Coal Waste Artificial Reef Program, Phase 1. Materials Screening and Characterization

I. W. Duedall[1]
P. M. J. Woodhead[1]
J. H. Parker[1]
R. Dayal[1]
H. B. O'Connors[1]
H. R. Carleton[2]
F. Wang[2]
T. O. Carroll[3]
D. Dicker[3]

[1] Marine Sciences Research Center
[2] Materials Science Laboratory, College of Engineering
[3] Institute for Energy Research

July 1984
(Report to Sponsors March 15, 1979)

State University of New York at Stony Brook, N.Y. 11794

Co-funded in Phase 1 by:

New York State Energy Research and Development Authority
Electric Power Research Institute, Palo Alto, Calif.
United States Department of Energy
United States Environmental Protection Agency
New York State Power Authority

SPECIAL REPORT 58

REFERENCE 84-5

Approved for Distribution

J. R. Schubel

MASIC
×
GC
1
.565
≈0.58

Table of Contents

Table of Contents (continued)

Table of Contents (continued)

Table of Contents (continued)

Table of Contents (continued)

List of Tables

List of Tables (continued)

List of Tables (continued)

List of Tables (continued)

List of Figures

List of Figures (continued)

List of Figures (continued)

List of Figures (continued)

List of Figures (continued)

I. INTRODUCTION

A. Definition of Problem

The present national energy policy encourages the rapid increase in the production and utilization of coal. To achieve this policy, however, it is necessary for new coal burning power plants to be fitted with flue gas desulfurization (FGD) scrubbers to remove harmful sulfur oxides in order that they comply with the standards of the Clean Air Act.

According to the U. S. Environmental Protection Agency, the use of FGD scrubbers is a reliable technology (Herlihy, 1977). The combustion of coal in furnaces fitted with scrubbers, however, results in the production of very large amounts of scrubber sludge, principally calcium sulfate and calcium sulfite. Fly ash, another waste product of coal combustion, is also produced in large volumes. The ratios of scrubber sludge to fly ash produced vary with the type of coal burned and the clean-up equipment used.

In areas with minimal land available for disposal, a major unsolved problem in the widespread use of scrubbers is the disposal of the calcium sulfate-sulfite sludge and fly ash. This problem must be overcome in order to develop the full potential for coal combustion using flue-gas

scrubbers.

Several methods for the disposal of these coal combustion wastes have been suggested and discussed (e.g. Lunt et al., 1977). They include disposal in mine shafts, land-fill applications and ocean disposal. Lunt et al. (1977) suggest that the disposal of untreated sludges (either as liquid slurries or as dewatered sludges) on the sea bed is probably environmentally unacceptable. One of the major potential problems suggested by Lunt et al. (1977) is the depletion of dissolved oxygen in the water column and the toxicity of sulfite to some organisms. Other potentially serious problems include increased turbidity in the water column, smothering of benthic communities on the seabed, and the release of trace metals that might be harmful to organisms. Lunt et al. (1977) do suggest, however, that the disposal of stabilized, scrubber sludge in solid, brick-like forms in the ocean appears promising.

Duvel et al. (1978) evaluated existing information obtained from several commerical installations in order to determine the utility of stabilized FGD sludges. Stabilization is usually accomplished by adding lime to a blend of raw FGD sludge and fly ash; fly ash is known for its excellent pozzolanic properties which makes it a desirable additive to concrete (Dikeou, undated). The reaction between the fly ash, lime, and FGD sludge results in formation of

ettringites (sulfo-alumina hydrates) and calcium silica hydrate (tobermorite) in the stabilized FGD sludge (Goodwin and Gleason, 1978). Duvel et al. (1978) found that of the several companies who have developed a stabilization process, it is only IU Conversion Systems, Inc. (IUCS) and the Dravo Corporation that have demonstrated fully commercial capability, with their end products exhibiting lower permeability, greater strength, and improved physical, chemical, and engineering properties compared to raw, untreated FGD sludges. As EPA considers land disposal of raw sludges environmentally unsound, an evaluation of the environmental effects associated with the disposal of the stabilized form in the sea has become necessary and is the subject of the present report.

B. Purpose and Scope of Report

This report describes the activities and presents the results of the initial activities (hereafter called Phase I) of the Coal Waste Artificial Reef Program (C-WARP) which started on October 11, 1978 and will involve the construction of an artificial fishing reef in the Atlantic ocean south of Fire Island Inlet (Figure I-1). In addition, the report presents supporting or supplementary data collected in our ongoing studies associated with the Conscience Bay site near Long Island Sound where blocks of stabilized FGD sludge and fly ash have been on the

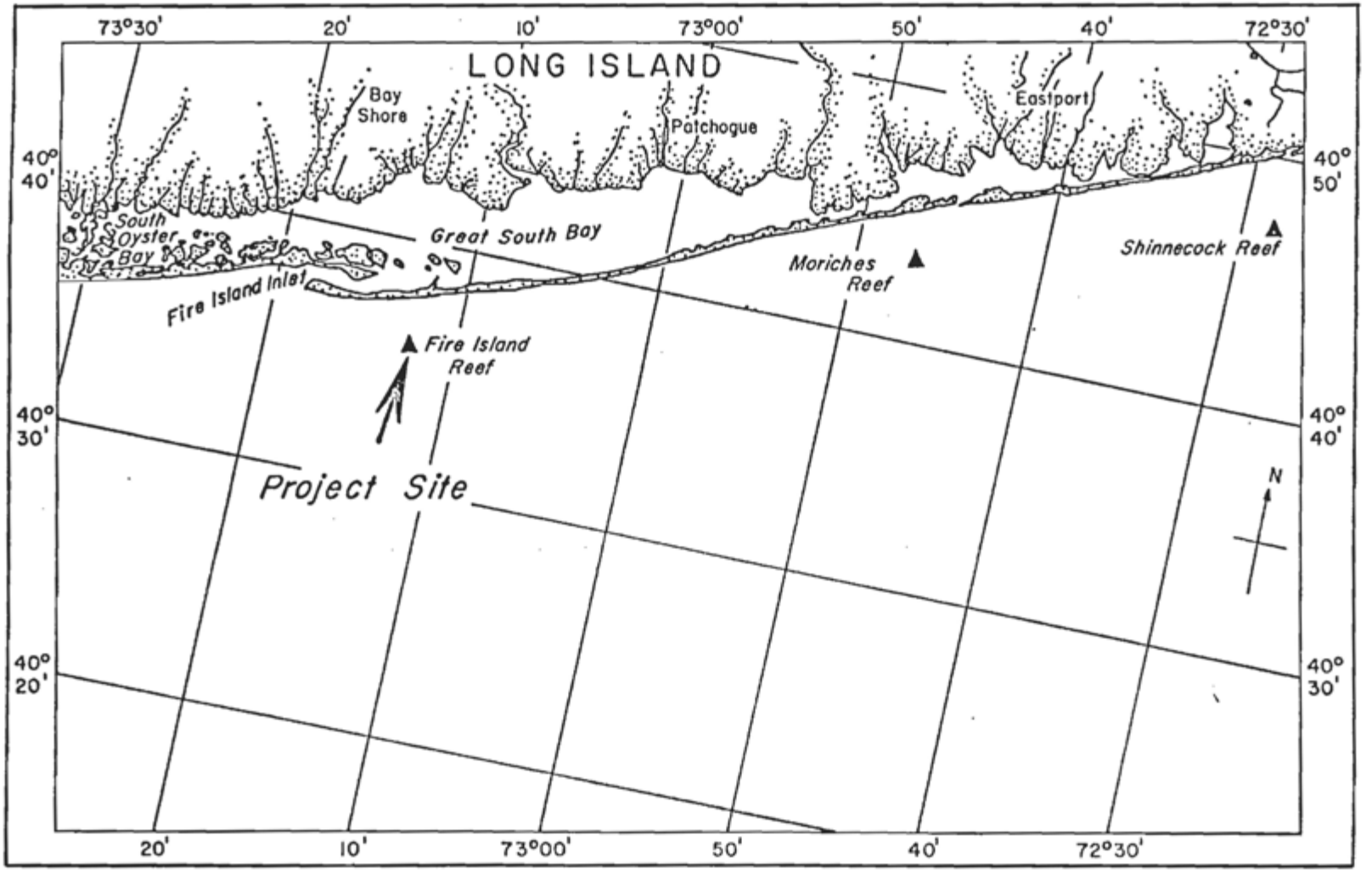

Figure I-1. C-WARP project site.

seabed for nearly two years.

The goal of The Coal Waste Artificial Reef Program (C-WARP) is to determine the environmental acceptability of stabilized coal wastes from coal fired electric generating plants when used for the construction of artificial reefs in the sea.

During C-WARP Phase I, research has started on four different formulations (mixes) of stabilized scrubber sludge and fly ash (POZ-O-TEC^{R} process) provided by IU Conversion Systems, Inc. (IUCS). The scrubber sludge used in the formulations originated from the Elrama station (near Pittsburgh) of Duquesne Light Company and the Conesville station of Columbus and Southern Ohio Electric.

For two Elrama mixes, we have gathered an extensive amount of data on composition, leaching behavior, physical properties, in situ behavior in relation to physical properties and biological colonization of small test blocks) at the Fire Island Reef site in the Atlantic and bioassays. Less information is available for the Conesville mixes obtained during C-WARP, although considerable long term data on one Conesville mix is available from the Conscience Bay study.

Concurrent with the C-WARP work on the properties and behavior of the test formulations was the completion of two

background oceanographic surveys to describe the baseline conditions at the Fire Island reef site where, during the next phase of the work, several hundred 1 yd^3 blocks will be placed. Other activities completed during Phase I include a preliminary economic assessment of coal waste disposal at sea and the fabrication by IUCS of proto-type 1 yd^3 blocks of stabilized FGD sludge and fly ash.

The scope of this report will be to present and discuss the principal findings of C-WARP Phase I and of the Conscience Bay study as they relate to the recommendation for full-scale production of several hundred 1 yd^3 blocks of stabilized FGD sludge and fly ash which would be placed in the sea in August 1979 as part of C-WARP Phase II operations.

C. Areas of Investigation

The areas of investigation in C-WARP Phase I covered a wide range of research activities involving chemistry, biology, materials science, oceanography, engineering, and economic assessment. The specific tasks associated with each area are given in Table I-1.

D. Schedule of Coal Waste Blocks Received

Several shipments of 1 ft^3 blocks of different mixes of stabilized FGD scrubber sludge and fly ash were received from IUCS during C-WARP Phase I. Table II-2 lists the mix types, their formulation (i.e., high sulfite, fly ash:sludge ratio, lime) and the date of receipt. The testing program conducted during C-WARP Phase I

Table I-1. Areas of Investigation during C-WARP Phase I.

Areas of Investigation	Specific Tasks
Chemical properties	Block composition and mineralogy, tank studies, accelerated dissolution, composition of sludge and fly ash end members
Physical properties	Density, porosity, permeability, water absorption, compressive strength, hardness, erosion, dissolution, elastic modulus, sound velocity, accelerated tests (hot bath, pressure)
Laboratory bioassays	Phytoplankton, animal assays: sand shrimp, winter flounder eggs and larva hard clams, minnows
Biological acceptability at blocks *in situ*,	Colonization studies at Flax Pond Laboratory, Conscience Bay, Atlantic project site
In situ block placement	Site marking, placement and handling
Baseline surveys	Water column, plankton abundances, benthic community, sediment properties residual currents
Production of 1 yd^3 prototype monoliths of stabilized scrubber sludge and fly ash	Mold release, lifting, transportation, curing, tests, cost estimates
Economic assessment of coal waste disposal at sea	Determine disposal costs on a commerical basis. Define areas where operation affects cost

Table I-2 . Schedule of blocks (1 ft^3) of stabilized FGD scrubber sludge and fly ash received from IUCS* during C-WARP Phase I. Elrama and Conesville denotes origin of sludges and fly ash; coarse (C) fine (F) refers to quicklime and hydrated lime respectively; 1:1 and 3:1 are fly ash to sludge ratios**.

Test Blocks	Code	Date Received	Remarks
Elrama Coarse 1:1	E1C1	Sept. 29, 1978	E1C1 and E1C3 experienced significant fracturing early in the testing program. This was due to incomplete maturation and the presence of excess amounts of unreacted lime (discussed later in text)
Elrama Coarse 3:1	E1C3	Sept. 29, 1978	
Elrama Coarse 1:1	E2C1	Nov. 29, 1978	
Elrama Coarse 3:1	E2C3	Nov. 29, 1978	
Elrama Fine 1:1	E3F1	Jan 22, 1979	
Conesville Fine 1:1	C3F1	Jan. 22, 1979	
Conesville Fine 3:1	C3F3	Jan. 22, 1979	

* IUCS also provided samples of the pure scrubber sludge and fly ash end members used for the preparation of the blocks. Analysis of these components was carried through in the chemical testing program.

** These are nominal ratios based on information supplied by IUCS and serve as useful diagnostic indicators for the fly ash: scrubber ratio; the actual ratio, from an analysis of the fly ash in the mixes, was determined in the testing program.

focused primarily on the Elrama mixes because it was decided at the first Program Managers meeting that the 1 yd^3 monoliths of FGD scrubber sludge and fly ash to be constructed in Phase II would be made at the Elrama power station. However, as will be discussed later in more detail, it was decided that the large monoliths should be constructed at the Conesville power station. A more efficient fly ash precipitator there prevents serious contamination of the scrubber sludge by fly ash, and the sludge produced is more representative of a newly built power station. Thus, an intensive testing program of the Conesville mixes has started. Some early results were available at the time of this writing.

E. Chronology of Testing Program

The C-WARP testing program is comprised of several related laboratory and field investigations, as indicated in Table I-1, in which tests have been performed on the mixes (Table I-2) received by IUCS. Table I-3 is a summary of the C-WARP cruise chronology. The main purpose of the cruise has been either baseline oceanography surveys or placement, location, and retrieval of test blocks; the chronology of specific test mixes placed at sea is given in Table I-4. In addition to the project site, several sets have been placed in sea tables at the Flax Pond field laboratory (Table I-5).

Table I-3. C-WARP Cruise Chronology.

Cruise No.	Dates	Main Purposes
1	October 9-11	Baseline oceanography surveys, surveys at Fire Island Reef, testing procedures for placement of test blocks.
2	October 18,19	Placement of test blocks.
3	November 13	Location and retrieval of test block samples.
4	December 5-8	Baseline oceanography, location placement of test blocks and retrieval of test blocks, collection of seawater for assays
5	January 10,12	Location and retrieval of test blocks, collection of seawater for bioassays.
6	February 9, 22 & 23 continuing	Location and retrieval of test blocks.

Table I-4. Chronology of test block placement and retrieval at project test site. Number in brackets represents test blocks placed in or retrieved from the project site near the Fire Island Reef.

Cruise No.	Date	Mixes and number of blocks placed	Mixes Retrieved
2	October 18	E1C1 (50) E1C3 (50) Concrete (50)	
3	November 13		E1C1 (6) E1C3 (6) Concrete (6)
4	December 8	E2C1 (50) E2C3 (50)	E1C1 All removed E1C3 (6) Concrete (6)
5	January 10		E1C3 (9) Concrete (6) E2C1 (3)
6	February 22	E3F1 (30) C3F3 (30) Concrete (30)	

Table I-5. Chronology of block placement at Flax Pond Laboratory. Numbers in brackets represent test blocks placed in or retrieved from sea tables.

Date	Mixes	Retrieval
December 15	MSL Blocks*	
	E2C1 (12)	
	E2C3 (12)	
December 26	Biol Blocks**	
	E1C1 (12)	
	E1C3 (12)	
January 30	Biol Blocks	
	E1C1 (4)	
	E1C3 (4)	
January 31		E2C1 (4)
		E2C3 (4)
February 23	Biol Blocks	
	E3F1 (2)	

*MSL Blocks; test blocks used by the Materials Sciences group for physical testing.

**Biol Blocks; test blocks used for biological work.

II. COMPOSITION, MINERALOGY AND CHEMICAL BEHAVIOR OF STABILIZED FGD SLUDGE AND FLY ASH

Knowledge of the composition, mineralogy, and seawater dissolution of stabilized FGD sludge and fly ash is fundamental in the interpretation of the physical behavior and biological impact of stabilized coal wastes in the ocean. Therefore, a systematic scheme of analysis was devised to assess: 1) the chemical homogeneity of a single stabilized coal waste block; 2) the mineralogy of unreacted (not exposed to seawater) and reacted (exposed to seawater) stabilized coal waste blocks; 3) the accelerated dissolution of chemical components in the stabilized coal waste blocks upon exposure to seawater; and 4) the chemical composition and mineralogy of the FGD sludge and fly ash end members used in the preparation of the stabilized coal waste blocks.

A. Methodology

1. Composition

a. Homogeneity of Elrama blocks. To determine the spatial variability in the chemical composition of the test blocks, 0.028 m^3 blocks of E2C1 and E2C3 were cut into 27 10 cm cubic subsections as shown in Fig. II-1. Four 10 cm cubic subsections were taken from each 0.028 m^3 block to include front and rear corners (F-9, F-1 or F-3, R-7) and

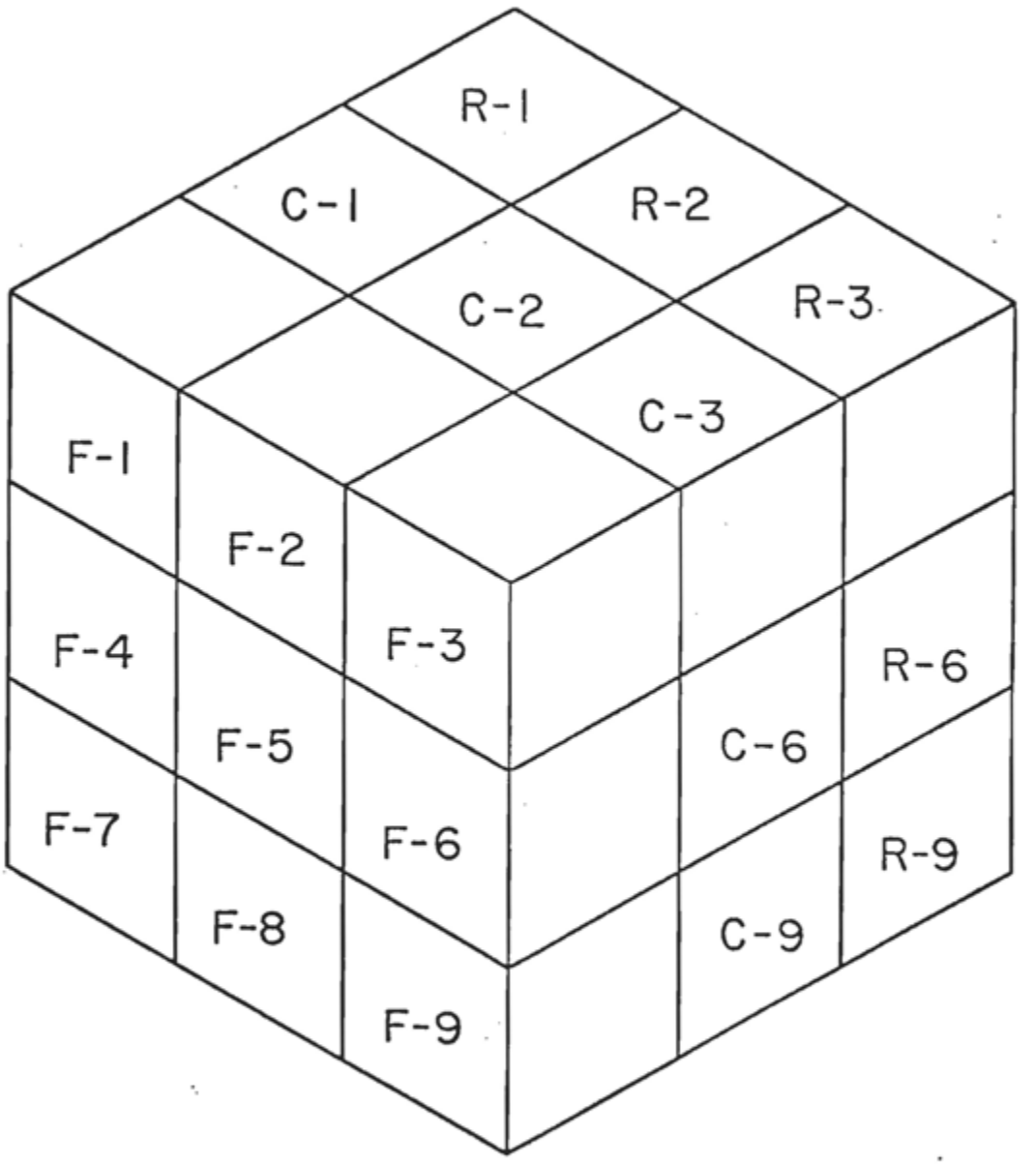

Figure II-1. Designations of subsections cut from 0.028 m^3 ($1ft^3$) blocks for homogeneity analysis.

center (C-5) subsections.

b. Sample preparation of Elrama blocks. The surface of each 10 cm cube was scraped off with a plastic blade to remove any contamination from the cutting and handling of the blocks. Further scrapings were taken from the remaining core to provide a representative sample which was ground in a ceramic mortar and pestle cleaned with Ottawa sand. The final powder was oven dried at 90°C for approximately 12 hrs.

For the determination of elemental composition by atomic absorption spectrophotometry, duplicate 2 g (weighed to the nearest 0.1 mg) aliquots of each dried subsection of powder were transferred to plastic digestion bottles. Ten ml of nitric acid were added and digestion at 90°C was carried out for 3 hours. The cooled digests were then filtered, brought up to 50 ml volume with Q-water and stored in plastic bottles prior to analysis. All containers were vigorously acid washed prior to use to ensure cleanliness. The identical preparation regime was used for the C4F1 and C4F3 proctors.

c. Determination of elemental composition. The nitric acid digests were analyzed for Ca, Cr, Cu, Fe, Mn, Ni, and Zn by flame atomic absorption spectrophotometry. Hg in the acid digests was analyzed by the flameless hydride generation atomic absorption spectrophotometry technique. Additional aliquots of the dried powder were sent to Dalhousie

University (Nova Scotia) and Brookhaven National Laboratory for thermal neutron activation analysis to provide a qualitative and quantitative analysis for a broad spectrum of elements in the stabilized coal waste blocks.

Arrangements are being made with Lawrence Berkeley Laboratory for x-ray fluorescence analysis for a broad spectrum of elements in the same blocks.

Through this on-going intercalibration, we can insure the most precise and accurate analysis of the elemental composition of the stabilized coal waste blocks.

d. Determination of sulfite (SO_3). The concentration of SO_3 in freeze-dried samples of the Elrama and Conesville sludges and the test mixes was determined using a modified version of the iodimetric titration (American Public Health Association, 1975). The rapid oxidation of SO_3 to sulfate(SO_4) in solution in the presence of oxygen proved to be a significant problem. Time series experiments using standard solutions of Na_2SO_3 indicated that $15.0 \pm 0.8\%$ (n=5) of the SO_3 originally present was oxidized to SO_4 within three minutes. The following precautions were taken to minimize SO_3 oxidation: 6N HCl was substituted for the 18N H_2SO_4 called for in the method (this modification minimized the oxidation of SO_3 by the H_2SO_4); the acid and the starch indicator were combined with Q-water to facilitate easier handling during analysis; both the titrant and the dilution water used in the analysis were deoxygenated by bubbling N_2 gas through

them for 30 min prior to analysis; the titration and all the steps involved in the transfer of liquids in the procedure were carried out in a glove bag which was initially evacuated and then purged with N_2 gas. Based upon a series of runs using Na_2SO_3 standards, the recovery of SO_3 was 92.2±2.7%(n=10).

Further problems appeared later in the actual analysis of the sludges and mixes because the solid samples had to be dissolved with 2 ml of 6N HCl. Direct dissolution of the samples by the acid resulted in an unacceptable recovery of SO_3, based on Na_2SO_3, of 81.2±5.5%(n=5). However, adding the acid after the addition of 50 ml of the acid-starch Q-water reagent proved satisfactory with a recovery of SO_3 from standard Na_2SO_3 of 93.8±0.8%(n=4).

e. Determination of sulfate. The $CaSO_4 \cdot 2H_2O$ and $CaSO_3 \cdot \frac{1}{2}H_2O$ in the test blocks are of considerable interest to the project. It is difficult, however, to determine SO_4 and SO_3 in the presence of each other in an acid digest because of the rapid oxidation of SO_3. Thus SO_4 was determined by subtracting the SO_3 concentration from a measurement of total sulfate plus sulfite. The measurement of total sulfate plus sulfite began with approximately 0.25g of replicate samples of freeze-dried Conesville and Elrama sludges or the test mixes being weighed into 250 ml erlenmeyer flasks. One-half ml of concentrated HCl was added to the samples followed by 25 ml

of Q-water. One ml of 30% H_2O_2 was then added to each sample to oxidize SO_3 to SO_4. The samples were warmed at 40°C for 1 hour after which they were filtered using Whatman No. 40 filters (75 ml of distilled water were used to rinse the flask and the filters). The filtrate was then heated to boiling and 12 ml of 5% solution of $BaCl_2$ were added drop by drop to precipitate the SO_4 as $BaSO_4$. The precipitated $BaSO_4$ samples were placed on a heating bath at 110°C for 2 hours and then allowed to cool for one half hour followed by filtering using Whatman No. 40 filters. The filters were carefully folded and placed neatly in size-0 porcelain crucibles where they were allowed to dry over night. The dried filters were charred by flame and then ignited at 800°C in an oven for one hour. After the ignition was complete, the crucibles were cooled to room temperature in a desiccator and reweighed to determine the $BaSO_4$. Based on a series of determinations using K_2SO_4 as the standard, the percent recovery was 98.3 ± 0.2 (n=6). Using Na_2SO_3 as the standard, the percent recovery was $96.7 \pm 2.2\%$ (n=6). The SO_4 in the test samples was calculated by subtracting the SO_3 from the sulfate plus sulfite measurement.

f. Determination of carbon. Total carbon, presumably in the form of carbonate carbon and/or elemental carbon, was determined for the sludges and mixes using a Hewlett Packard CHN analyzer (model 185). The combustion temperature was 1140°C, and acetanalide was used as the

standard. The coefficient of variation was ±7.4%(n=5). Elemental carbon in the sludges was determined by combusting the acid residue (from the fly ash determination) in the CHN analyzer. Carbonate carbon was calculated by difference.

g. Determination of fly ash. The fly ash content of test mixes C4F1 and C4F3 and the Elrama and Conesville sludges were determined by two different methods. The first method involved adding weighed 0.3-0.5 g portions of freeze-dried samples of the mixes or sludges to 50 ml of 6N HCl in an erlenmeyer flask followed by stirring for 8 minutes at 25°C. The remaining residue was filtered through a 0.45 µm Millipore filter and dried in a dessicator until constant weight was achieved. In the second method, similarly prepared samples were dissolved in 0.1M Na_4EDTA using the same filtering and drying procedures as in the HCl method. For both analysis, an Elrama ash was carried through the procedure as a check on the dissolution of any fly ash in the sludges. The results obtained from the two methods are compared in Table II-1 for the fly ash, the sludges, and the Conesville 1:1 and 3:1 mixes. The EDTA method would be the preferred technique since a small amount of the ash can be solubilized by the action of HCl (see results for the control, Table II-2). However, for the sludges, the EDTA method gave ash values significantly higher then those obtained by the HCl method. The increased ash content

Table II-1. Comparison of HCl and EDTA methods for determining fly ash concentration (percent fly ash on a dry weight basis).

Method	Elrama Ash (control)	Sludges		Mixes	
		Conesville	Elrama	C4F1	C4F3
HCl	96.1 ± 0.2	2.8 ± 1.0	43.2 ± 0.4	48.1 ± 1.3	70.9 ± 0.2
EDTA	97.9 ± 0.2	5.5 ± 2.8	53.0 ± 0.6	57.5 ± 0.4	77.7 ± 0.4

found, using the EDTA method, is most likely due to incomplete dissolution of non-ash components by the Na_4EDTA. The correct fly ash content in the samples tested lies somewhere between the values obtained from the two methods. Work is in progress to improve the accuracy of EDTA methods and, for the present, the reported fly ash concentrations are based on the HCl method.

2. Mineralogy

a. X-ray diffraction analysis. Methods used for x-ray diffraction analysis were similar to those used by Dayal et al. (1978). The x-ray diffractometer was set up for a broad range of diffraction angles ($5\text{-}65^{\circ}2\theta$). Since none of the mineral phases present have layer-silicate structure, our main aim was to obtain characteristic (hkℓ) reflections rather than (00ℓ) basal reflections on the diffractogram. For this purpose, random mounts were prepared for x-ray diffraction analysis.

b. Light microscopy. Permanent mounts of fly ash samples were prepared using Caedex immersion oil (refractive index = 1.58). These slides were examined under the microscope using plane polarized, crossed nicols, and reflected light settings or a combination of transmitted and reflected light. Magnetite is opaque in transmitted light and exhibits a characteristic grey lustre in reflected light. Hematite can be easily distinguished from magnetite by its reddish-brown lustre. Transparent glassy

(alumino-silicate) spherules are relatively easy to identify based on their spherulitic morphology and isotropic optical properties under crossed nicols. Mullite, quartz, and calcite are optically anisotropic and exhibit birefringent properties under crossed-nicols.

c. Scanning electron microscopy (SEM). Selected samples were prepared for SEM work by gold-plating the sample placed upon a stainless steel stub. The analysis was carried out on Cambridge Geoscan scanning electron microscope.

3. Accelerated Dissolution Studies

a. Tanks. Ten cm cubic subsections from the same E2C1 and E2C3 0.028 m^3 blocks used for spatial chemical variability analysis were cut into duplicate 97, 287 and 831 cm^3 blocks with geometric surface areas of 130,261 and 516 cm^2. The weighed blocks were suspended in acid washed plastic tanks which were filled with 1, 2 or 4 liters of filtered sea water from the proposed Fire Island reef site (Table II-2). Duplicate tanks with 2 liters of seawater were set up as controls. The ratio of the surface area to volume of seawater was held constant at 130:1. Each tank had a 0.45µm membrane placed over an opening in its cover to insure aeration without contamination. All tanks were placed on individual magnetic stirrers for 8 hrs everyday to accelerate the dissolution process. An acid washed outlet tube was attached to the bottom of each

Table II-2. Experimental design for tank study.

Mix Type	Tank #	Surface Area Blocks (cm^2)	Seawater in Tank (l)
E2C1	1	130	1
	2		
	3	261	2
	4		
	5	516	4
	6		
E2C3	7	130	1
	8		
	9	261	2
	10		
	11	516	4
	12		
	13	Controls: 2 liters seawater alone	
	14		

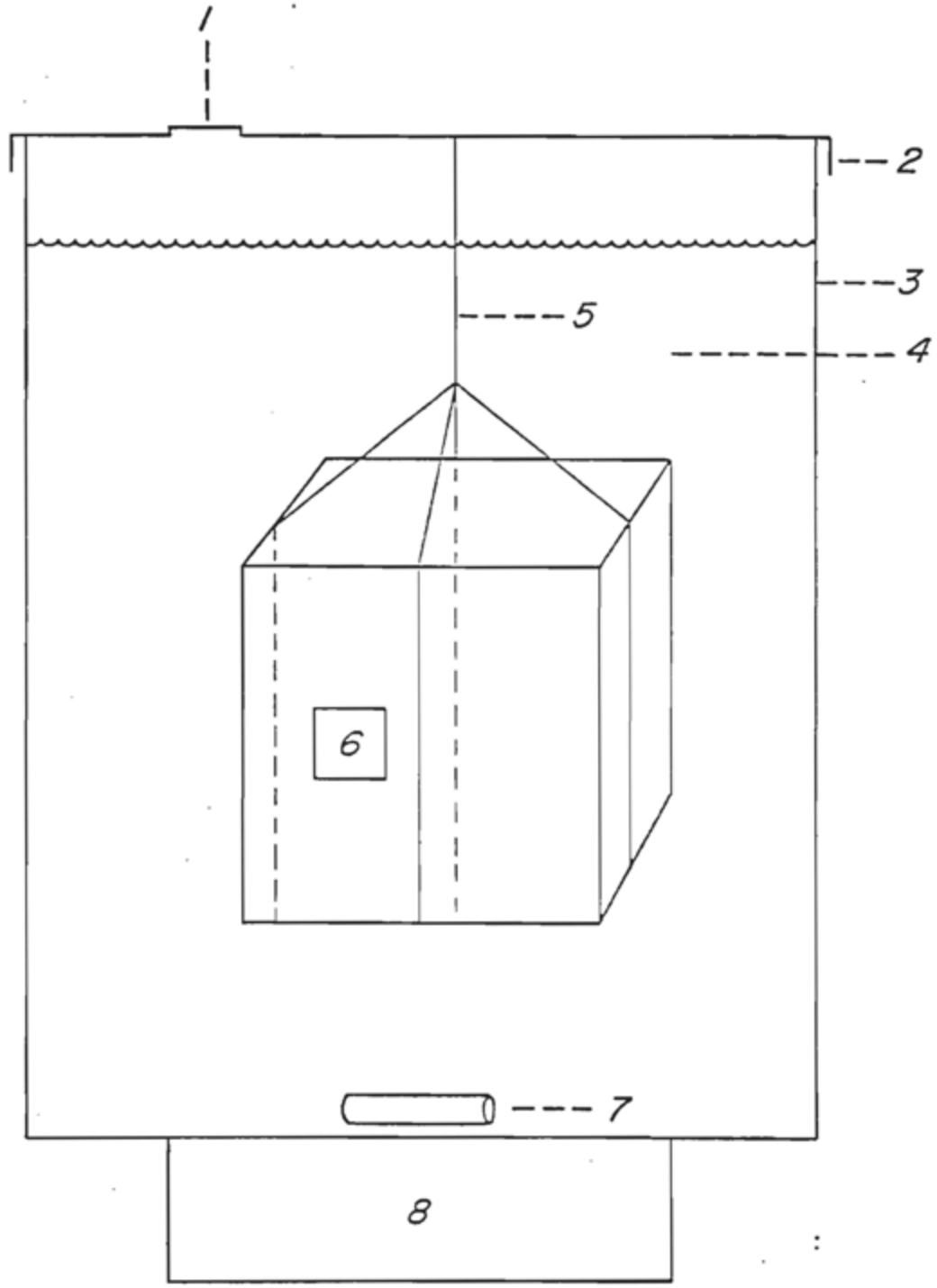

Figure II-2. Tank configuration: 1. 0.45µm filter; 2. cover; 3. tank; 4. filtered seawater; 5. monofilament fishing line; 6. coal waste block; 7. magnetic stirring bar; 8. magneti stirrer.

tank for sampling (Figure II-2).

To avoid saturation of the seawater in the tanks with a resultant reduction in leaching rates, the entire volume of seawater was replaced at 2 week intervals with filtered seawater from the proposed Fire Island reef site. At 2-3 day intervals during the 2 week leachings, 5 ml of seawater were sampled from each tank for calcium analysis. These samples were taken with acid washed plastic syringes and filtered through acid washed 0.45μm membrane filters attached to the syringe. The filtrates were acidified and refrigerated immediately.

At the end of the 2 week leaching period, a 100 ml aliquot of seawater was taken for pH and sulfate analysis, and immediately frozen. A separate 500 ml filtered aliquot was taken for dissolved trace metal analysis. The trace metal samples were immediately acidified to pH 2 with Ultrex nitric acid and refrigerated. The remainder of the seawater was discarded and the tanks were rinsed with Q-water and refilled with filtered seawater. Aliquots of the reef site seawater were periodically taken for blank analysis to characterize the elemental composition of this water.

Extreme care was taken in sample handling to insure a minimum of contamination. Seawater filtration (filling and emptying tanks) was carried out by attaching an acid washed surgical silicone rubber tubing to the source. The tubing was connected through a Masterflex peristaltic pump and connected downstream to an acid washed plastic filter

holder housing an acid washed 0.45μm membrane filter. Therefore, the seawater was never exposed to the laboratory atmosphere or non acid-washed material during the filtering process. This is mandatory for low level trace metal studies and the contamination-free nature of our experiments is reflected in the results.

Calcium in the seawater leachates was analyzed by flame atomic absorption spectrophotometry after the addition of 1% La^{3+} to both samples and standards. Copper in the seawater leachates was analyzed by flameless atomic absorption spectrophotometry using the method of standard additions. Mercury in the seawater leachates was analyzed by the flameless hydride generation atomic absorption spectrophotometry technique. Methods are currently being developed for the analysis of more transition metals of interest in the leachates.

b. Columns. Ten cm cubic sub sections from the same E2C1 and E2C3 0.028 m^3 blocks used for spatial chemical variability were filed into duplicate 5 cm diameter x 5 cm long cylinders. The weighed cylinders were epoxied into the bottoms of 5 cm I.D. x 1.2 m long acid washed PVC columns. A fifth column was assembled without a stabilized coal waste cylinder to serve as a blank. The tops of the columns were fitted with a screw cap assembly connected to a nitrogen tank for pressurizing the column. An acid washed filtering funnel and a 500 ml teflon separatory funnel were attached to the column for the collection of the

leachate (Fig. II-3). The columns were filled with approximately 2.2 ℓ of filtered seawater from the proposed Fire Island reef site.

Prior to pressurizing the columns, the time interval between filling the individual columns with seawater and the collection of 20 ml of leachate was measured to calculate the coefficient of permeability. Nitrogen pressure was then applied at 3-4 psi until 500 ml of leachate were collected in the teflon separatory funnels.

When all funnels were filled, a 100 ml aliquot of the seawater was taken for pH and sulfate analysis and immediately frozen. A separate 500 ml filtered aliquot was taken for dissolved trace metals analysis. The trace metal samples were immediately acidified to pH 2 with Ultrex nitric acid and refrigerated.

Four 500 ml aliquots of the seawater leachate from each column were collected in this manner. At the end of the fourth collection, the columns were refilled with filtered Fire Island reef site seawater. Aliquots of the reef site seawater were continually taken for blank analysis to characterize the elemental composition of this water.

The same methods and care were used for filtration, sample handling, and analysis as described in the tank dissolution studies.

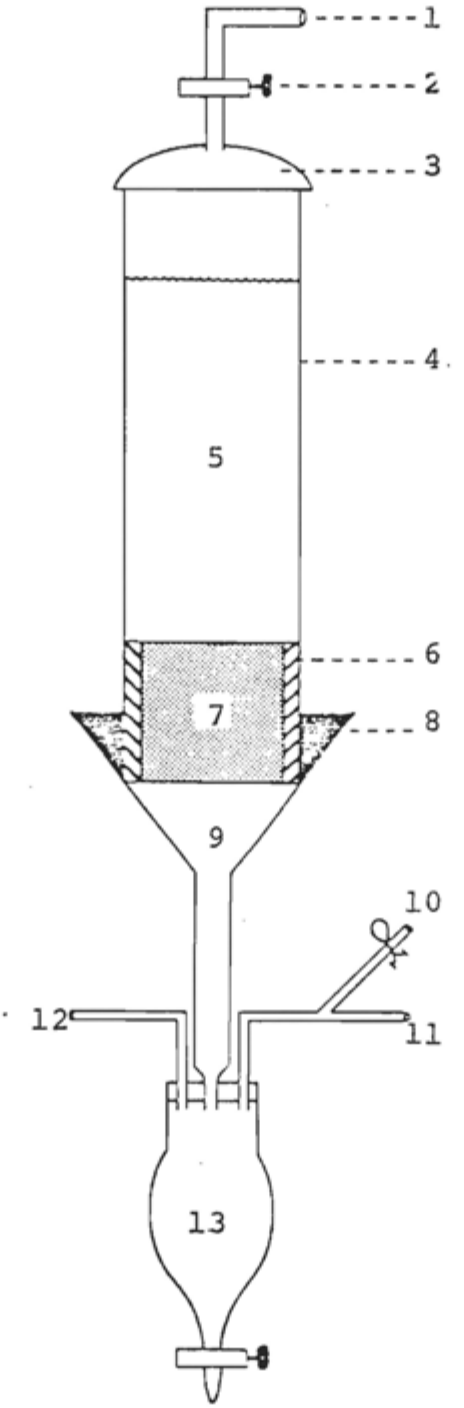

Figure II-3. Column configuration: 1. nitrogen tank; 2. flow control valve; 3. screw-on end fitting; 4. PVC pipe; 5. filtered seawater; 6. epoxy resin; 7. coal waste block; 8. silicone caulk; 9. plastic funnel; 10. vent; 11. to nitrogen tank; 12. to bubbler; 13. teflon separatory funnel.

B. Results and Discussion

1. Composition.

a. The blocks. Before leaching tests can be undertaken, we must be assured that the stabilized coal waste blocks are homogenous with respect to the major and minor elements. Table 11-3 details the spatial variability in the chemical composition of the E2C1 and E2C3 blocks used for the dissolution experiments. The null hypothesis ANOVA statistical test was applied to the values reported for the four subsections from each individual mix (intra-block variation), and to the average values reported for the two mix types (intermix block variation). The ANOVA test gives four levels of significance that variance exists: $p<0.05$, $p<0.01$, $p<0.001$ and not significant (NS). As reported in Table II-3, there is no significant intra-block variance of Cr, Cu, Fe, Mn, Ni and Zn in both the E2C1, and E2C3 blocks. Therefore these blocks are homogenous with respect to these trace metals. There is a large significant intrablock variance with respect to fly ash with a decreasing, but significant intra-block variance of Ca and Hg. There is a large ($p<0.001$) significant variance for all the metals and fly ash concentrations between the average values reported for the E2C1 and E2C3 blocks. Therefore, as expected, intermix variation exists.

Table II-3. Major and minor element composition of test mixes. Subsamples refer to samples taken from 1 ft^3 test blocks that were subdivided to determine block homogeneity.

Sample Mix Type	Sub Sample	Fly Ash (%)	Total C (%)	Total S (%)	Ca (%)	Cr ($\mu g\ g^{-1}$)	Cu ($\mu g\ g^{-1}$)	Fe ($mg\ g^{-1}$)	Hg ($\mu g\ g^{-1}$)	Mn ($\mu g\ g^{-1}$)	Ni ($\mu g\ g^{-1}$)	Zn ($\mu g\ g^{-1}$)
E2C1	F-9	52.48±0.27	2.97	5.49	10.83±0.17	11.79±0.07	9.26±0.62	6.71±0.68	.34	46.31±0.65	7.82±0.04	20.74±0.35
	R-7	50.81±0.20	3.50	6.05	12.26±0.31	12.24±0.62	9.34±0.10	5.65±1.27	.46±0.06	44.49±2.82	7.62±1.14	19.42±1.42
	C-5	56.96±0.89	2.98	4.49	10.54±0.58	12.03±0.58	9.16±0.11	6.12±0.25	.38±0.02	46.72±2.21	7.80±0.67	20.15±0.79
	F-1	51.98±0.16	3.12	5.39	11.55±0.19	11.60±0.37	9.01±0.05	5.93±0.30	.41±0.01	42.92±1.37	7.71±0.25	19.42±0.56
	$\bar{x}$	53.06	3.14	5.36	11.3	11.9	9.2	6.1	.40	45.1	7.7	19.9
	p	p<.001			p<.01	NS	NS	NS	p<.05	NS	NS	NS
E2C3	F-3	72.23±0.70	4.01	2.44	6.52±0.01	13.82±0.76	10.00±0.15	8.09±1.50	.28	52.18±4.32	8.14±0.95	23.37±3.81
	R-7	73.92±1.40	2.87	2.35	6.52±0.17	13.32±0.31	10.28±0.67	6.89±2.21	.32±0.01	51.60±0.98	7.98±0.45	23.52±2.43
	F-9	72.56±0.32	3.10	2.44	6.34±0.05	13.23±0.12	10.36±0.12	6.98±1.33	.29±0.01	49.94±1.30	8.03±0.03	25.33±5.71
	C-5	73.66±0.30	3.88	2.9	6.56±0.00	13.55±0.43	11.06±1.32	7.58±1.05	.27±0.00	52.61±2.20	8.24±0.80	22.09±1.17
	$\bar{x}$	72.82	3.47	2.36±	6.5	13.5	10.4	7.4	.29	51.6	8.1	23.8
	p	p<.001			p<.01	NS	NS	NS	p<.05	NS	NS	NS

Table II-4. Average concentrations of major and minor elements and fly ash in the Elrama and Conesville mixes.

Sample Mix Type	Fly Ash (%)	Total C (%)	CO_3 (%)	Total S (%)	SO_3 (%)	SO_4 (%)	Ca %	Cr $\mu g\ g^{-1}$	Cu $\mu g\ g^{-1}$	Fe $mg\ g^{-1}$	Hg $\mu g\ g^{-1}$	Mn $\mu g\ g^{-1}$	Ni $\mu g\ g^{-1}$	Zn $\mu g\ g^{-1}$
E2C1	53	3.14	10.4	5.36	11.4	2.40	11.3	11.9	9.2	6.1	.40	45.1	7.7	19.9
E2C3	73	3.46	12.0	2.36	3.47	2.91	6.5	13.8	10.4	7.4	.29	31.6	8.1	23.8
C4C1	48	0.50	1.20	8.07	20.8	0	12.9	12.4	12.6	8.6	.30	85.9	7.6	29.7
C4C3	71	0.39	0.65	4.12	10.5	0	8.1	8.8	13.2	7.4	.16	43.0	9.2	25.9

Table II-5. Ratios of fly ash and total calcium in the Elrama and Conesville mixes.

Sample	% sludge	sludge ratio (1:1/3:1)	% Ca	% Ca ratio (1:1/3:1)
E2C1	47	1.7	11.3	1.6
E2C3	27		6.5	
C4F1	52	1.8	12.9	1.7
C4F3	29		8.1	

Table II-6. Massbalance for the Elrama and Conesville mixes.

Mix	Fly Ash (%)	$CaCO_3$ (%)	$CaSO_3 \cdot 1/2H_2O$ (%)	$CaSO_4 \cdot 2H_2O$ (%)	$Ca(OH)_2$ (%)	$\sum$ (%)
Elrama						
E2C1	53	17.4	18.4	4.30	-	93
E2C3	73	20.1	5.60	5.22	-	104
C4C1	48	2.0	33.6	-	3.14	87
C4C3	71	1.08	16.9	-	4.50	93

as $CaCO_3$. $Ca(OH)_2$, which was not determined quantitatively but calculated based on the difference between total Ca determined in the strong acid leach and the Ca associated with the mineral phases $CaSO_3 \cdot \frac{1}{2}H_2O$, $CaSO_4 \cdot 2H_2O$, and $CaCO_3$, is also added to the balance

b. The end-members and calculation of a sludge mass balance. The chemical composition of the Elrama and Conesville end members (the sludges and fly ash used to prepare the mixes) provides valuable information on the origin of the major and minor elements in the test mixes. Table II-7 shows the fly ash, SO_3, SO_4, and CO_3 content for the Elrama and Conesville sludges. From the results in Table II-7 a mass balance can also be calculated for the sludges in the same way as for the mixes. Here it was assumed that the excess Ca in Elrama sludge was present as CaO rather than $Ca(OH)_2$. For the Elrama sludge, a mass balance was achieved. For the Conesville sludge, the mass balance gave 86% total solids.

Table II-9 summarizes the concentrations of trace elements found in the Elrama, Conesville and Phillips fly ash measured by neutron activation analysis at Brookhaven National Laboratory (BNL). With few exceptions (i.e. Fe, Ba, and Zn), the trace element concentrations for the fly ashes were very similar. The composition of the Phillips and Elrama ashes would be expected to be the same or similar since these two ashes came from the same coal (see IUCS

Table II-7. Ash, sulfur, and carbon content (%) in the Elrama and Conesville sludges.

Sludge	Ash	Sulfur			Carbon	
		Totals	SO_3	SO_4	Total C	CO_3*
Elrama	43.2±0.4	8.78±2.53	20.6±1.5	1.65	2.24±0.62	4.35
Conesville	2.84	18.08±0.60	48.9±0.3	0	0.41±0.01	0.71

* CO_3 was determined by subtracting the total carbon in the sludge from the carbon measured in sludge residue which had been leached by acid.

Table II-8. Mass balance for the Elrama and Conesville sludges.

Sludge	Ash (%)	$CaCO_3$ (%)	$CaSO_3 \cdot \frac{1}{2}H_2O$ (%)	$CaSO_4 \cdot 2H_2O$ (%)	CaO (%)	Σ (%)
Elrama	43.2	7.3	33.2	2.9	14.3	101
Conesville	2.84	1.25	79.0	≈1.2*	1.9	86

* Based on x-ray diffraction results.

Table II-9 . Trace element* concentrations ($\mu g\ g^{-1}$) of fly ash end members.

Element	Fly Ash		
	Elrama	Conesville	Phillips
Iron	74700	138000	71800
Barium	555	940	581
Chromium	107	105	111
Rubidium	102	122	105
Cerium	99	107	100
Zinc	98	169	103
Lanthanum	38	45	40
Cobalt	25	27	22
Scandium	24	25	24
Thorium	15.8	17.0	16.0
Samarium	8.8	10.8	9.4
Cesium	8.4	9.1	9.3
Hafnium	4.6	4.5	4.9
Ytterbium	4.4	6.3	5.1
Europium	2.1	2.7	2.1
Antimony	2.0	2.5	1.52

* These results, using neutron activation analysis, were kindly provided by Dr. G. Harbottle, Chemistry Department, Brookhaven National Laboratory, Upton, New York. U.S. Geological survey standard rocks were used as standards; the error in the values is $\pm$ 3-5%.

Report, Chapter VIII). A mass balance for the fly ash awaits further quantitative analysis of the major components to include Al, Si, Na and O by Dr. Chatopadhay of Dalhousie University, (Nova Scotia). He is determining the concentration of natural radionuclides and thermal neutron-induced gamma spectra of the fly ash, scrubber sludge, and the Elrama mixes. So far, he has been able to identify 40 elements in the fly ash samples provided. Quantitative analysis will be received soon.

2. Mineralogy

a. Fly ash. Frequency size distributions of fly ash samples derived from Elrama, Conesville, and Phillips plants are shown in Fig. II-4, 5, 6. The Elrama and Phillips fly ash exhibit a bimodal distribution whereas the Conesville fly ash distribution is unimodal. A comparison of the particle size distributions of the three fly ash types is shown in Fig. II-7. The Elrama fly ash contains as much as 20% clay fraction by weight. On a total weight basis, the fine clay-fraction is practically absent in Conesville and Phillips fly ash (Fig. II-7).

The mineralogical composition of fly ash derived from Elrama and Conesville plants consists of quartz, mullite, magnetite, hematite, calcite, and glassy amorphous material (Table II-10). Diffractograms of the two fly ash samples are shown in Fig. II-8. Microscopic examination of fly ash under plane polarized-light reveals the presence of opaque and transparent glassy spherules, large ir-

e II--10. X-ray diffraction results of the fly ash types, scrubber sludges, and their mixtures.

Sample Type	Sample Code	Phases Identified	Peak Intensity Ratios * SO_3/Q_z	SO_3/SO_4	SO_3/CO_3	Remarks
Elrama Scrubber Sludge	-	gypsum,Ca-sulphite, quartz,hematite, magnetite,mullite	3.7	2.5	-	Moist sample analyzed. See diffraction pattern (Fig. II-21)
Conesville Scrubber Sludge	-	Ca-sulphite,gypsum, (no quartz and fly ash)	-	15.5	-	Moist sample analyzed. See diffraction pattern (Fig. II-21)
Elrama Fly Ash	-	quartz,mullite, magnetite,hematite,calcite	(Mu/Q_z) 0.7	(Mu/Mag) 1.6	(Q_z/Mag) 2.5	Diffraction pattern (Fig. II-8)
Conesville Fly Ash	-	quartz,mullite, magnetite, hematite,calcite	(Mu/Q_z) 0.7	(Mu/Mag) 0.8	(Q_z/Mag) 1.1	Diffraction pattern (Fig.II-8) Note higher background than Elrama fly ash indicating presence of more amorphous material.
Elrama Coarse 1:1	(E2C1)	Ca-sulphite,calcite,quartz,ettringite,(no gypsum peak),mullite, magnetite,hematite	0.8	-	1.0	Upon exposure to seawater, the sample diffraction pattern shows no change except for an increase in peak sharpness. (Fig. II-22,23)
Elrama Coarse 3:1	(E2C3)	Ca-sulphite,quartz, calcite,mullite, ettringite,hematite, magnetite(no gypsum)	0.3	-	0.9	Upon exposure to seawater, the value ISO_3/ICO_3 ratio decreases (see Fig.II-22,33). Note higher background than in E2C1.
Elrama Fine 1:1	(E3F1)	Ca-sulphite,ettringite,quartz mullite,vw SO_4 peak, hematite,magnetite	-	-	-	Diffraction pattern (Fig. II-22)
Conesville Fine 1:1	(C4F1)	Ca-sulphite,quartz (no gypsum),ettringite	2.6	-	-	Diffraction pattern (Fig. II-26)
Conesville Fine 3:1	(C4F3)	Ca-sulphite,quartz (no gypsum), ettringite	1.0	-	-	Diffraction pattern (Fig. II-26)
Grey Inclusions in Elrama 1:1	(E1C1)	Gypsum,Ca-sulphite quartz,calcite	-	0.94	-	Upon exposure to seawater the sulphite peaks become stronger with a higher SO_3/SO_4 peak intensity ratio. (Fig.II-28)
White Inclusions in Elrama Coarse 1:1	(E1C1)	$Ca(OH)_2$,calcite, quartz	-	-	-	Upon exposure to seawater, strong brucite peaks are observed. $Ca(OH)_2$ & calcite go into solution (Fig.II-30)

* The following x-ray reflections were used for peak intensity ratio calculations: gypsum - (020) at 7.61 Å; $CaSO_3 \frac{1}{4}H_2O$ - 100% intensity reflection at 3.16 Å (no (hkl) indices available); quartz - (100) at 4.26 Å; magnetite - at 1.485 Å; mullite - (110) at 5.35 Å; calcite - calcite - at 3.04 Å.

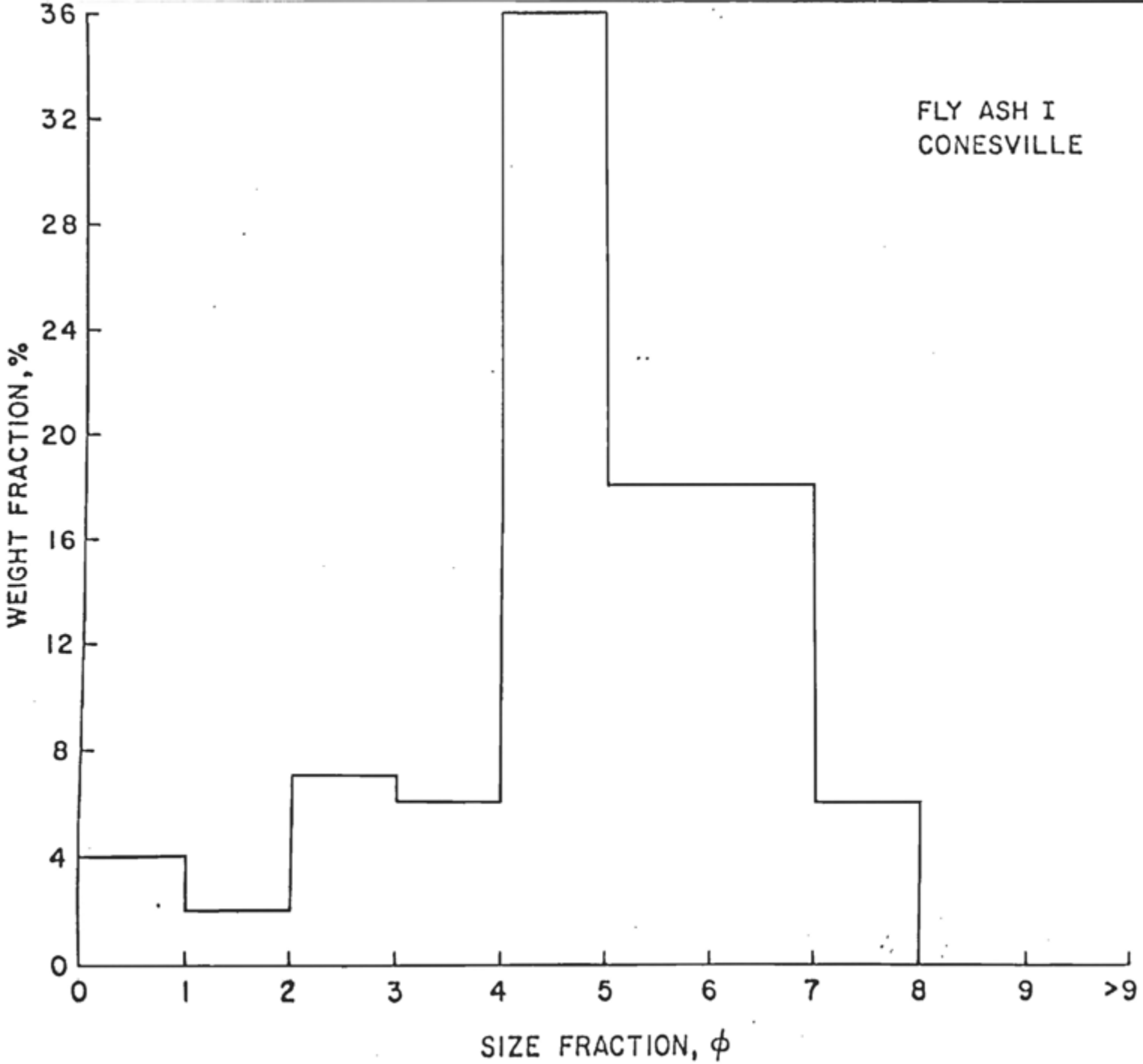

Figure II-4. Frequency distribution of Conesville fly ash.

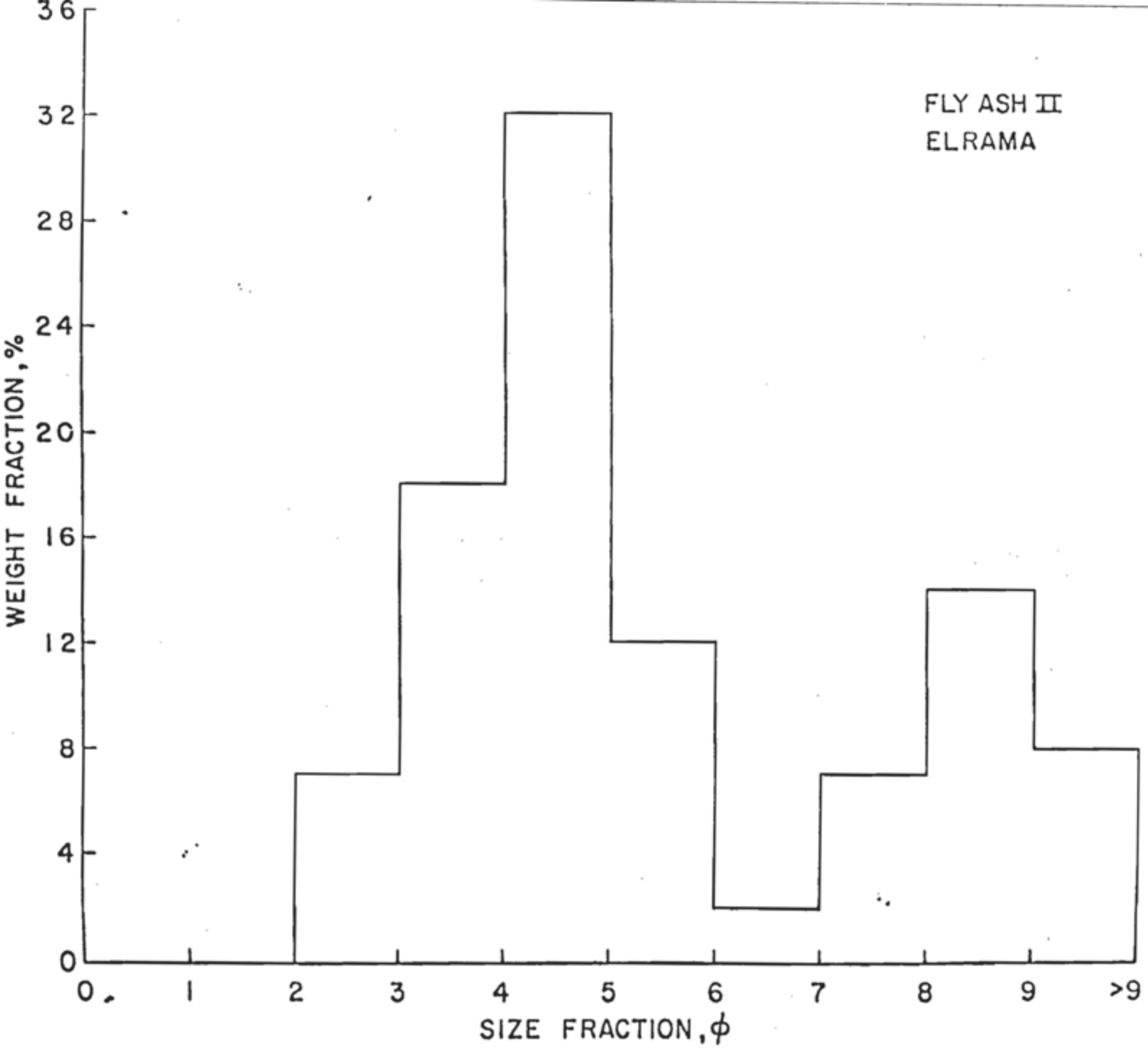

Figure II-5. Frequency-size distribution of Elrama fly ash.

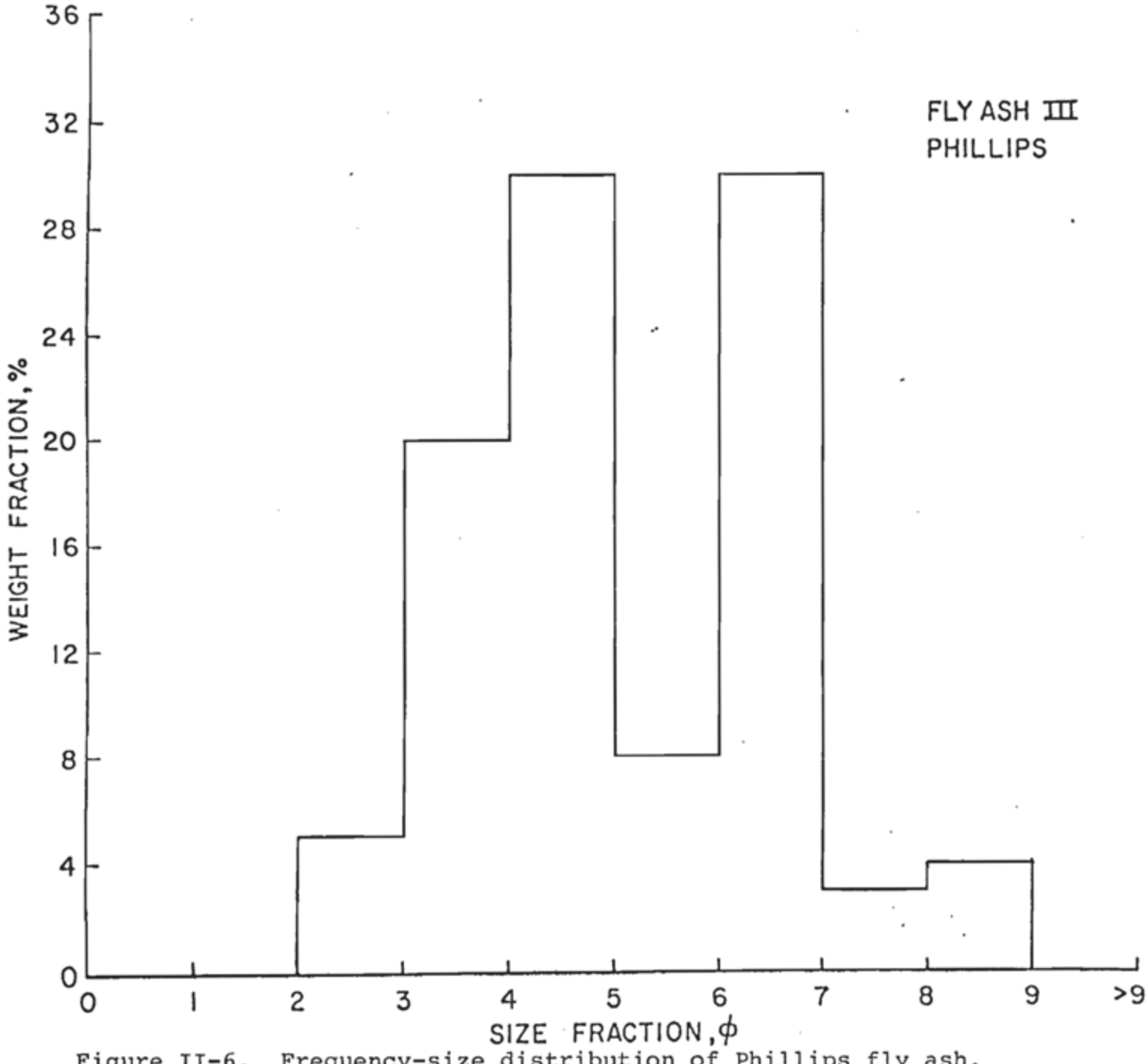

Figure II-6. Frequency-size distribution of Phillips fly ash.

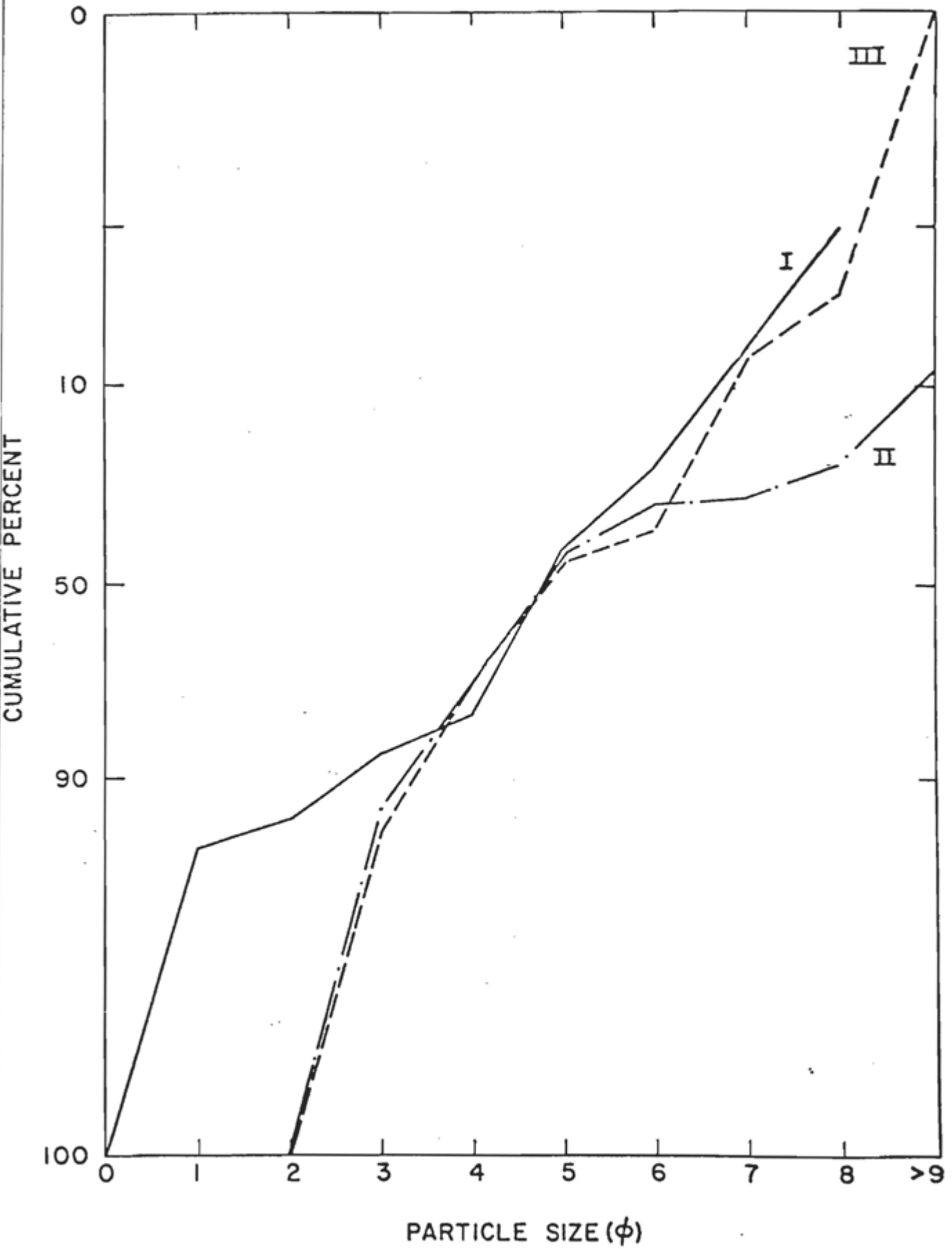

Figure II-7. Cumulative percent particle size distributions for Conesville, Elrama, and Phillips fly ash types.

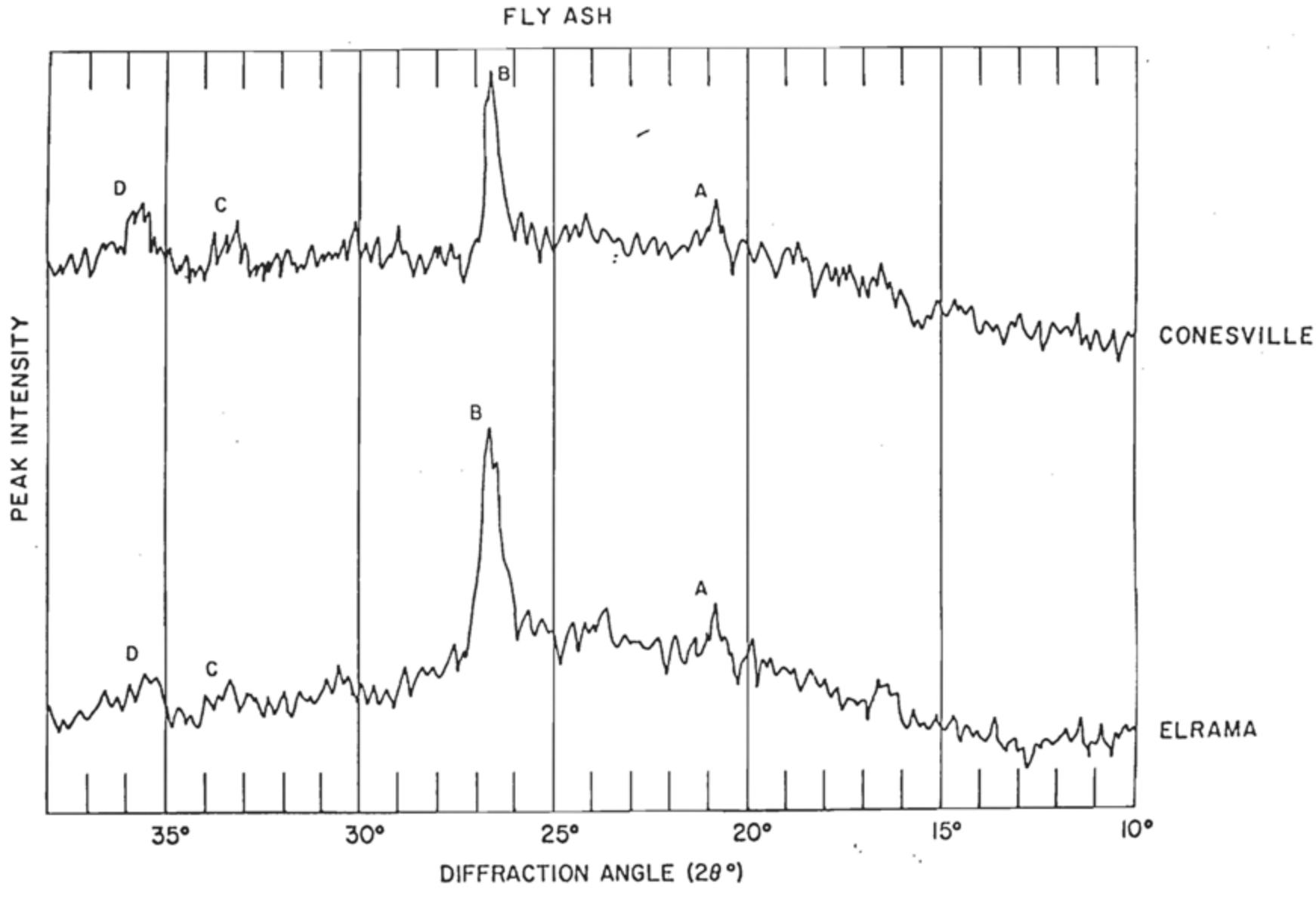

Figure II-8. X-ray diffractograms of Conesville and Elrama fly ash types.

regular opaque particles, and birefringent minerals. Under reflected-light, most of the opaque spherules exhibit a grey lustre characteristic of magnetite. Some show a characteristic reddish-brown lustre of hematite. The glassy spherules are isotropic under crossed nicols. The birefringent minerals were identified as quartz and mullite. Calcite was easy to identify based on its high birefringence and rhombohedral cleavage. Light micrographs of the three fly ash types examined under transmitted and reflected light are shown in Fig. II-9-14.

Scanning electron microscopic examination of fly ash reveals some interesting features (Fig. II-15 to II-20). The large variation in particle size is quite evident from the electron micrographs. They also show variation in particulate morphology from one fly ash sample to another. Often small spherules are fused onto the surface of larger spherules. Large hollow spherules with infillings of smaller spherules having varying particle sizes are quite common. Also note the pitted porous surface of the large spherules. The vesicular character of the fly ash spherules may be the main determinant, in terms of reactive surface area, in controlling the fly ash reactivity.

X-ray diffractograms of fly ash samples (Fig. II-8) exhibit higher background than that observed for scrubber sludges and mixes (Fig II-21 to II-23). This can be attributed to the presence of large amounts of amorphous

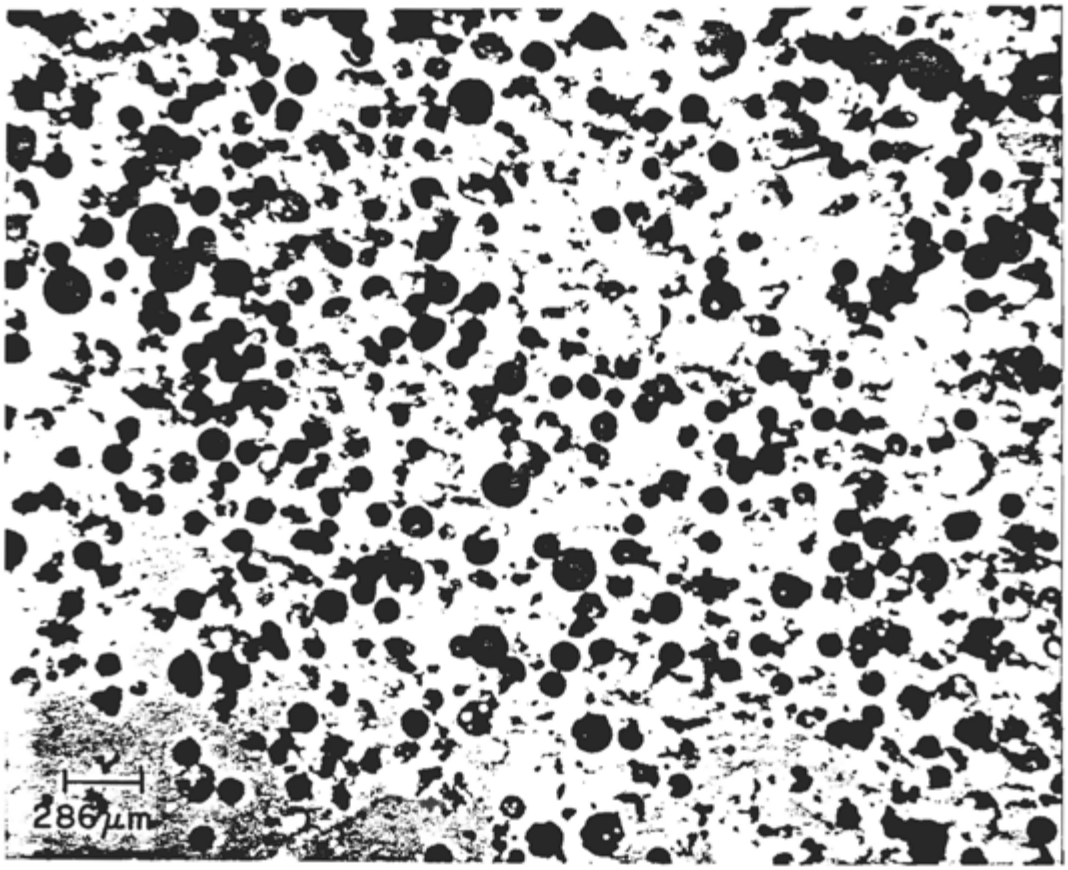

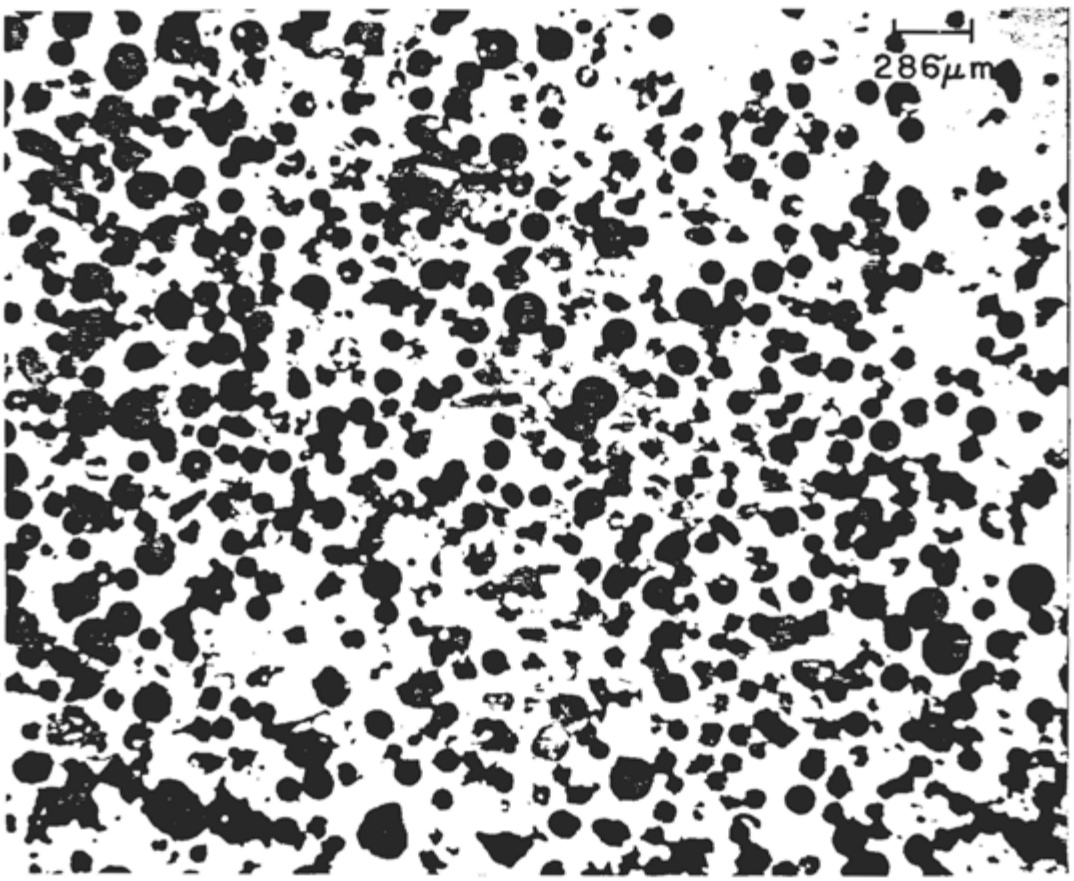

Figure II-9. Light micrographs of Conesville fly ash in transmitted and reflected light.

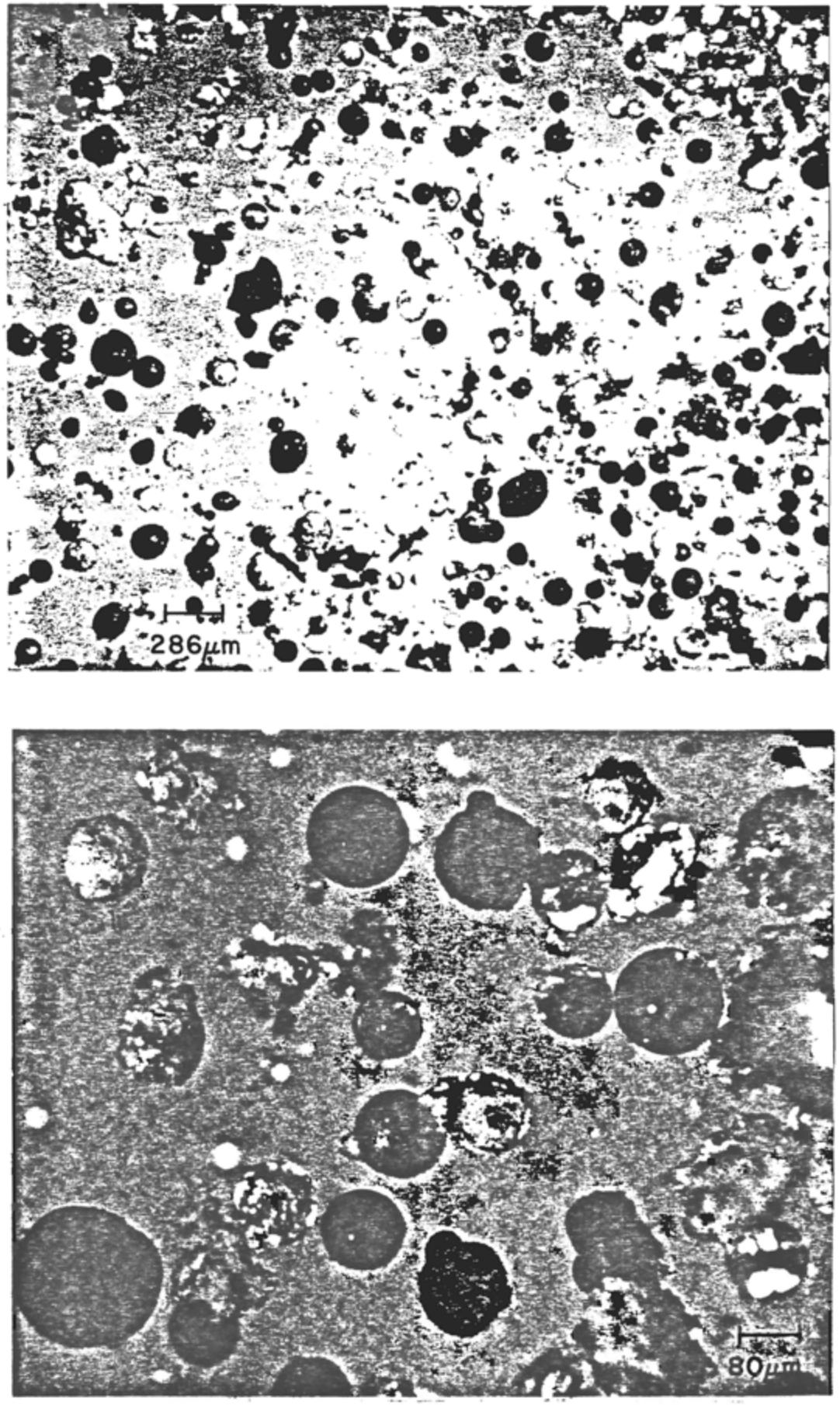

Figure II-10. Light micrographs of Conesville fly ash in transmitted and reflected light.

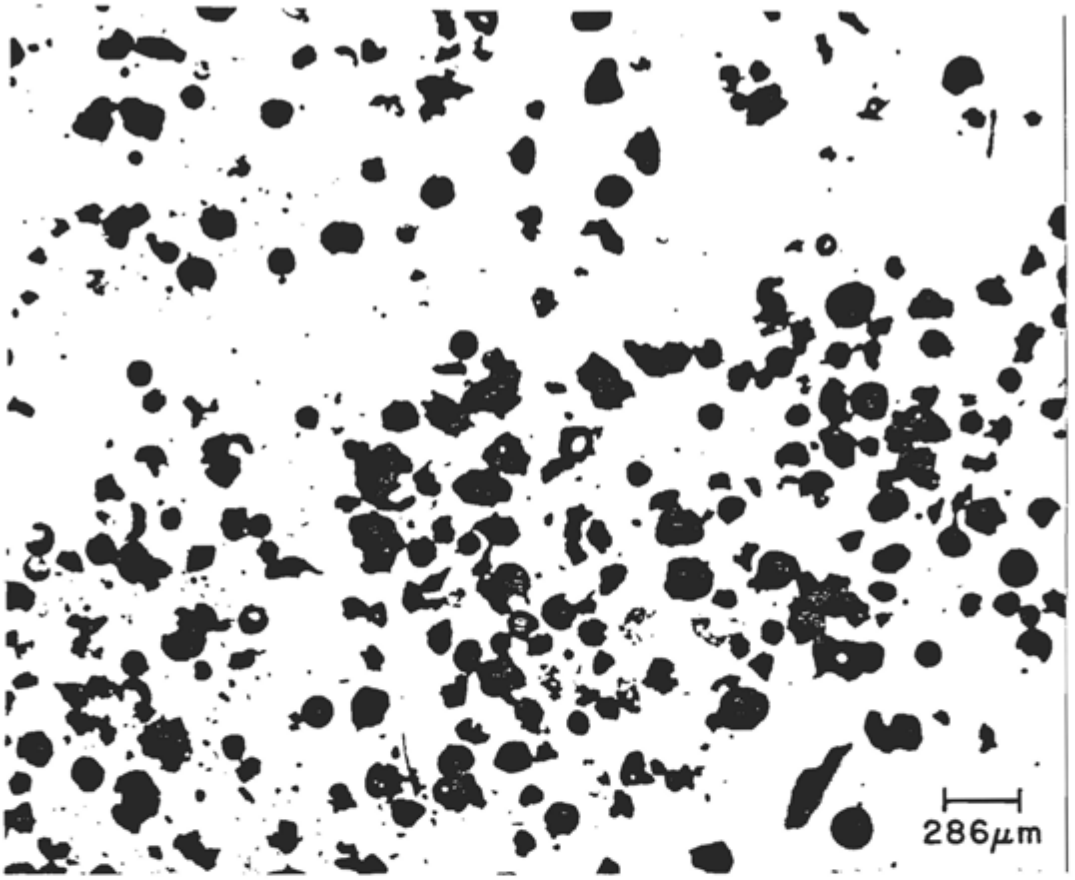

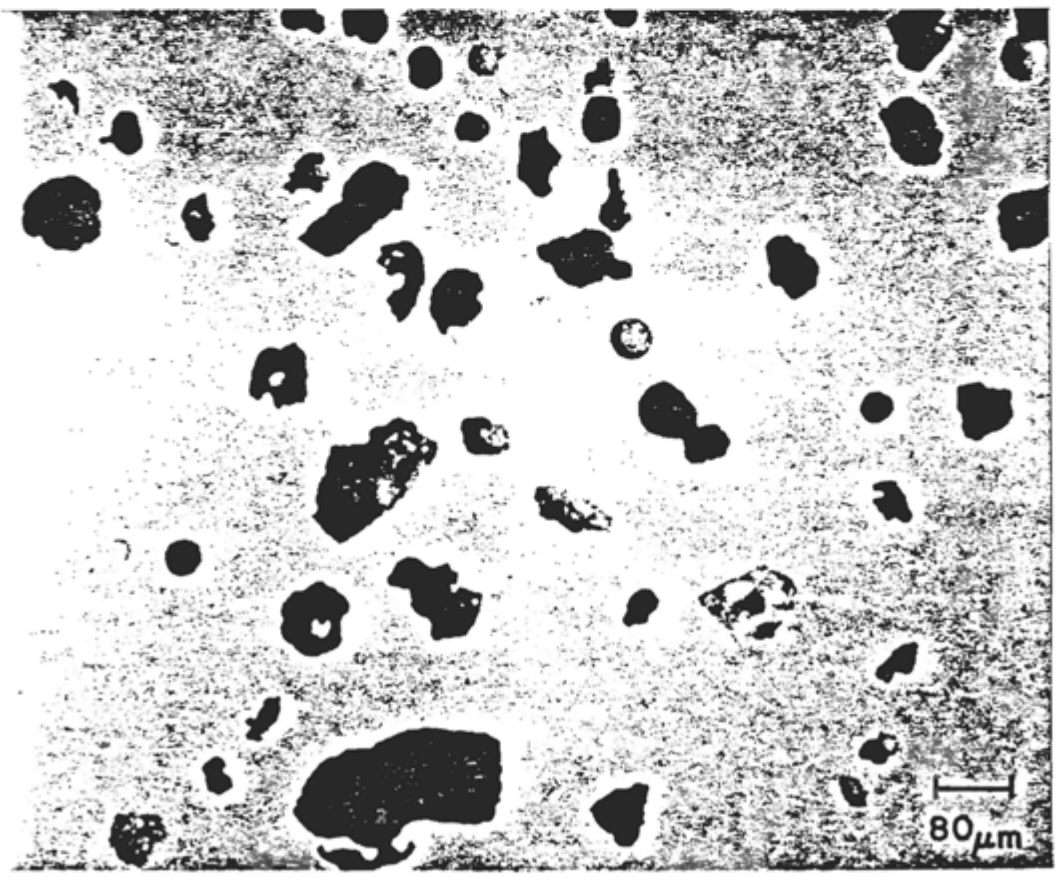

Figure II-11. Light micrographs of Elrama fly ash in transmitted plane polarized light.

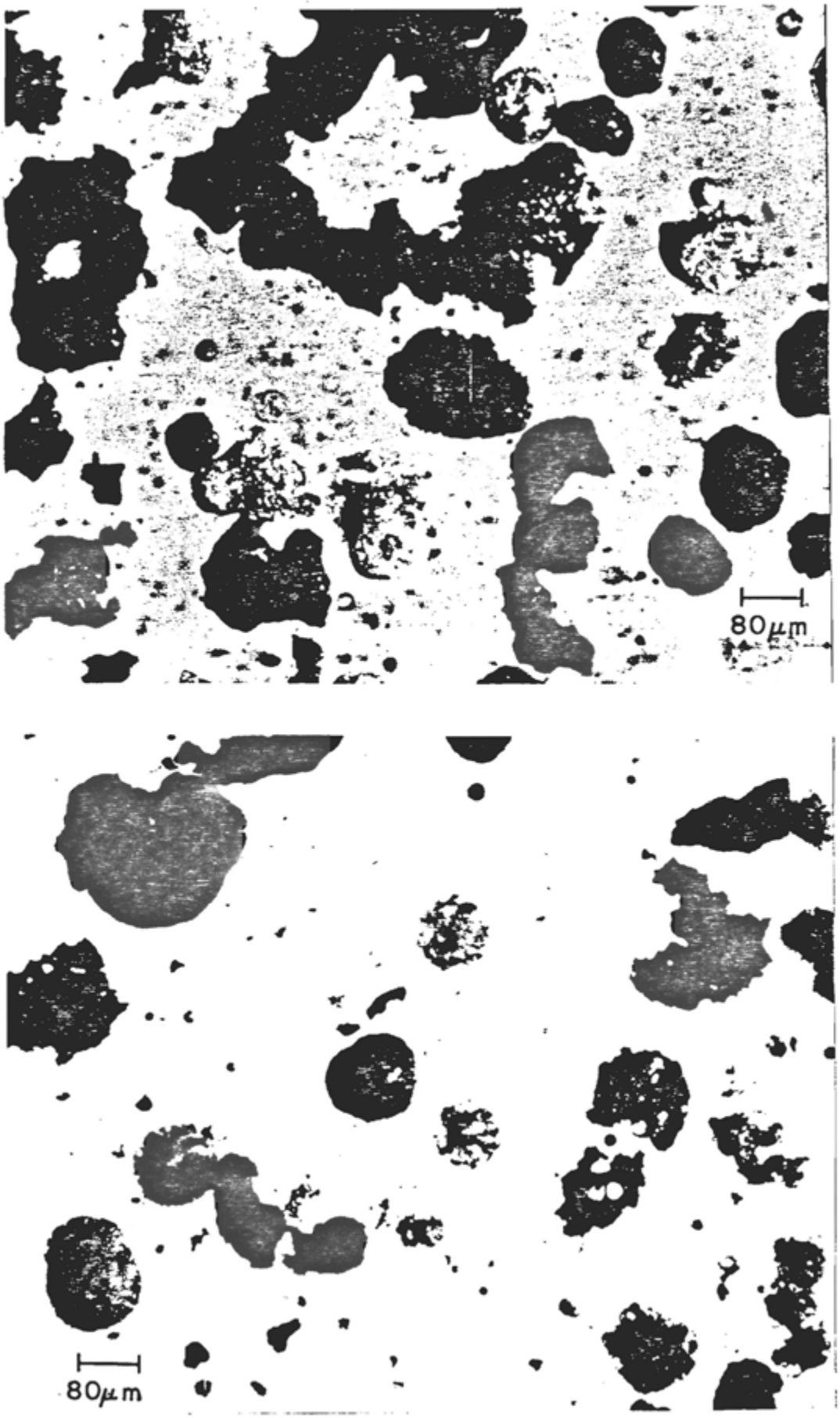

Figure II-12. Light micrographs of Elrama fly ash in transmitted and reflected light.

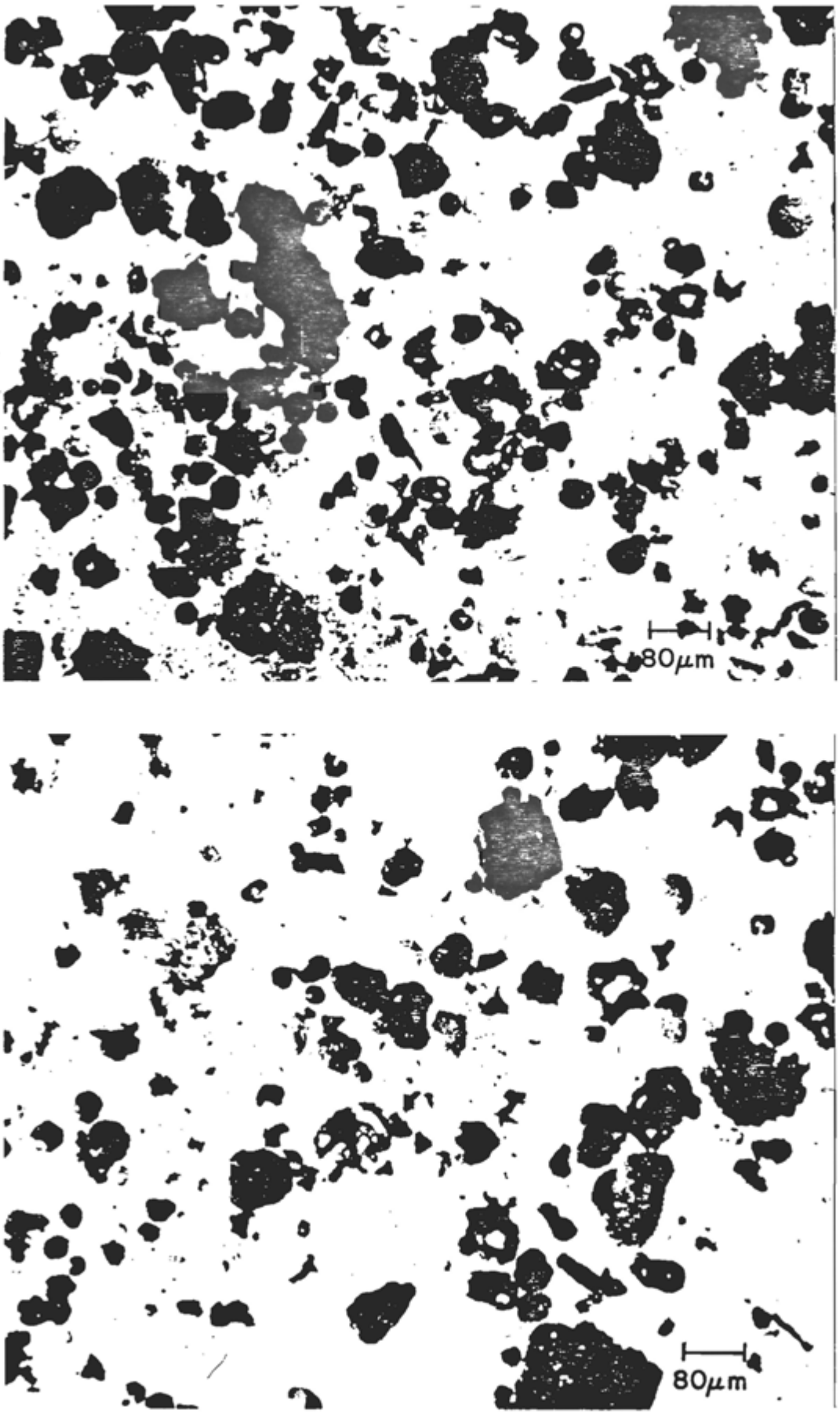

Figure II-13. Light micrographs of Phillips fly ash in transmitted and reflected light.

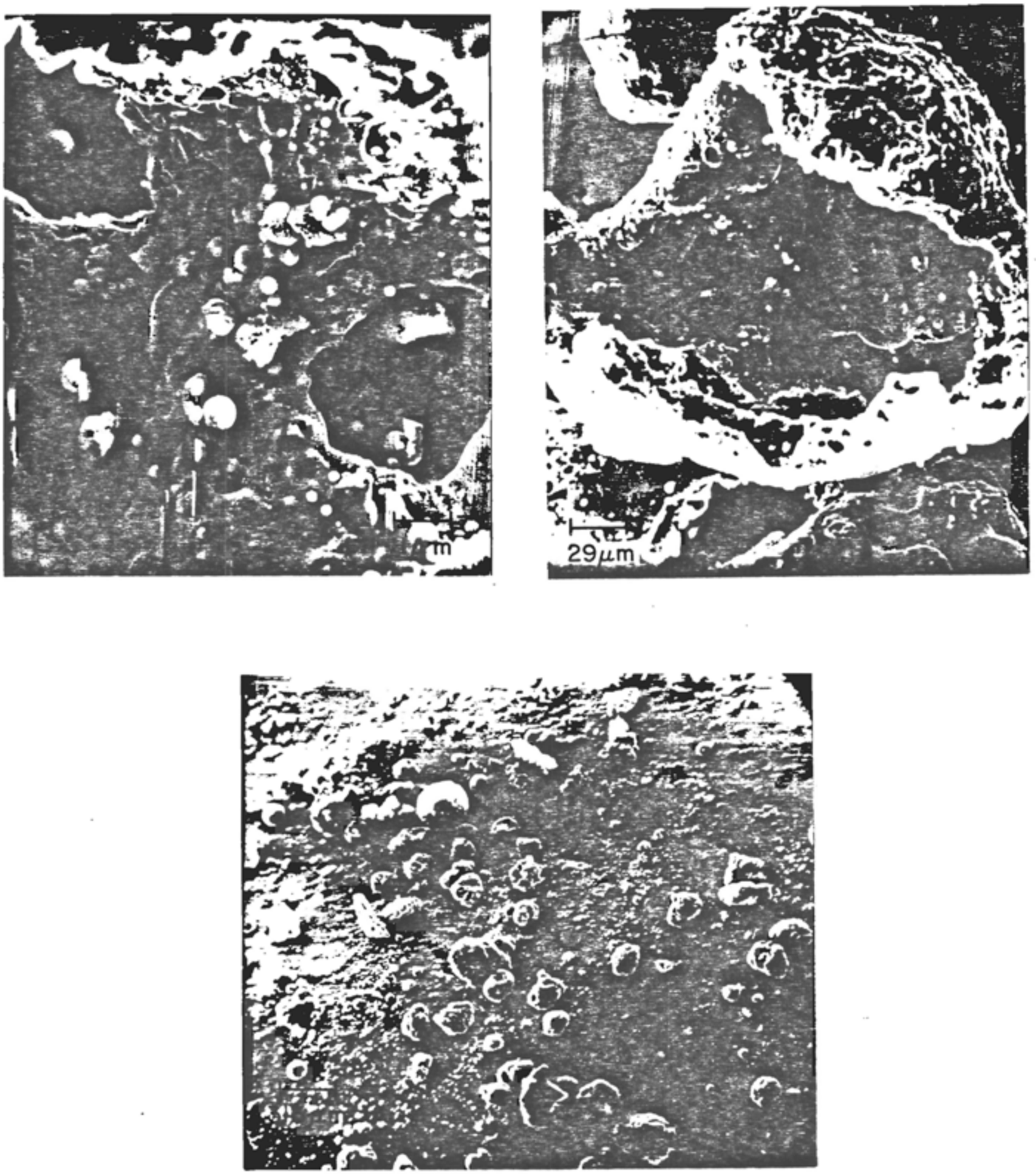

Figure II-17. Electron micrographs of Elrama Fly Ash.

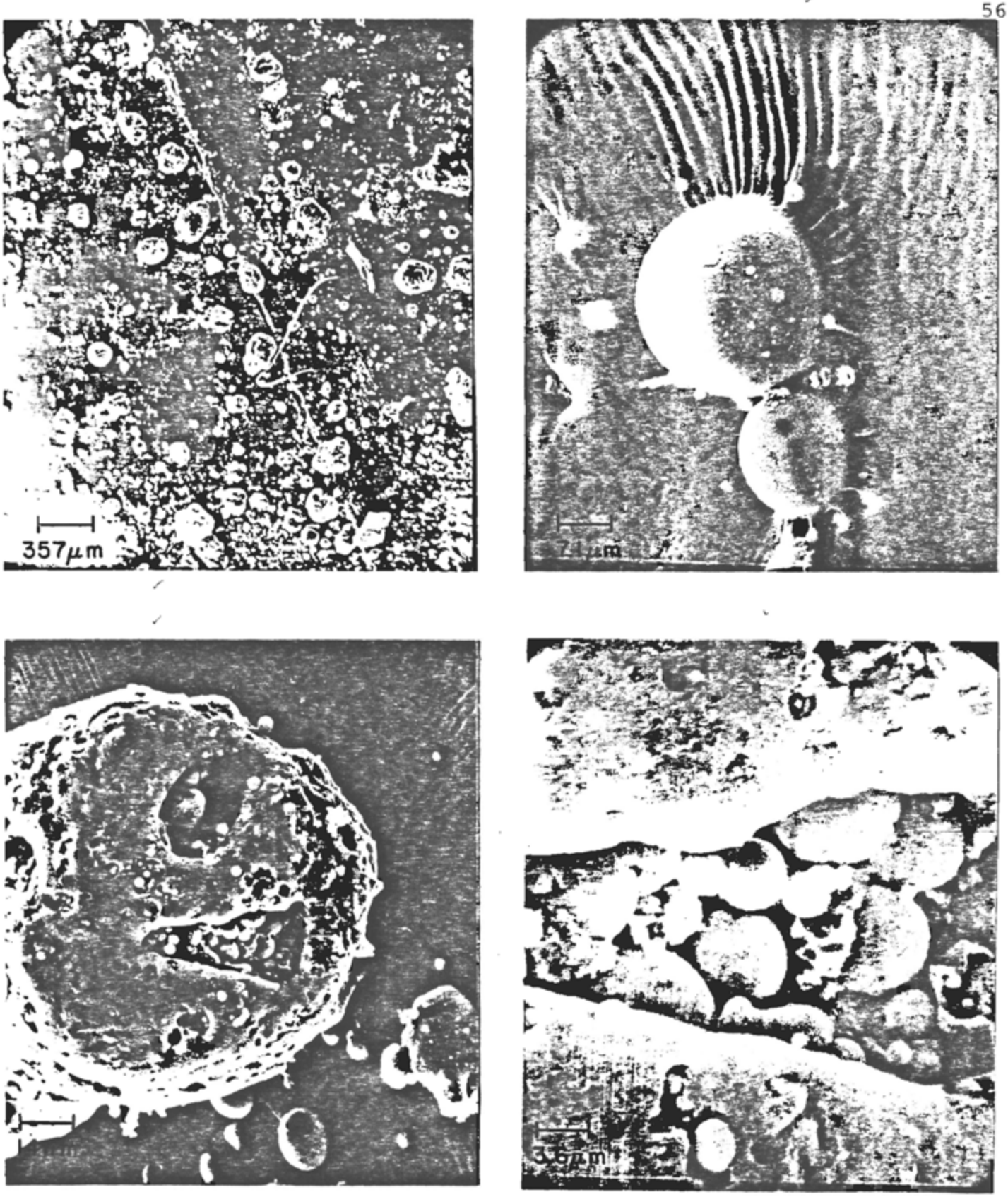

Figure II-18. Electron micrographs of Elrama Fly Ash.

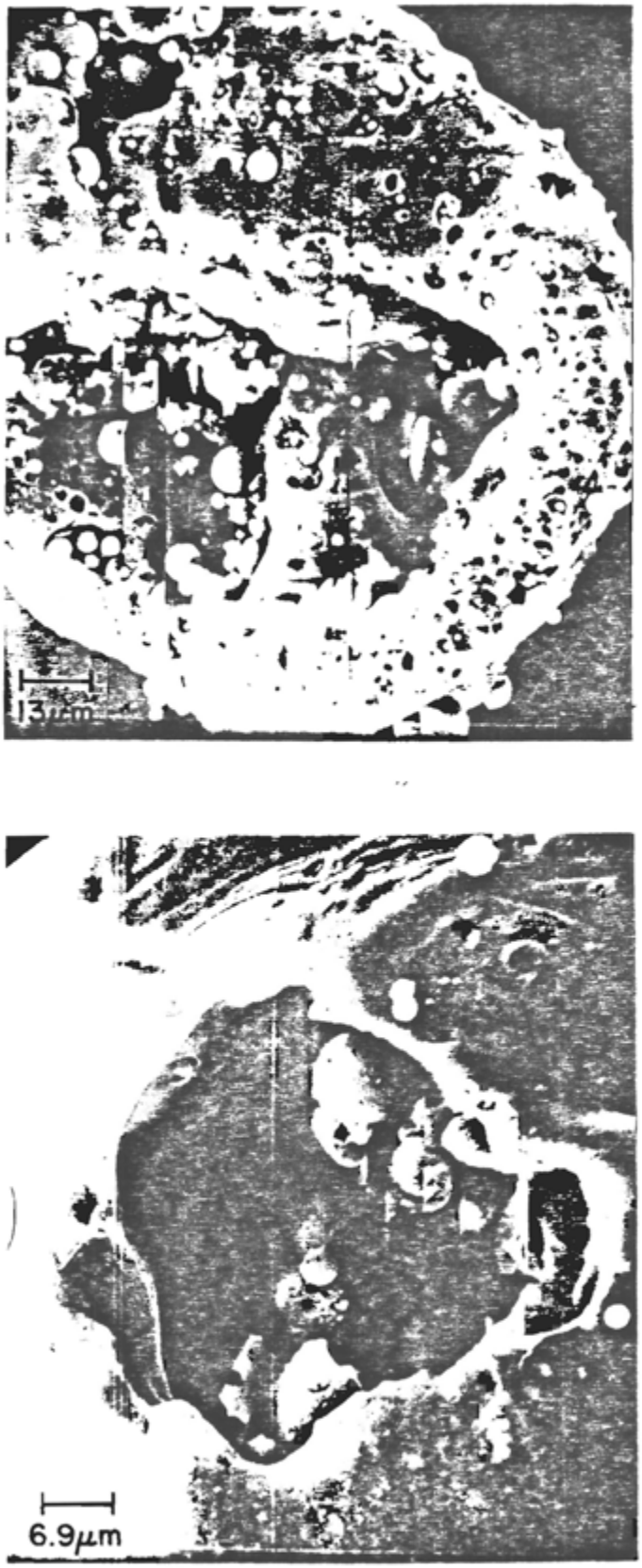

Figure II-19. Electron micrographs of Phillips Fly Ash.

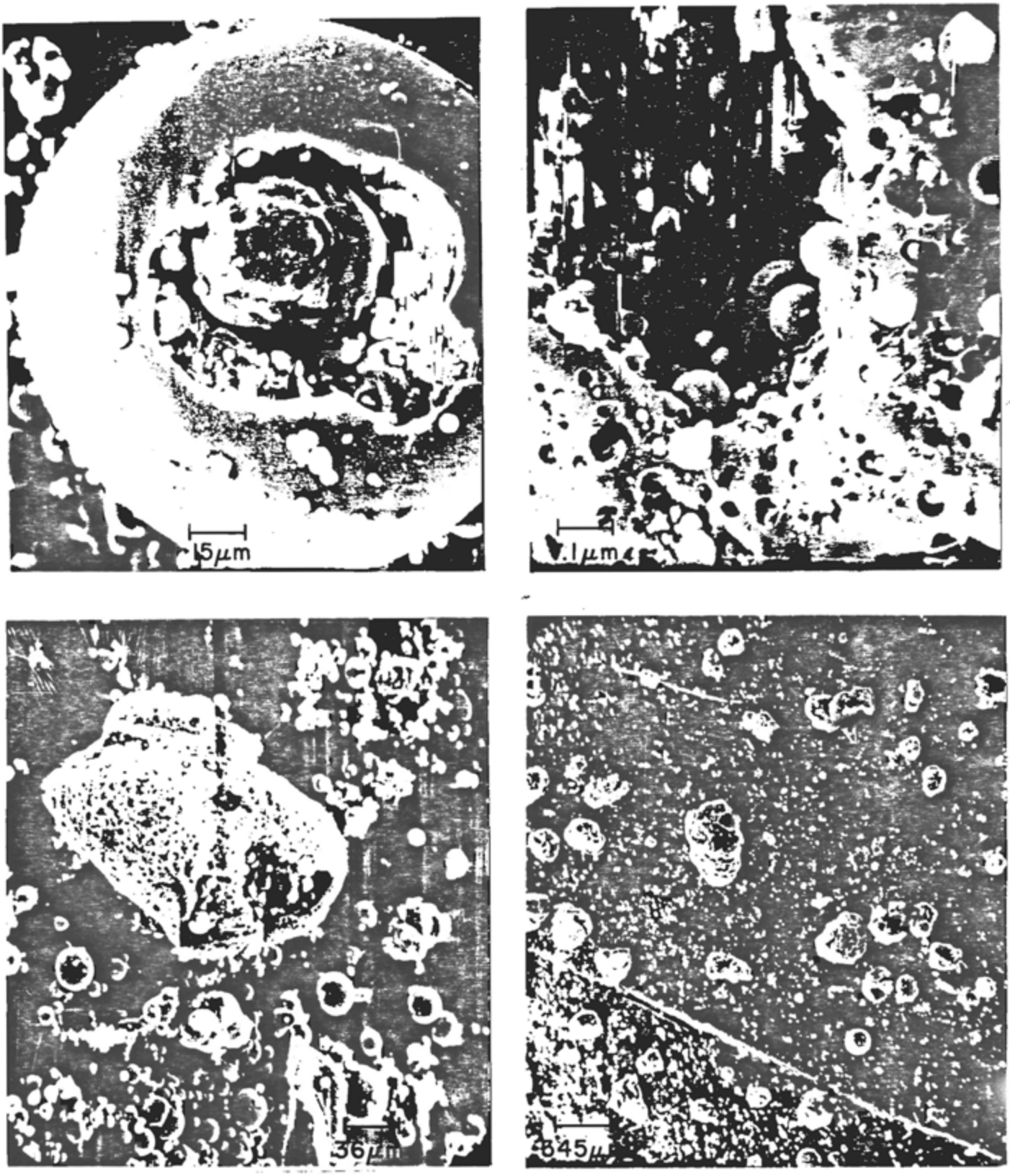

Figure II-20. Electron micrographs of Phillips Fly Ash.

material. As discussed earlier, microscopic examination of fly ash under crossed-nicols reveals the presence of transparent glassy spherules that exhibit isotropic optical properties. It is interesting to note that Conesville fly ash shows a higher background than Elrama fly ash (Fig. II-8). This could very well reflect a greater amount of amorphous material in Conesville fly ash.

The presence of mullite and quartz phases reflects the aluminosilicate and silica composition of the non-amorphous fly ash constituents, respectively. Hematite and magnetite reflect the metallic composition of the fly ash. The large, irregular, opaque particles, shown in the light micrographs of fly ash samples (Fig. II-9 to II-14), are basically carbonaceous and reflect the carbon composition of fly ash. Calcite is present in trace amounts and does not contribute significantly to the total carbon content of fly ash. Chemical analysis of fly ash shows elemental carbon to be less than 2% by weight.

The magnetite reflection at 1.485 Å was used for quartz/magnetite and mullite/magnetite intensity ratio calculations. Table II-10 shows that the mullite/quartz intensity ratio of the two fly ash samples is identical. This indicates that the aluminosilicate/silica composition of the non-amorphous non-metallic component of the two fly ash samples is quite similar. However, the mullite/magnetite and quartz/magnetite peak intensity ratios are

higher for Elrama fly ash by a factor of two (Table II-10). Since the mullite/quartz peak intensity ratio is similar for both fly ash types, the implication is that the magnetite content of Elrama fly ash is lower than that of Conesville fly ash. Microscopic examination under transmitted and reflected light reveals a larger number of magnetitic opaque spherules in Conesville fly ash. Elemental composition of fly ash samples confirms that Conesville fly ash has twice as much elemental iron than Elrama fly ash (Table II-9).

b. Elrama scrubber sludge. The mineralogical composition consists of gypsum, $CaSO_3 \cdot \frac{1}{2}H_2O$, quartz, hematite, magnetite, mullite, and traces of calcite (Fig. II-21). The presence of non-calcium-sulfur phases indicates that the scrubber sludge contains appreciable amounts of fly ash. Fly ash contamination of Elrama scrubber sludge is also evident from its dark grey color. Chemical analysis shows that the non-acid soluble component (fly ash) to be approximately 43% by weight (Table II-7). On a dry weight basis, this corresponds to a fly ash/scrubber sludge ratio of 1:1.3.

In order to obtain information on the relative amounts of sulfite and sulfate present in the sludge, peak intensity ratios were calculated. The 100% intensity reflections of $CaSO_3 \cdot \frac{1}{2}H_2O$ at 3.16 Å and (020) gypsum at 7.61 Å were used for calculating their peak intensity ratios. A peak intensity ratio of 2.5 is calculated for I_{SO_3}/I_{SO_4} (Table II-10). Based on the chemical analysis

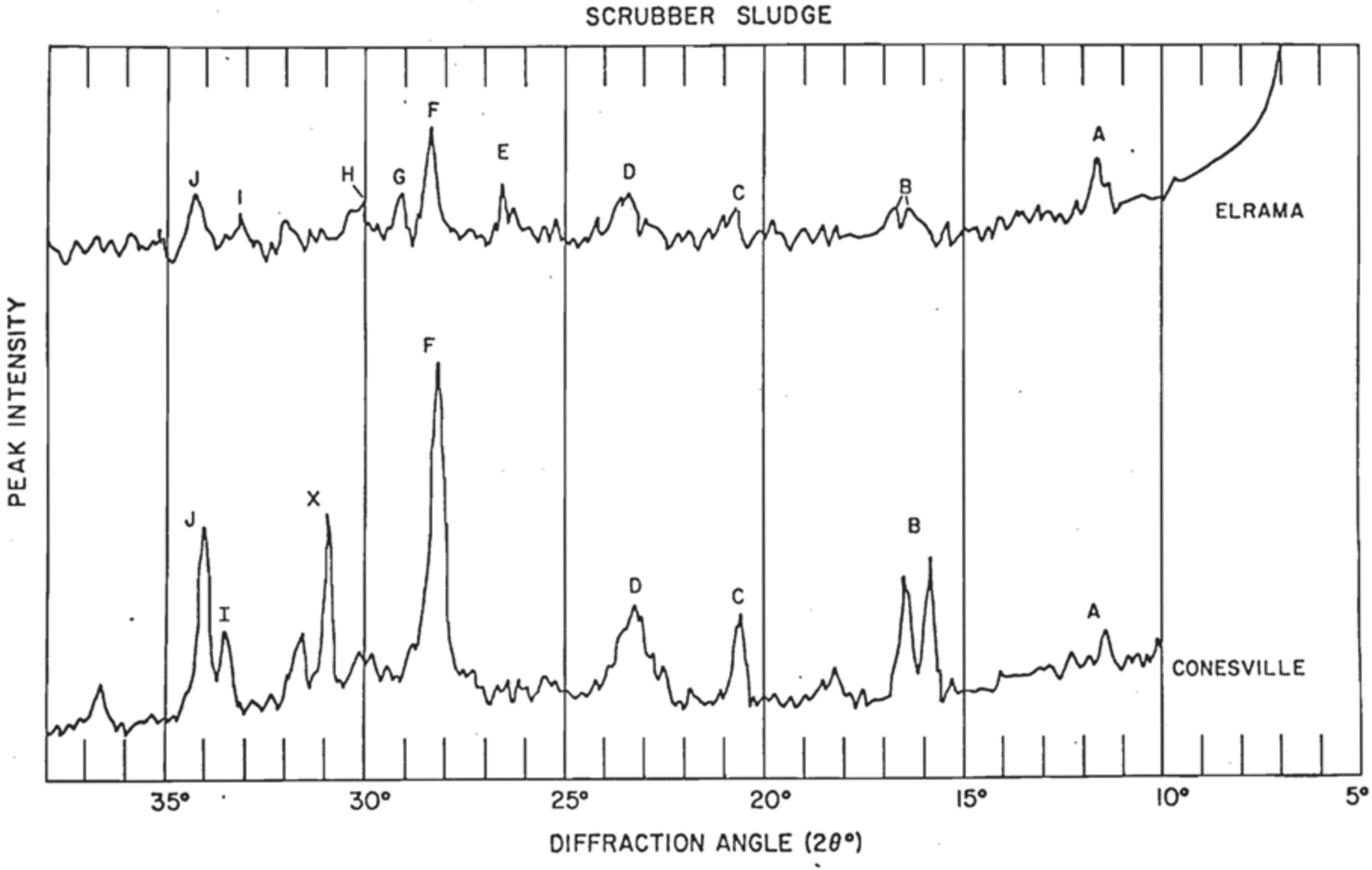

Figure II-21. X-ray diffractograms of scrubber sludges derived from Elrama and Conesville plants. A = gypsum (020); B,D,F,H,I,J = $CaSO_3 \cdot 1/2H_2O$; C = gypsum ($12\bar{1}$); E = quartz (101); G = gypsum ($14\bar{1}$); X = gypsum (002).

given in Table II-8, this calculated peak intensity ratio corresponds to a $CaSO_3 \cdot \frac{1}{2}H_2O$/gypsum compositional ratio of approximately 11.5. Using the (100) quartz reflection at 4.26 Å, ISO_3/Iquartz is calculated to be 3.7. Since quartz is associated with fly ash, a comparison of ISO_3/Iquartz ratios of different sludges and mixes having varying sludge/fly ash compositions can provide some information on the variation in the relative amounts of the two end components.

c. Conesville scrubber sludge. Conesville scrubber sludge consists of $CaSO_3 \cdot \frac{1}{2}H_2O$ and gypsum. No fly ash mineral phases were observed on the x-ray diffractogram (Fig. II-21). Chemical analysis shows that the non-acid soluble component of Conesville sludge is less than 3% by weight (Table II-8). $CaSO_3 \cdot \frac{1}{2}H_2O$ is the dominant mineral phase. The calculated value of ISO_3/ISO_4 is 15.5 (Table II-10). Comparison of this value with that calculated for Elrama scrubber sludge indicates that the $CaSO_3 \cdot \frac{1}{2}H_2O$ content in Conesville sludge is approximately 71 % by weight. Chemical analysis given in Table II-8 shows that the sulfite content in Conesville sludge is 79% by weight and gypsum content is practically negligible.

d. Elrama mix E2C1. X-ray diffraction analysis shows that this mix consists of $CaSO_3 \cdot \frac{1}{2}H_2O$, calcite, quartz, ettringite, mullite, magnetite, and hematite (Fig. II-22). No gypsum reflection was observed on the

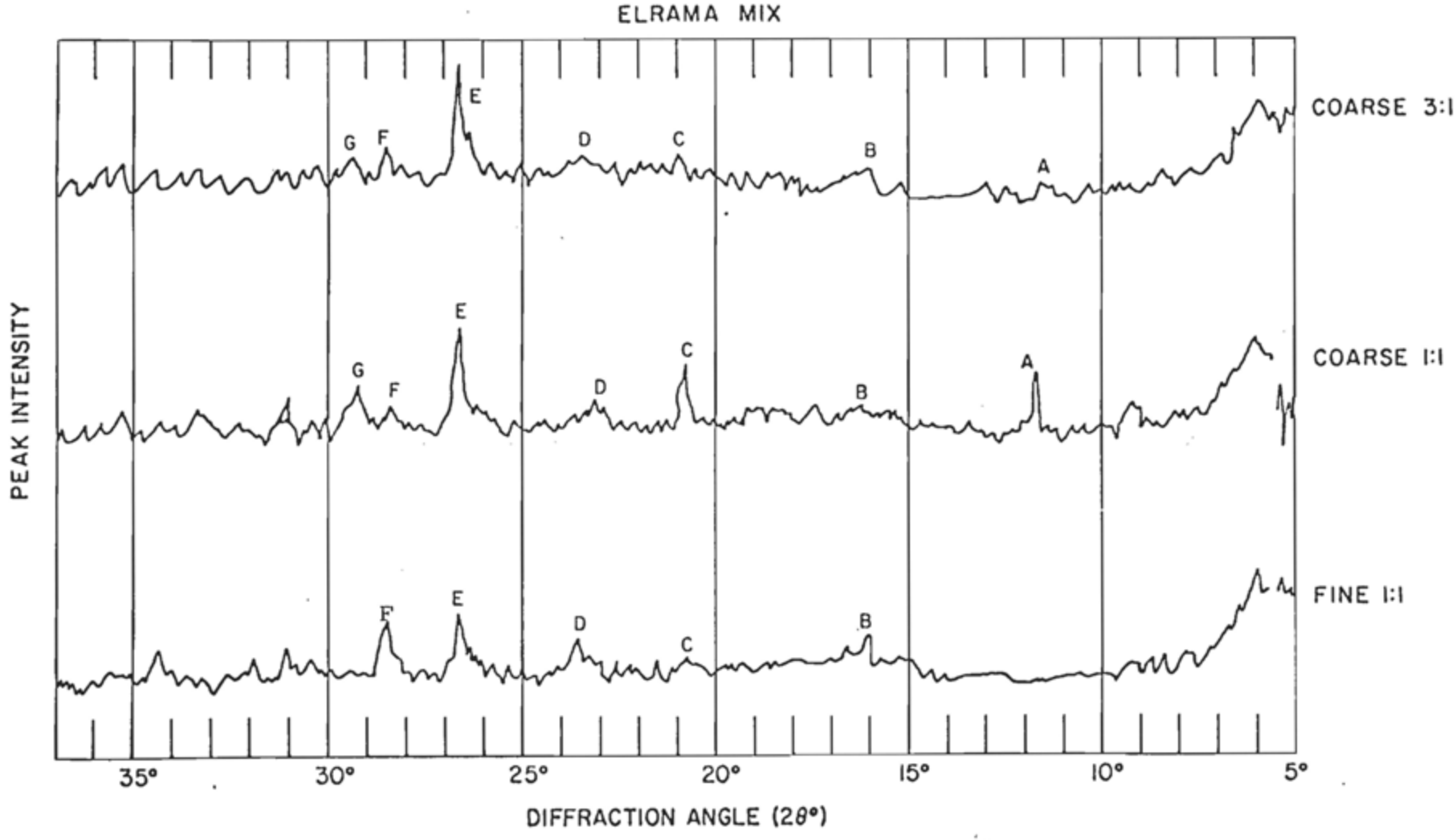

Figure II-22. X-ray diffractograms of Elrama mixes with coarse and fine lime as an additive. A = gypsum (020); B, D, F = $CaSO_3 \cdot 1/2H_2O$; C = gypsum ($12\bar{1}$); E = quartz (101); G = gypsum ($14\bar{1}$)

diffractogram. Ettringite, a hydrated calcium sulfo-aluminate, is present as a reaction product of the reactants present in fly ash and scrubber sludge. It is important to note that some of the mineral phases of the reactants are also present in the cured mix. Gypsum reflection, however, is not observed. This suggests that gypsum undergoes chemical transformation during the curing process and is used up in the formation of ettringite. The ISO_3/I_{quartz} and ISO_3/ICO_3 values are calculated to be 0.8 and 1.0, respectively. Calcite content reflects the amount of unreacted additive (limestone) present in the mix. A comparison of the ISO_3/Iquartz values of Elrama scrubber sludge and E2C1 shows that the scrubber sludge value is greater by a factor of 4. This is to be expected considering that quartz (fly ash) is present in scrubber sludge as a contaminant and in mix E2C1 as one of the main components. X-ray diffraction analysis of reacted mix powder resulting from the elutriate experiment shows no significant change in the diffraction pattern (Fig. II-23). However, a general increase in the sharpness of the peaks is observed. This may be a result of an increase in the crystallinity of some of the phases present. Scanning electron micrographs of mix E2C1 powder show fly ash and sludge particulates and nodules of fly ash coated with sludge (Figure II-24).

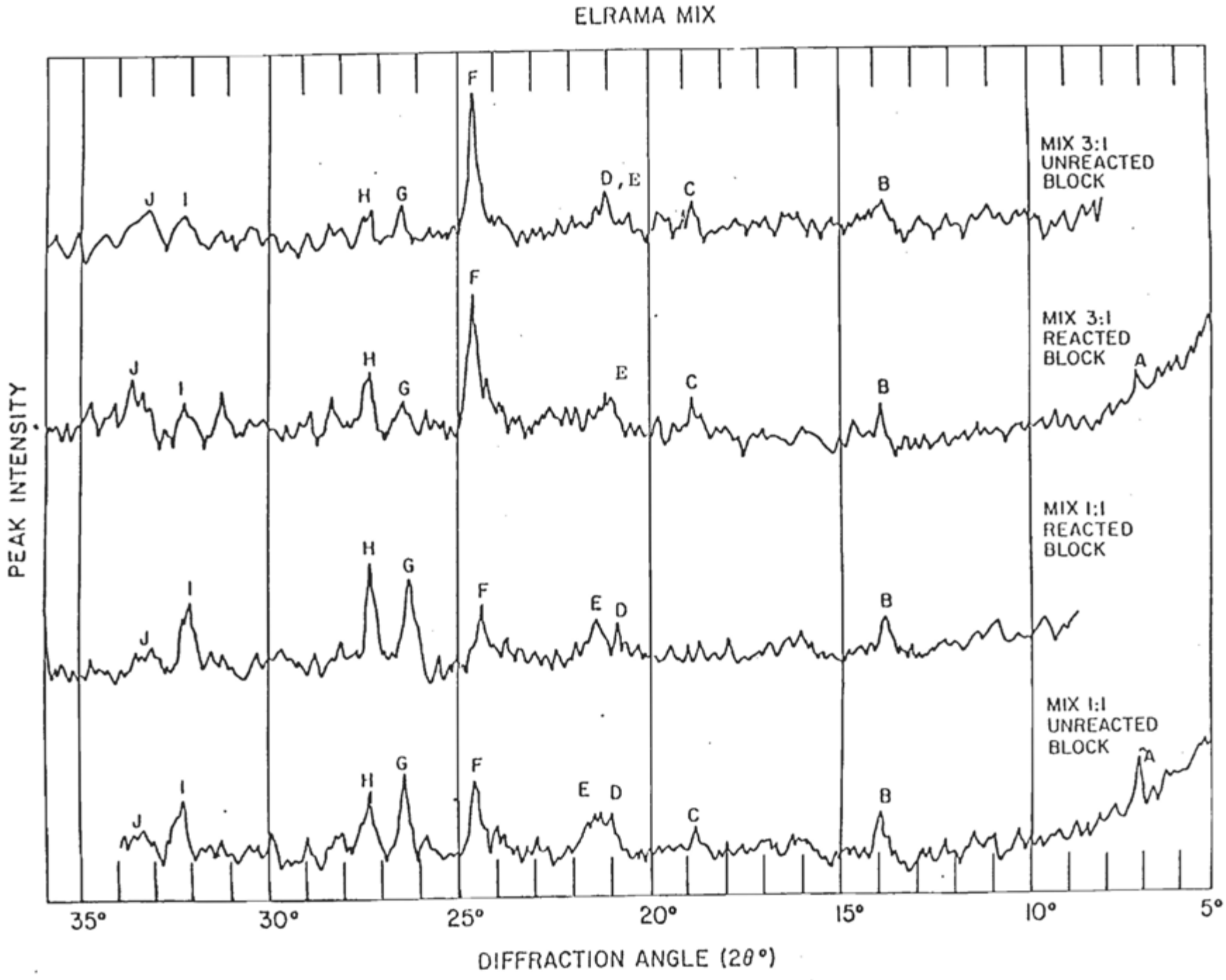

Figure II-23. X-ray diffractograms of unreacted and reacted Elrama mix E2C1. A = ettringite (100); B, E, G, I = $CaSO_3.1/2H_2O$; C = quartz (100); F = quartz (101); H = calcite (111); D = ettringite (114); J = (magnetite+hematite).

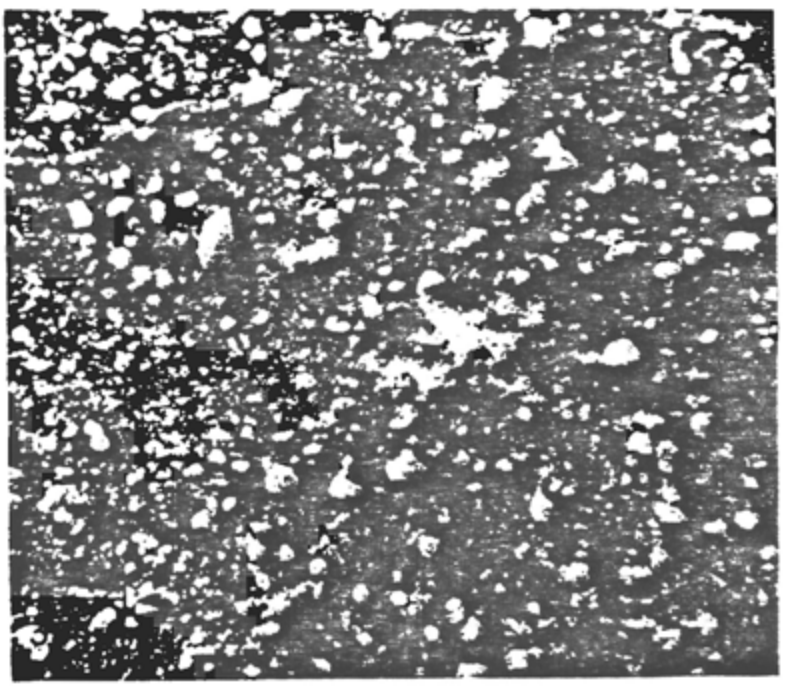

Figure II-24. Electron micrographs of Elrama mix E2Cl show scrubber sludge particulates and nodules of fly ash coated with sludge.

e. Elrama mix E2C3. This mix has the same mineralogy as mix E2C1. The elevated background observed for E2C3 mix as compared with E2C1 mix (Fig. II-22) may reflect a higher concentration of amorphous material. This is quite possible considering that the fly ash in mix E2C3 has a three-fold higher concentration. Based on light microscopic examination of the end components, we have found that all amorphous material present in the mix is associated with fly ash. The absence of the 100% intensity (020)gypsum reflection at 7.56 Å indicates that sulfate is used up in the precipitation of calcium sulfoaluminate. An ettringite reflection is observed on the diffractogram. The I_{SO_3}/Iquartz value is approximately three times smaller than that of mix E2C1. Since quartz represents the fly ash component of the mix, the smaller peak intensity ratio of mix E2C3 can be attributed to its higher fly ash content. The I_{SO_3}/I_{CO_3} value for mix E2C3 is quite similar to that of mix E2C1 (Table II-10). Mix E2C3,upon reaction with seawater,does not exhibit any significant change in the diffraction trace. The calculated I_{SO_3}/I_{CO_3} ratio, however, is smaller than that for unreacted mix E2C3. Electron micrographs of this mix powder are shown in Fig. II- 25. Nodular particulates of fly ash and sludge are quite common. Fly ash spherules embedded in cavities in sludge matrix are also observed.

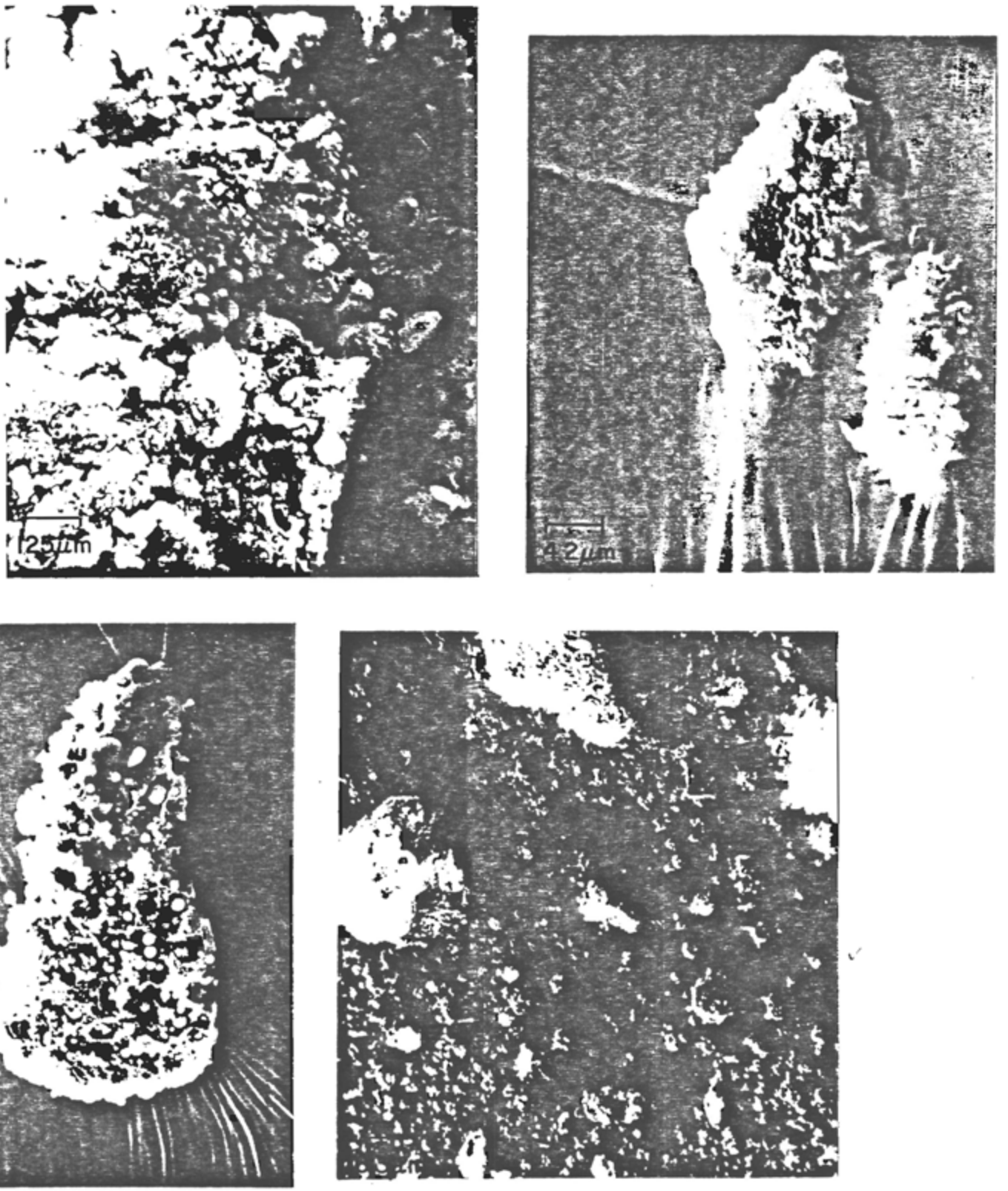

Figure II-25. Electron micrographs of Elrama mix E2C3 showing showing scrubber sludge particulates, nodules of fly ash coated with sludge, and fly ash spherules embedded in cavities in sludge matrix.

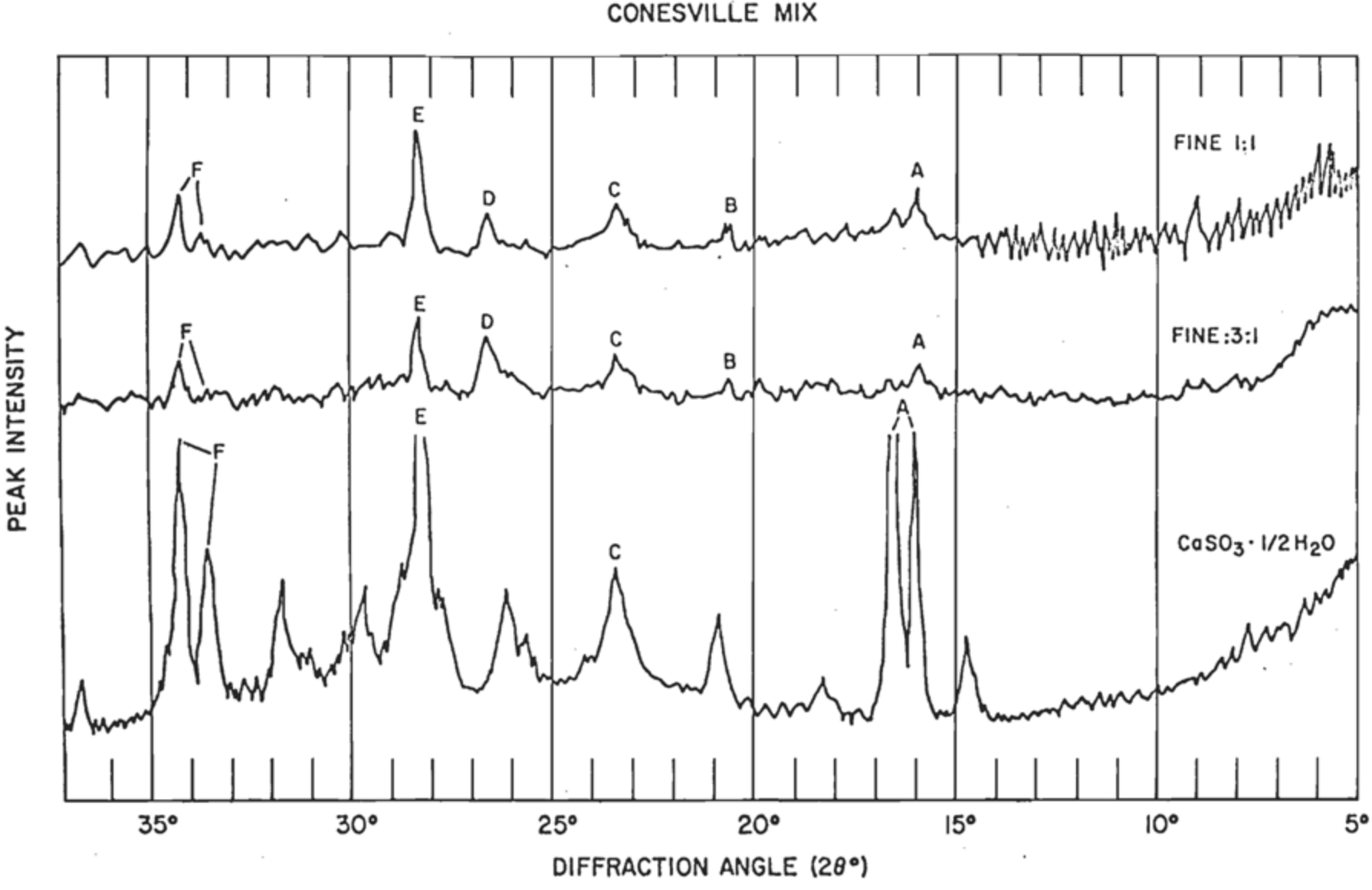

Figure II-26. X-ray diffractograms of Conesville mixes with fine lime as an additive. X-ray trace of pure $CaSO_3 \cdot \frac{1}{2}H_2O$ is also shown. All reflections are for $CaSO_3 \cdot 1/2H_2O$ except D at 3.33A for quartz (101).

can be attributed to its higher fly ash content. In most cases, x-ray diffraction results reflect the mineralogy of the reactant phases and the compositional ratio for a certain mix type. However, for a cured block, the mineralogy of the final reaction products should be different from that of the initial reactants present in an uncured block. Although the presence of ettringite, as one of the reaction products, confirms chemical reaction during the curing process, the presence of reactant phases in a cured block is suggestive of an incomplete chemical reaction.

i. Inclusion mineralogy of Elrama mix E1C1.

The very first set of Elrama mix E1C1 blocks developed internal cracks during the curing process. A number of the cracks observed originated at the location of the white inclusions in the blocks. Upon exposure to seawater, many of these blocks fell apart along the stress cracks.

In order to determine the factors that caused block failure, a detailed mineralogy of the inclusions was carried out on the unreacted and reacted blocks. Sections of an unreacted and a reacted block are shown in Fig. II-27. Grey inclusions were extracted from unreacted and reacted block surfaces and analyzed by x-ray diffraction. Table II-10 shows that the mineralogy consists of gypsum, $CaSO_3 \cdot \frac{1}{2}H_2O$, quartz, and calcite. Mineralogy of the grey

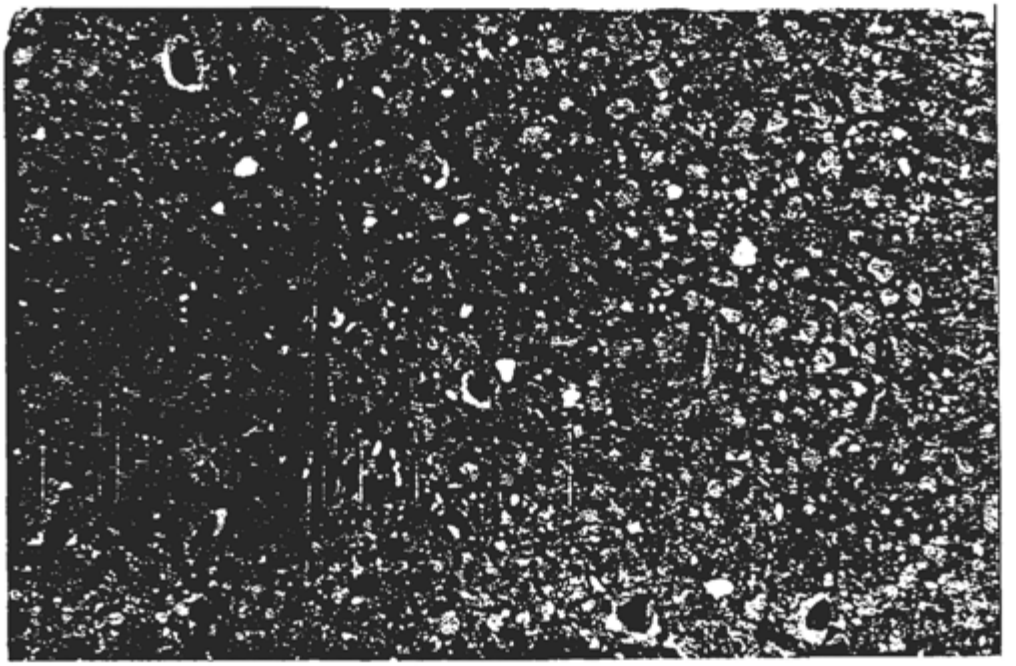

Figure II-27. Sections of Elrama block (ElCl) before (top) and after (bottom) exposure to seawater. The effect of seawater is quite obvious from the weathered surface of the reacted block. The holes represent grey and white inclusions extracted for x-ray mineralogy.

inclusions in reacted block is basically the same, except for an increase in the SO_3/SO_4 intensity ratio (Fig. II-28).

The mineralogical composition of the white inclusions in unreacted block consists of portlandite ($Ca(OH)_2$), calcite, and quartz. In the reacted block, however, the calcite and portlandite phases are absent and strong brucite peaks develop as shown on the diffractogram in Fig. II-29. This indicates that $Ca(OH)_2$ reacts with Mg^{2+} present in seawater to form brucite. Dissolution of portlandite gives rise to highly alkaline conditions in the immediate environment. Brucite is known to form under high pH conditions (Garrels and Christ, 1965). The chemical transformation of portlandite into brucite can be represented by the reaction:

$$Ca(OH)_2 + Mg^{2+} \rightleftarrows Mg(OH)_2 + Ca^{2+}$$

From a knowledge of the partial molar volumes of the reactants and the reaction products (Berner, 1971), a change in the molar volume resulting from the dissolution of portlandite and formation of brucite can be calculated. Therefore,

$$\Delta v = [v_{Mg(OH)_2} + \bar{v}_{Ca^{2+}}] - [v_{Ca(OH)_2} + \bar{v}_{Mg^{2+}}]$$

$$= [24.64 - 17.7] - [33.06 - 20.9]$$

$$\Delta v = -5.22 \text{ cm}^3 \text{ mole}^{-1}$$

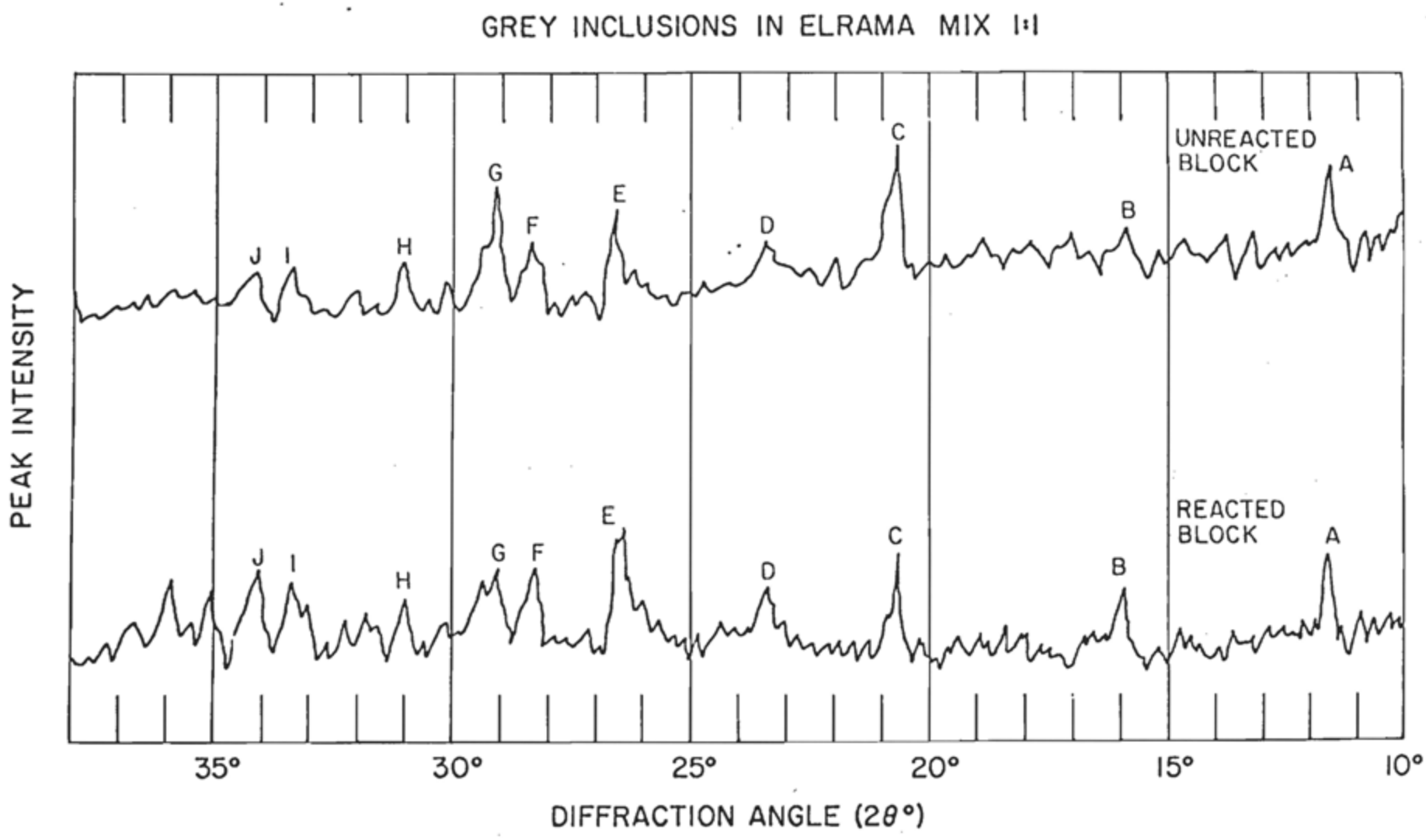

Figure II-28. X-ray diffractograms of grey inclusions contained in Elrama mix E1C1 for unreacted and reacted blocks. A = gypsum (020); B,D,F,I,J = $CaSO_3 \cdot 1/2H_2O$; C = gypsum ($12\bar{1}$); E = quartz (101); G = gypsum ($14\bar{1}$); H = gypsum (002).

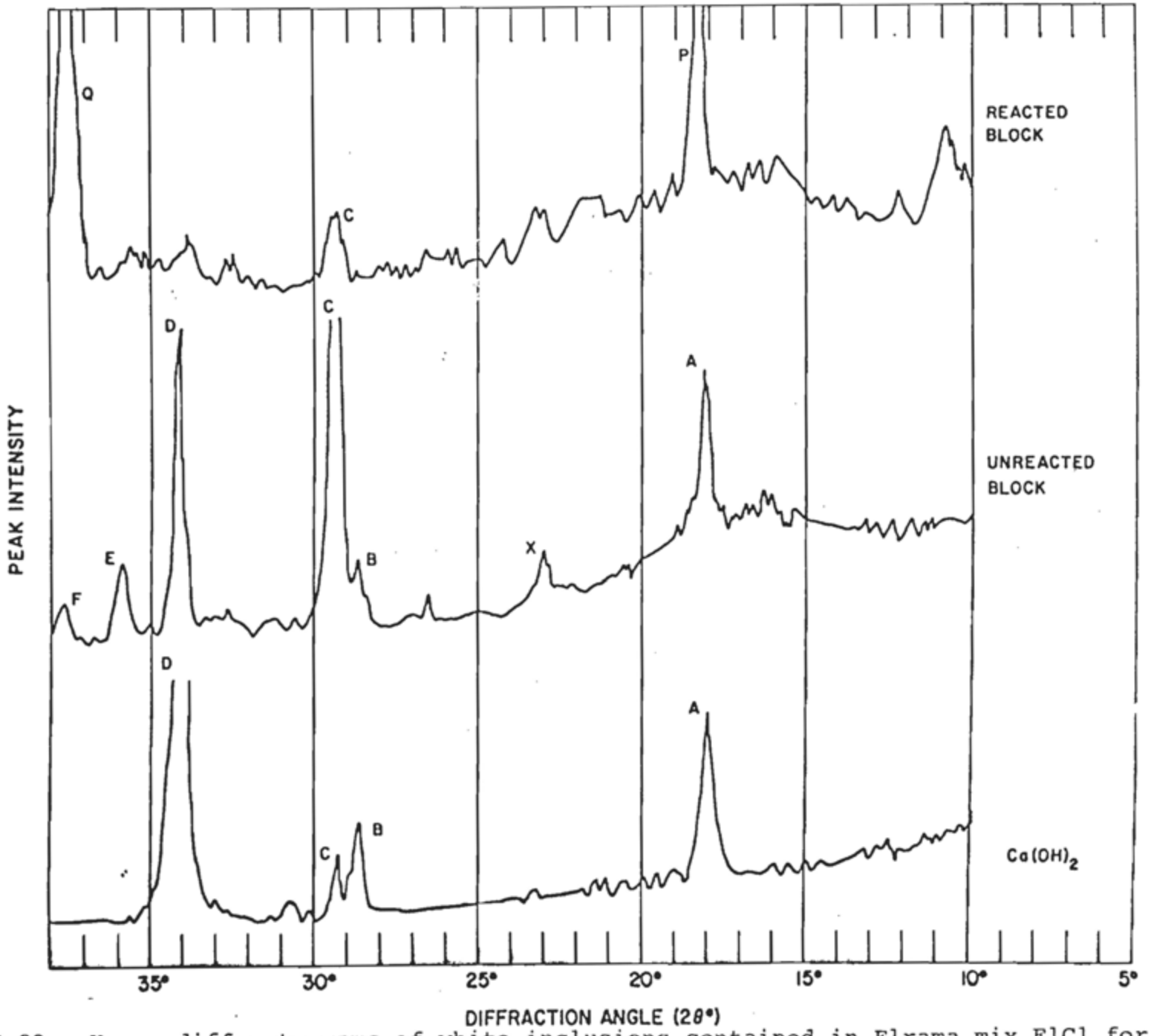

Figure II-29. X-ray diffractograms of white inclusions contained in Elrama mix ElCl for unreacted and reacted blocks. X-ray diffractogram of $Ca(OH)_2$ (portlandite) is is also shown. A = portlandite (001); P = brucite (001); X = calcite (102); B = calcite (100); C = calcite (104); D = portlandite (101); E = calcite (110);

A negative change in molar volume implies an increase in void space and porosity of the material resulting in a more vesicular texture. This may have been the main determinant of block failure.

3. Accelerated Dissolution Studies.

a. Tanks. The accelerated dissolution tank study most closely approximates the leaching effects that we can expect in the natural environment, in that, the tank water is replaced before saturation conditions slow the leaching rate, is in equilibrium with the stmosphere, and is stirred. We refer to the tank study as accelerated dissolution since the temperature of the tank water ($\approx 25^{o}C$) exceeds natural water temperatures at the proposed site ($\approx 4\text{-}20^{o}C$) and the stirring rate exceeds the bottom current flow rates.

The use of duplicate tanks in this experiment permits measurement of the variability in the data. More importantly, the design allows for analysis of the effect of surface area of the test block on the leaching rates and, thus, provides an estimate of the lower limit for the life span of the $0.76\ m^3$ ($1\ yd^3$) blocks in seawater.

Figs. II-30, 31, and 32 show the rate of calcium leaching for the E2C1 and E2C3 test blocks at surface areas of 130, 261, and 516 cm^2. After an initial rapid increase in the leaching of calcium, the leaching rate is essentially constant over the 43 day period shown.

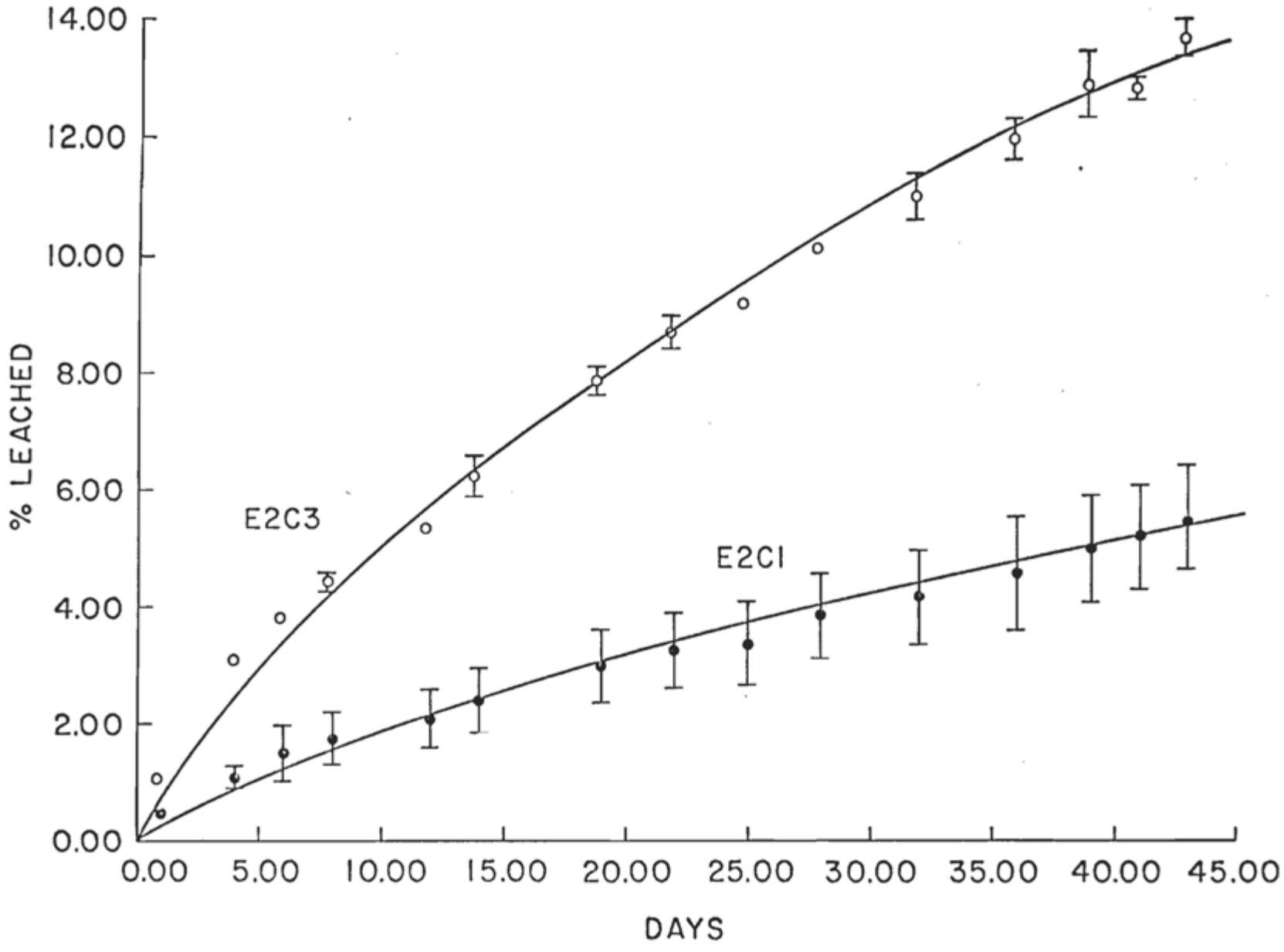

Figure II-30. Calcium leached from coal waste blocks in tanks; 130 cm^2 surface area: 1 liter seawater.

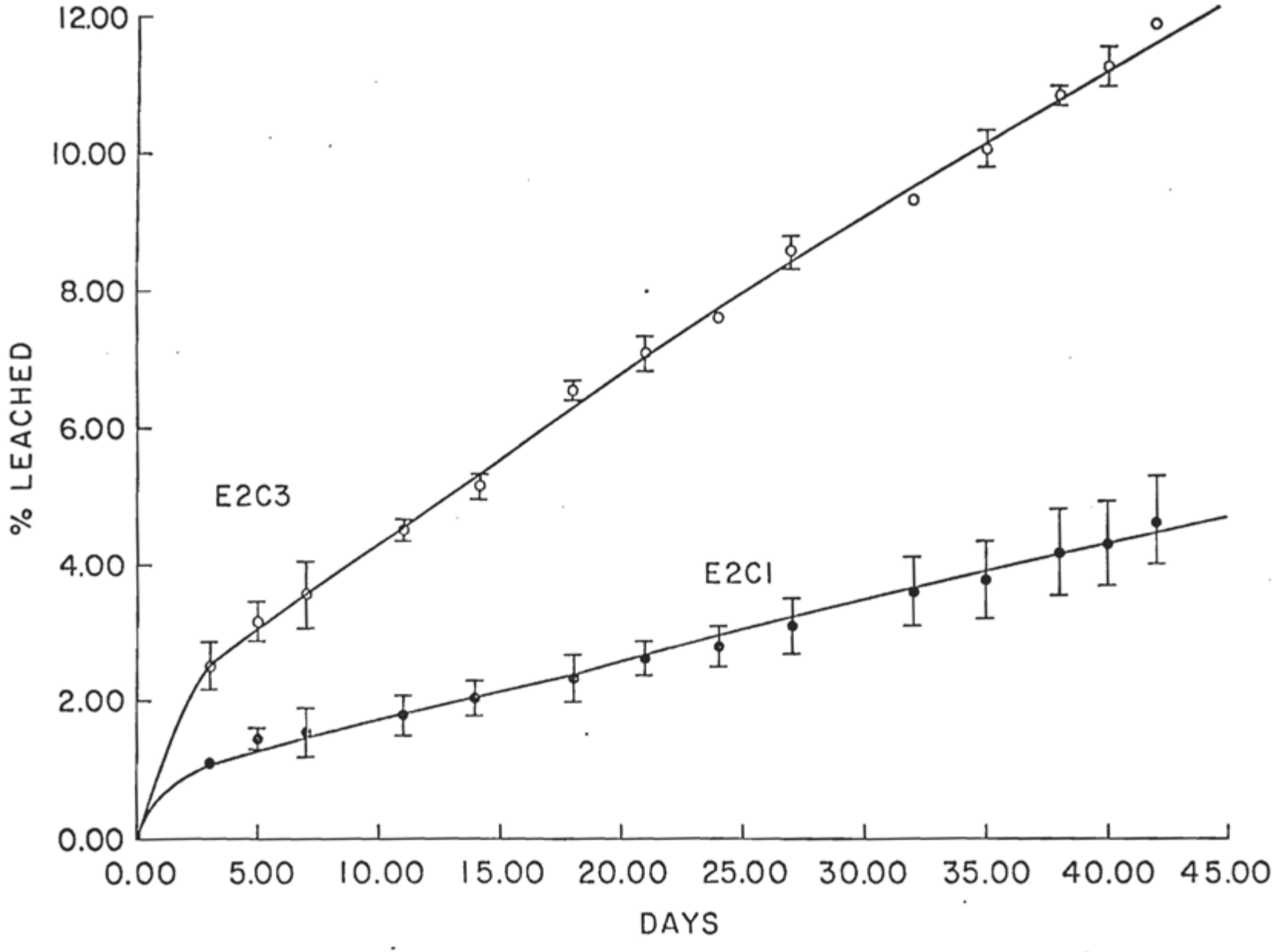

Figure II-31. Calcium leached from coal waste blocks in tanks; 261 cm^2 surface area:2 liters seawater.

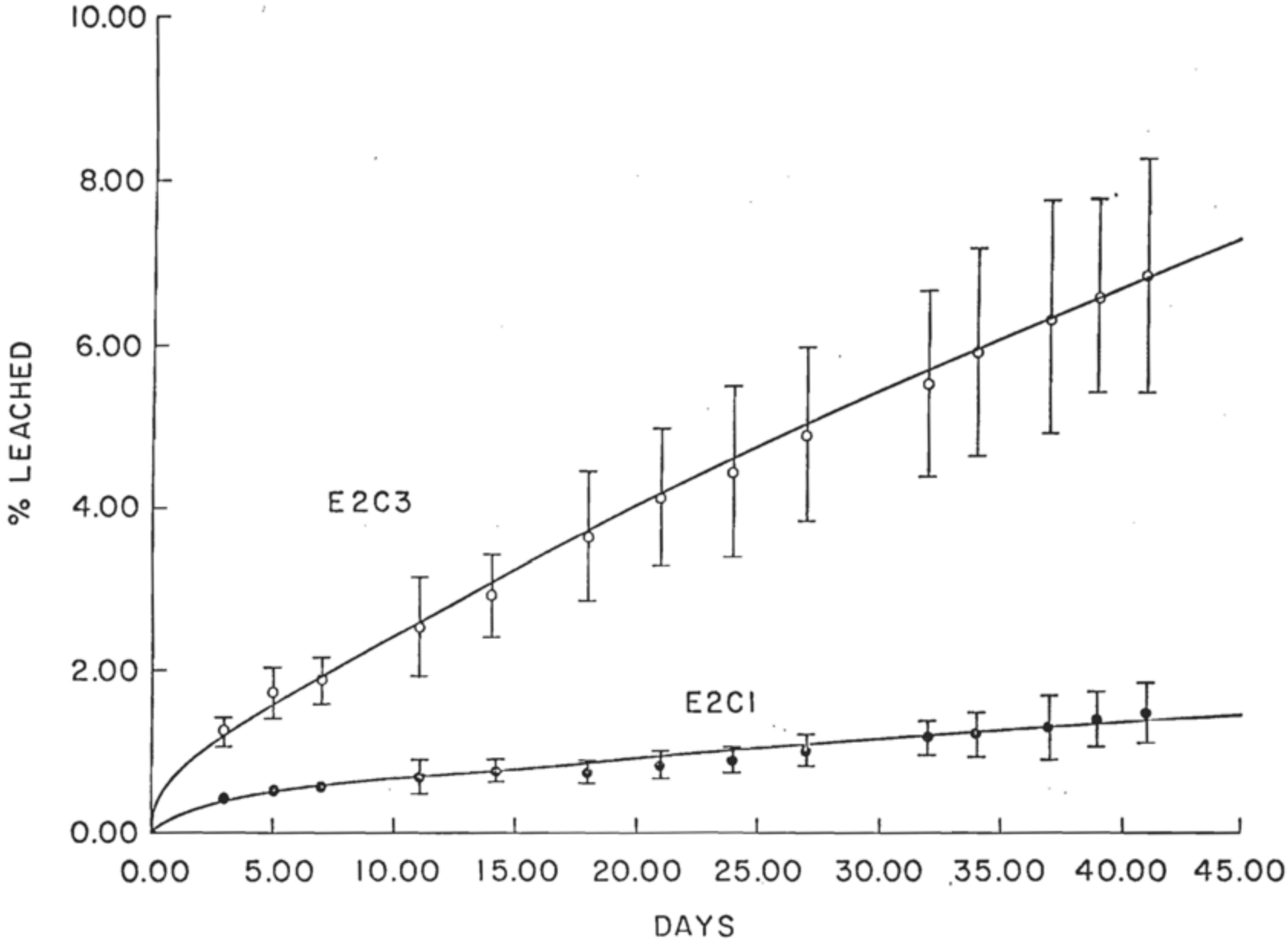

Figure II-32. Calcium leached from coal waste blocks in tanks; 516 cm^2 surface area: 4 liters seawater.

However, in all cases, within the limits of error considered, the calcium leaching rate for the E3C3 blocks far exceeds that for the E2C1 blocks. This is also shown for the column percolation study. As discussed later (Chapter III), it was found that the increase in the strength of the E2C1 blocks during seawater immersion is far superior to the increase of strength of the E2C3 blocks. The difference in calcium leaching rates exhibited here may substantiate this observation.

Table II-11, which predicts the lifetime of the E2C1 and E2C3 blocks in seawater, is a direct result of the calcium leaching data. In order to predict the lifetimes of the blocks used in the tank experiments, we make the following assumptions:

i. The block will lose its structural integrity when all of the calcium has been leached (%Ca=100).

ii. The linear range of the leaching curve (slope=k) will maintain its linearity until the block collapes ($t=t_{max}$).

From assumption (ii)

$$\% \text{ Ca} = Kt$$

Using assumption (i) the equation becomes

$$\% \text{ Ca} = 100 = Kt_{max}$$

or

$$t_{max} = 100/K$$

From Table II-11, it can be seen that the predicted lifetime of the blocks increases with increasing block

Table II-11. Leaching rate and predicted lifetime of the blocks in tank study.

Mix	Block Characteristics: Dimensions	Surface Area (cm^2)	Volume (cm^3)	Water Volume (l)	Day	Calcium Leached (%)	Predicted Lifetime (years)
E2C1	$(4.6\ cm)^3$	130	97	1	43	5.5	2,6
	$(6.6\ cm)^3$	261	287	2	42	4.6	3.1
	$(9.3\ cm)^3$	516	831	4	41	1.5	11.0
E2C3	$(4.6\ cm)^3$	130	97	1	43	13.6	1.1
	$(6.6\ cm)^3$	261	287	2	42	11.9	1.2
	$(9.3\ cm)^3$	516	831	4	41	6.8	1.9

surface area and block volume. Therefore, we would expect the predicted lifetime of the $0.76\ m^3$ monoliths for Phase II to far exceed the lifetimes predicted for our smaller test blocks. Due to the assumptions above,and to elevated temperatures of the laboratory, the experiment represents a worst case model. We would expect a longer lifetime for these blocks at the proposed reef site.

The tank waters were also analyzed for copper and mercury. Copper was chosen as being representative of the transition metals of concern, and mercury was chosen for its negative environmental implications. Copper and mercury in the tank waters were all less than or equal to the seawater blanks of 0.5ppb Cu and 0.2ppb Hg. Therefore, the test blocks were actually acting as scavengers of transition metals. This agrees well with previous tank studies (Seligman, 1978). This scavenging phenomenon is also borne out in the bioassay elutriates (Chapter IV). In preparing the elutriates, powdered Elrama and Conesville mixes were added to seawater and shaken. The filtered elutriate water and the original seawater were analyzed for calcium, copper and mercury. For both mixes, calcium was leached from the powder. However, the copper concentration in the original seawater was 70% adsorbed by the powders and the mercury concentration in the elutriate waters was equal to or less than the 0.2ppb Hg concentration found in the original seawater.

The reduction in dissolved trace metal concentrations in the tank waters cannot be explained by an increase of pH in the waters upon exposure to the blocks with the resultant "loss" of dissolved metals through hydroxide precipitation and co-adsorption, since the pH of the tank waters did not significantly change from the pH of the original seawater throughout this study.

b. Columns. The percolation study maximizes the dissolution of the components present throughout the internal structure of the test block. Leaching of the soluble components was enhanced by percolation since the leaching was not limited to the dissolution of the surface area.

Fig. II-33 shows the leaching rate of calcium as successive volumes of seawater are percolated through the test blocks. The duplicate E2C1 test blocks show excellent agreement in percolation rates for calcium. This rate shows two distinct linear regions with the linear rate after 2.5 liters of seawater passage increasing over the initial rate. The duplicate E2C3 test blocks do not show agreement in their percolation rates for calcium. The rate for the E2C3 #1 block is similar to but greater than the rate for the E2C1 blocks which agrees with the tank results for calcium leaching. However, the percolation of calcium for the E2C3 #2 block proceeds at a rapid linear rate. We attribute this anomaly to an artifact which is dissolving at a rapid rate in this particular block.

This hypothesis seems to be confirmed by the percolation rates for copper and the permeability observations which are to be discussed below.

Fig. II-34 shows the leaching rate of copper as successive volumes of seawater are percolated through the test blocks. Again, the duplicate E2C1 test blocks show good agreement in percolation rates for copper. The error bars for the E2C1 copper leaching rates are significant but appear to be a function of the permeability of the individual blocks (Table II-12) rather than measurement error. The effects of permeability on observed percolation rates will be discussed below. As for calcium, the duplicate E2C3 blocks do not show agreement in their percolation rates for copper. This anomaly serves as further proof of the artifact in the E2C3 #2 block.

The major observation to be drawn from Figs. II-33 and II-34 is that while the calcium leaching follows an increasing rate pattern, the copper leaching is slowing down to what appears to be a steady state leaching rate. If we can assume that copper behaves like the other transition metals to be considered in this study, a steady leaching rate should exist for all transition metals. The fact that the pH of the leachate has decreased to the pH of the original seawater (Fig. II-35) substantiates this theory.

As shown in this discussion of the dissolution studies, the percolation studies differ from the tank studies with

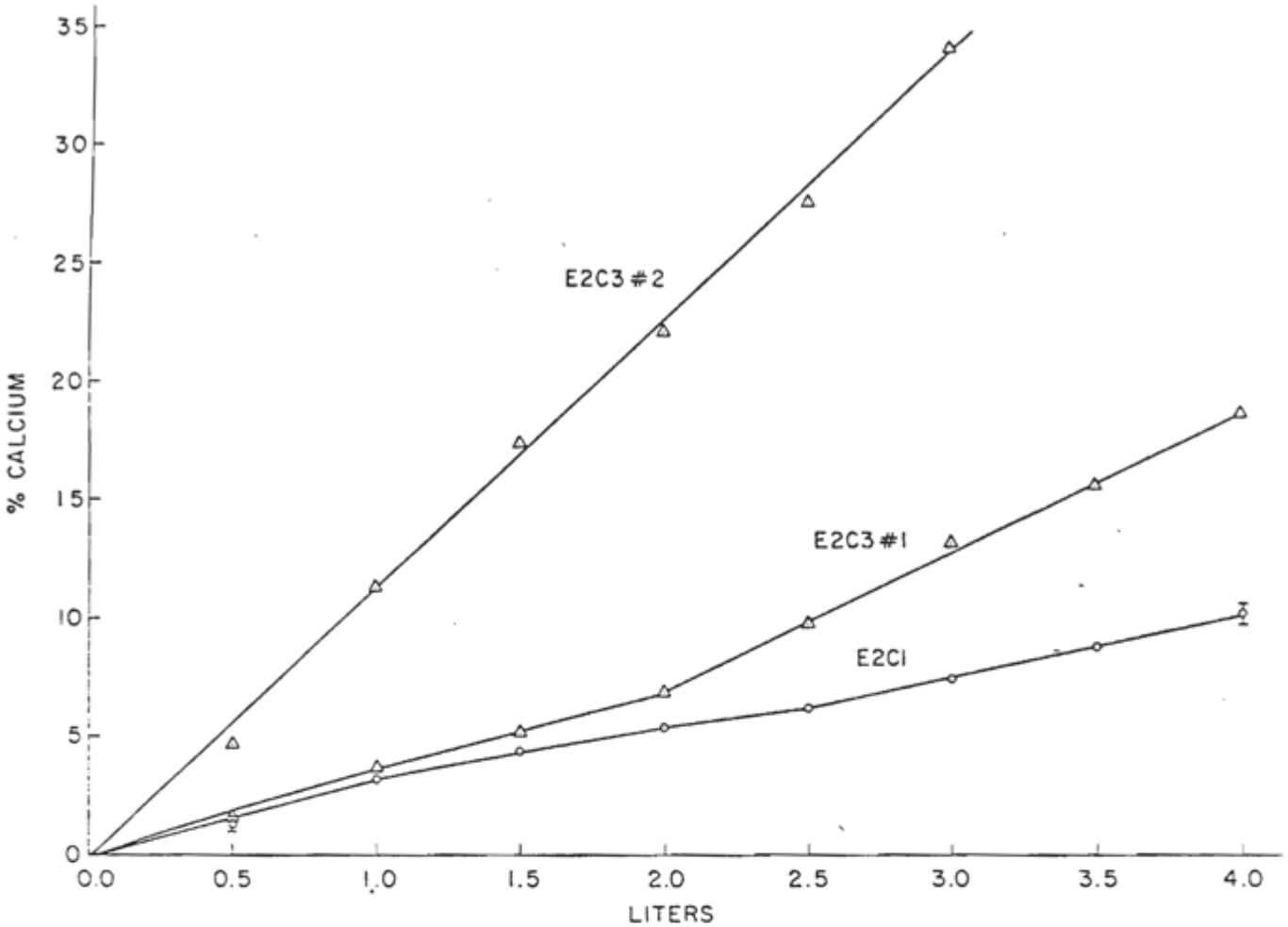

Figure II-33. Copper percolation from coal waste block in column.

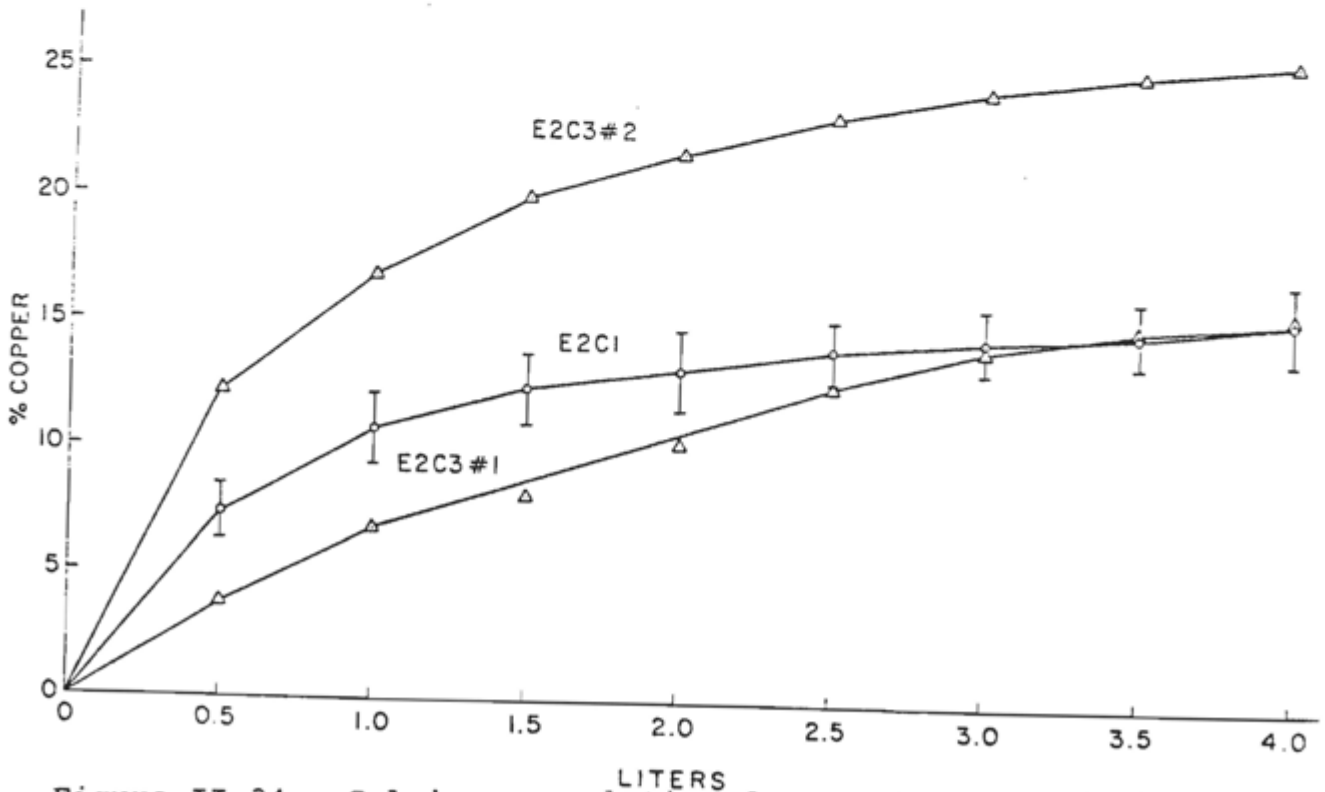

Figure II-34. Calcium percolation from coal waste block in column.

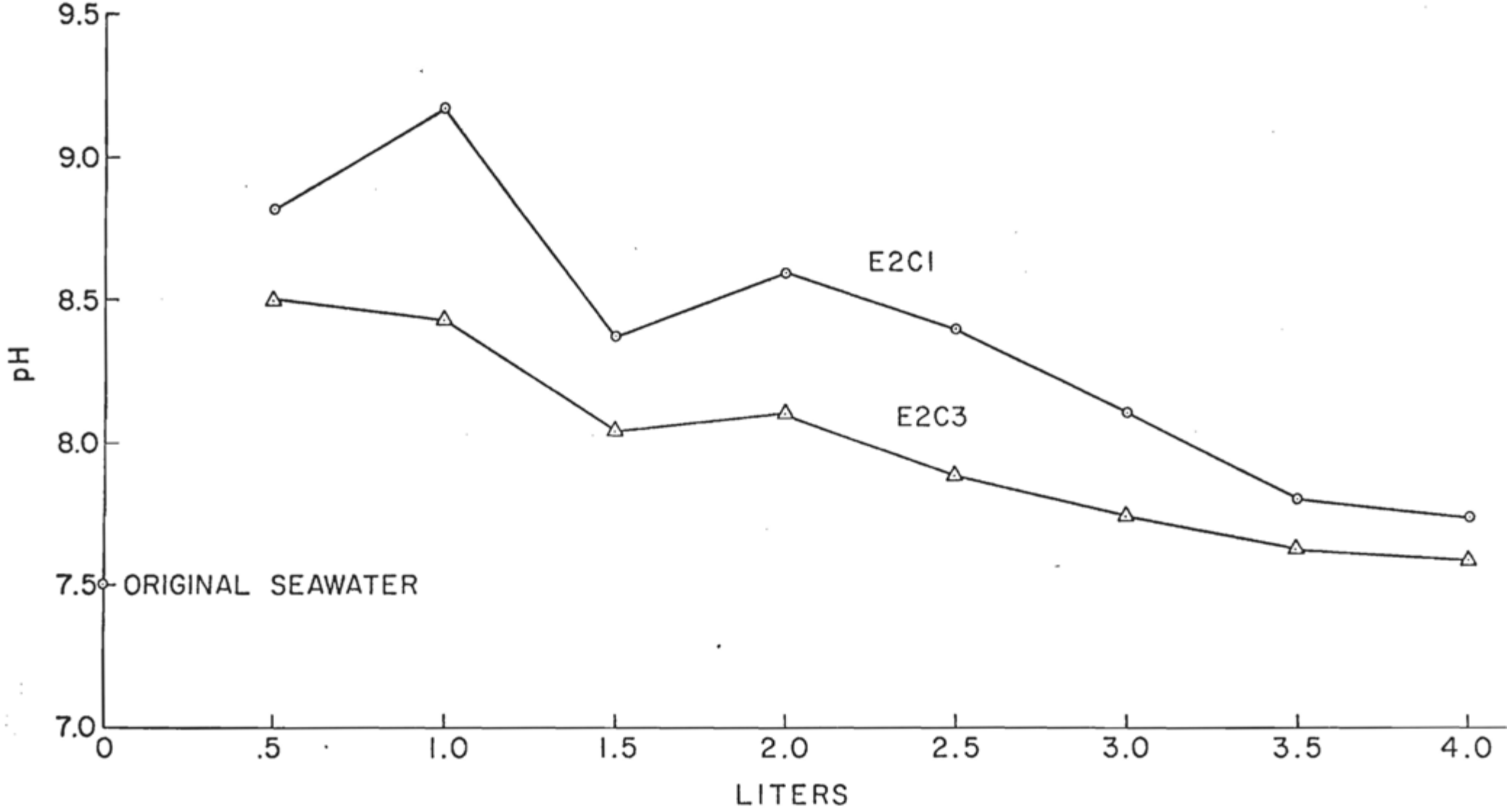

Figure II-35. pH of column percolated seawater.

regard to trace metal leaching. In the "worst case" study, i.e. the percolation study, the trace metal leaching is significant but reaches a steady state rate whereas in the study that most resembles the natural environment, i.e. the tank study, there is no trace metal leaching but, rather a trace metal adsorption effect.

Finally, Table II-12 is an attempt to explain the artifact theory observed for the E2C3 #2 block, and to correlate permeability with percolation leaching rates. Since the permeability measurement was made at the start of the percolation study, the leaching of calcium and copper for the first 0.5 liter of seawater percolation is considered here. Two important observations can be drawn from this data:

i. The ratios of percent Ca and percent Cu leached in the #1 and #2 blocks from each mix type are similar. Therefore, contamination and/or measurement error cannot explain the large error bars for the E2C1 copper leaching. In addition, the artifact theory is substantiated by the agreement of the ratios for the E2C3 blocks.

ii. There is an inverse relationship between permeability and leaching rates. This relationship may be accounted for by the fact that a higher permeability signifies more fissures in the block which decreases the residence time of the percolated water in the block, leading to a decrease in leaching.

Table II-12. Percent calcium and copper leached during first 0.5 l passage of seawater and permeability coefficient.

Mix	Ca (% leached)	Ratio	Cu (% leached)	Ratio	K ($cm\ sec^{-1}$)
E2C1 #1	1.53		8.17		2.8×10^{-7}
		1.4		1.2	
E2C1 #2	1.09		6.61		4.3×10^{-7}
E2C3 #1	1.52		3.76		7.5×10^{-7}
		3.1		3.2	
E2C3 #2	4.68		12.2		1.2×10^{-7}

III. MATERIAL PROPERTIES

A series of interrelated tests have been devised and implemented which provide a basis for determining the ultimate block strength from the nondestructive measurements of block properties. Such measurements not only provide a basis for predicting ultimate block strength, but they also make it possible to monitor the evolution of block properties with time, which may provide a basis for lifetime prediction.

A. Test Environments

Test sample blocks cut from 0.028 m^3 coal waste blocks were divided into sub-groups, pre-tested, and then aged in different environments.

1. Ambient Conditions

Test blocks to be aged under ambient conditions were placed in: a) the Atlantic Ocean at the project site at a 21 m depth, b) tanks of fresh and seawater at a laboratory temperature of 20°C, and c) tanks of circulating seawater at an outside temperature of 4°C.

2. Accelerated Conditions

As part of the testing program, experiments using a hot bath and a pressure cell were designed to accelerate the physical and chemical evolution of the blocks. The results of such tests should aid in predicting lifetime of the block material in the ocean.

a. Hot bath. A set of tests was carried out on selected mixes held in freshwater and seawater tanks at

an elevated temperature of 40°C. Pumps provided constant circulation of the water within each test tank.

b. Pressure cell. A pressure cell was constructed with the use of a 6 in. ID steel tube with 1/4 in. wall thickness. It was welded to a steel base and its top was threaded and fitted with an aluminum alloy cap. A small 1/2 in. tube was inserted to the tube wall to introduce compressed air at 18 psi. A gas gauge was placed in the aluminum cap to record the gas pressure inside the cell. Test samples were placed inside the cell and seawater from the Fire Island Project site was used to cover them.

B. Test Block Properties

Every sample was characterized by measurments of size, volume, dry weight, and elastic modulus at the beginning of each aging cycle. At approximately monthly intervals, certain test blocks were selected from the project site off Fire Island and tested along with blocks from the laboratory tanks for apparent density, volume, and for longitudinal and transverse sound velocity and attenuation. After each test, all blocks were returned to the test tanks with the exception of the blocks removed from the reef site and those used for compressive strength measurements which destroys the blocks . These measurements make it possible to monitor the evolution, with time, of the following properties of each block:

1. water uptake
2. material loss due to dissolution
3. porosity
4. elastic modulus
5. elastic anisotropy
6. surface anisotropy in dissolution
7. mix inhomogeneities
8. internal friction

This last property is directly related to the absorption of ultrasonic energy measured in the test sample and provided a basis, in combination with the elastic modulus, for the prediction of the compressive strength of the block material.

A chronology of this part of the test program is displayed in Table III-1.

1. Density and Porosity

The apparent densities of several groups of control blocks were carefully evaluated using the following procedures. $0.028 m^3$ test blocks were first cut into smaller 7.5 cm x 10 cm x 15 cm test blocks which were labeled. Each small block was carefully weighed in the dry state to determine its mass. Apparent dry weight density was determined by the weight of the test speciment divided by its bulk volume. In their dry states, there were large ranges of apparent density values within each formulation mix, as well as within each test block, as shown in Table III-2.

Table III-1. Summary of engineering tests by block type.

Test No.	Block Type	Start Date	Location	Temp.	No. Pieces	Environment
1	E1C1	12/21/78	Lab	Amb[1]	1	Freshwater
2	E1C1	1/15/79	"	40°C	1	Seawater
3	E1C1	1/15/79	"	40°C	4	Seawater
4	E1C3	1/15/79	"	40°C	3	Seawater
5	E2C1	1/15/79	"	40°C	1	Freshwater
6	E2C1	1/15/79	"	40°C	4	Freshwater
7	E2C3	1/15/79	"	40°C	3	Freshwater
8	E2C1	12/7/78	Reef	Amb[2]	10	Seawater
9	E2C3	12/7/78	Reef	Amb[2]	12	Seawater
10	E2C1	12/21/78	Lab	Amb[2]	4	Freshwater
11	E2C3	12/21/78	Lab	Amb[2]	4	Freshwater
12	E2C1	12/20/78	F.P.*	Amb	3	Seawater
13	E2C3	12/20/78	F.P.*	Amb	3	Seawater
14	E3F1	2/3/79	Reef	Amb[2]	16	Seawater
15	C3F3	2/3/79	Reef	Amb[2]	16	Seawater

* Flax Pond field test lab.

1 Approx. 20°C

2 Approx. 4°C

Table III-2 Apparent density ranges and apparent porosity (based on a true density of 2.35) of test samples in the dry state.

Test Mix	Apparent Density ($g\ cm^{-3}$) within each formulation	Apparent Density ($g\ cm^{-3}$) within each block (1 cu.ft.size)	Apparent Porosity (%) within each formulation	Apparent Porosity (%) within each block (1 cu.ft.size)
E1C1	1.377 - 1.554	1.281 - 1.537	33.9 - 41.4	34.6 - 45.5
E1C3	1.233 - 1.506	1.160 - 1.459	35.9 - 47.5	37.9 - 50.6
E2C1	1.190 - 1.434	1.409 - 1.538	39.0 - 49.4	34.6 - 50.0
E2C3	1.250 - 1.466	1.281 - 1.537	37.6 - 46.8	34.6 - 45.5

The small blocks were then soaked in either freshwater or seawater, depending on the intended environment of the block, for a period of approximately two hours. It was found that this time was required for the blocks to degass to a point where they could be weighed. Each block was then weighed again on the balance pan (W_A) and while suspended in a net in water (W_w). The volume of each block was calculated from

$$V = \frac{W_A - W_w}{\rho_w}$$

where ρ_w is the density of water. From the volume (V), the apparent density ϕ_A is computed from $\phi_A = W_A/V$. A gravimetric displacement technique was then used to accurately monitor the apparent density (P_A) and volume (V) of each test sample even though material was being lost during the aging process.

We found that the blocks had a nominal dry weight of about 1800 g. The variations in densities between the blocks at each weighing were due to actual differences between blocks, demonstrating a certain degree of inhomogeneity in the $0.028 m^3$ blocks. The evolution of the apparent densities of each test group is indicated in Figure III-1. Apparent densities of the test blocks indicate a systematic increase in density of about 2.2% over a 31 day immersion period (see also Table III-3). Although the initial growth in density can be readily attributed to the uptake of water into pores of the blocks, the continued increase is more likely due to chemical reaction. The

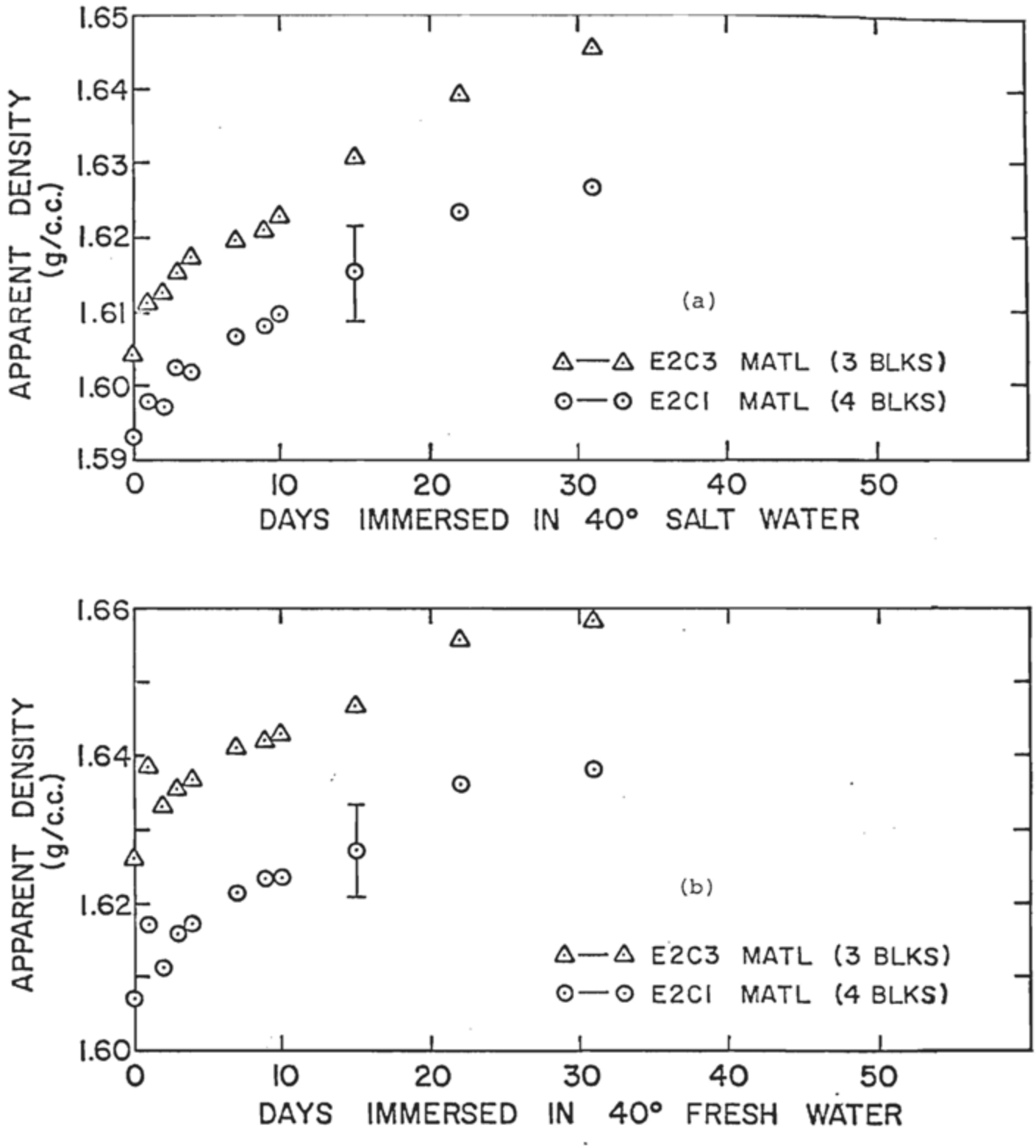

Figure III-1. Variation in apparent density with time of immersion in freshwater or seawater at 40°C. (a) Average of four E2C1 and three E2C3 blocks in seawater. (b) Average of four E2C1 and three E2C3 blocks in freshwater.

Table III -3. Variation of apparent density with time of test blocks at 40°C.

	Seawater		Freshwater	
Days Elapsed	E2C1	E2C3	E2C1	E2C3
0	1.5931	1.6042	1.6071	1.6260
1	1.5980	1.6116	1.6171	1.6386
2	1.5974	1.6120	1.6116	1.6334
3	1.6023	1.6152	1.6161	1.6360
4	1.6021	1.6173	1.6170	1.6367
7	1.6067	1.6199	1.6218	1.6411
9	1.6081	1.6210	1.6238	1.6421
10	1.6098	1.6228	1.6239	1.6427
15	1.6159	1.6308	1.6273	1.6468
22	1.6237	1.6395	1.6362	1.6560
31	1.6268	1.6455	1.6381	1.6594

error bars shown are attributed to block inhomogeneities (and represent the statistical spread of the group). The standard deviation for the apparent density within a given block mix is typically less than $\pm$ 0.4%. The error in the density measurements is less than $\pm$ 0.1%. In these tests, the density of test blocks with a 3:1 fly ash:sludge ratio was about 1% higher than that of 1:1 material and remained that way over the period of immersion.

The initial density of the test mixes placed in seawater was uniformly lower than that of those placed in freshwater. This feature is significant and is presumed to be related to chemical processes which occur in the first few hours of immersion. The subsequent increase in density was the same, within experimental error, for both seawater and freshwater immersion.

These results are the opposite of what could be expected for a model in which the fluid is directly drawn into the pores of the material. Such a model would suggest an increase in specific gravity proportional to the specific gravity of the immersion fluid. Since seawater has a density about 2% higher than freshwater, the higher density should have been achieved when the blocks were submerged in seawater; the opposite was observed. On the other hand, our observations indicate a rapid uptake of water for about two hours after initial immersion - after which the rate slows down by orders of magnitude. If we accept a model in which the blocks are saturated after 1-2 days, then we must attribute density increases to other mechanisms.

Because the materials in the test sample were physically mixed, it was difficult to obtain a representative specimen to measure its true density as a solid substance. By assuming an arbitrary density of 2.35 g cm^{-3} for the dry solid substances in the test sample, apparent porosities were calculated (see Table III-2). The apparent porosity is the sum of open pores and closed pores.

Immersion of test samples in water under an atmospheric condition showed that the water absorption proceeded in two stages. In the first stage, a large percentage of porosity in the test sample was filled by water. It took place within 1/2 hour of its contact with water. In the second stage, the additional water intake took place at a very slow rate. In certain cases, the test sample never reached a steady state wet density even after immersion in water in excess of 7 days. For example, test sample E1C1 had an initial apparent porosity of 44.2%. After the immersion in water for 1/2 hour, it gained in density equivalent to a water intake of 33.6%. Thereafter, the rate of water intake continued at an approximate rate of 1.8% loss in porosity per day. It did not reach a steady state density until after 7 days immersion in water. In another sample, the first stage of water intake exceeded the apparent porosity. This suggests that, in addition to the water adsorption which replaced the pores in the test sample, chemical reactions which consumed water as a reactant may have occurred. In cases where there were no chemical

reactions which consumed water, the sample should have reached a steady state wet density after 1 day immersion in water for the sample sizes used in this experiment. The possibility or occurrence of chemical reactions between the test samples and water must be further investigated.

2. Water Permeability and Absorption

Previous work by Seligman (1978), and results in Chapter II of the present report, show that the test samples of waste block mixes have a low coefficient of permeability in the range 10^{-6} to 10^{-7} cm sec^{-1}. Due to the results indicating possible chemical reactions between the block and water, the exact meaning of permeability is unclear. Special tests must be developed to take into account the presence of chemical reactions.

In order to investigate further the water absorption characteristics of the test samples, an accelerated test using a pressure cell was performed. Results for the uptake of water in the test mixes are shown in Table III-4. For the E2C1 and E2C3 mixes, considerable water uptake occurred within the first one-half hour. For these mixes, the pressure cell showed large amounts of gas bubbles. The surfaces of mix E2C3 showed deformation (wrinkle-like) after 24 hours in seawater. In sample E1C1 and E1C3, there were no visible effects.

3. Compressive Strength

Previous studies (Seligman, 1978; Roethel,personal communication) used a Riehle Universal Testing Apparatus

Table III-4. Water uptakes of test samples in the pressure cell at 18 psig.

Number Code	apparent density g cm-3	time of water immersion (hrs)	% volume equivalent to water intake
E1C1	1.370	94.0	34.7
E1C3	1.230	97.0	38.0
E2C1	1.190	0.5	28.3
		24.0	36.4
E2C3	1.250	0.5	30.2
		24.0	37.6

to determine the compressive strength. The load, at which the test specimen was fractured at a loading rate of 0.064 cm min^{-1}, is divided by the area of the cross-section to give the compressive strength value. Figure III-2 shows the extensive compressive strength record for a test mix in the marine environment. The experiment was terminated after 508 days because of the extensive boring activity of biota. Table III-5 presents data on additional mixes submerged in Conscience Bay (Roethel, personal communication).

Concrete had higher compressive strength than the test samples but lost a signficiant amount of its compressive strength after 146 days immersion in seawater at the Conscience Bay site. However, test samples showed significant (44% for the Elrama sample; and 99% for the Conesville sample) gains in their compressive strengths during this period. The large gain in compressive strength observed for the first 146 days of study at Conscience Bay, relative to the initial dry values for the Elrama and Conesville test mixes, suggests that there were chemical reactions between the mixes and water which produce beneficial results with respect to the physical integrity of the blocks.

In the present program several determinations of compressive strength were conducted with the Elrama mixes (E1 and E2) soaked in seawater prior to testing (Table III-6). The following conclusions were reached based on

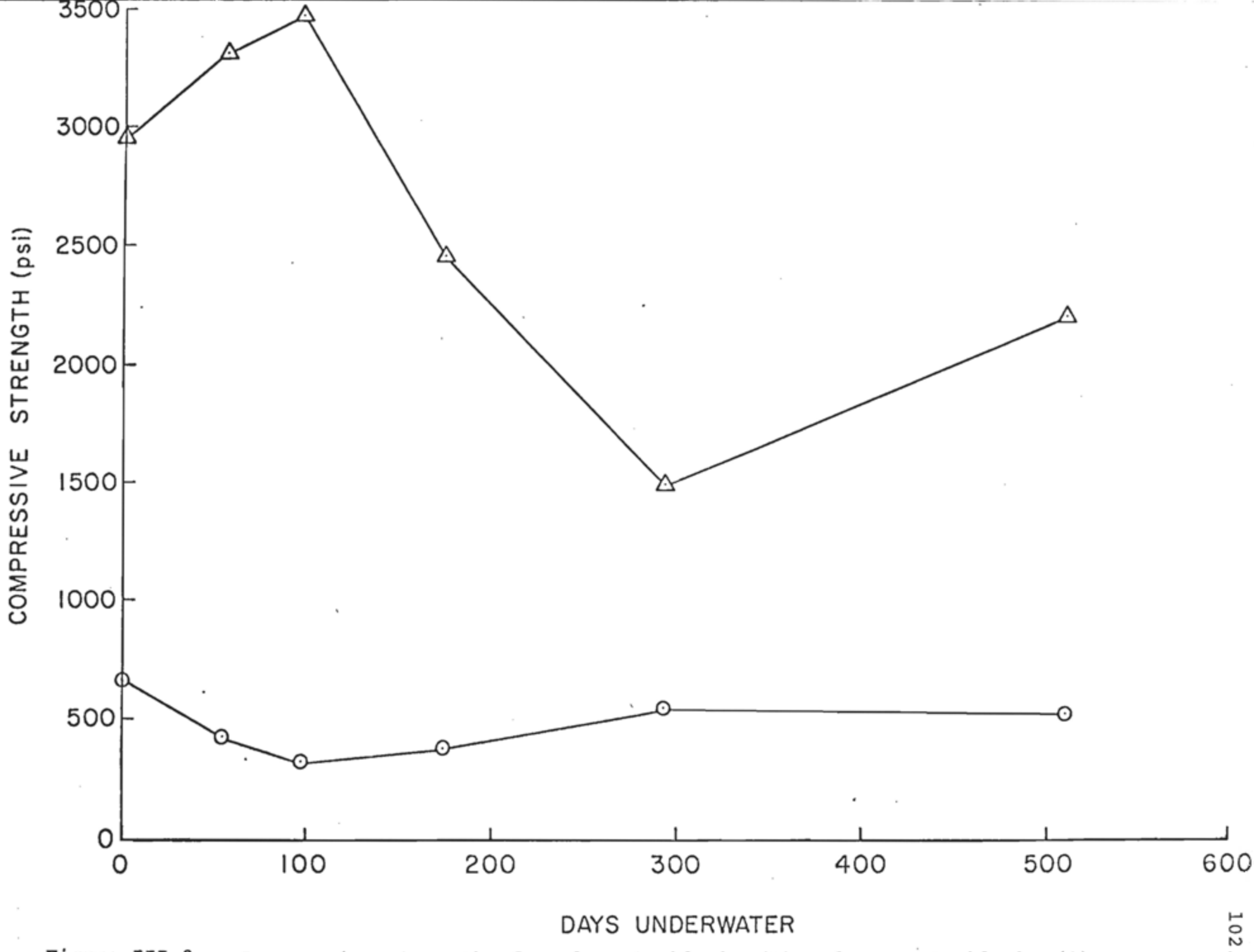

Figure III-2. Compressive strength of coal waste blocks (O) and concrete blocks (Δ)

Table III-5. Compressive strength of *in situ* blocks in Conscience Bay (Roethel, personal communication).

Test Mix	Days of Immersion	Compressive Strength (psi) (n=3)
Elrama 1:1	0 (dry)	1101±122
	146	1585± 79
	238	1029±405
Conesville 1:1	0 (dry)	321± 18
	146	640± 51
	238	597± 95
Concrete	0 (dry)	2124± 99
	146	1483± 30
	238	2014±185

the compressive strength results.

a) The compressive strength values after 30 days immersion were considerably lower than the initial compressive strength values.

b) High sludge content produced higher compressive strength values than high fly ash content.

c) Water immersion under pressure (accelerated testing) decreased the compressive strength values.

d) The compressive strength values were at least ten times greater than the actual compressive load each block will experience at the project site.

4. Fracture Patterns

Fratography can provide information about the material characteristics. Figures III- 3 to 5 show the results of compressive strength tests for six samples. All six faces of each sample are shown with the top photo showing the back side. The row of three photos show the left and the

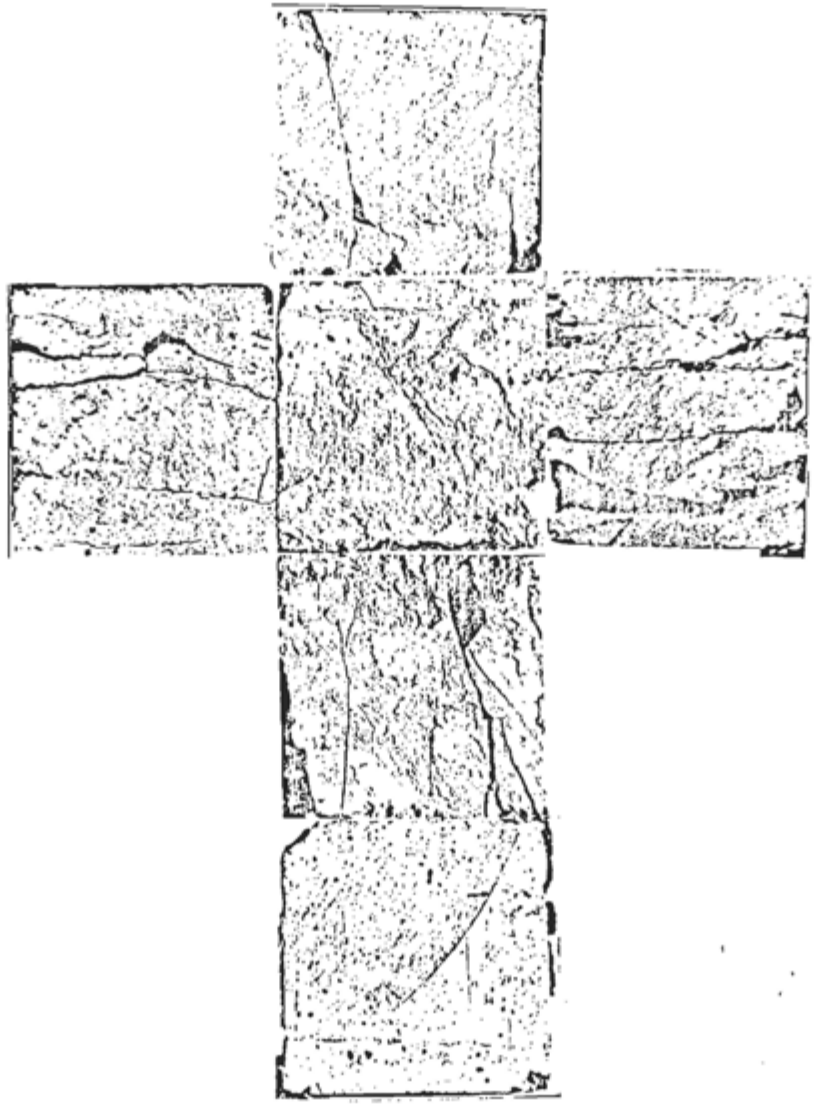

Figure III-3. Conesville 1:1 after the compressive strength (321.4 psi) test.

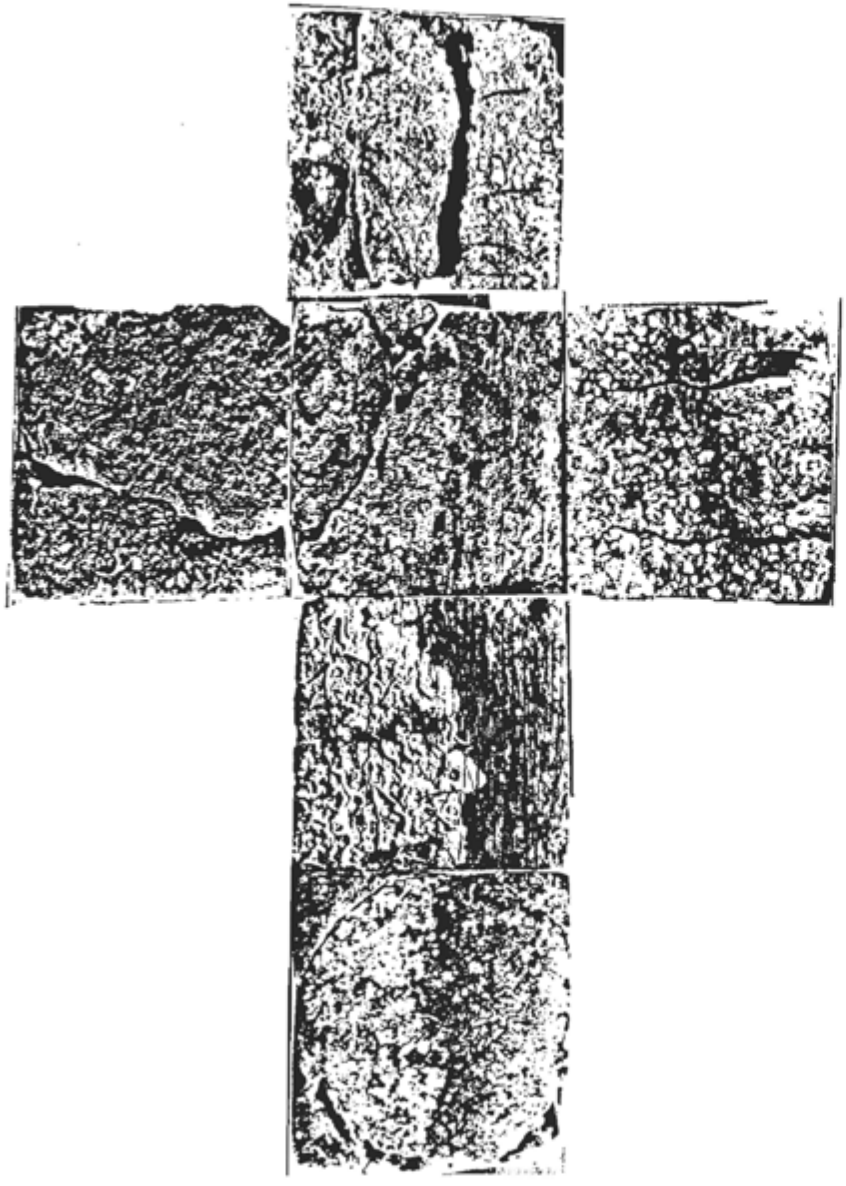

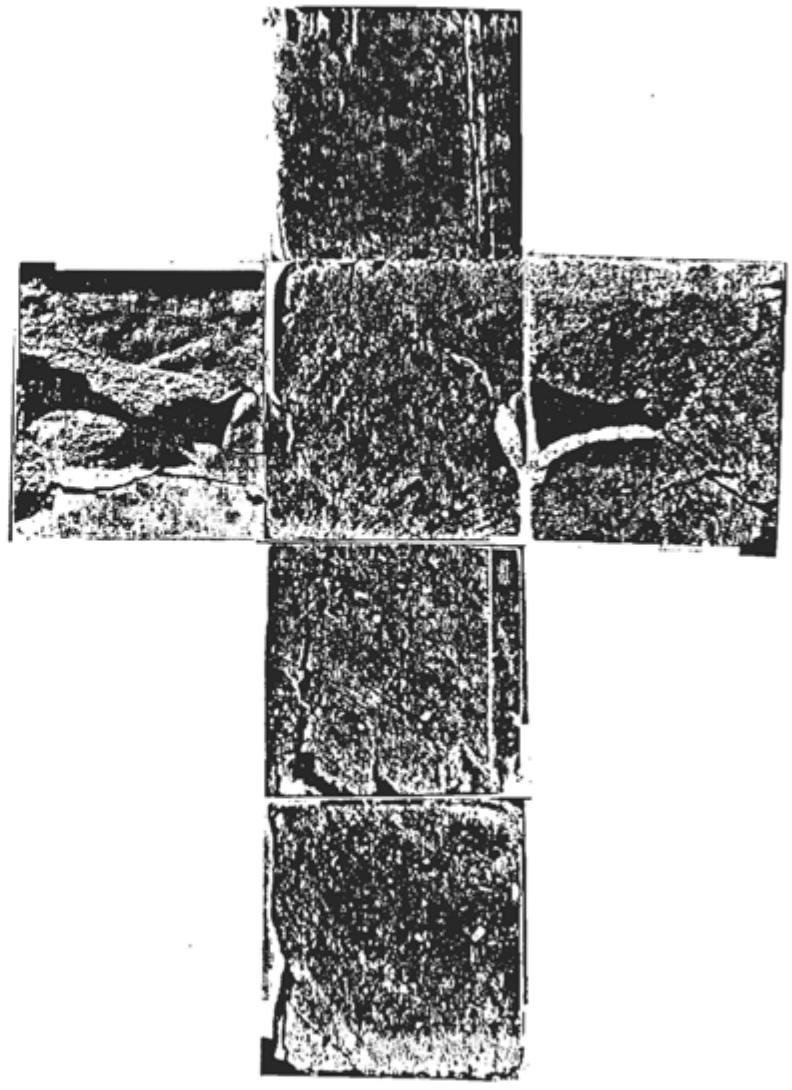

Figure III-4. (left) Concrete sample, immersed in seawater for 146 days, after the dry compressive strength (1483.2 psi)test.

(right) Elrama 1:1 sample after the compressive strength (1101.3 psi) test.

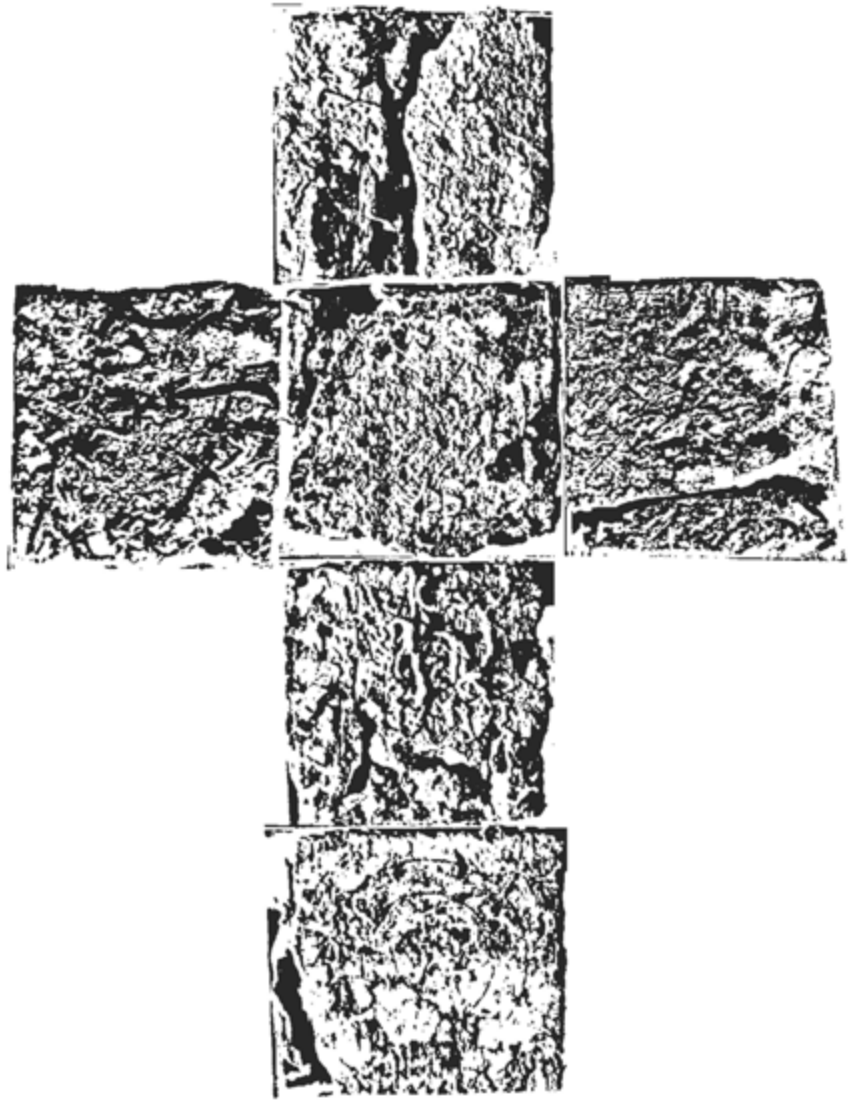

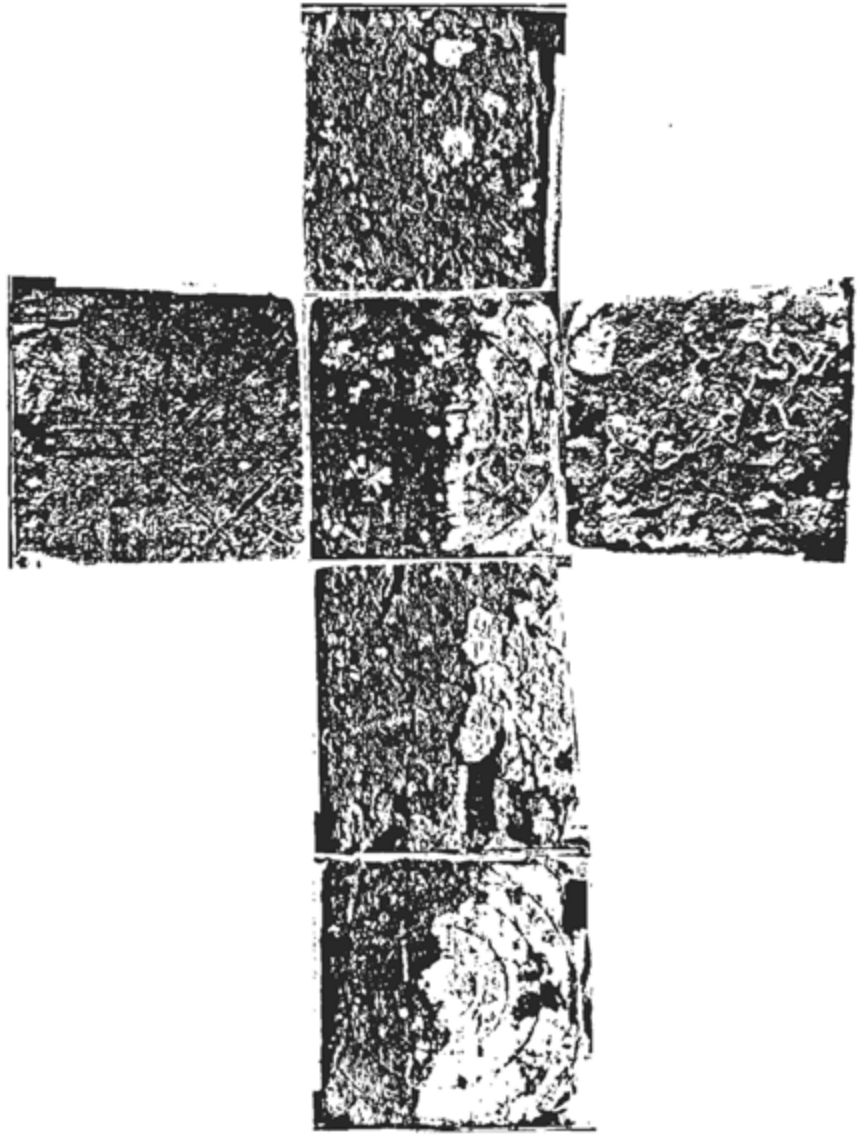

Figure III-5. (left) Conesville 1:1 sample, immersed in seawater for 146 days, after the compressive strength (640.5 psi) test.

(right) Elrama 1:1 sample, immersed in seawater for 146 days, after the dry compressive strength (1585.7 psi) test.

right sides at the left and right, respectively. The center photo in the row was the top face. The front side was shown in the photo beneath the top face, and the last photo was the bottom side. The load was applied to both the top and bottom side. In Figure III-3, the left part showed the Conesville 1:1 sample (dry compressive strength of 321 psi Table III-5)after the test. The right part of Figure III-4 shows a dry Elrama 1:1 sample (dry compressive strength 1101 psi), and the left part shows a concrete block (dry compressive strength 1483 psi) after its immersion in seawater for 146 days. The left part of Figure III-5 shows Conesville 1:1 (dry compressive strength 641 psi), and the right part showed Elrama 1:1 (dry compressive strength 1586 psi). Both were immersed in seawater for 146 days. Although the dry compressive strength values varied, the fracture patterns were very comparable. The Conesville 1:1 sample in Figure III-4 lost many pieces after the compressive strength test. The test samples, which were subject to compressive strength test, are shown in Figure III-6. In Figure III-6, six blocks were immersed in seawater at the Fire Island project site for 30 days, two blocks were immersed in the sea tables in the Flax Pond Laboratory for 35 days; three blocks were immersed in the seawater in the pressure cell at 18 psi. The wet compressive strength values for all these treatments are shown in Table III-6. In Figure III-6, samples are shown in one view. Here the load was applied to the left and

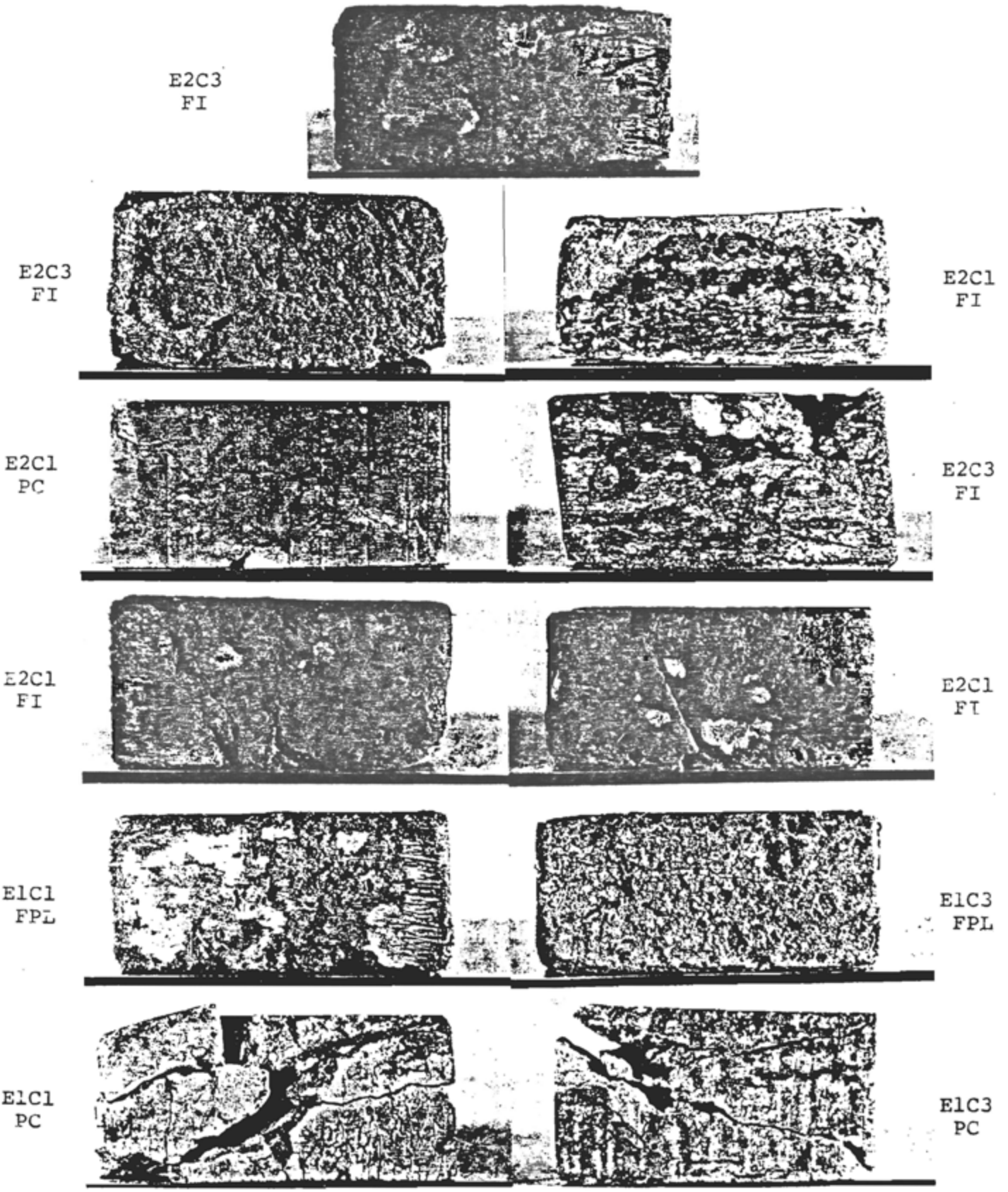

Figure III-6. Samples after wet compressive strength test
FI = Fire Island site, 30 days; FPL = Flax Pond Lab, 35 days
PC = Pressure cell, 97 hrs

Table III-6. Compressive strength of test samples aged in a) Flax Pond Laboratory, b) Fire Island site, and c) pressure vessel (18 psi)

Mix	Compressive strength (dry) psi	Period of Immersion	Compressive strength (wet) psi
a) E1CI	1067±134	35 days	324
E1C3	1169±164	35 days	172
b) E2C1	542±88	30 days	395±26 (n=3)
E2C3	588±93	30 days	292±58 (n=3)
c) E1C1	1067±134	94 hrs	582
E1C3	1169±164	97 hrs	472
E2C1	542±88	24 hrs	381
		97 hrs	275
E2C3	588±93	24 hrs	339
		97 hrs	370

right faces of the samples as shown in the photographs. Again, their fracture patterns were comparable.

5. Hardness, Erosion, Dissolution

Test blocks showed inhomogeneous spots on their surfaces. The spots ranged from white to grey to dark grey. Brinnell hardness tester was used to determine the hardness for each distinctive spot on the surface. The hardness values ranged from 12.5 to 75.5, for a 1.6 mm diameter ball and 15 kg load. The hardness values indicated the test samples to possess relatively soft substances. However, there was no correlation between the hardness value and the distinctive spots on the surface.

A surface abrasion test was devised to abrade the test sample with a glass surface. The surfaces were maintained wet and the sample weight (about 1.5 kg) was the sole load on the sample. The sample movement was maintained at approximately 1 km hr^{-1}. The dry test samples produced weight losses which were equivalent to abrasive material removal rates of about 2.5×10^{-2} mm day^{-1}. Test samples, which were immersed in seawater in the pressure cell for 24 hours, resulted in abrasive material removal rates of about 0.38 mm day^{-1}. This test represents abrasion at a continuous and substained fashion and, consequently, best represents an accelerated testing condition for a low velocity (1 km hr^{-1}) range. Thus, under these removal rates, there is no danger for the

the test block to be abraded away. Similar tests will be made later at higher velocities.

The mechanism of edge breaking by mechanical impact is difficult to quantify and no attempt was made to conduct impact tests. Random impacts in handling while carrying and various tests and tasks did produce occasional loss of material in the form of broken corners or edges. Quantitatively, this effect was somewhat more pronounced in 1:1 than 3:1 mixes for both the Elrama and Conesville at the beginning of tests, where the greatest propensity to breakage seems to occur. The broken pieces did not exhibit faster degeneration by other mechanisms (discussed below) than the parent block. This suggests that the breakage is accidental and was associated, to some degree, with flaws that may have occurred when the material was first fabricated.

Certain mixes were visibly very inhomogeneous in nature, particularly mixes C3F1, C3F3 and E2C3, in which globules of scrubber sludge and lime were distinguished by their white or grey color. Results from the chemical investigation of homogeneity in element concentrations demonstrated that there was significant spatial variation in the levels of Ca in $0.028 m^3$ blocks. When submerged in test tanks, the exposed white areas would begin breaking up and eventually fell to the bottom of the tank; the amount of material lost was in direct proportion to the size and number of white occlusions. However, very little dissolution occurred.

A small but observable loss of material attributable to surface dissolution in proportion to the surface area of each block was observed for the test mixes. This loss was a maximum in the first 2-3 days after immersion and decreased to an imperceptible rate thereafter. The rate of weight loss of 0.01% for mix C3F3 occurred in the first two hours with a rapid decrease in the rate thereafter. This weight loss is higher than can be attributed to dissolution processes alone because of the unstable state of the surfaces of the test blocks after cutting from larger blocks.

6. Elastic Modulus

Every attempt was made to monitor the elastic moduli of each test block at the beginning of each test and periodically thereafter. The previous results (density) have verified the sensitivity of the elastic modulus to physical changes occurring within the block and to the yield stress of the block. A brief discussion of the measurement technique is given in Section C.

Using this instrumentation, it was possible to accurately measure the velocity of sound in each test block without physically disturbing the surfaces by placing the test sample in the path of an ultrasonic beam in the test tank. These observations lead to precise

readings of the ultrasonic velocities in various directions in each block as the sample assumes various orientations within the tank. It can be shown that the velocity of sound C_ℓ depends on the elastic modulus M and the apparent density ρ_A through the relation

$$C_\ell^2 = M/\rho_A \ .$$

The sound velocity will vary with both the water uptake and any change in modulus. Since the modulus strongly depends on the chemical composition and structure of the block material, it is a sensitive indicator of these internal changes of the block.

a. Ambient control blocks. Sets of control blocks from each composition and site group were weighed to obtain the dry mass before submerging in laboratory test tanks at room temperature. The blocks exhibit rapid uptake of water for the first few hours after placement. After the blocks degassed, it was possible to obtain the first ultrasonic readings. For each reading, weight and volume measurements were taken on each block in order to obtain ρ_A and other data. The evolution of the sound velocity in this test is shown in Figure III-7 and tabulated in Table III-7. These data show a continuous increase in C_ℓ for both Elrama 1:1 and 3:1 mixes throughout the length of the tests. The increase in strength is most dramatic

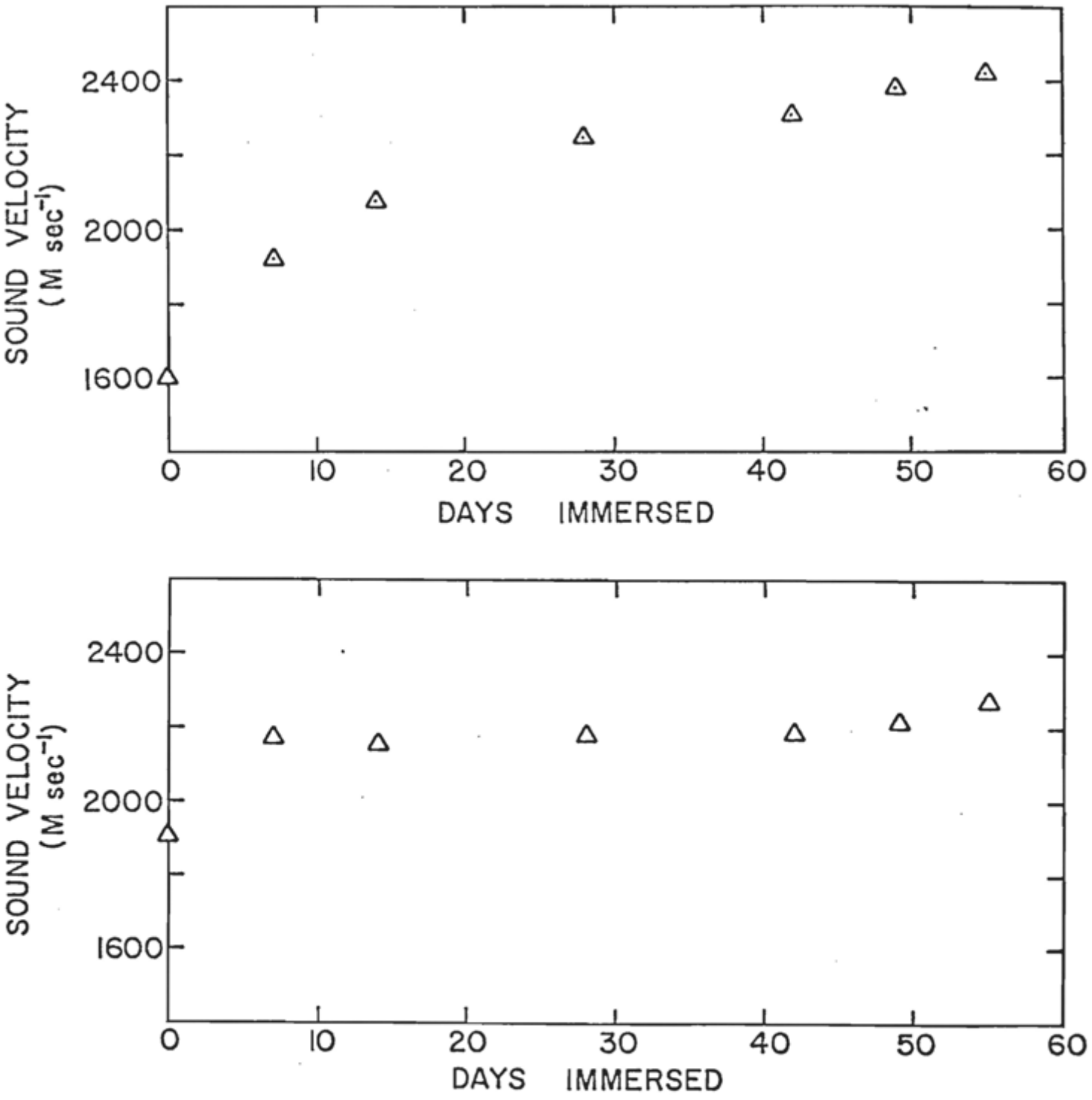

Figure III-7. Evolution of sound velocity with time of immersion in freshwater at room temperature.
(a) Average of four E2C1 type blocks.
(b) Average of four E2C3 type blocks. Individual data on each of these blocks can be found in Table III-7.

Table III-7. Sound velocity of test blocks kept in freshwater tanks at room temperature. (Velocity in m sec^{-1})

	Days Immersion						
Block	0	7	14	28	42	49	55
E2C1-1	1723	1839	2023	2186	2264	2342	2394
E2C1-8	1690	-	2129	2233	2274	2346	2398
E2C1-L7	1745	1958	2086	2247	2330	2379	2433
E2C1-L11	1697	1967	2081	2338	2400	2462	2490
Mean	1714	1921	2080	2251	2317	2382	2429
E2C3-3	1987	2170	2199	2199	2216	2235	2281
E2C3-14	1850	2249	2148	2162	2178	2203	2247
E2C3-22	1986	2168	2168	2182	2199	2239	2286
E2C3-31	1844	2131	2131	2187	2168	2207	2261
Mean	1917	2180	2162	2183	2190	2221	2269
E1C1-3	2098	2138	2152	2264	2182	2221	2247

for the E2C1 mix which initially had a C_ℓ of 2000 m sec^{-1} and increases to 2500 m sec^{-1} after 48 days. This corresponds to an increase of modulus of 50%. On the other hand, mix E2C3 had a higher sound velocity (and modulus) at the outset of the test, but increased more slowly with time, so that the sound velocity in this material is about 10% lower than that of the E3C1 mix after 48 days. This observation correlates with the results of the yield tests reported below.

The increase in sound velocity C_ℓ is associated with a strengthening of the blocks with time. It is dramatically illustrated in the high yield strength for test blocks which were removed from the Fire Island test site and subsequently tested for correlations of C_ℓ and yield strength. The results for test mix E2C3 is illustrated in Figure III-8. Yield strengths for laboratory test blocks and those retrieved from the Fire Island test site after 30 days (plus tank aging) are also shown.

Considerable scatter was found in the yield strength data. This can be attributed to the irregular shape of each block which can cause a stress anomaly in the test fixture. In spite of this, the correlation of yield strength to the ultrasonic velocity is clear. If the yield strength

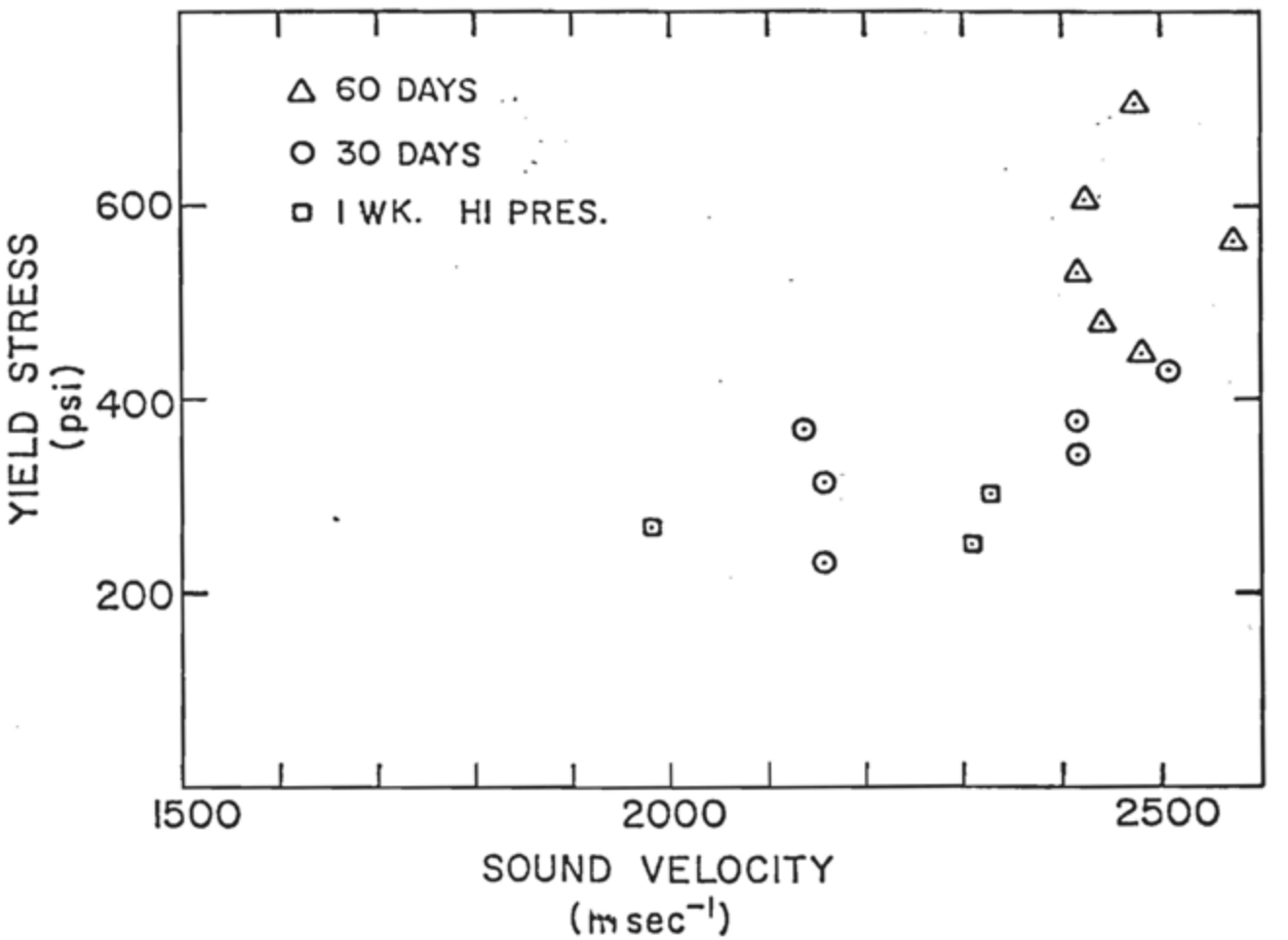

Figure III-8. Correlation of yield stress of test blocks to sound velocity. The coefficient of variation for average sound velocities in a given block is about 1% while the statistical variation due to block inhomogeneity is about 5%. The largest statistical error is attributable to the mechanism of yield.

is directly proportional to the modulus, a quadratic dependence on C_ℓ would be expected in Figure III-8. Although the data are suggestive of this dependence, verification will have to wait yield testing on a larger number of samples in order to reduce the statistical uncertainty of the yield-stress data.

b. Accelerated tests at 40°C. Data on ultrasonic velocity, which most closely reflects structural evolution of the blocks, are shown in Figure III-9 (see also Table III-8). The data from the ultrasonic velocity measurements again verify the greater propensity of E2C1 material to increase in strength in either freshwater or seawater. There appears to be no significant difference between the evolution sound velocity for test blocks in freshwater or seawater when taken by a given mix type as can be seen from the detailed data of Table III-8. In addition, as in other observations of this type, the trajectory of C_ℓ for each block taken by itself is typical for a given mix type. Three other features of these tests should be noted. The density of the blocks increase with time under accelerated tests (Table III-3). The sound velocity for the mixes at 40°C (especially 1:1 mixes) increased at about twice the rate of that for blocks at ambient temperature (25°C). There is also clear evidence that a "saturation" in the sound is setting in after 15 or so days, which may indicate that the ultimate strength of these blocks is being reached.

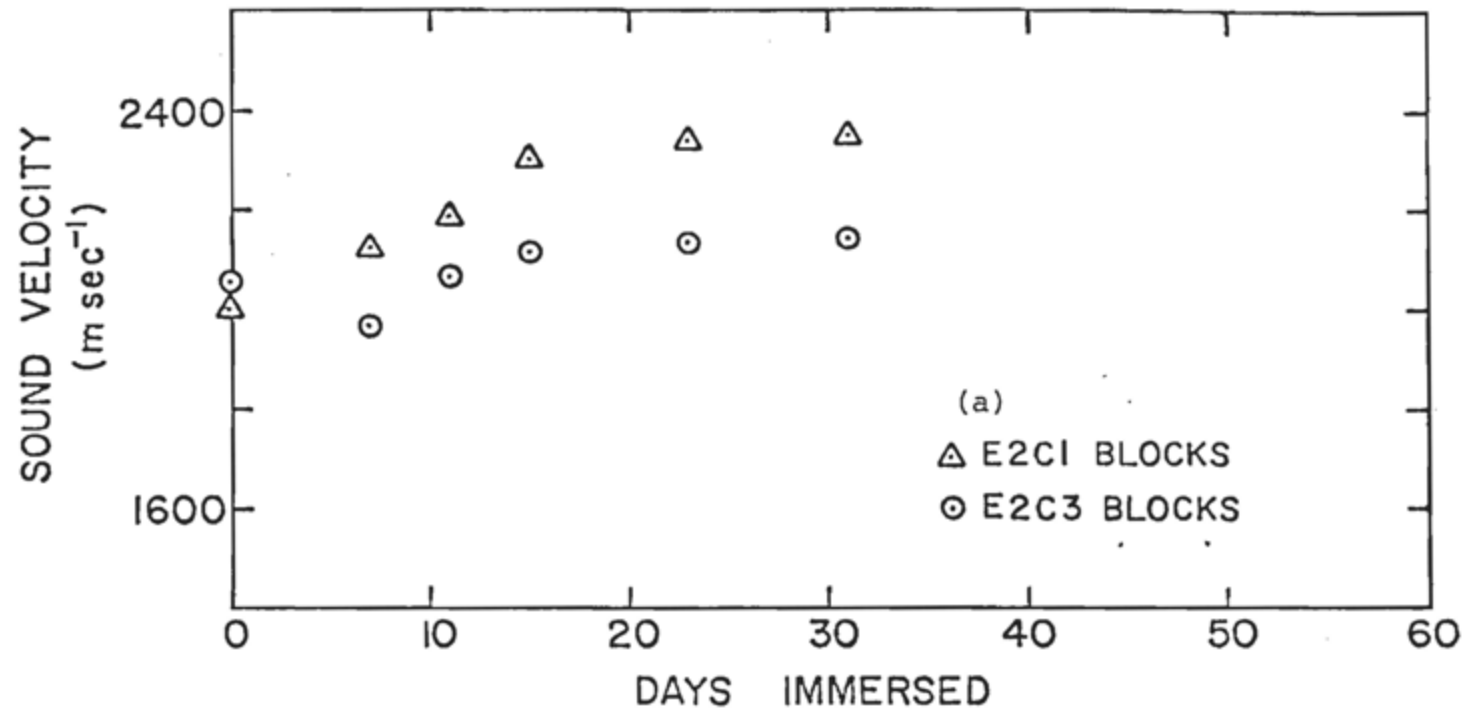

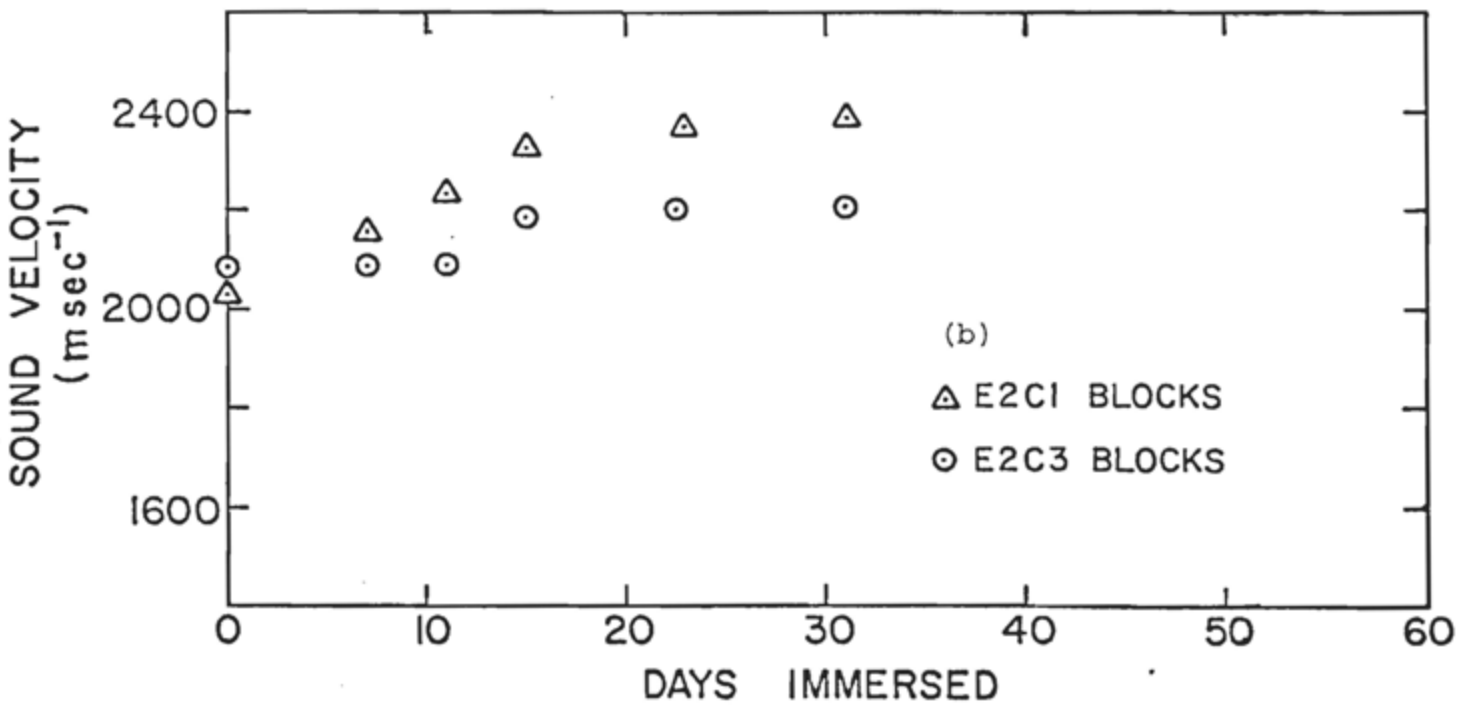

Figure III-9. Evolution of sound velocity with time of immersion in freshwater or seawater at 40°C. (a) Average of four E2C1 and three E2C3 blocks in seawater. (b) Average of four E2C1 and three E2C3 blocks in freshwater. Individual data for these blocks can be found in Table III-8.

Table III- 8. Sound velocity (m sec^{-1}) of test blocks in 40°C accelerated aging tanks

Days immersed in 40°C saltwater

Block	0	7	11	15	22	31
E2C1-2A	2004	2149	2222	2333	2349	2373
E2C1-12A	1955	2109	2210	2256	2329	2361
E2C1-L8A	2100	2156	2201	2312	2320	2352
E2C1-L10A	2064	2219	2314	2418	2464	2480
E2C1 Avg.	2031	2158	2237	2330	2365	2392
E2C3-4B	2136	2136	2150	2238	2241	2268
E2C3-15B	2029	2054	2005	2133	2154	2159
E2C3-36B	2086	2099	2112	2181	2207	2222
E2C3	2084	2096	2089	2184	2201	2216

Days immersed in 40°C freshwater

Block	0	7	11	15	22	31
E2C1-5A	2103	2232	2310	2429	2466	2482
E2C1-L3A	1862	1961	2021	2110	2180	2222
E2C1-L9A	2036	2102	2187	2296	2345	2294
E2C1-7A	2070	2193	2237	2381	2381	2388
E2C1 Mean	2018	2122	2189	2304	2343	2347
E2C3-11B	2027	2003	2077	2090	2101	2115
E2C3-13B	2110	1972	2097	2146	2159	2171
E2C3-32B	2031	1936	2043	2121	2156	2161
E2C3 Avg.	2056	1970	2072	2119	2139	2149

C. Internal Structure by Non-Destructive Testing

A major effort was expended in the experimental design of improved ultrasonic technique for the measurement and characterization of scrubber reef test samples and projected *in situ* tests. In order to carry out the large number of repetitive tests on many samples, the conventional method of bonding test transducers on each test block had to be abandoned. A non-contact method was developed which utilized a liquid test-tank in which each test block was held in the path of an ultransonic beam within the tank. The change in time delay brought about by interruption of the beam is measured by precision apparatus. This data is used in calculations to determine the velocity of sound within the scrubber block which can be accurately determined if the length of the block and the velocity of sound in the immersion liquid are known.

Since no contact is required of the test block, sound velocities can be measured along any axis of the block by simply changing orientation. Experience has shown that the delay can be measured to an accuracy of 1% in any single reading. This accuracy is being improved by the addition of improved instrumentation.

Techniques have also been investigated for attaching permanent transducers to the $0.028\ m^3$ test blocks in anticipation of *in situ* monitoring at sea for C-WARP Phase II. Studies

have shown that it will be advisable to provide a mechanical anchor for these transducers, probably in the form of a recessed section of each block about 2 cm deep into which a transducer assembly is case. This precaution is necessary in anticipation of the rough handling which the blocks will be subjected to during barge operations.

Measurements of sound velocity have shown that the acoustic energy is subject to high attenuation within the blocks, but that this attenuation drops markedly as the blocks strengthen. In order to obtain adequate penetration of the blocks, an operating frequency of 162.5 khz has been chosen (the exact frequency determined by commerically available ultrasonic transducers). This frequency will provide a resolution of slightly larger than 1 cm when signal processing techniques are applied to the data obtained from scattered energy reflected back to the sending structural changes associated with block inhomogeneities.

IV. BIOASSAYS

A. Laboratory Studies

1. Assay Procedures and Test Organisms

The bioassays followed the procedures set out by the EPA Ocean Disposal Bioassay Working Group in the publication "Bioassay Procedures for the Ocean Disposal Permit Program" (EPA-600/9-78-010). These bioassays were established to provide methods for conducting biological evaluation of materials to be disposed of in the ocean. Tests conducted according to the bioassay procedures would provide information on the toxicity of the material.

Elutriates from a number of different stabilized coal waste mixtures were assayed with laboratory organisms, the largest number being used in multi-parameter assays with cultures of unicellular algae. Algae, shrimp, and fish eggs and larvae were all tested using elutriates from mixes E2C1, E2C3, C3F1, and C3F3. The algae bioassay using the C3F3 elutriate is in progress.

2. Elutriate Preparation

The seawater elutriates were prepared in accordance with Bioassay Procedure I., "Entire life-cycle toxicity test using grass shrimp, Palaemonetes pugio Holthuis" (Tyler, Schroeder, 1978). Test blocks ($0.028 m^3$) of stabilized scrubber sludge and fly ash were broken down into small pieces and manually ground to powder with a mortar and pestle. Knowing the density of the block material, the weight of a unit volume of powdered material was diluted with four volumes of filtered (0.45 μm) seawater. After 24 hours of mechanical

agitation, the slurry was allowed to settle for at least 36 hours. From the settled mixture, the supernatant liquid was decanted and filtered through an 0.80 µm filter. The filtered solution was adjusted to the pH of the seawater and used at a range of concentrations for bioassay on the marine organisms.

3. Phytoplankton Bioassays

The basic experimental methods followed were Bioassay Procedure A. and B. in Section II "Bioassay Procedures for Routine Application," (EPA-600/9-78-010).

The experiments consisted of replicate (n = 3) 500 ml volumes each of treated (50 ml volume of elutriate added to 450 ml cell suspension) and control (50 ml volume of filtered seawater added to 450 ml cell suspensions) suspensions of Thalassiosira pseudonana cells (clone 3H) grown in nutrient enriched seawater. The elutriate concentration was 10% (V/V) of the cell suspension.

Control and treated volumes were placed in a 20°C, fluorescent tube-illuminated incubator. The suspended cell volume concentration (particle concentration, ppm by volume), chlorophyll a concentration (mg l^{-1}), and quantity of ^{14}C incorporated (counts $minute^{-1}$ ml^{-1} or cpm ml^{-1}) were determined daily in each control and treated cell suspension using methods outlined in Strickland and Parsons (1972). The amount of carbon-14 incorporated is an index of the rate of photosynthesis in the cultured algal cells. Replicate samples (n = 2) were analyzed for each variable for each control and treated flask. The results of the two replicate analyses were averaged and

estimated the value of the variable for the flask for each day.

The results of the bioassays are presented in Tables IV-1 to IV-3. A single classification ANOVA (Sokal and Rohlf, 1969) was used to test for statistically significant differences between control ($\bar{X}_C$) and treatment ($\bar{X}_T$) means (n=3). No significant differences were found for the bioassays employing the Elrama elutriates. The data analysis in Table IV-3 for day 1 suggest that $\bar{X}_T > \bar{X}_C$ for chlorophyll a and cell volume concentrations for cells exposed to the elutriate prepared from the Conesville fine 1:1 material.

These results indicate that the elutriates employed in these bioassays produced no inhibitory effects on the growth of the algal species used.

4. Animal Bioassays

The basic experimental methods followed were Bioassay Procedure K., "Static method for acute toxicity tests using fish and macroinvertebrates" (Hansen, Schimmel, Nimmo and Lowe, 1978). At least 20 test animals were exposed to four or more concentrations of a seawater elutriate of the coal waste material; replicate treatments were run when possible. An equal number of animals in test vessels of seawater were used as controls. Representative samples of test animals were distributed impartially to test containers by adding one or two animals at a time to each container repeatedly until the desired number of test animals was reached in each container.

Table IV-1 Elrama coarse 1:1 elutriate test - Thalassiosira pseudonana

	Chlorophyll a ($\mu g\ l^{-1}$)	Suspended Cell Volume (ppm)	^{14}C Uptake ($cpm\ ml^{-1}$)
Day 0	$\bar{X}_O = 4.69$ $s_o = 0.78$	$\bar{X}_O = 1.11$ $s_o = 0.01$	$X_O = 68$ $s_o = 32$

Single classification ANOVA tables: $H_o: \bar{X}_C = \bar{X}_T$, $F(0.025, 1, 4) = 12.2$; $F(0.01, 1, 4) = 21.20$

Day 1

	Chlorophyll a ($\mu g\ l^{-1}$)	Suspended Cell Volume (ppm)	^{14}C Uptake ($cpm\ ml^{-1}$)
	$\bar{X}_C = 26.07$ $s_C = 2.85$	$\bar{X}_C = 6.61$ $s_C = 0.70$	$\bar{X}_C = 176$ $s_C = 22$
	$\bar{X}_T = 25.23$ $s_C = 0.48$	$\bar{X}_T = 5.70$ $s_T = 0.21$	$\bar{X}_T = 195$ $s_T = 40$

	SS	df	MS	F	SS	df	MS	F	SS	df	MS	F
TREATMENT	1.07	1	1.07	0.26	1.25	1	1.25	4.72	580	1	580	0.55
ERROR	16.70	4	4.18		1.06	4	0.27		4,203	4	1,050	
TOTAL	17.77	5			2.31	5			4,783	5		

Day 2

	Chlorophyll a ($\mu g\ l^{-1}$)	Suspended Cell Volume (ppm)	^{14}C Uptake ($cpm\ ml^{-1}$)
	$\bar{X}_C = 185.11$ $s_C = 10.70$	$\bar{X}_C = 30.73$ $s_C = 0.87$	$\bar{X}_C = 1,289$ $s_C = 108$
	$\bar{X}_T = 179.16$ $s_T = 19.83$	$\bar{X}_T = 29.39$ $s_T = 3.50$	$\bar{X}_T = 1,374$ $s_T = 111$

	SS	df	MS	F	SS	df	MS	F	SS	df	MS	F
TREATMENT	53.16	1	53.16	0.21	2.72	1	2.72	0.42	10,795	1	10,795	0.90
ERROR	1,015.65	4	253.91		26.03	4	6.51		47,822	4	11,955	
TOTAL	1,068.81	5			28.75	5			58,617	5		

Day 3

	Chlorophyll a ($\mu g\ l^{-1}$)	Suspended Cell Volume (ppm)	^{14}C Uptake ($cpm\ ml^{-1}$)
	$\bar{X}_C = 527.57$ $s_C = 33.03$	$\bar{X}_C = 82.12$ $s_C = 12.51$	$\bar{X}_C = 2,356$ $s_C = 84$
	$\bar{X}_T = 528.59$ $s_T = 45.64$	$\bar{X}_T = 84.24$ $s_T = 8.96$	$\bar{X}_T = 1,974$ $\bar{X}_T = 173$

	SS	df	MS	F	SS	df	MS	F	SS	df	MS	F
TREATMENT	1.55	1	1.55	.001	6.72	1	6.72	0.006	218,695	1	218,695	11.82
ERROR	6,347.6	4	1,586.90		473.47	4	118.37		73,997	4	18,499	
TOTAL	6,349.15	5			480.19	5			292,692	5		

Since none of the F values calculated exceeds $F(0.025, 1, 4) = 12.2$; $F(0.01, 1, 4) = 21.20$ the null hypothesis can not be rejected. Control and treatment means are not significantly different.

	Chlorophyll a ($\mu g\ l^{-1}$)	Suspended Cell Volume (ppm)	^{14}C Uptake ($cpm\ ml^{-1}$)
Day 0	$\bar{X}_o = 3.46$ $s_o = 0.08$	$\bar{X}_o = 1.48$ $s_o = 0.03$	$\bar{X}_o = 38$ $s_o = 8$

Single classification ANOVA tables: $H_o: \bar{X}_C = \bar{X}_T$, $F(0.025, 1, 4) = 12.2$; $F(0.01, 1, 4) = 21.20$

Day 1

	$\bar{X}_C = 25.09$ $s_C = 0.93$ $\bar{X}_T = 24.66$ $s_T = 1.02$				$\bar{X}_C = 6.42$ $s_C = 0.35$ $\bar{X}_T = 6.42$ $s_T = 0.53$				$\bar{X}_C = 166$ $s_C = 37$ $\bar{X}_T = 145$ $s_T = 56$			
	SS	df	MS	F	SS	df	MS	F	SS	df	MS	F
TREATMENT	0.28	1	0.28	0.29	2×10^{-5}	1	2×10^{-5}	8×10^{-5}	641	1	641	0.29
ERROR	3.82	4	0.96		0.804	4	0.201		8,978	4	2,245	
TOTAL	4.10	5			0.804	5			9,619	5		

Day 2

	$\bar{X}_C = 226.97$ $s_C = 23.82$ $\bar{X}_T = 221.65$ $s_T = 11.39$				$\bar{X}_C = 37.99$ $s_C = 2.62$ $\bar{X}_T = 34.87$ $s_T = 4.54$				$\bar{X}_C = 1,599$ $s_C = 199$ $\bar{X}_T = 1,629$ $s_T = 182$			
	SS	df	MS	F	SS	df	MS	F	SS	df	MS	F
TREATMENT	42.40	1	42.40	0.12	14.66	1	14.66	1.07	1,411	1	1,411	0.04
ERROR	1,394.68	4	348.67		54.90	4	13.73		145,873	4	36,468	
TOTAL	1,437.08	5			69.57	5			147,284	5		

Day 3

	$\bar{X}_C = 622.36$ $s_C = 17.43$ $\bar{X}_T = 587.27$ $s_T = 53.78$				$\bar{X}_C = 43.76$ $s_C = 1.82$ $\bar{X}_T = 48.41$ $s_T = 6.02$				$\bar{X}_C = 2,073$ $s_C = 45$ $\bar{X}_T = 1,408$ $s_T = 384$			
	SS	df	MS	F	SS	df	MS	F	SS	df	MS	F
TREATMENT	1,846.61	1	1,846.61	1.16	32.48	1	32.48	1.64	663,338	1	663,337	3.47
ERROR	6,392.11	4	1,598.03		79.08	4	19.77		764,991	4	191,248	
TOTAL	8,238.72	5			111.56	5			1,428,329	5		

Since none of the F values calculated exceeds $F(0.025, 1, 4) = 12.2$; $F(0.01, 1, 4) = 21.20$ the null hypothesis can not be rejected. Control and treatment means are not significantly different.

Table IV-3 Conesville fine 1:1 elutriate test - *Thalassiosira Pseudonana*

	Chlorophyll *a* ($\mu g\ l^{-1}$)	Suspended Cell Volume (ppm)	^{14}C Uptake (cpm ml^{-1})
Day 0	$\bar{X}_o = 0.92$ $s_o = 0.08$	$\bar{X}_o = 0.50$ $s_o = 0.02$	$\bar{X}_o = 111$ $s_o = 31$
	Single classification ANOVA tables: $H_o \bar{X}_C = \bar{X}_T$, F (0.025, 1, 4) = 12.2; F (0.01, 1, 4) = 21.20		
Day 1	$\bar{X}_C = 3.94$ $s_C = 0.25$	$\bar{X}_C = 1.96$ $s_C = 0.12$	$\bar{X}_T = 151$ $s_T = 49$
	$\bar{X}_T = 4.60$ $s_T = 0.10$	$\bar{X}_T = 2.57$ $s_T = 0.18$	$\bar{X}_C = 217$ $s_C = 85$

	SS	df	MS	F	SS	df	MS	F	SS	df	MS	F
TREATMENT	0.65	1	0.65	18.76	0.57	1	0.57	24.66	6,600	1	6,600	1.38
ERROR	0.14	4	0.03		0.09	4	0.02		19,185	4	4,796	
TOTAL	0.79	5			0.66	5			25,785	5		

Day 2	$\bar{X}_C = 32.52$ $s_C = 0.91$	$\bar{X}_C = 6.98$ $s_C = 0.70$	$\bar{X}_T = 243$ $s_T = 37$
	$\bar{X}_T = 35.43$ $s_T = 2.40$	$\bar{X}_T = 8.41$ $s_T = 1.01$	$\bar{X}_C = 346$ $s_C = 73$

	SS	df	MS	F	SS	df	MS	F	SS	df	MS	F
TREATMENT	12.64	1	12.64	3.83	3.05	1	3.05	4.07	15,811	1	15,811	4.74
ERROR	13.20	4	3.30		3.00	4	0.75		13,346	4	3,336	
TOTAL	25.84	5			6.05	5			29,157	5		

Day 3	$\bar{X}_C = 186.13$ $s_C = 15.29$	$\bar{X}_C = 29.00$ $s_C = 2.07$	$\bar{X}_C = 612$ $s_C = 30$
	$\bar{X}_T = 232.88$ $s_T = 18.38$	$\bar{X}_T = 34.02$ $s_T = 4.34$	$\bar{X}_T = 828$ $s_T = 118$

	SS	df	MS	F	SS	df	MS	F	SS	df	MS	F
TREATMENT	3,277.41	1	3,277.41	11.46	37.70	1	37.70	3.26	69,768	1	69,786	9.49
ERROR	1,143.49	4	285.87		46.23	4	11.56		29,419	4	7,355	
TOTAL	4,420.90	5			83.93	5			99,187	5		

The ANOVA for Day 1 suggests that $\bar{X}_C < \bar{X}_T$ for chlorophyll *a* ($P<0.025$) and cell volume concentrations ($P<0.01$). For the remainder of the results, the null hypothesis can not be rejected.

The assays were carried out in polyethylene containers held in controlled laboratories with constant temperature, humidity, and lighting conditions throughout the experiments. The tests were run over 96 hrs and the organisms were examined daily with records being made of the number of dead or affected animals at 24 hr intervals throughout the test. Dead animals were removed if observed. On completion of each bioassay, the elutriates were replaced with seawater and the test organisms were observed for a further 24 hr period.

a. Sand shrimp. Sand shrimp, Crangon septemspinosa, were taken from Flax Pond, an arm of Long Island Sound, using a beach seine. As recommended in the EPA bioassay procedures, the shrimp used in the assays were all less than 10 cm (rostrum to telson length ranging from 9 mm to 25 mm). The shrimp were acclimated in the laboratory for 4 days at ambient temperatures of 6°C, the sea temperature at which they had been caught, before being used in the bioassays run at the same temperature. The shrimp were fed during the holding period but not during the 96 hour assay exposure to the various elutriate concentrations.

During initial screening tests made with very high concentrations of the elutriates, the only significant mortalities occurred in tests with full 100% concentrations of elutriate when 25% of the shrimp died over a 96 hour test period. The results of the elutriate assay with sand shrimp are given in Table IV-4.

b. Flounder eggs and larvae. The eggs and larvae of fish are

Table IV-4. Bioassay of coal waste elutriates on sand shrimp.

Material	Elutriate	# Dead (day) 1	2	3	4	# Live	% Mortality
Conesville 1:1	10%	0	0	0	0	25	0
	25%	0	0	0	0	25	0
	40%	0	0	0	0	25	0
Conesville 3:1	10%	0	0	0	0	25	0
	25%	0	0	0	0	25	0
	40%	0	0	0	0	25	0
Control		0	0	0	0	25	0
Elrama 1:1	10%	0	0	0	0	22	0
	30%	0	0	0	1	20	5
	60%	0	0	0	0	27	0
Elrama 1:1 Replicate	10%	0	0	0	0	22	0
	30%	0	0	0	0	19	0
	60%	0	0	0	0	23	0
Elrama 3:1	10%	0	0	0	0	24	0
	30%	0	0	0	0	25	0
	60%	0	0	0	0	27	0
Control 1		0	0	0	0	26	0
Control 2		0	0	0	0	26	0

especially sensitive developmental stages and are particularly appropriate for use in bioassays. The winter flounder, Pseudopleuronectes americanus, spawns in inshore waters around Long Island, laying demersal eggs which are attached to substrates on the sea bed. Winter flounder occur very commonly at the Fire Island artificial reef site.

Eggs of winter flounder, spawned and fertilized at 5°C, were held at that temperature for several days in flow-through seawater aquaria at the Flax Pond Lab prior to bioassay. The assays were made at the advanced embryo stage H (Klein-McPhee, 1978) shortly before activation of the hatching process. At hatching, some mortalities occurred in all samples, including the controls. Statistical analysis revealed no significant differences between the mortalities occurring in the various concentrations of elutriates and in the replicate control samples (Table IV-5).

After the hatching of the flounder eggs was completed, the yolk-sac stage larvae were used in a future set of assays. Almost no mortalities occurred at any elutriate concentrations or in the replicate control samples over the four day assay period (Table IV-5). The exposure to the elutriate concentrations was extended for two further days but no additional mortalities were recorded.

Table IV-5. Bioassay of coal waste elutriates on winter flounder eggs a
larvae.

Stage	Material	Elutriate	(day)	# Dead 1	2	3	4	# Live	% Mortali
Larvae	Conesville	1:1	10%	0	0	0	0	25	0
			25%	0	0	0	0	25	0
			40%	0	0	0	0	25	0
	Conesville	3:1	10%	0	0	0	0	26	0
			25%	0	0	0	0	25	0
			40%	0	0	2	0	26	8
	Elrama	1:1	10%	0	0	0	0	26	0
			25%	0	0	0	0	25	0
			40%	0	0	0	0	27	0
	Elrama	3:1	10%	0	0	0	0	24	0
			25%	0	0	0	0	25	0
			40%	0	0	0	0	25	0
	Control 1			0	0	0	0	23	0
	Control 2			0	0	0	0	25	0
Egg	Conesville	1:1	10%	3	1	1	1	18	25
			25%	5	1	0	0	19	24
			40%	4	1	0	0	21	19
	Conesville	3:1	10%	3	3	0	0	21	22
			25%	3	2	0	0	20	25
			40%	6	0	0	0	22	21
	Elrama	1:1	10%	2	4	0	0	20	23
			25%	2	1	3	1	22	24
			40%	3	2	1	0	19	24
	Elrama	3:1	10%	2	3	0	0	20	25
			25%	1	6	0	0	21	25
			40%	6	1	1	0	18	31
	Control 1			0	4	0	0	19	17
	Control 2			2	3	0	0	20	25

The results of the flounder egg bioassays (Table IV-5) were analyzed using a two way ANOVA without replication (Sokal and Rohlf, 1969). The results of the analysis are given in Table IV-6.

It was concluded that there was no significant differences between the mortalities of the eggs in the control assay and any of the coal waste elutriate concentrations for any of the coal waste mixes.

5. Discussion

The results of the laboratory bioassays carried out to date suggest that the elutriates from both the Elrama and Conesville coal waste mixes did not have toxic effects on either the cultures of phytoplankton or the animals used. It was noteable that fish eggs and larvae are sensitive early life stages for such assays but experienced no significant increases in mortalities for the elutriates at any concentration. It is emphasized that the elutriate concentrations used for these assays far exceeded any that might occur in situ.

B. Biological Acceptability of Blocks In Situ

1. Colonization of Test Blocks

a. Atlantic project site. Test blocks of stabilized coal wastes were placed in trays on the seabed at the project test site. The blocks were of two sizes, 7.5 x 10 x 15 cm and 7.5 x 10 x 5 cm. Concrete blocks of the same size were also set out in trays at the site at the same time. The test

Table IV-6. ANOVA of flounder egg bioassays.

Source of Variation	df	ss	Ms	Fs
Coal Mix	3	12.51	4.17	1.369 ns
Elutriate Conc.	3	13.15	4.38	1.439 ns
Error	9	27.42	3.05	
Total	15	53.07		

blocks were subsequently retrieved for various laboratory tests and were examined for biological settlement and colonization.

Although winter is the season when the early, larval life stages of benthic organisms are few in number in the plankton, biological settlement was observed on the test-blocks within one month of placement. Subsequent recoveries of test blocks from the site revealed continued settlement of increased numbers of organisms. Analysis of the size frequencies of some of the settled organisms showed that growth had occurred on the test blocks with overall sizes of the organisms increasing with time.

The material most sampled in this first period was coal waste mix E1C3. Biological settlement and growth on blocks of this material in the Atlantic are compared below with settlement on concrete blocks over the same period from October to January. During that three month period, at least eight different species settled upon blocks of both types. The organisms were two species of tubicolous polychaetes, two species of stonofierous hydroids, two species of encrusting bryozoans, one species of sessile bryozoan, and a barnacle. The numbers of organisms belonging to different groups which had settled on sample blocks of E1C3 and concrete during the period are given in Table IV-7. The total numbers of animals settled upon individual blocks retrieved from the Atlantic are shown for both E1C3 and concrete in Figure IV-1.

Table IV-7. Number of animals settled on test blocks placed in the Atlantic in October 1978*.

Animals	November		December		January	
	E1C3	Conc	E1C3	Conc	E1C3	Conc
Hydroids	2	15	-	-	3	5
Bryozoa	72	57	104	188	87	175
Polycheates	11	50	28	61	9	62
Barnacles	1	1	-	-	-	-
Total	86	123	122	259	99	242

* The numbers are for the total animals settled on three test-blocks of each material, at each time of sampling.

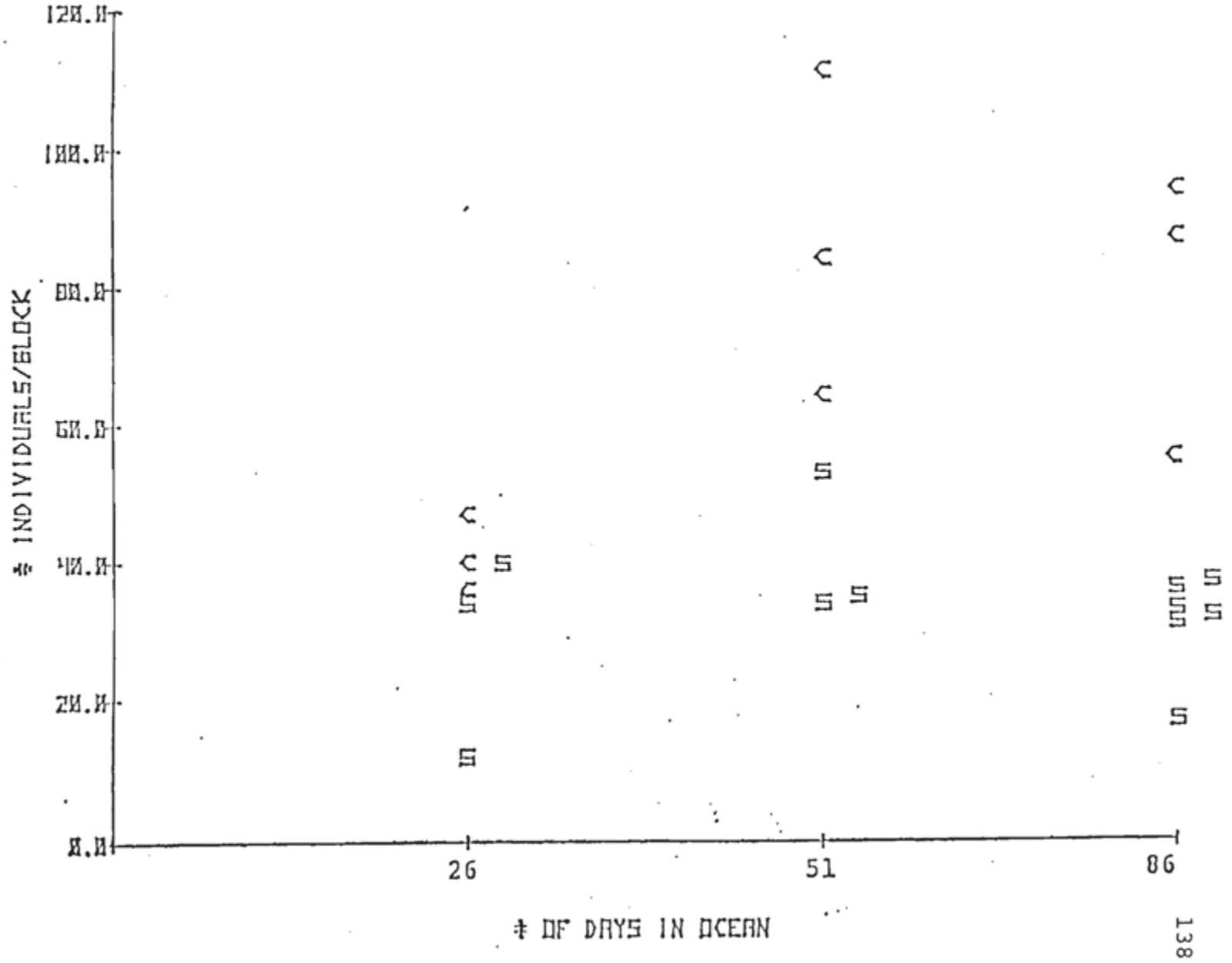
120.0
100.0
80.0
60.0
40.0
20.0
0.0
INDIVIDUALS/BLOCK
26
51
86
OF DAYS IN OCEAN

Less animals had settled on the stabilized coal waste blocks than on the concrete controls at each occasion of sampling, but some settlement occurred on both materials from the start. Animals of the same species occurred on both materials. There may have been some preferential settlement by bryozoa (particularly of foliose bryozoa) on the coal waste relative to other organisms settling on that material, but sample variability was probably too great to confirm this at this stage. Between November and December, the numbers of settled organisms increased on both materials, but no further settling appeared to have occurred after this period. The hiatus in settling may have been due to relatively few larval forms being available in mid-winter, or because transient sand waves on the seabed were observed to partially cover the trays of blocks during this stormy period, inhibiting settling or causing the death of some organisms.

The animals which settled on the test blocks grew as individuals, or, in the case of colonial species, increased in colony size. Measurements of growth and size distributions of organisms may provide valuable indices in making assessments of colonization by animals. Some of the most numerous animals colonizing the test blocks were encrusting colonies of bryozoans, probably Membranipora sp. The diameter measured of these encrusting colonies increased from one sample set to the next. This is illustrated in Figure IV-2 as size

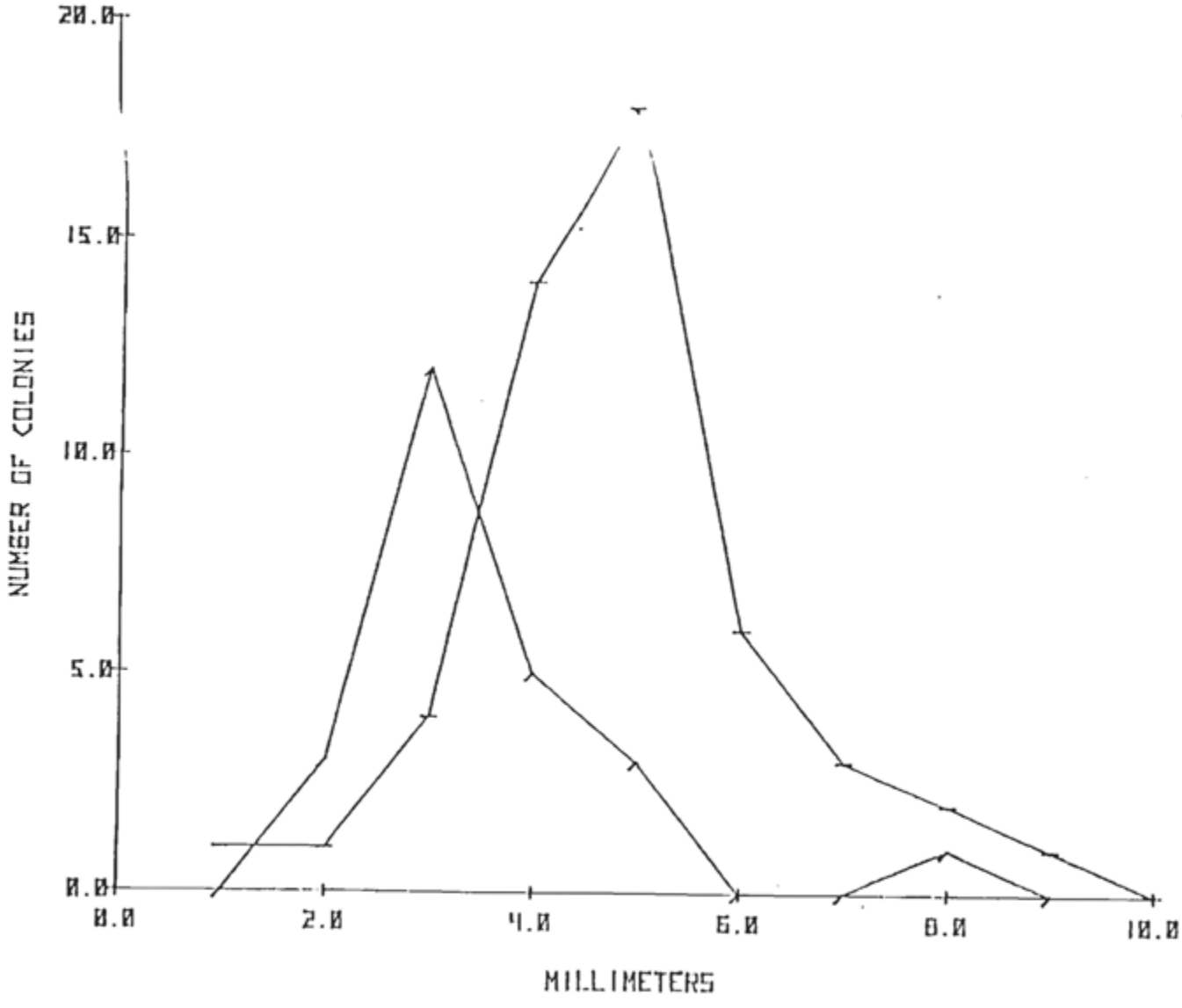

Figure IV-2a. Diameter of encrusting colonies of bryozoa growing on E1C3 (S) and concrete (C) after 26 days.

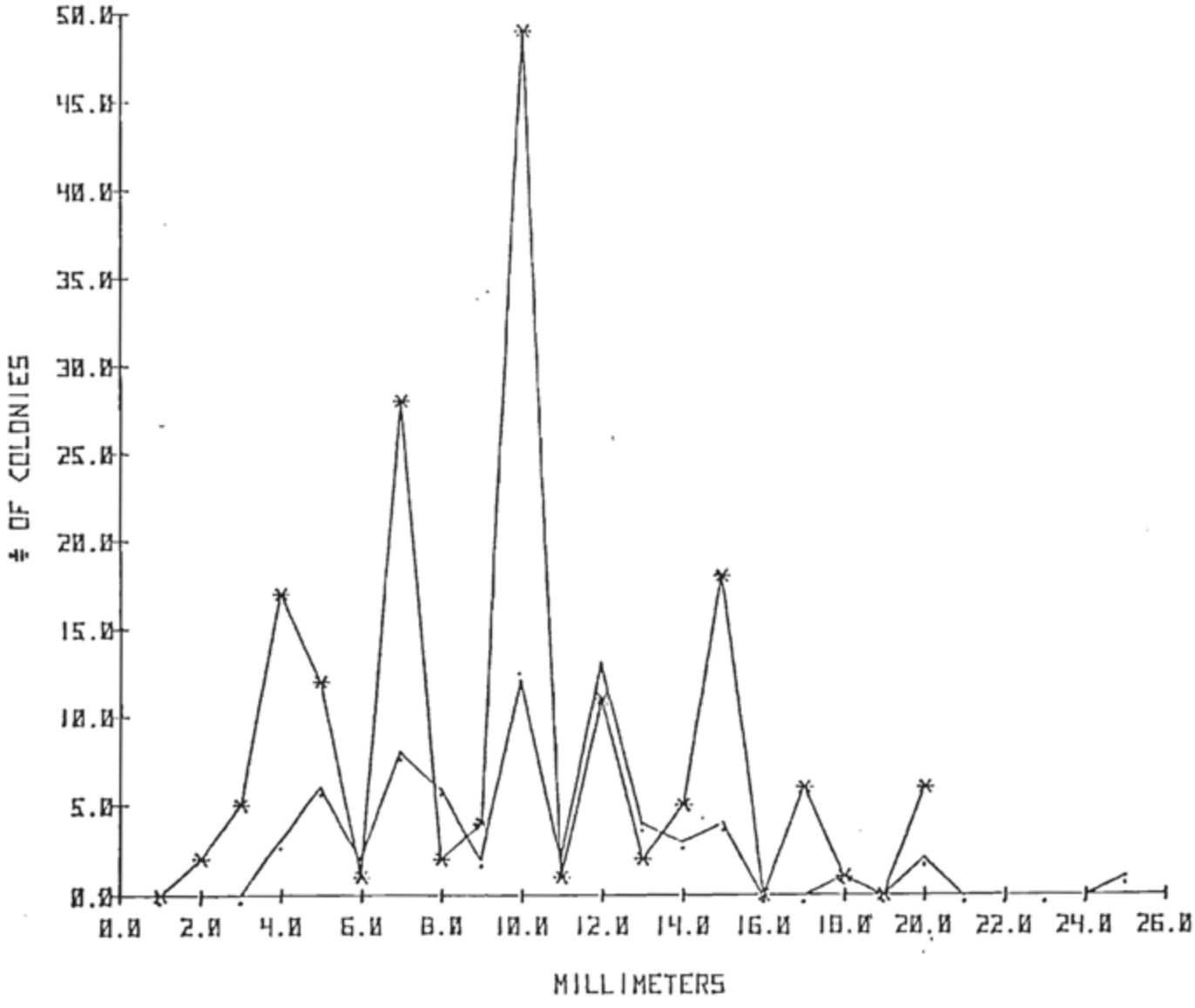

Figure IV-2b. Diameter of encrusting colonies of bryozoa growing on E1C3 (S) and concrete (C) after 51 days.

distributions for colonies of encrusting bryozoans after 26 days and 51 days exposure of the test blocks of material E1C3 and concrete controls. On both materials, the colonies were of rather similar sizes after 26 days (2 to 8 mm), and also after 51 days (4 to 20 mm diameter). Thus, although smaller numbers of encrusting bryozoans occurred on coal waste E1C3 than on concrete blocks, once settled, the colonies on blocks of both materials were of similar size distributions and were apparently growing at the same rates.

An incidental observation of coal waste test block habitation by macroinvertebrates at the Atlantic project site was made in November and again in December, when divers found rock crabs, Cancer irroratus, and a few lobsters, Homarus americanus, settled among the trays of test blocks. The crabs and lobsters were not seen on the open seabed in the vicinity and it was concluded that they had aggregated at the site. Numerous gammarid amphipods, Gammarus duebeni, were also found swimming around the blocks, but it is less clear whether they were aggregated at the site, or were more generally distributed. Similar behavior, but by fish, had been reported for the Conscience Bay project site, when bergals, Tautogolabrus adspersus, were observed to swim in among the test blocks and take up habitation almost as soon as the blocks were placed at the site.

b. Flax Pond laboratory. The Marine Sciences Research Center (MSRC) maintains an excellent marine laboratory at Flax Pond, on an arm of Long Island Sound. The laboratory

has large sea table aquaria, 12 ft. x 4 ft. x 2 ft. deep, supplied by running seawater pumped from the Sound. The seawater is at natural ambient temperature and salinity and carries plankton, including the spores and larvae, of many marine benthic organisms.

In mid-December, blocks of the stabilized coal waste materials, E1C1, E1C3, E2C1, and E2C3 were placed in illuminated sea table aquaria with a slow, continuous flow of seawater, Table I-5. Few larval forms or spores were present in the plankton in mid-winter when Long Island Sound, including Flax Pond, was frozen over by the severe weather conditions. Nevertheless the test blocks were settled by algae and an associated community of microorganisms within weeks of being placed in the aquaria. After only five weeks, the surfaces of the blocks were covered by growths of a chain-forming diatom, Melosira varians. After eight weeks, the chains of Melosira formed extensive overgrowths on the blocks. The diatom colonies contained a diverse community of micro-organisms including other diatoms, the blue-green alga, Oscillatoria, and numerous rotifers, nematodes, and protozoa living in intimate association with the coal waste blocks.

c. Conscience Bay. In May 1977, nine 0.028 m^3 blocks of Elrama coal waste, with a fly ash:sludge ratio of 5:1 were placed in Conscience Bay, Long Island Sound. At low tide, the blocks were about 5 m deep, at high tide about 7 m deep. The blocks were arranged (Figure IV-3) to expose surfaces to seawater and, at the same time, provide crevices for the biological colonization. A duplicate set of concrete blocks was placed in the

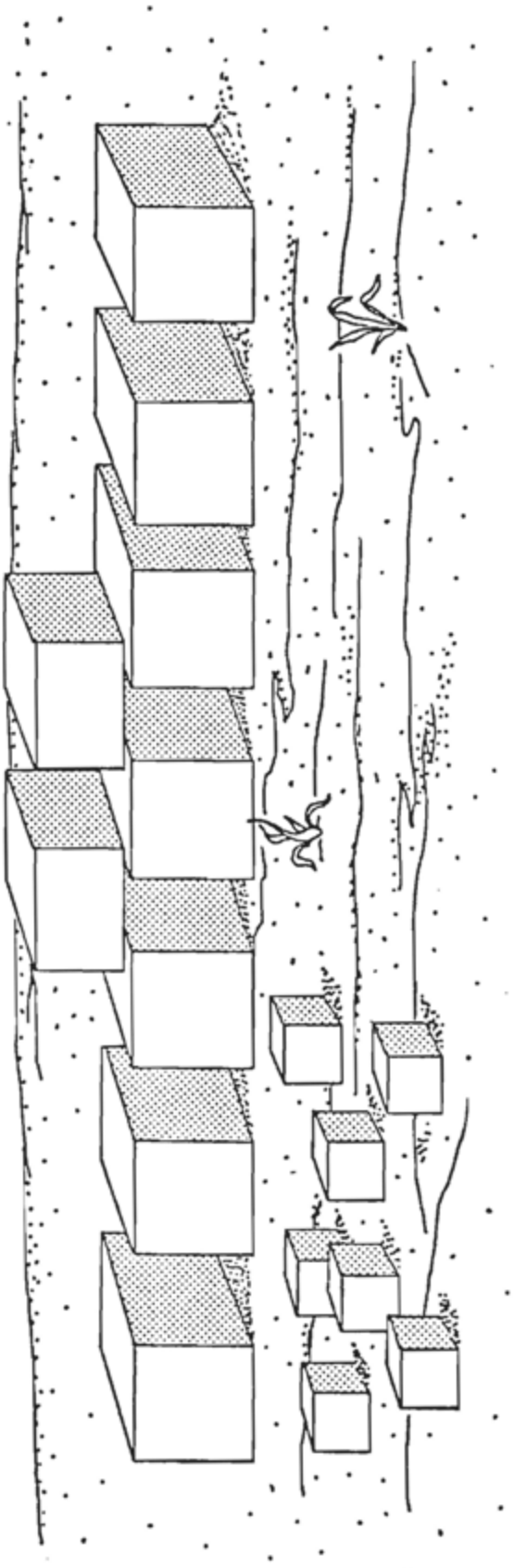

Figure IV-3. Conscience Bay reef block configuration.

same arrangement on the seabed nearby. The site was periodically visited by divers to make observations on biological colonization on the blocks and to photograph them.

Of the organisms observed growing on the blocks, hydroids were early colonizers on both coal waste and concrete. The colonies were first observed only 20 days after block placement and were about 1 cm long. By 55 days following placement, small patches of both red and green algae were observed on both substrates, while many small encrusting colonizes of bryozoans were encountered on the coal waste blocks. Eighty-two days after placement the algal colonies were observed to have increased in abundance and size and covered about 30% of the surface area of the coal waste blocks. The hydroid colonies reached a length of 5-10 cm. Numerous slipper limpets were observed attached to the concrete surfaces. Calcareous casings of polychaete tube worms (spirorbids) were also observed on both materials. By the 111th day following placement, bryozoan colonies were seen on concrete surfaces but less extensively than on the coal blocks. Many limpets were encountered on concrete, but none were seen on the coal waste blocks. One hundred seventy-four days after placement, there were very heavy growths of diverse colonizers, dominated by algae, on the tops of both the coal waste and concrete blocks. Snails, and their grazed tracks, could be seen on the top surfaces of these blocks.

In the second year of observation, more than 460 days after placement, bryozoan, hydroid, and algal growths were very extensive, covering all exposed surfaces. The differences in colonization of coal wastes and concrete which were seen at the earlier stages of colonization in the study were no longer evident. The bryozoan colonies and tube worms dominated the sides of the blocks, with algae and hydroids attached to the tops, sides, corners, and edges. The colonizers appeared to form a stable community. Fish, crabs, and snails were commonly found grazing and browsing on the dense growths. The macroinvertebrates and fish are listed in Tables IV-8 and IV-9.

More stablizied coal waste blocks of new materials were placed at the Conscience Bay test site in May 1978. The new blocks were set out in groups of nine in the same arrangement that had been adopted in May 1977 (Figure IV-3). The materials consisted of Elrama and Conesville mixes, both of the fly ash:sludge ratio of 1:1. The control materials were blocks of concrete and also six large natural rocks (glacial erratics).

The blocks of different materials were again used as substrates for biological settlement and overgrown by colonizing organisms in very similar manner to that observed in the 1977 in situ studies. Colonization of the two stabilized scrubber sludges, Elrama 1:1 and Conesville 1:1, closely resembled each other and followed the colonization

Table IV-8. Macroinvertebrates associated with the coal waste blocks placed in Conscience Bay.

Phylum Porifera (sponges)

Cliona celata
Microciona prolifera

Phylum Coelenerata

Tubularia sp.
Bougainvillea superciliaris
Obelia dichotoma
Sertularia sp.

Phylum Annelida (segmented worms)

Hydroides dianthus
Serpula vermicularis
Diopartra cupraea
Hydroides dianthus

Phylum Mollusca (snails and bivalves)

Acmaea testudinalis
Busycon canaliculatum
Venus mercenaria
Ostrea virginica
Polinices heros
Barnea truncata
Crepidula fornicata

Phylum Bryozoa

Schizoporella unicornis
Lepralia pallasiana
Membranipora pilosa

Phylum Echinoderma (star fish)

Arbacia punctulata
Asterias forbesi

Phylum Arthropoda (crabs)

Pagurus longicarpus
Neomysis americana
Libinia emarginata

Table IV-9. Fish associated with the coal waste blocks placed in Conscience Bay

Common name	
Blackfish	*Tautoga onitis*
Silversides	*Menidia menidia*
Scup	*Stenotomus chrysops*
Toadfish	*Opsanus tau*
Cunner	*Tautogolobrus adspersus*
Winter flounder	*Pseudopleunonectes americanus*
Killifish	*Fundulus heteroclitus*

process observed for the Elrama (5:1) blocks of the previous year. Hydroids were early colonizers, as were small colonies of encrusting bryozoans. The coal waste blocks could be distinguished from the concrete blocks by their colonizing communities in the first months of placement in Conscience Bay. After the blocks had been completely overgrown, the diversity of organisms colonizing both groups of blocks tended to converge and the blocks became indistinguishable from each other.

The processes of colonization and subsequent dense overgrowth of the blocks, their habitation by motile animals, and the interactions occurring within these communities were very complex, - much more so than appears in the short descriptions above. To more completely illustrate the colonizing community, a 4-minute underwater film was made.

2. Uptake of Metals By Biota

Samples of organisms living on the surfaces of the coal waste blocks were collected from the Conscience Bay site by SCUBA divers. The samples of encrusting organisms were removed from the Elrama 5:1 mix and concrete blocks at the center of each arrangement during August and September 1977. The organisms removed encompassed a sufficient area of the blocks to include a representative sample of invertebrates and algae present. In the laboratory, samples were rinsed in triple-distilled water to remove surface particles and salt. Organisms were freeze-dried for 48 hours; the dehydrated biomass was finely ground with a

Table IV-10. Metals concentration (ppm by weight) in encrusting biomass. Data are means of replicate (n=3) analyses of samples collected on 16 August and 13 September 1977.

Metal	Collection date	Concentration in Coal Waste Biomass Sample ($\bar{X}_s$)	Concentration in Concrete biomass sample ($\bar{X}_{con}$)	"t" test result **
Cd	8/16	0.29	0.60	N.S.
	9/13	0.43	0.55	N.S.
Pb	8/16	40.2	37.7	N.S.
	9/13	33.4	40.4	*
Cu	8/16	46.2	49.7	N.S.
	9/13	59.8	63.5	N.S.
Cr	8/16	22.8	26.8	N.S.
	9/13	22.4	23.1	N.S.
Zn	8/16	287	232	N.S.
	9/13	201	239	*

Hg and Ag concentrations were below instrumental detection limits.

**The hypotheses $H_o: \bar{X}_s = \bar{X}_{con}$, $Ha: \bar{X}_s > \bar{X}_{con}$ or $\bar{X}_s < \bar{X}_s$ were tested for each date, using Student's "t" distribution $\alpha = 0.10$ (Sokal and Rohlf, 1969), where $\bar{X}_{con}$ and $\bar{X}_s$ are mean metals concentrations measured on replicate analyses of samples obtained from concrete and SCPW surfaces, respectively. N.S. indicates no significant difference observed, i.e. H_o: could not be rejected.

*Indicates the rejection of $H_o: \bar{X}_s = \bar{X}_{con}$; in both cases, $\bar{X}_{con}$ was signficantly larger than $\bar{X}_s$.

quartz mortar and pestle. Three 1 g aliquots of each sample were weighed, digested with concentrated HNO_3 and analyzed for Cd, Pb, Cu, Cr, Zn, Hg and Ag using atomic absorption spectrophotometry and our previously described methods (MSRC, 1978).

The results of metals analysis of colonizer biomass collected in August and September 1977 are presented in Table IV-10. There was no evidence of elevated levels of trace metals in the biomass collected from the Elrama blocks when compared with biomass collected from the concrete controls. Only two sets of analyses showed significant differences between metals concentration in biomass obtained from coal wastes and concrete. The biomass obtained from the concrete block contained more Pb and Zn than did the biomass obtained from the Elrama blocks.

During the fall of 1977, divers observed the presence of boring pholid clams (Barnea truncata) living within the Elrama scrubber block. On January 13, 1978, divers withdrew from Conscience Bay one of the 0.028 m^3 scrubber blocks. The clams removed from the block ranged in shell length from 0.7 to 2.5 cm. The shells were removed and the soft tissues of the organism were rinsed in distilled-deionized water (DDW) and freeze-dried. After freeze drying, each sample was subdivided to permit replicate analyses and then subjected to a hot HNO_3 digestion. Each sample was analyzed for Cu, Cd, Pb, Cr, Zn, Se, As, Ag, Hg. The results of these analysis are

shown in Table IV-11. The trace metal concentrations found in the boring clams, which were in intimate contact with the waste materials completely surrounding them, were less than the concentrations measured in the biomass of epibenthic colonizers collected from the surfaces of the blocks.

During the course of the 1978 program on in situ coal waste studies in Conscience Bay, further analyses for trace metals were made on biomass growing over coal waste blocks. The coal materials in the 1978 program included stabilized blocks of Elrama 1:1 and Conesville 1:1 mixes. The controls were both concrete blocks and natural hard rocks placed at the site at the same time.

On August 16, 1978, divers removed from each of the structures in Conscience Bay samples of hydroids, primarily Sertularia sp., with small amounts of Tubularia sp. All samples were returned to the laboratory immediately, where they were rinsed in DDW to remove surface particles and salts and then processed and analyzed by the same methods used in the 1977 program. The results of the analyses are shown in Table IV-12.

As had been found in the extended study in 1977, the concentrations of trace metals in the colonizer biomass

Table IV-11. Metal Concentration (ppm) in Barnea truncata

Cu	Pb	Zn	Se
20.455	8.441	153.35	11.713

Cr, Cd, Hg, As, Ag were below instrument detection limits.

Table IV-12. Metals concentration (ppm by weight) in encrusting biomass. Data are means of replicate (n=3) analyses of samples collected on August 16th and October 15th, 1978.

Metal	Collection Date	Metal Concentration in Biomass Elrama	Conesville	Concrete	Rock	ANOVA Analysis†
Zn	8/5		136.76	149.68	170.29	n.s.
	10/15	124.93	121.32	138.54	159.65	n.s.
Pb	8/5		21.51	23.34	31.06	n.s.
	10/15	26.64	17.81	16.16	23.81	n.s.
Cr	8/5		16.56	23.95	25.50	n.s.
	10/15	18.35	15.62	13.43	15.95	n.s.
Cu	8/5		72.63	78.06	82.82	n.s.
	10/15	50.10	50.59	46.99	58.11	n.s.
Se	8/5		16.43	15.74	23.72	n.s.
	10/15					
Cd	8/5	0.71	1.02	0.84	1.76	*

† ANOVA analysis (Sokal and Rohlf, 1969) performed to indicate significant (*) or non-significant (n.s.) variation among materials for each metal at $\alpha = .05$.

removed from the coal waste blocks in the 1978 study were not greater than the concentrations measured in the colonizing biomass removed from control concrete blocks or from natural rock controls. Only analyses for cadmium showed a significant difference in concentration in biomass, being significantly higher in biomass collected from hard rock than from other materials.

3. Discussion of Biological Acceptability

Biological settlement occurred successfully on blocks of a wide variety of fly ash and scrubber sludge mixes, exposed in different natural seawater systems. During the fall, blocks of Elrama 1:1 and 3:1 on the seabed below the photic zone in the Atlantic were settled exclusively by animals. Growth of species was clearly demonstrated. The same materials, placed in illuminated seatable aquaria at the Flax Pond Lab through the winter, were quickly overgrown by a diverse community of microorganisms dominated by the growth of photosynthetic algae. The most extensive studies of colonization were made over two years in Conscience Bay in Long Island Sound. Elrama 1:1 and 5:1 and Conesville 1:1 mixes were placed within the photic zone, in the spring. These blocks were colonized by diverse communities of seaweeds, macroinvertebrates and microorganisms. As the blocks were progressively overgrown,

numbers of fishes, crabs, urchins and other motile animals inhabited the blocks, frequently browsing on the colonizing epibenthic communities.

The observations of successful block colonization in such different marine environments, strongly suggested that the coal waste blocks represented unoccupied solid substrates suitable for settlement by larvae and spores. Toadfish, Opsanus tau, treated the new blocks in Conscience Bay as a spawning substrate by attaching their fertilized eggs to the blocks within three weeks of placement.

The surface properties of the fly ash-scrubber sludge blocks were different from those of the concrete and rock controls in that the surfaces were texturally finer and also softer in seawater than the controls. Numerous studies have established that early life stages of benthic organisms, when settling, may be highly selective with respect to the surface properties of potential substrates. Such settlement substrate selection could well account for the initial differences in colonizing species noted on the test blocks and controls in the Conscience Bay studies. But with time, the calcareous skeletons of encrusting bryozoa and polycheate tube worms dominated the sides of blocks, with algae and hydroids on the tops, sides and corners. With in situ exposures of longer than about five months, all blocks were heavily overgrown by colonizers. The communities

colonizing the different types of blocks tended to lose their differences and increase in similarity.

Despite the demonstrated suitability of the coal waste blocks as substrates for biological colonization in the sea, a very important consideration was whether uptake of trace metals by the colonizing organisms occurred. Repeated microchemical analysis for trace metals in the epibenthos collected from the surfaces of blocks exposed for several months in Conscience Bay showed that concentrations of such trace metals were not any higher than trace metal concentrations in similar biomass collections from control materials of concrete and hard rock placed at the site at the same time.

V. IN SITU BLOCK PLACEMENT

A. Site Location, Marking

Precise navigation available on board the R/V ONRUST permits the positioning of the vessel within 200-400 feet of the test site location. Yet, for divers to locate the test blocks on the sea floor, with visibility almost zero at times, a more accurate method is required. Surface buoys are found to disappear within a few weeks or attract curious sport divers and fishermen if they remain.

Ultrasonic pingers (40 khz and 62 khz) were set at the test site near the sea floor. A deck receiver leads the vessel to a position directly overhead and the underwater receiver directs divers to the test blocks even in zero visibility. Sub-surface polystyrene floats were set approximately 3 m above the bottom for detection by side scan sonar as an alternate system for vessel positioning.

B. Placement and Handling of Test Blocks

Due to the quantity of test blocks of the various mixes placed on the bottom, plastic compartmentized trays were used to contain and differentiate the test blocks. The hard sand bottom allowed direct placement of the trays on the sea floor during the fall, but, as the winter storms developed, consistently poor visibility and extensive sand movement reduced the divers' ability to locate and identify the trays of test blocks. Also, the possibility of sand covering some blocks affects rates of colonization being monitored. Epoxy-coated tables were constructed to contain and elevate

the trays just above the sea floor. This also facilitated location and identification as well as promoted colonization on the bottom surfaces of blocks.

The plastic trays permitted raising and lowering of many test blocks by means of lift bags and divers with inflatable vests. A small safety boat on the surface easily picks up and lowers the trays since the large vessel could not manuever accurately enough for this task. Individual 1 cu ft test blocks are also raised and lowered in this manner.

C. Discussion

Continued development and improvement of site location and block handling techniques will facilitate all on-site tasks after the placement of the large 1 cu yd blocks. Having encountered less than satisfactory conditions at the underwater project site, development of alternate underwater study methods has progressed rapidly.

A system of diver-to-vessel communication is being developed to aid in investigations requiring attachment of cables to the ship.

VI. BASELINE SURVEYS

Samples for water column properties, plankton abundances and primary productivity, and benthic biomass and number were collected during oceanographic cruises at the reef site (Figure I-1) on October 9-11th and December 5-8th, 1978. During the October cruise, grab samples for sediment characterization and analysis were also collected. This work, along with the results from future cruises during the coming spring, summer, and fall and results from previous studies (Marine Sciences Research Center, 1973), will provide a baseline against which the coal waste reef will be evaluated. Previous studies at or near the reef site indicated that (1) the water in this region is well mixed from October to early May; (2) dissolved oxygen is usually high throughout the water column; and (3) the prevailing wind during the winter is west to northwest resulting in a surface drift away from the shore.

A. Water Column

1. Methodology

The water column was sampled in October and December at 6 depths at each of the 12-14 stations (Figure VI-1, Stations 1-12) with up to five sample replicates being taken at selected stations. Stations 21 and 22 were added during the December cruise. The stations were sampled from the R/V ONRUST.

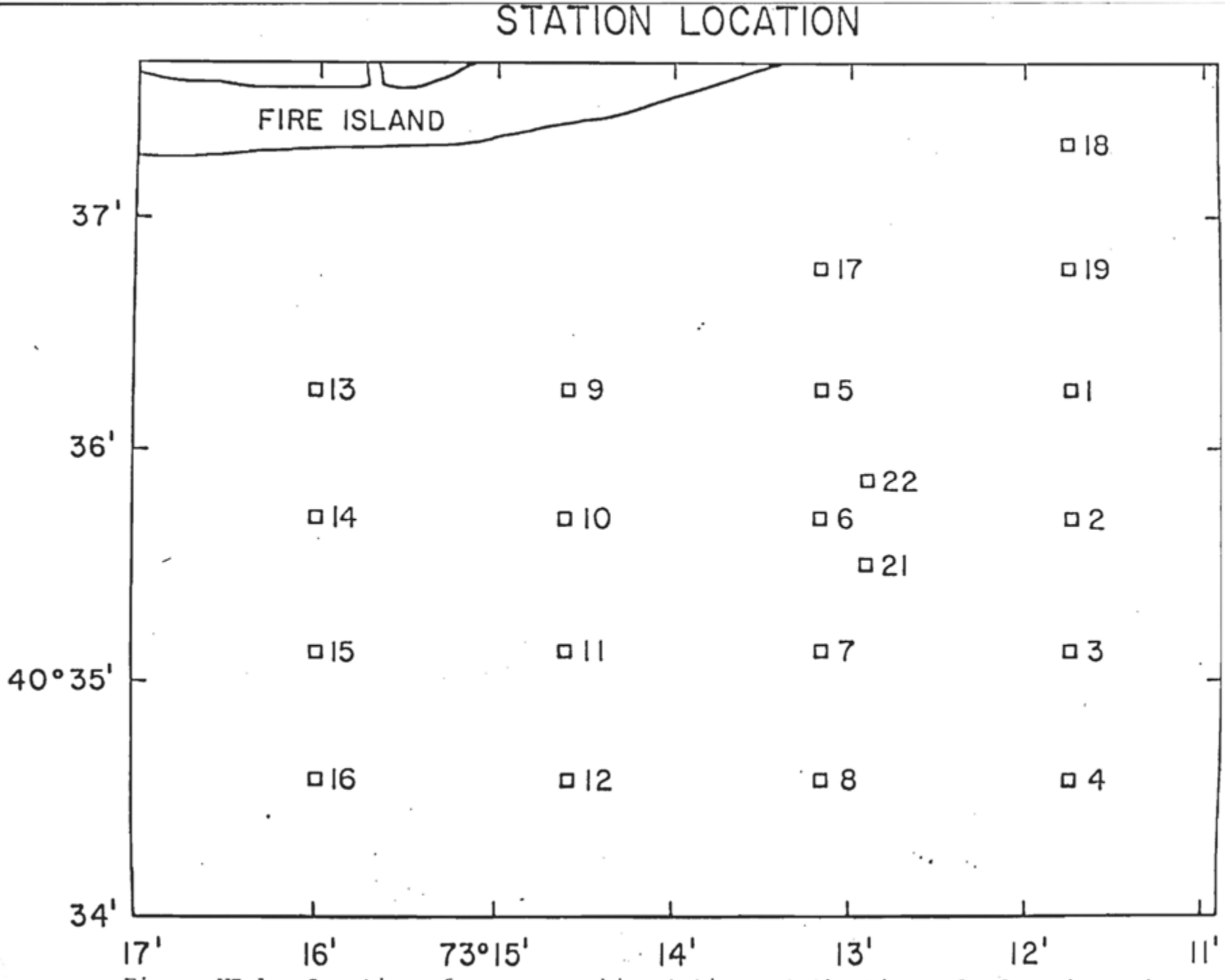

Figure VI-1. Location of oceanographic stations at the Fire Island project site.

The sampling grid was designed to observe spatial variations in the water properties over a broad region in the vicinity of the Fire Isalnd artificial reef site. Replicate samples (i.e. repeated sampling at depth) were collected to estimate the variability in our analytical procedures.

The Plunket system (Hulse, 1975) was used to measure temperature and salinity and to obtain samples for the analysis of dissolved oxygen, nitrite (NO_2^-), nitrate (NO_3^-), ammonium (NH_4^+), phosphate (PO_4^{3-}), silicic acid ($Si(OH)_4$), suspended solids (for gravimetric analysis), and particulate carbon and nitrogen. The Plunket is a shipboard, semi-automated, data acquisition system in which seawater is continuously pumped from depth, via a submersible pump, to a manifold (located inside the ship) which directs water to various sensors. Niskin bottles (Top Drop and Go-Flo) were used to sample for particulate trace metals.

a. Dissolved oxygen. Water samples for dissolved oxygen were carefully drawn into 55-57 ml calibrated iodine flasks from the Plunket and immediately pickled using a specially designed dispenser that added both oxygen reagents simultaneously. The pickled samples were analyzed for dissolved oxygen by means of the micro-Winkler method (Carpenter, 1956).

b. Nutrients. During the October cruise, glass-fiber filtered (8 um porosity) water samples for NH_4^+, NO_2^-, NO_3^-,

PO_4^{3-}, and $Si(OH)_4$ were collected in small glass and plastic test tubes (with Teflon screw caps) from the Plunket. Immediately after collection these samples were stored at 4°C until they could be analyzed in the laboratory.

During the December cruise, 0.4 µm porosity glass-fiber filters were used for NH_4^+, NO_2^-, NO_3^-, and PO_4^{3-} collection; the filtrates were collected in 30 ml glass test tubes. Samples for $Si(OH)_4$ were filtered through a Millipore filter (0.45 µm porosity) and collected in 15 ml plastic test tubes. Immediately after collection, all nutrient samples were frozen and brought back to the laboratory for analysis. The sampling and storage methods used in December represent an improved procedure over that used during the October cruise.

NH_4^+, which includes about 5% by weight of dissolved NH_3, was determined 20 to 30 hr after collection using an automated indophenol method. NO_2^-, NO_3^-, PO_4^3 and $Si(OH)_4$ were determined from 2 to 3 days after each cruise using automated colorimetric methods.

c. Suspended solids. Samples for gravimetric analysis of suspended matter were collected in 500 ml glass bottles from the Plunket spigot. These samples were filtered in the laboratory using pre-weighed 0.8 µm Nucleopore (47 mm diameter) filters. The filters were dried in a dessicator and then reweighed.

d. Particulate carbon and organic nitrogen. Samples for particulate carbon and particulate organic nitrogen determination were collected on 0.3 µm porosity glass fiber filters. The filters were stored frozen until the analysis could be performed. A Hewlett-Packard CHN analyzer (Model 185) was used for the analysis. The combustion temperature was 1140°C, and acetanalide was used as the standard.

e. Particulate trace metals. Samples for particulate metals analysis were collected using 10 liter Niskin Top Drop (PVC) samplers during the October cruise and 5 liter Go-Flo Niskin (PVC) samplers in December. The water samples collected during both cruises were filtered onboard the research vessel using glass fiber filters (0.8 µm porosity) fitted in Swinex filter holders. The filters were frozen until digestion could be performed in the laboratory. The digestion was carried out by placing each filter in a 30 ml polyethylene bottle to which 2.5 ml of a 1:1 concentrated Ultrex HCl:concentrated Ultrex HNO_3 solution was added. After heating at 75°C for four hours, the leachate was filtered through a No. 42 Whatman filter, taken up to 10 ml in a volumetric flask with Q-water, and immediately transferred to a polyethylene container. The digests were refrigerated prior to analysis.

2. Results

a. Salinity. During the October cruise, vertical salinity gradients were very small, usually less than 0.10‰ with salinity ranging very near 32.1-32.3 °/₀₀.

Figures VI-2, a-b show the horizontal distributions of surface and bottom salinities, respectively. Decreasing salinities were found in the northern portion of the station grid.

During the December cruise, a similar pattern was observed (Figures VI-2,c-d). A tongue of high salinity water was observed both in the surface water and at the bottom near the southeast portion of the study area. Lower salinity surface water was found at the northwest section of the station grid.

The freshening observed during both sampling periods is presumably due to the transport of lower salinity water from Great South Bay. Hardy (1972), based on previous residual tidal data, reported that a net tidal volume leaves the Bay at Fire Island Inlet.

b. Temperature. The water column was essentially isothermal vertically with temperatures ranging between about 16.0 and 16.6°C in October; Figures VI-3,a-b show the horizontal distributions of the surface and bottom temperatures during this cruise. At the surface and the bottom, the coldest waters were found in the northwest corner of the station grid. By December (Figures VI-3, c-d), the water column had cooled substantially, with surface temperatures ranging between 7.8 and 8.5°C and bottom temperatures in the range 8.3-9.2°C. At the bottom, the coldest waters were found in the northern portion of the sampling grid while, at the surface, the coldest waters were found at the western

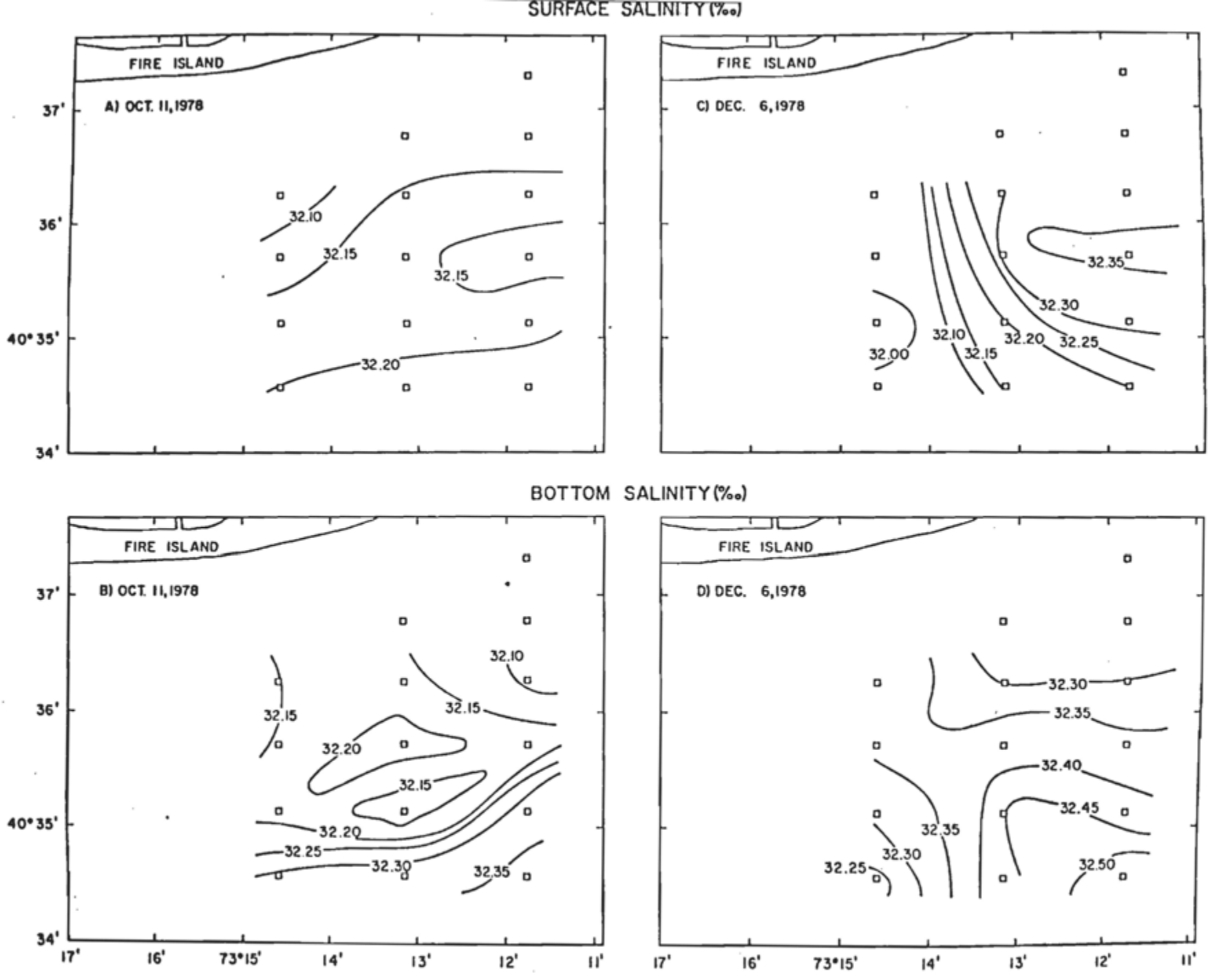

Figure VI-2. Distribution of surface and bottom salinity (°/oo) during October and December baseline cruises.

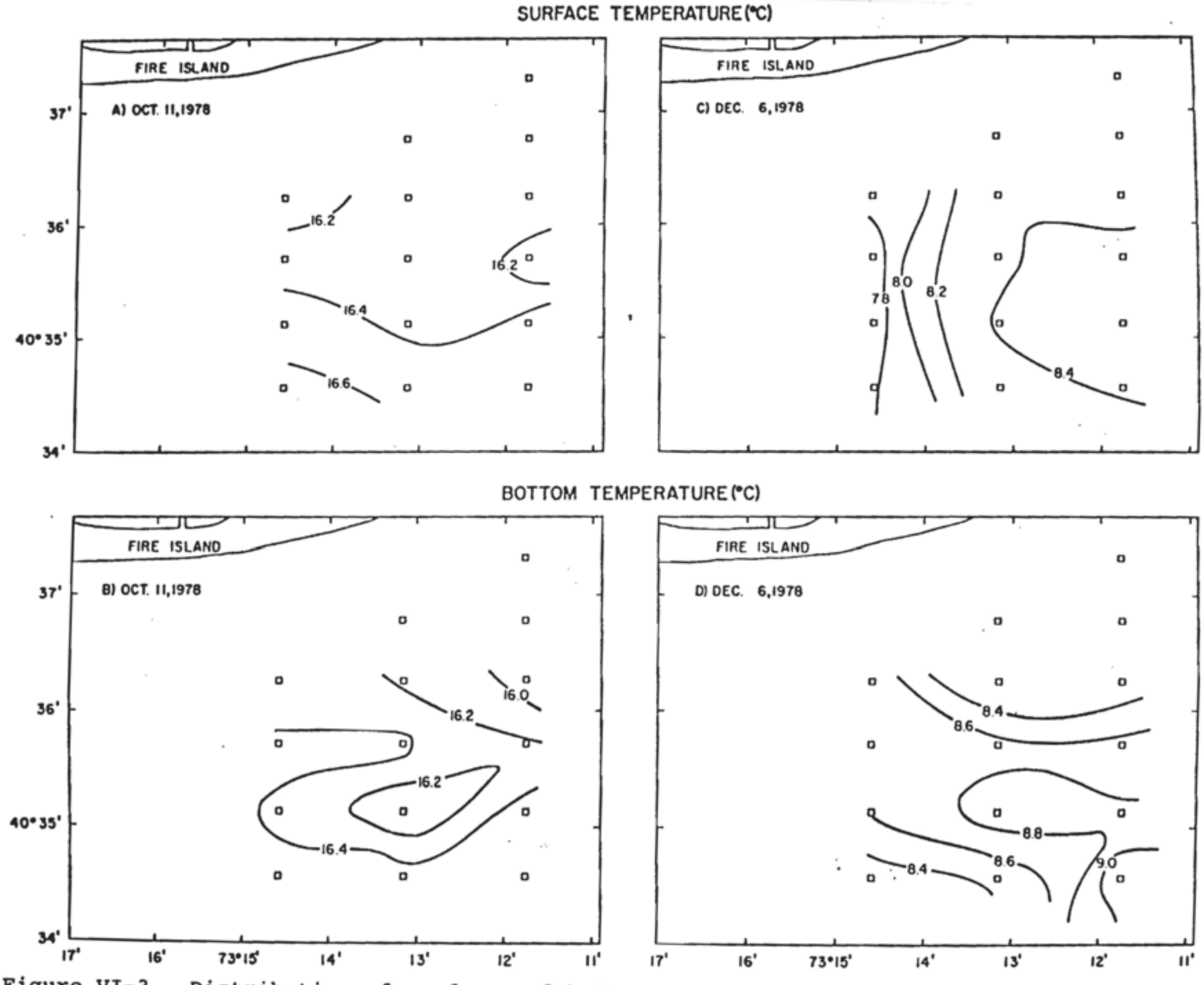

Figure VI-3. Distribution of surface and bottom temperature (°C) for October and December baseline cruises.

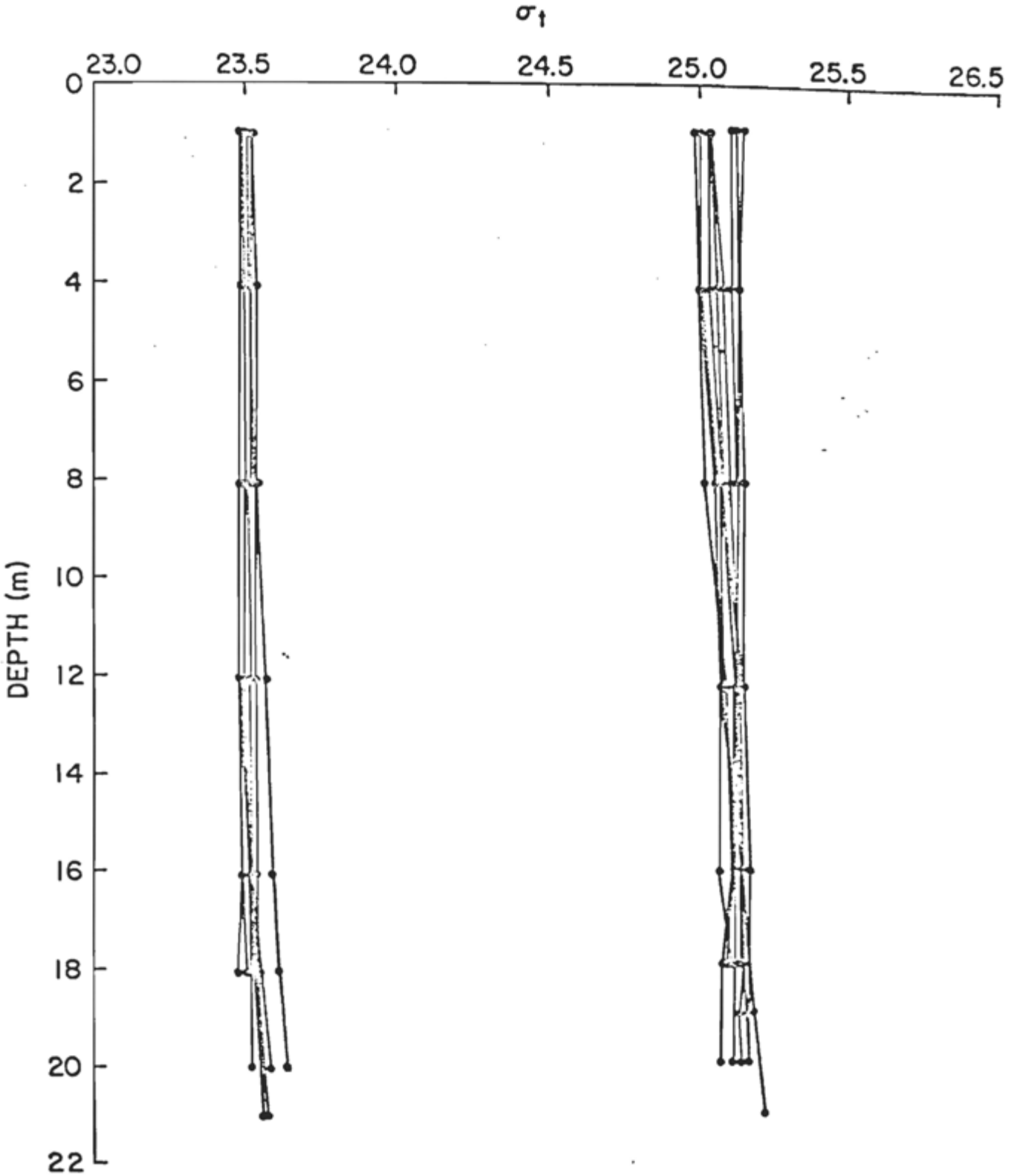

Figure VI-4. Depth distribution of density (σ_t= (Density-1)X1000) for October and December.

end of the grid. The presence of cold, low salinity water at the western and north-western region of the sampling grid during the sampling periods further suggests that water from the Great South Bay was being advected into the study area.

c. Water column stratification. The water column was very well-mixed during both cruise periods as evidenced by the uniform density distributions (Figure VI-4). As the salinity remained nearly unchanged between the two cruises, the increased density observed in December was due to the presence of colder water.

d. Dissolved oxygen. The waters in the study area were either saturated or very close to saturation with respect to dissolved oxygen. Highest concentrations were observed in the surface waters where percent oxygen saturation values usually ranged between 100 and 104 percent (Figure VI-5,a). Bottom oxygen concentrations were slightly lower than those observed in the surface waters; the corresponding percent oxygen saturation values for the bottom waters ranged between 95 and 100 percent of saturation (Figure VI-5,b). These relatively high and uniform concentrations of dissolved oxygen observed throughout the water column demonstrate that the water column was well-mixed during this period.

e. Ammonium. Considerable variation (0.48-44 μM) was found in the concentrations of ammonium (NH_4^+) in October with some anomalously high values observed at a few stations; these high values may have been due to either biological activity or contamination.

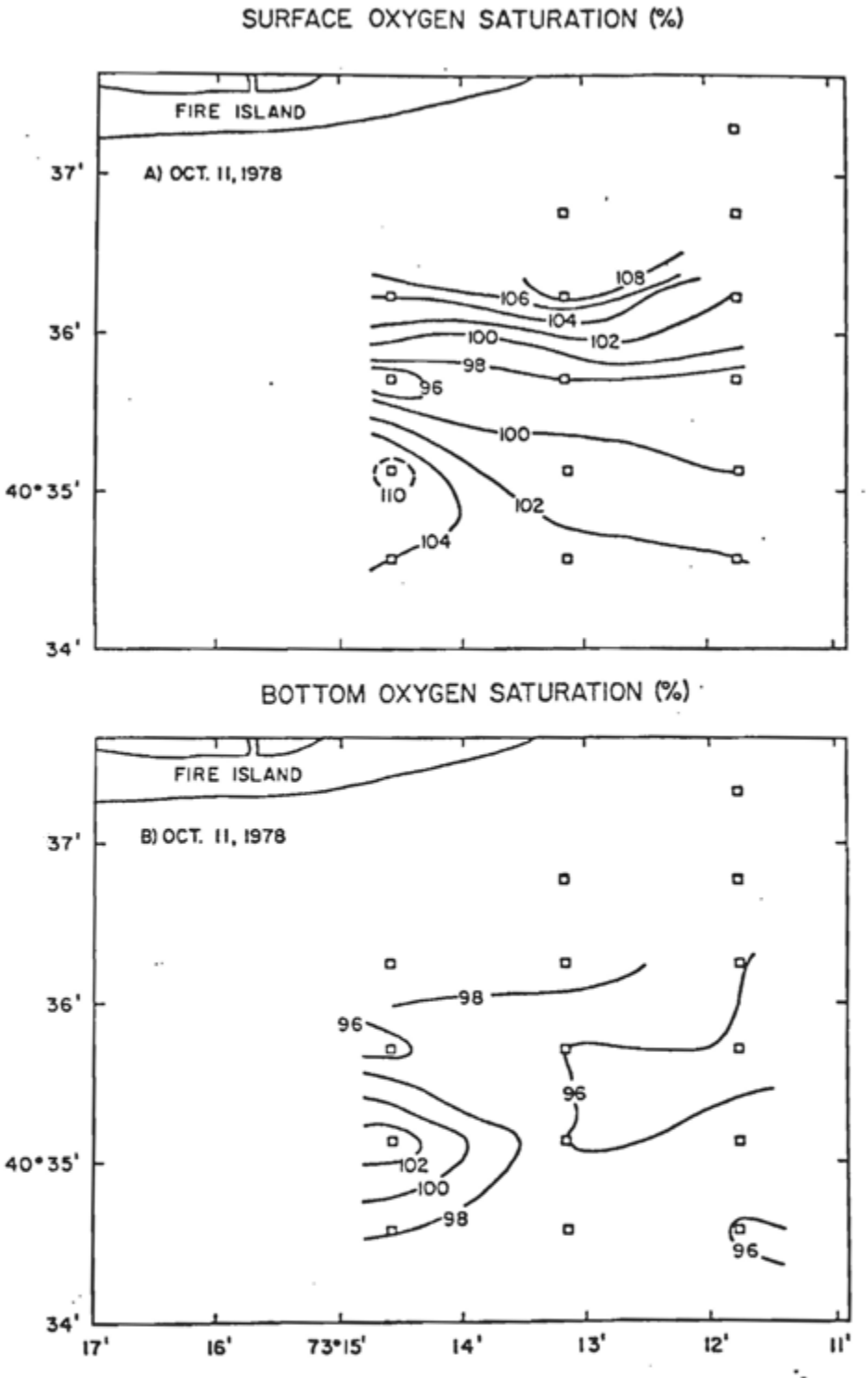

Figure VI-5. Distribution of surface and bottom dissolved oxygen concentration (as percent of saturation) during October basline cruise.

In December, concentrations of NH_4^+ were generally elevated throughout the area with surface values (Figure VI-6, a) ranging from 3.2 µM to 7 µM. The highest NH_4^+ concentrations were consistently found at the western end of the sampling grid. Bottom NH_4^+ values (Figure VI-6,b) ranged from 2.6 µM to 7.4 µM. Again, the highest NH_4^+ concentrations were usually found at the western portion of the sampling grid.

f. Nitrite and nitrate. Concentrations of nitrite (NO_2^-) were uniformly low throughout the study area, where values ranged between 0.1-0.3 µM in October and 0.5-0.9 µM in December. Nitrate (NO_3^-) concentrations ranged between 0.07 and 0.77 µM in October with the lowest observed in the northern region of the study area (Figures VI-7,a-b). In December, NO_3^- concentrations ranged between 1.6-3.7 µM in surface and bottom waters (Figure VI-7,c-d). During this period, concentrations of NO_3^- were the highest at the western portion of the sampling grid.

g. Phosphate and silicic acid. Concentrations of phosphate (PO_4^{3-}) were uniformly low and in the range 0.8 to > 1.0 µM (Figures V-8,a-d). Concentrations of silicic acid [$Si(OH)_4$] ranged between 4.6 and 5.2 µM, with highest surface values observed in the northern portions of the sampling grid (Figure VI-9,a-d). Concentrations of $Si(OH)_4$ were somewhat patchy near the bottom.

h. Suspended solids. Considerable variability was observed in the concentrations of suspended solids (Figure VI-10,a-d).

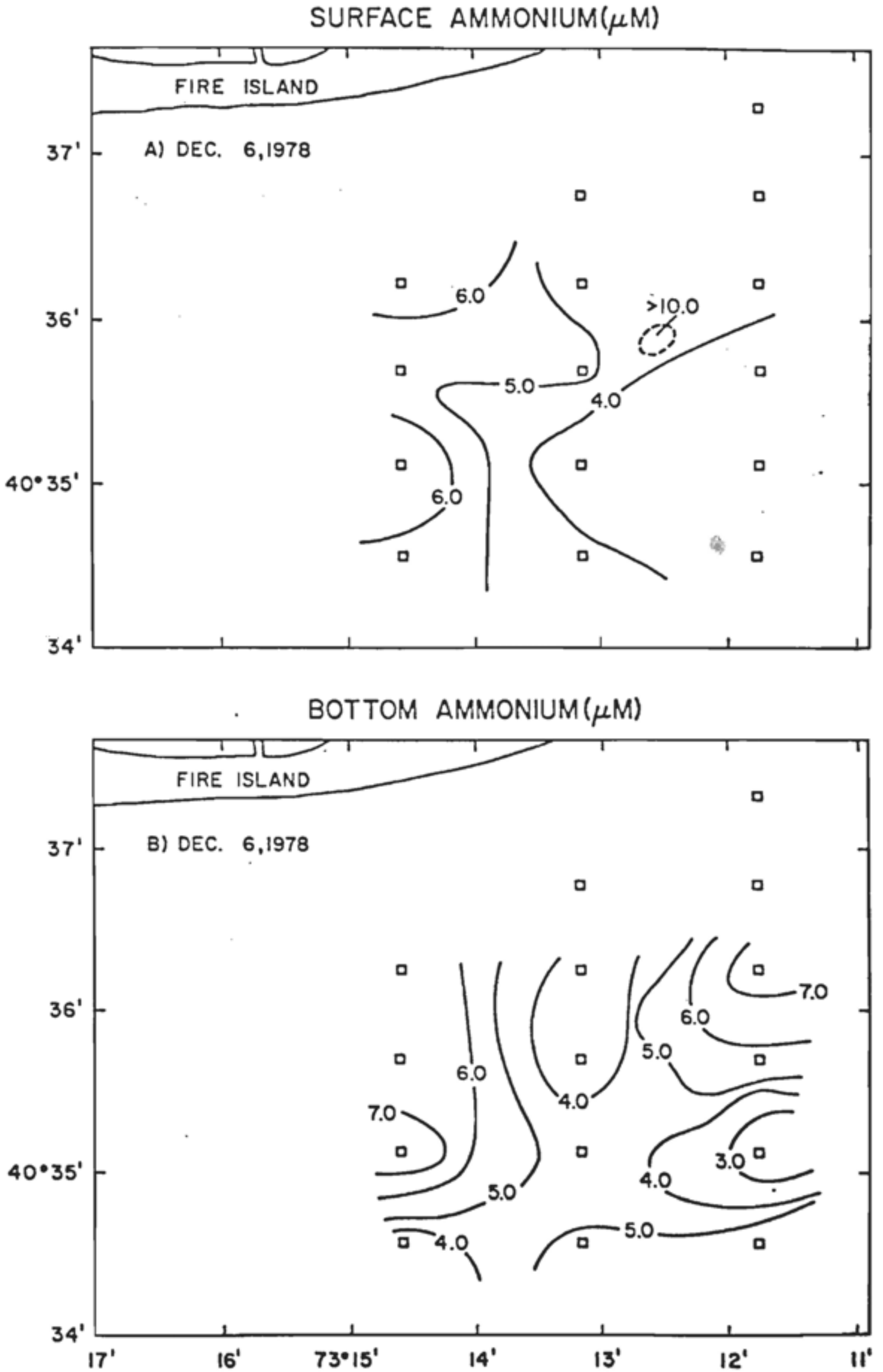

Figure VI-6. Distribution of surface and bottom ammonium concentration (μM) during December baseline cruise.

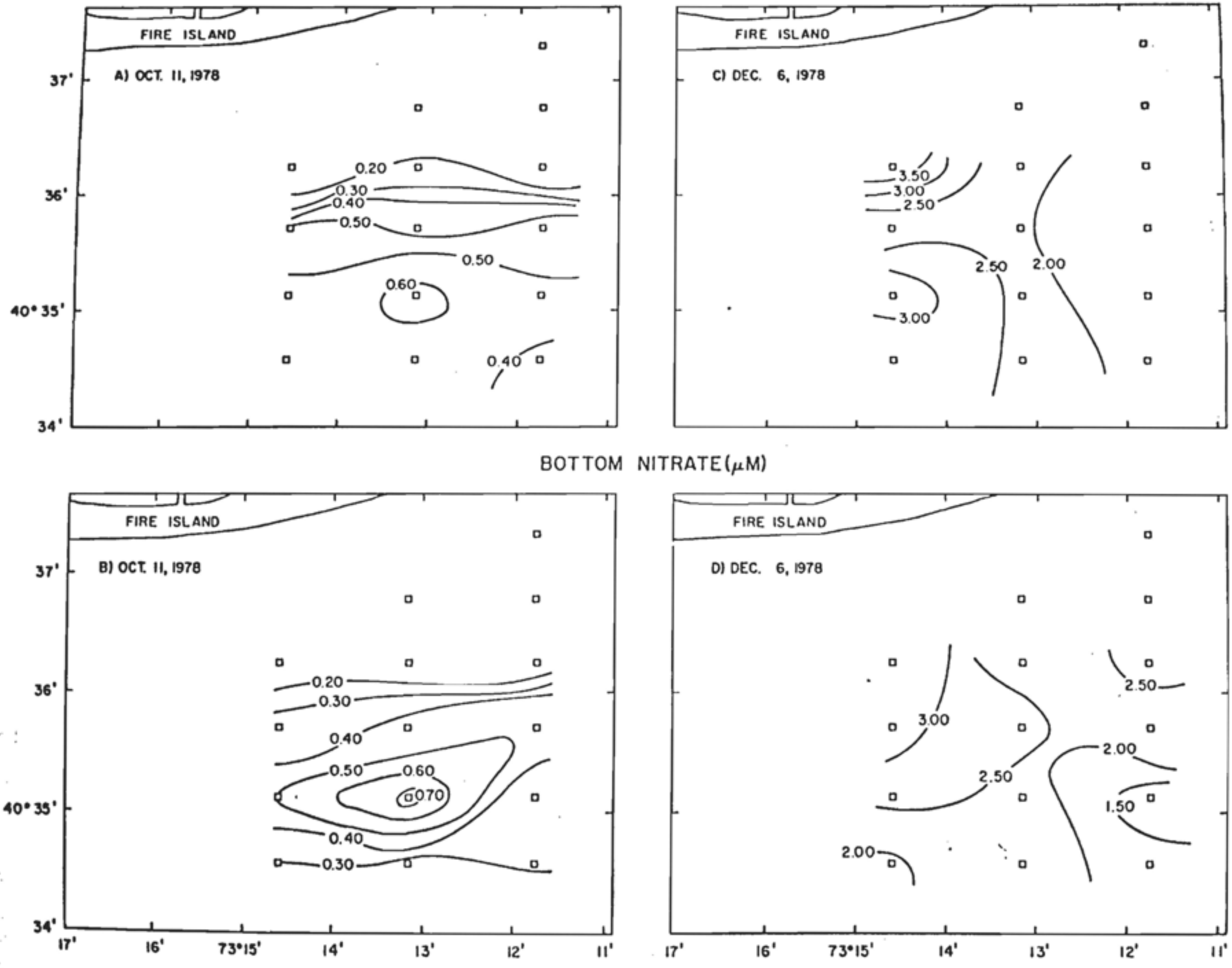

Figure VI-7. Distribution of surface and bottom nitrate concentration (μM) during October and December baseline cruises.

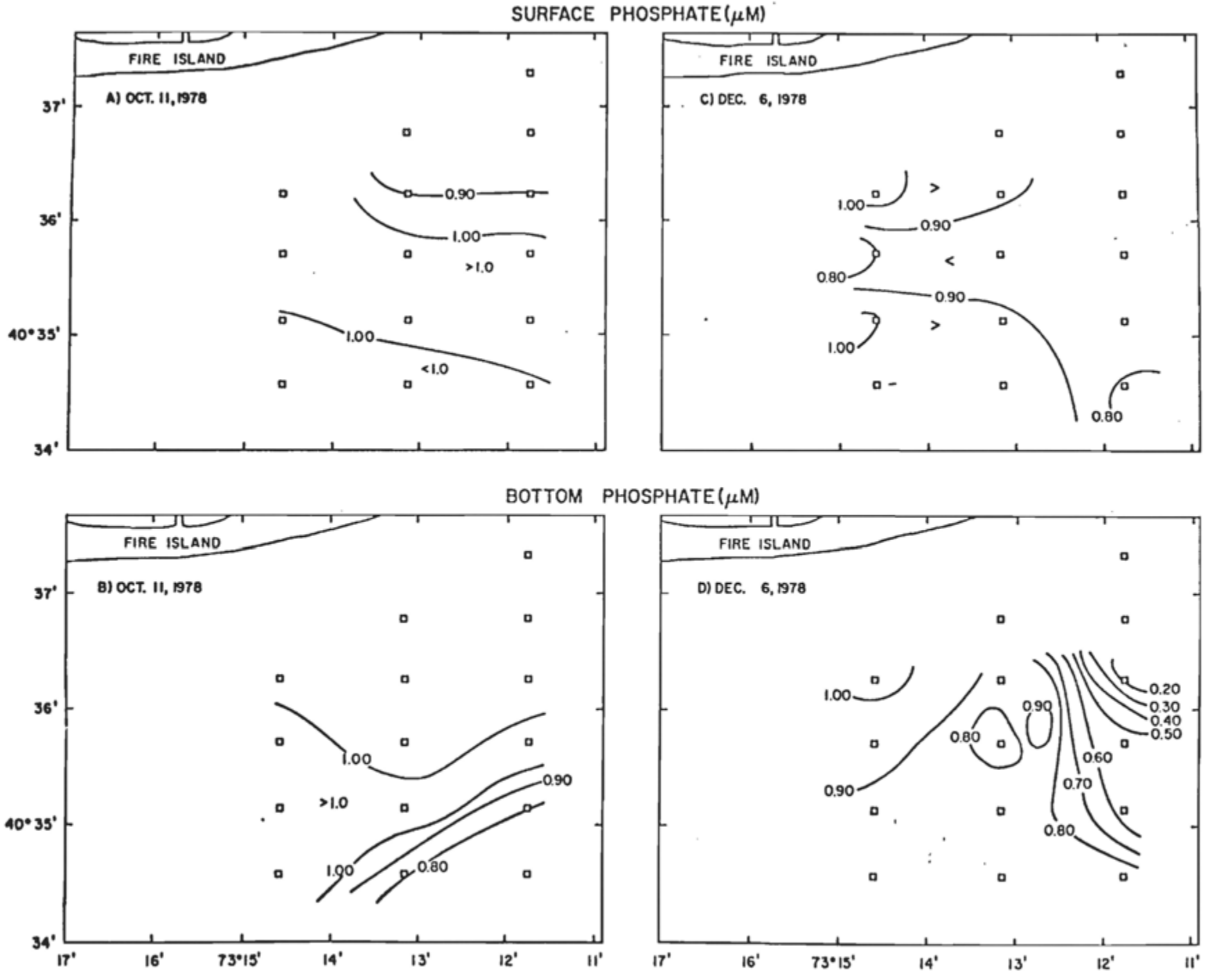

Figure VI-8. Distribution of surface and bottom phosphate concentration (μM) during October and December baseline cruises.

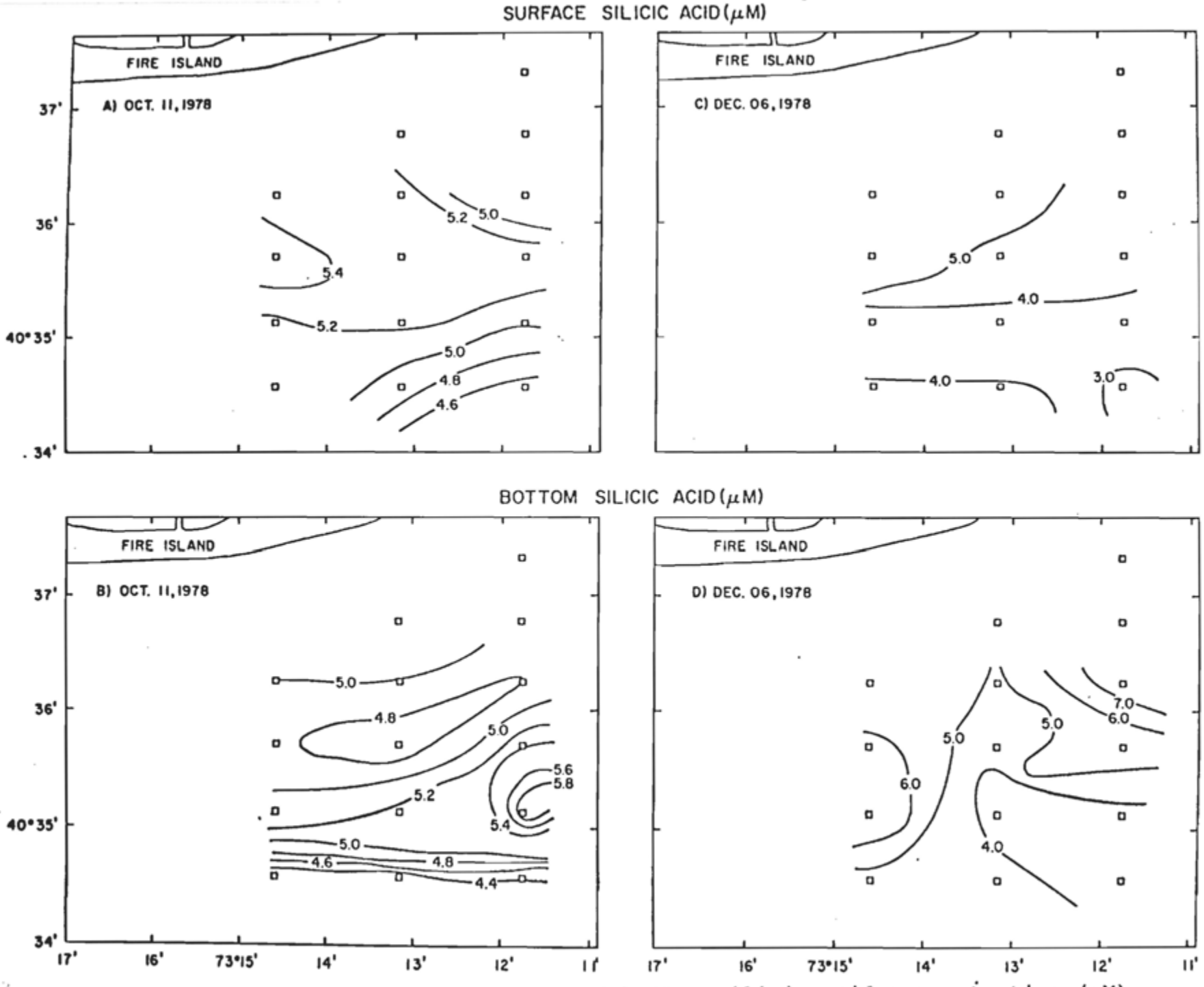

Figure VI-9. Distribution of surface and bottom silicic acid concentration (μM) during October and December baseline cruises.

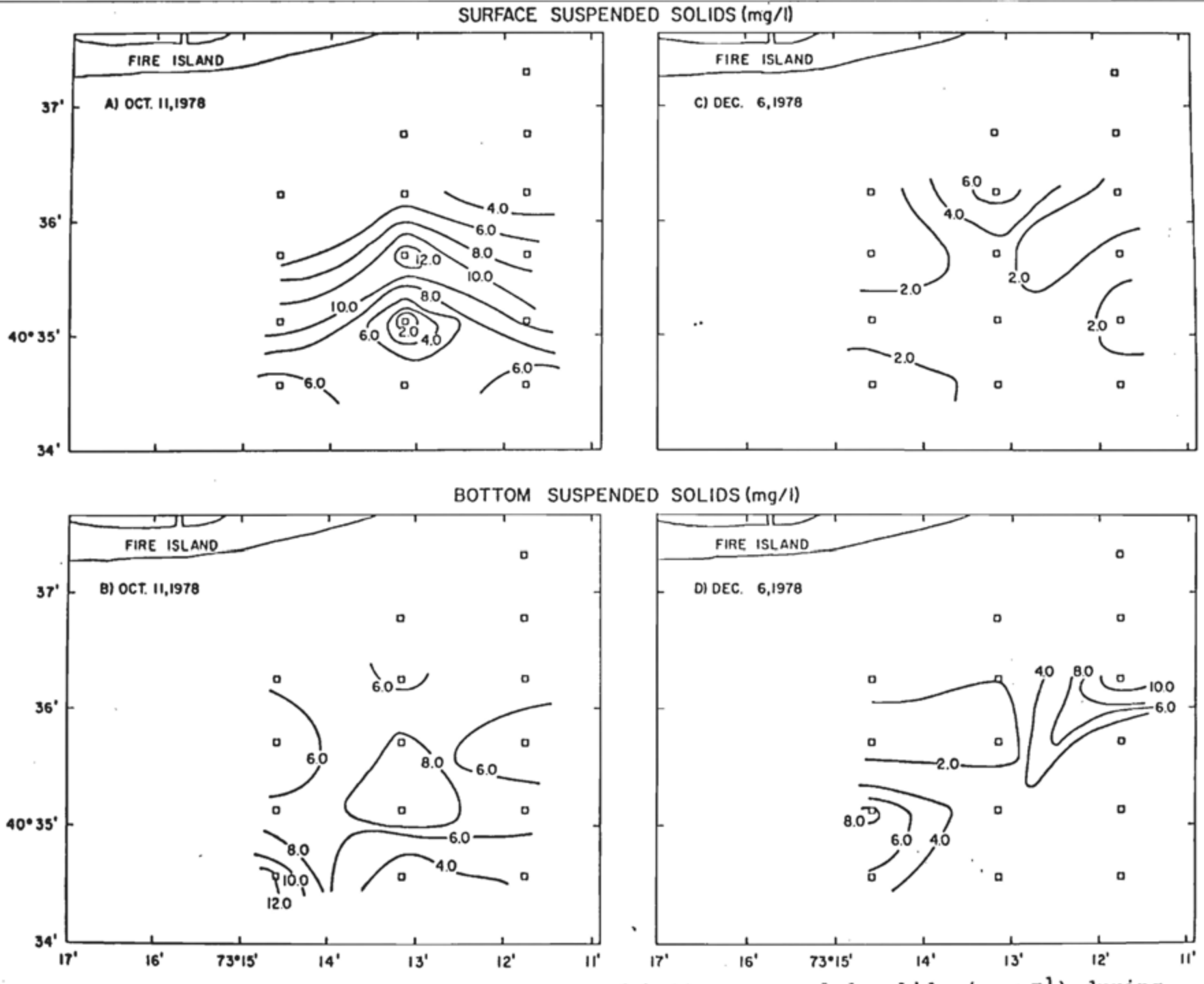

Figure VI-10. Distribution of surface and bottom suspended solids (mg m^{-1}) during October and December baseline cruises.

During the October cruise, the range in concentrations was 0.44 to 15 mg l^{-1}. During the December cruise, concentrations of suspended solids ranged between 0.40 and 11 mg l^{-1}. The variability in suspended solid concentrations was confirmed by the divers at the project site who reported a definite patchiness in the turbidity of the water column.

i. Particulate carbon and nitrogen. Concentrations of surface particulate carbon (Figure VI-11,a and c) and particulate nitrogen (Figure VI-12,a and c) were highest on the northwest portion of the sampling grid, again suggesting that Fire Island Inlet is a source for material entering the project site. The gradient in concentrations decrease seaward.

B. Plankton Abundance, Distribution and Primary Production

1. Methodology

a. Phytoplankton biomass. Samples for chlorophyll analysis were collected from the spigot of the Plunket system. Chlorophyll a and phaeophytin a concentrations were determined by fluorometric methods (Strickland and Parsons, 1972).

b. Phytoplankton species composition. Five hundred ml samples of water collected at the surface and mid-depths at several stations were preserved with Lugol's iodine solution and allowed to settle. The particulates were examined by microscopy for phytoplankton species composition.

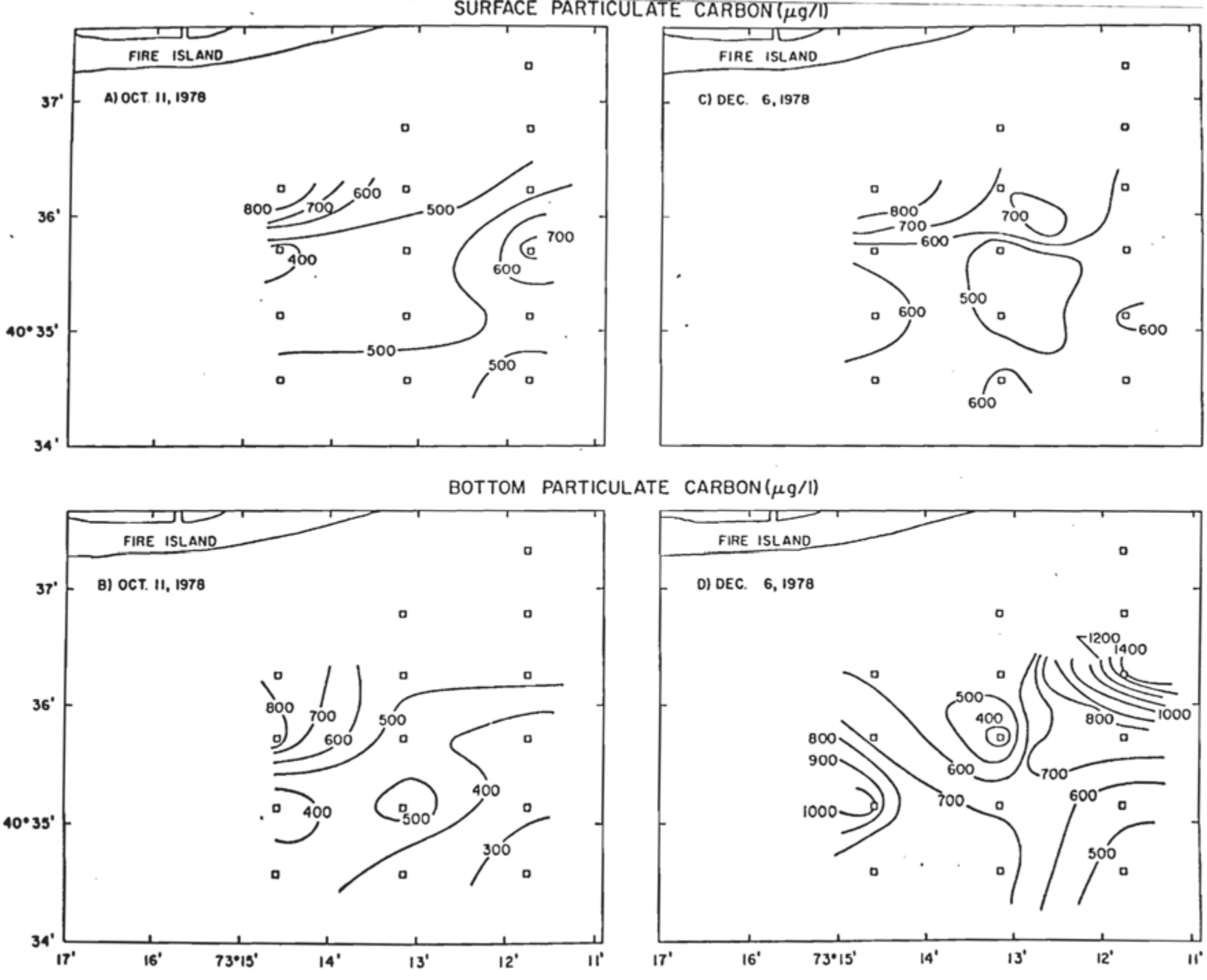

Figure VI-11. Distribution of surface and bottom particulate carbon concentration (μg l-1) during October and December baseline cruise.

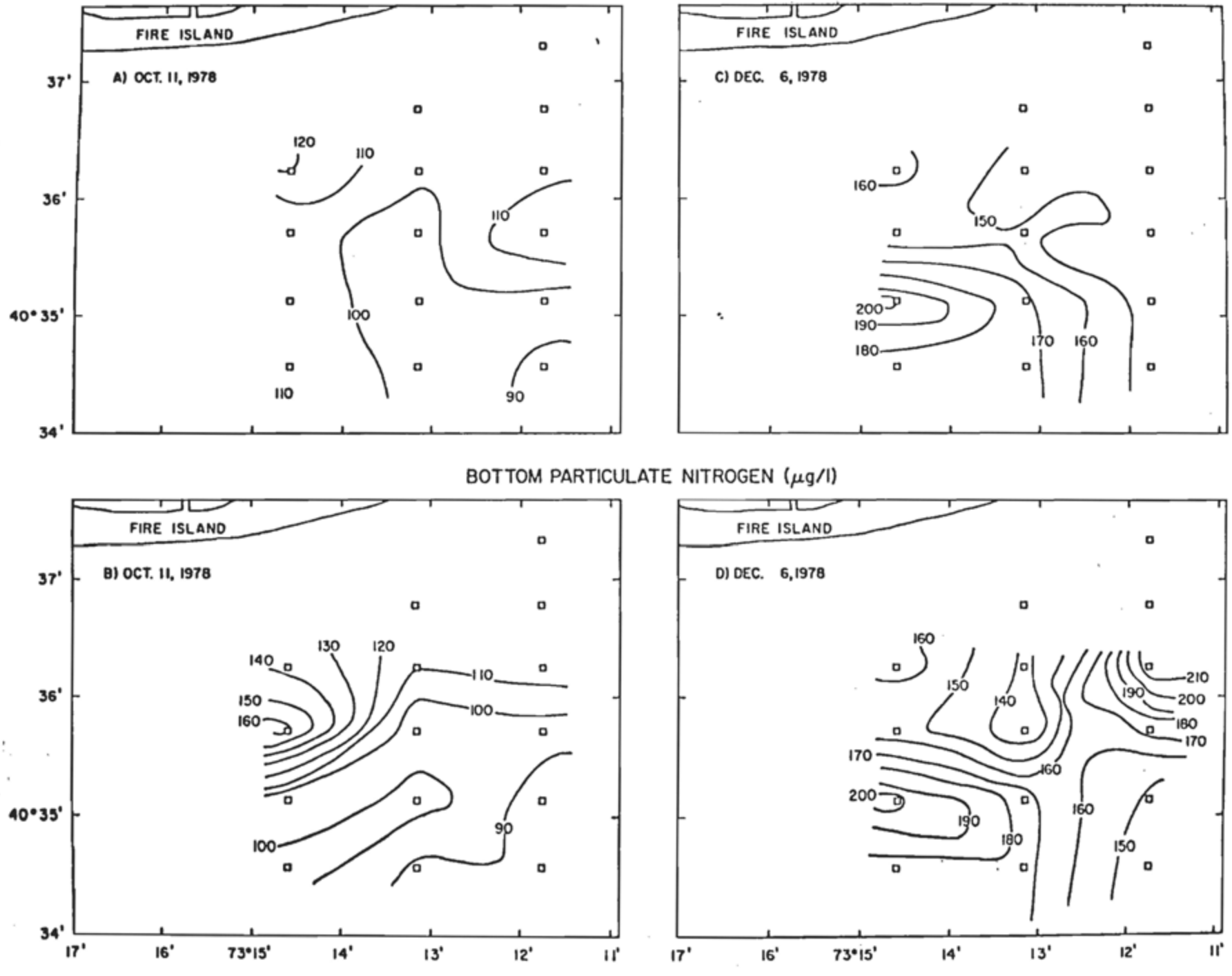

Figure VI-12. Distribution of surface and bottom particulate nitrogen concentration (μg l-1) during October and December baseline cruise.

c. Primary production. Rates of primary production were measured using the carbon-14 technique (Strickland and Parsons, 1972). Incubations were accomplished during 1000 and 1500 hr period at two stations. Water samples were collected at depths equivalent to 100, 60, 40, 16, 5% and 1% of the incident solar radiation, I_o. Each water sample was incubated for 2-3 hrs in a dark mounted incubator at a simulated light intensity equivalent to that occurring at the collection depth. The incubator was supplied with flowing surface water. The extinction coefficient, k, was measured using a submarine photometer.

d. Zooplankton. Zooplankton samples were obtained at several stations via vertical tows, bottom to surface, using 0.6 m diameter net equipped with 200 mm mesh and a TSK flow meter.

2. Results and Discussion

a. Phytoplankton. Concentrations of chlorophyll a measured at the surface at each station during the October cruise are shown in Figure VI-13. Chlorophyll a measurements were also made at selected depths from the surface to the bottom at each station. These concentrations were integrated over the water column depth, and are presented in Figure VI-14.

The patterns taken by the chlorophyll a concentration isolines indicate that the spatial distribution of phytoplankton was inhomogeneous, with patches occurring at areal scales several times as large as the station grid sampled. The surface chlorophyll a gradient decreased by a factor of 5 from the southwest towards the northeast (Figure VI-13). The integrated water column concentration gradient decreased in a similar direction, but by a factor of approximately 3.5 (Figure VI-14).

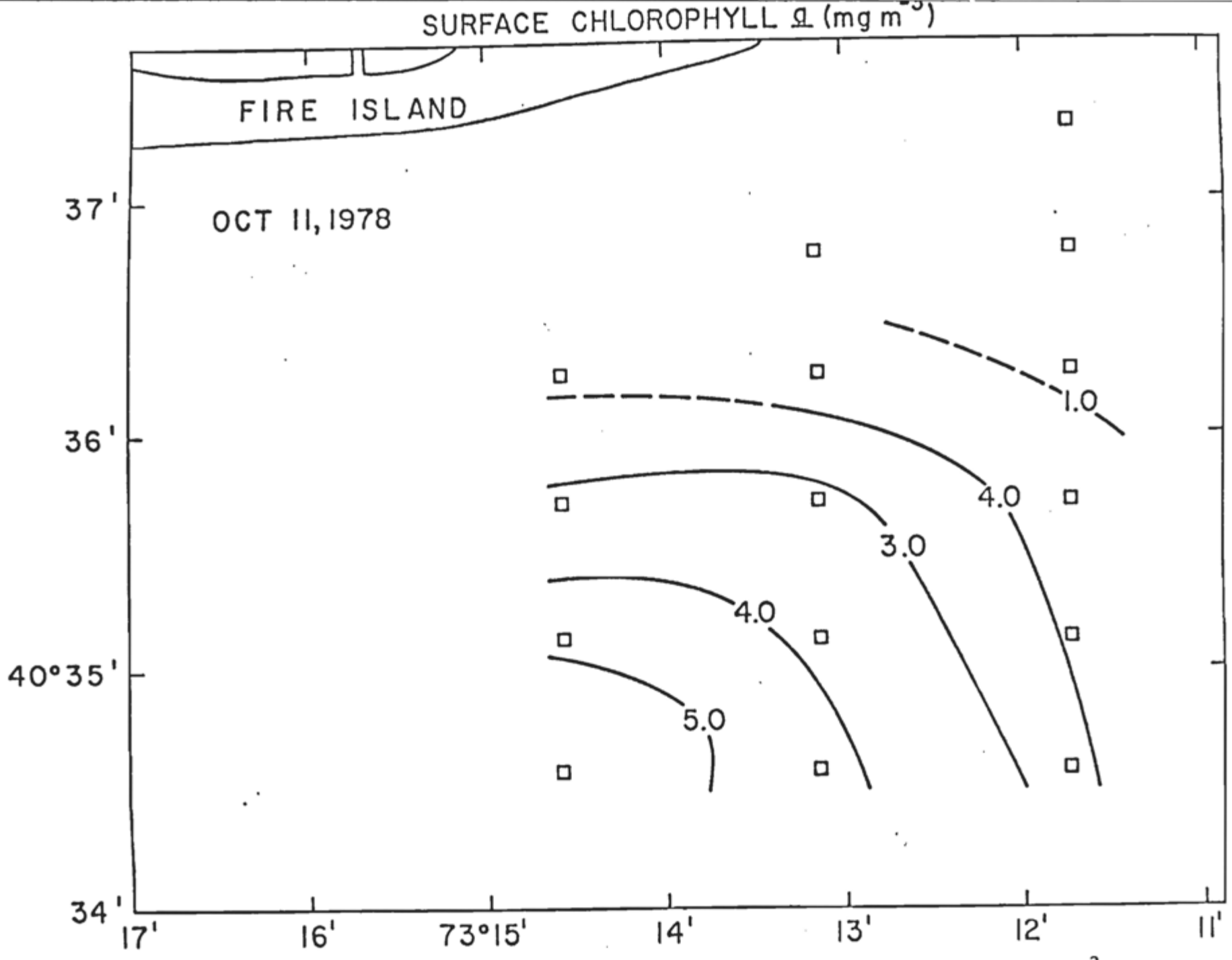

Figure VI-13. Distribution of surface chlorophyll a concentration (mg m^{-3}) during October baseline cruise.

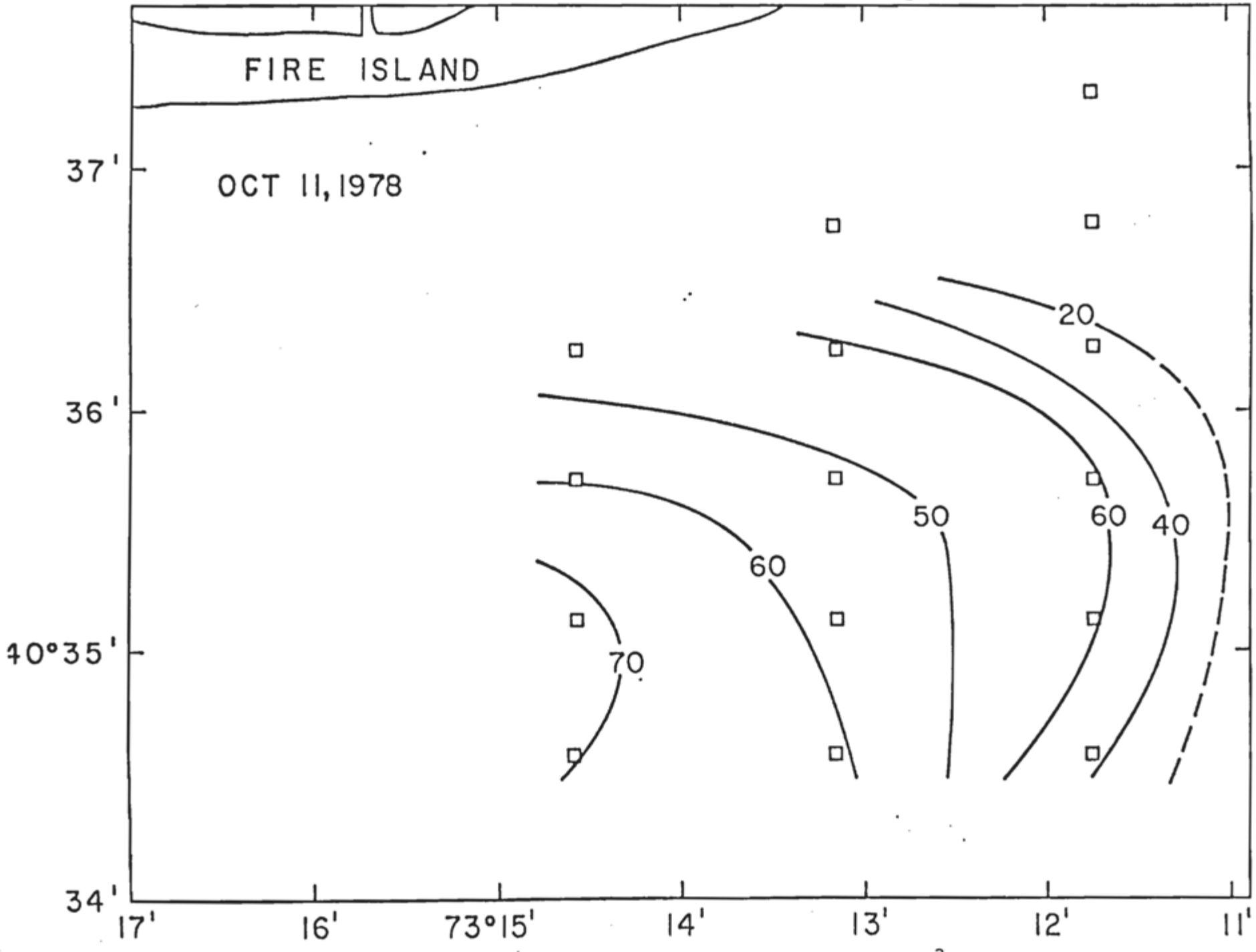

Figure VI-14. Distribution of integrated chlorophyll a (mg m^{-3}) at the project site.

The depth distribution of chlorophyll a concentration for the two eastern offshore transects (stations 5 through 8 and stations 1 through 4) are given in Figure VI-15 for the October cruise.

The depth distribution of chlorophyll a was variable in October but frequently exhibited sub-surface maxima in the upper 9 meters of the water column. A depth of 9 meters corresponded to the 1% I_o isolume.

The ratios of phaeophytin a:chlorophyll a were computed for depth at each station and are presented vs. depth in Figure VI-16. Phytoplankton exhibited increasing values of phaeophytin a:chlorophyll a with increasing depth in October. Phaeophytin a is the initial decomposition product of chlorophyll a; physiologically vigorous phytoplankton contain virtually no phaeophytin a. An increased quantity of detrital particles, containing phytoplankton remnants, was observed at depth in October. The magnitude and increase with depth of the ratio suggests that the standing crop of phytoplankton samples was exhibiting declining physiological vigor. This interpretation is supported further by the occurrence of low NO_3^- concentrations (0.5 μM or less) in the water column (Figure VI-17). Low concentrations similar to these are often associated with nutrient depletion and sinking of a phytoplankton crop.

Concentrations of chlorophyll a measured at the surface and depth at each station are shown in Table VI-1 for the December cruise. The mean ($\bar{x}$) and standard deviation (s) for

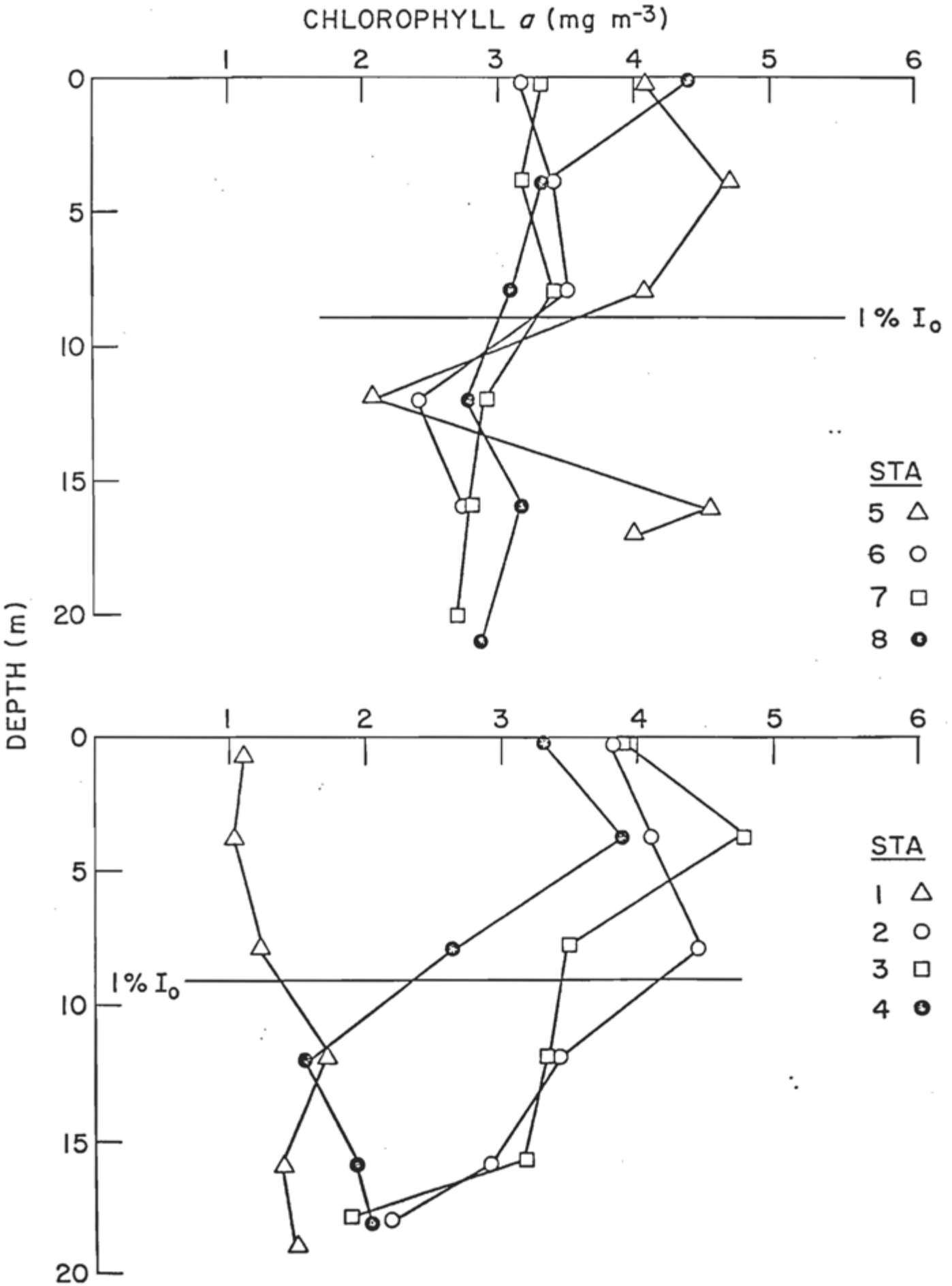

Figure VI-15. Depth distributions of chlorophyll a at: (a) stations 5-8, (b) stations 1-4, during October baseline cruise.

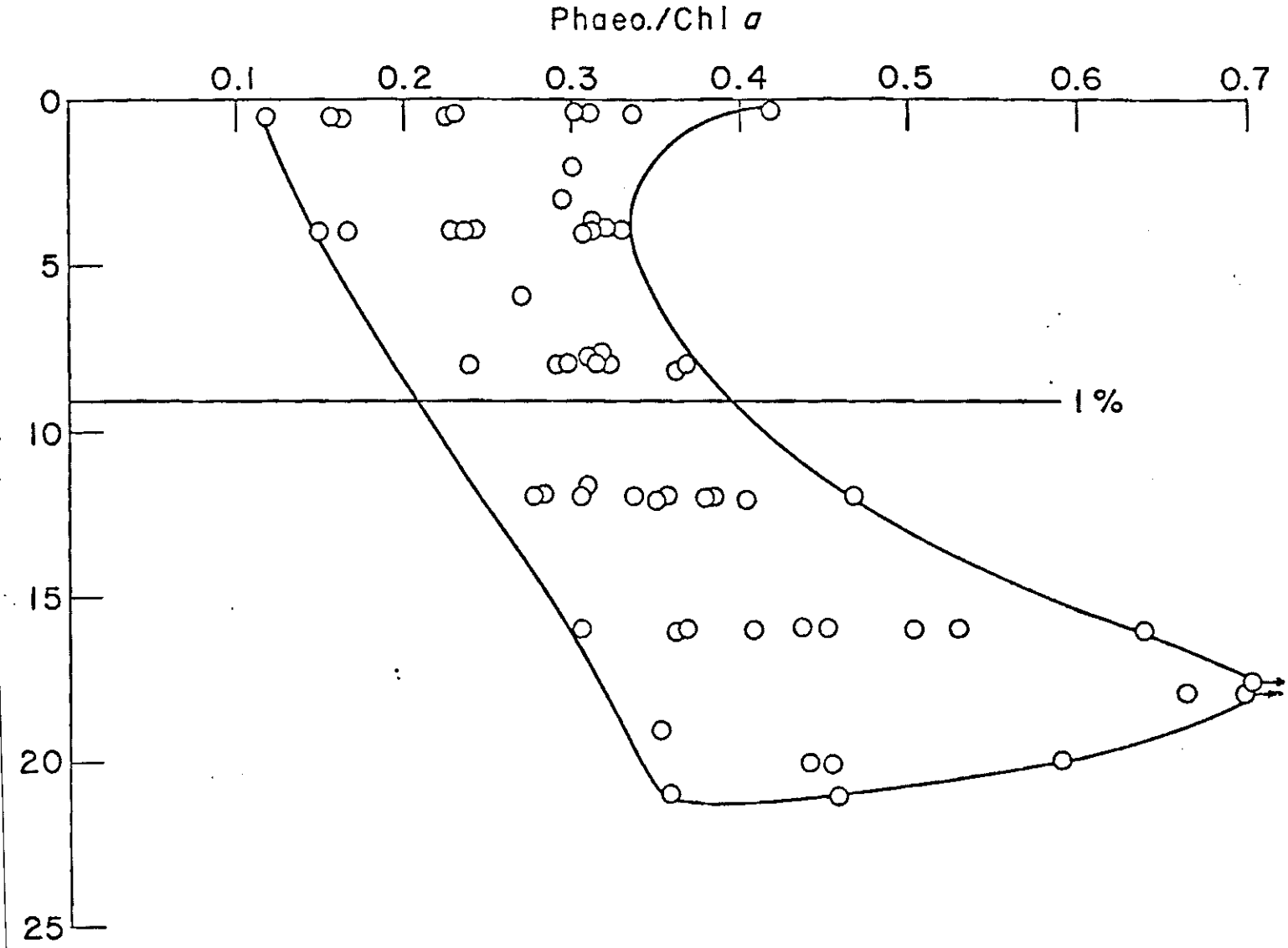

Figure VI-16. Depth distribution of the ratio phaeophytin a: chlorophyll a for all stations and depths.

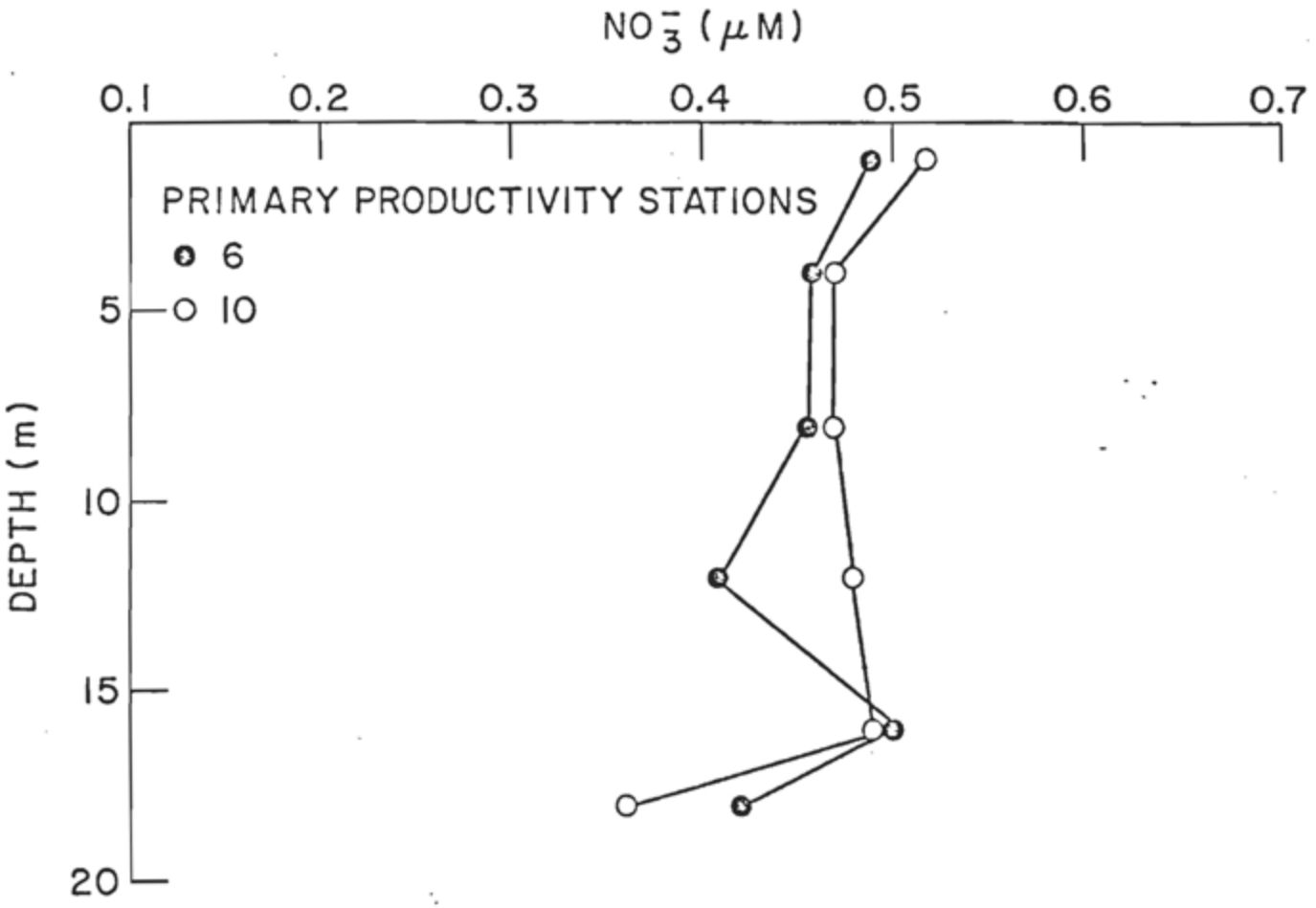

Figure VI-17. Depth distribution of NO_3^- (μM) at stations 6 and 10 during October baseline cruise.

able VI-1. Chlorophyll a, mgm^{-3} (a)[1] and phaeophytin a/chlorophyll a (b) December

Stations

Depth (M)	1 (a)	1 (b)	2 (a)	2 (b)	3 (a)	3 (b)	4 (a)	4 (b)	5 (a)	5 (b)	6 (a)	6 (b)	7 (a)	7 (b)	8 (a)	8 (b)	9 (a)	9 (b)	10 (a)	10 (b)	11 (a)	11 (b)	12 (a)	12 (b)	20 (a)	20 (b)	21 (a)	21 (b)
1	3.6	.24	4.3	.16	5.9	0	4.9	.14	3.9	.20	4.1	.19	4.0	.34	4.2	.26	4.1[2]	.37[2]	3.7	.43	4.2	.40	4.3	.39	3.7	.17	4.1	.22
4	3.5	.38	4.0	.16	4.8	.11	4.4	.13	3.8	.30	4.1	.24	4.2	.15	4.9	.13	4.0	.34	3.9	.41	4.4	.40	4.0	.38	3.5	.23	4.4	.20
8	4.2	.32	4.6	.17	5.2	.11	3.4	.27	3.6	.40	3.9	.21	3.2	.25	1.7	.42	-	-	3.5	.38	3.1	.38	3.6	.43	4.6	.22	4.3	.16
12	-	-	4.4	.22	3.8	.12	3.8	.15	2.9	.53	4.0	.35	4.2	.11	3.5	.19	4.9	.26	4.0	.31	3.8	.20	3.3	.31	3.6	.24	4.5	.11
16	4.4	.71	4.4	.14	5.4	.12	4.2	.14	3.9	.36	4.7	.40	5.1	.13	5.3	.02	4.0	.50	4.1	.33	5.3	.34	3.4	.45	3.9	.26	5.2	.23
18	4.4	1.2							1.9	.49							4.4	.32	4.0	.40	7.9	.49						
19											4.8	.31	6.2	.38											4.5	.37		
20					6.5	.18	5.7	.10							7.3	.33							4.8	.47			5.8	.17

for all stations and depths (n=81)
$\bar{x}$ = 4.30 s = 0.95

replicate samples (n=5)

chl a (mgm^{-3})	Phaeo a/chl a
$\bar{x}$ = 4.1	0.37
s = 0.3	0.02

all stations and depths sampled during this period was 4.30 and 0.95 mg chlorophyll *a* m^{-3}, respectively. Ricker's (1937) coefficient, $s^2/\bar{x}$, can be used to determine whether these data are randomly distributed, spatially, - do the data fit the Poisson distribution? Theoretically, if the value of $s^2/\bar{x}$ is greater than 1, the population is over-dispersed, or exhibits aggregation, spatially. If the population is randomly distributed in space, $\bar{x}$ becomes the expected value of s^2 and the ratio is distributed as $\chi^2/N-1$ with (N-1) degrees of freedom (Holmes and Ridrig, 1956). In the present case $\chi^2_{0.05}/N-1 = 101.88/80 = 1.27$. Hence, a value of $s^2/\bar{x}$ less than 1.27 would indicate that the hypothesis of satisfactory Poisson distribution fit could not be considered false. For these data, $s^2/\bar{x} = 0.21$, indicating random distribution with station and depth for the chlorophyll *a* concentrations at the 95% confidence level.

In a similar manner, the depth integrated chlorophyll *a* values (Table VI-2) were found to be randomly distributed ($\chi^2_{0.05}/N-1 = 22.36/13 = 1.72$; $s^2/\bar{x} = 1.47$) at the 95% confidence level. Therefore, contoured maps of chlorophyll *a* concentrations were not indicated for the data collected in December. The random distributions suggest a well-mixed water column resulting from the strong winds occurring in the sampled area several days prior to and during the December cruise. The tendency for higher values of phaeophytin *a*:chlorophyll *a* (Table VI-1) to occur at depth nearer the bottom suggests an upward mixing of detrital phytoplankton pigments.

Table VI-2. Depth integrated values of chlorophyll *a*, December 1978

Station	mg chlorophyll *a* m^{-2}
1	69.2
2	65.3
3	96.3
4	79.8
5	58.8
6	75.7
7	77.4
8	80.0
9	90.7
10	65.5
11	73.1
12	71.2
20	71.0
21	89.1

$n = 14$, $\bar{x} = 75.94$, $s = 10.58$

b. Phytoplankton species composition. No difference in species composition was noted among the samples collected at stations 4, 7, 8, 9 and 11 during the October cruise. The most numerous algae seen was the dinoflagellate Prorocentrum scutellum. A few examples of the dinoflagellate Dinophysis accuminata were seen. These dinoflagellates were about 10% as numerous as P. scutellum. In the middepth samples, a high frequency of detrital particles were encountered. These aggregates were composed largely of undifferentiated organic matter, but also contained partially filled frustules of the diatom Skeletonema costatum sp., Chaetoceros sp., and a small Thalassiosira sp. which resembled T. pseudonana.

Examination of the particulates collected at the surface and mid-depth at stations 9 and 10 in December revealed primarily detrital organic aggregates. However, a few cells of Thalassiosira decipiens and lesser quantities of Skeletonema costatum were encountered.

c. Primary production. Primary production measurements for the October cruise are presented in Figure VI-18, a-b as mgC m^{-3} hr^{-1} and mgC mg chlorophyll $a^{-1}hr^{-1}$, respectively. The rate of primary production per unit volume (mgC m^{-3} hr^{-1}) and primary production rate per unit phytoplankton (mgC mg chl a^{-1}) exhibited near surface minima and sub-surface maxima at stations 6 and 10 (at approximately 3.5 m). The extinction coefficient, k, measured at these stations was 0.52 m^{-1}. The observed depth distribution of photosynthesis

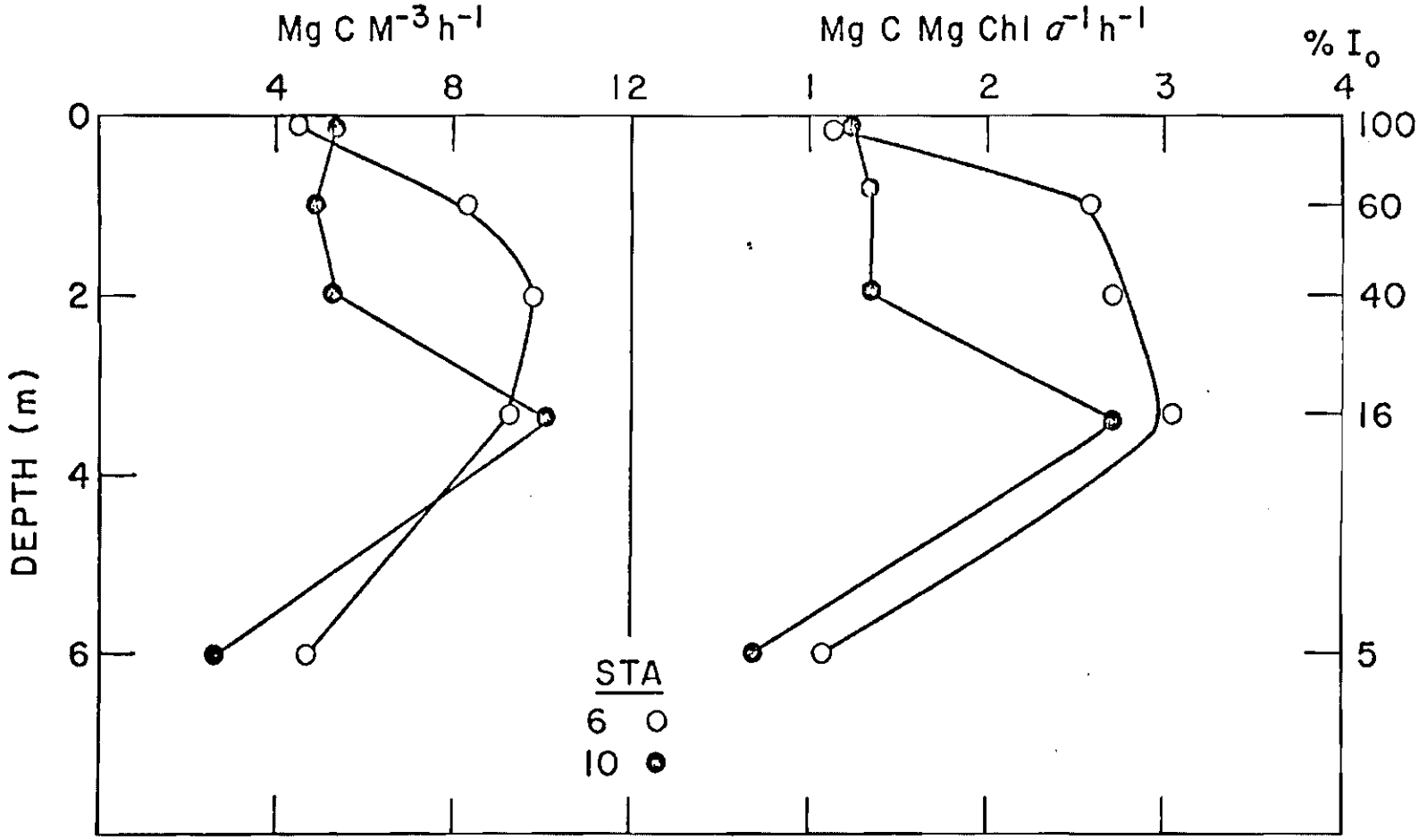

Figure VI-18. Depth distribution of carbon assimilation (mgC m^{-3} hr^{-1}) and assimilation index (mgC [mg chl a]$^{-1}h^{-1}$) for the October baseline cruise.

was likely due to photoinhibition induced at light intensities greater than 16% I_o, which occurred in the water column above a depth of 3.5 m. At intensities less than 16% I_o, photosynthesis was light limited. The depth distribution of available nutrients was relatively uniform (0.5 µM or less) in the 9 m deep euphotic zone and therefore did not influence the depth distribution of photosynthesis (Figure VI-17).

The assimilation index (mgC mg chl $\underline{a}^{-1}hr^{-1}$) at light saturation (16% I_o at 3.5 m) was 3.03 at station 6 and 2.70 at station 10, values which may indicate nutrient depletion (Curl and Small, 1965) in October. The rates presented in Figures VI-18, a-b are similar in magnitude to the rates measured by Mandelli *et al.* (1970) for nearby stations during October 1966. The depth integrated primary production rate was 46.57 and 37.16 mgC m^{-2} for stations 6 and 10, respectively.

The rate of primary production was measured during 1000 to 1500 hr at depths with illunination equivalent to 100, 60, 16, 5 and 1% I_o at stations 2 and 100, 60, 40, 16, 5, and 1% at station 6 in December. The extinction coefficient, k, was 0.58 m^{-1} for station 2 and 0.53 m^{-1} for station 6. The depth distributions of the primary production rate, chlorophyll *a* concentration, and assimilation index are

shown in Figures VI-19 and VI-20 for stations 2 and 6 respectively. Primary production was 36.87 mgC $m^{-2}h^{-1}$ for stations 2 and 42.53 for station 6.

The depth-distributed and depth-integrated primary production rates measured in December are similar to those observed during the October cruise. The values obtained in December, however, are probably over-estimates of in situ rates. The incubation procedure retained phytoplankton, collected at depth in a turbulent water column, at relatively constant simulated in situ light intensities for 3 hours. In the water column, the cells were mixed over a depth range in which they would have experienced a sharp light gradient. The constant light exposure was a consequence of the procedure required for those measurements and likely led to an over-exposure of the algae to light, when the incubation light regime is compared to the in situ exposure. This may account for the near surface suppression of measured photosynthesis. The algae, which were probably adapted to a low level of light, may have received sufficient illumination to produce some photoinhibition.

d. Zooplankton. Ctenophores and scyphomedusea encountered on the October cruise were abundant at all stations, clogging the nets and interfering with the quantitative collection and sub-sampling of the crustaceous zooplankton. Gelatinous zooplankton can not be quantitatively collected with nets, nor do they preserve well, but field observations suggest

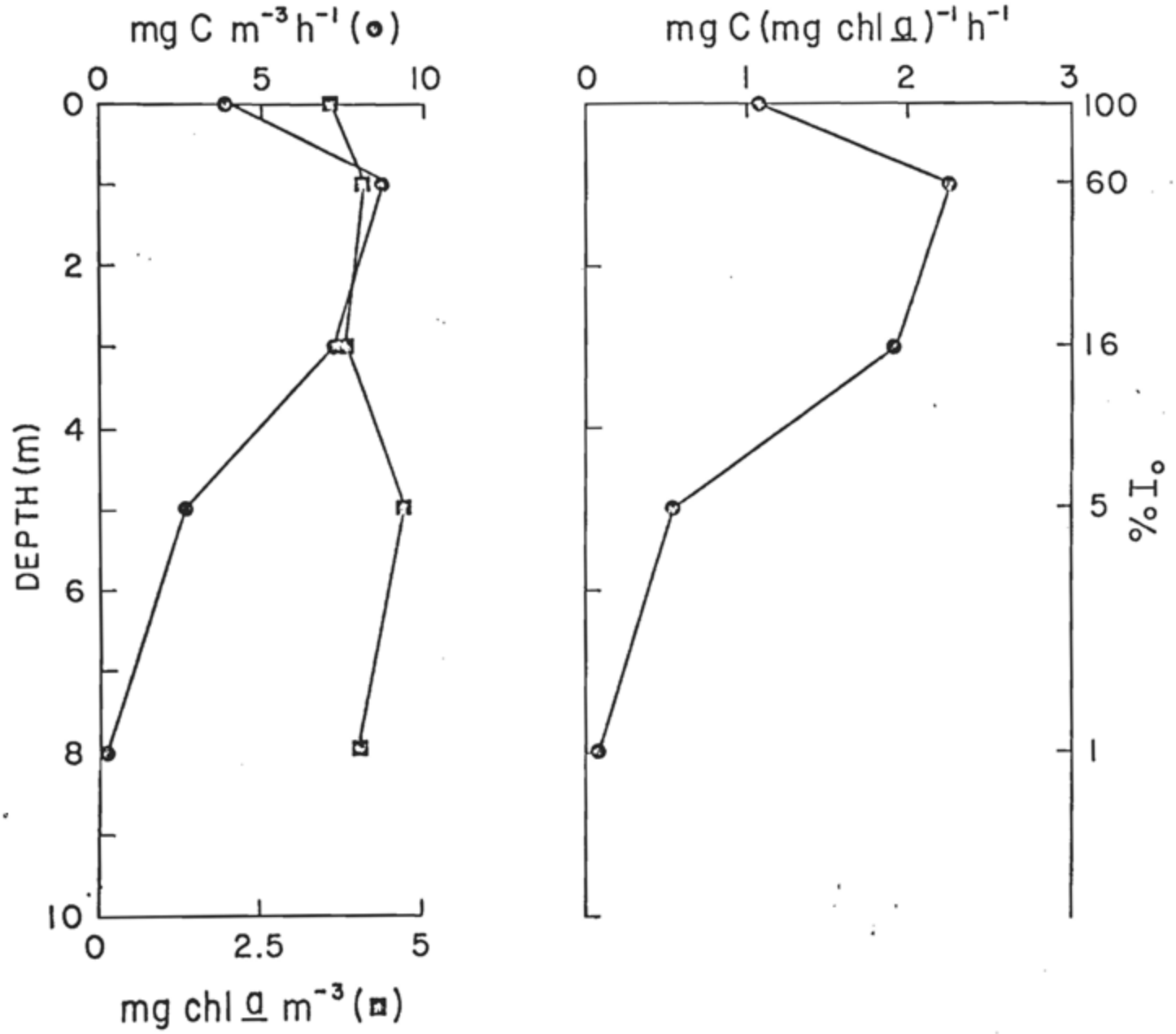

Figure VI-19. Depth distribution at station 2 of carbon assimilation (mgC m^{-3} hr^{-1}), chlorophyll a concentration (mg chl a mg^{-3}) and assimilation index [mgC (mg chl a)$^{-1}$ hr^{-1}] for the December baseline cruise.

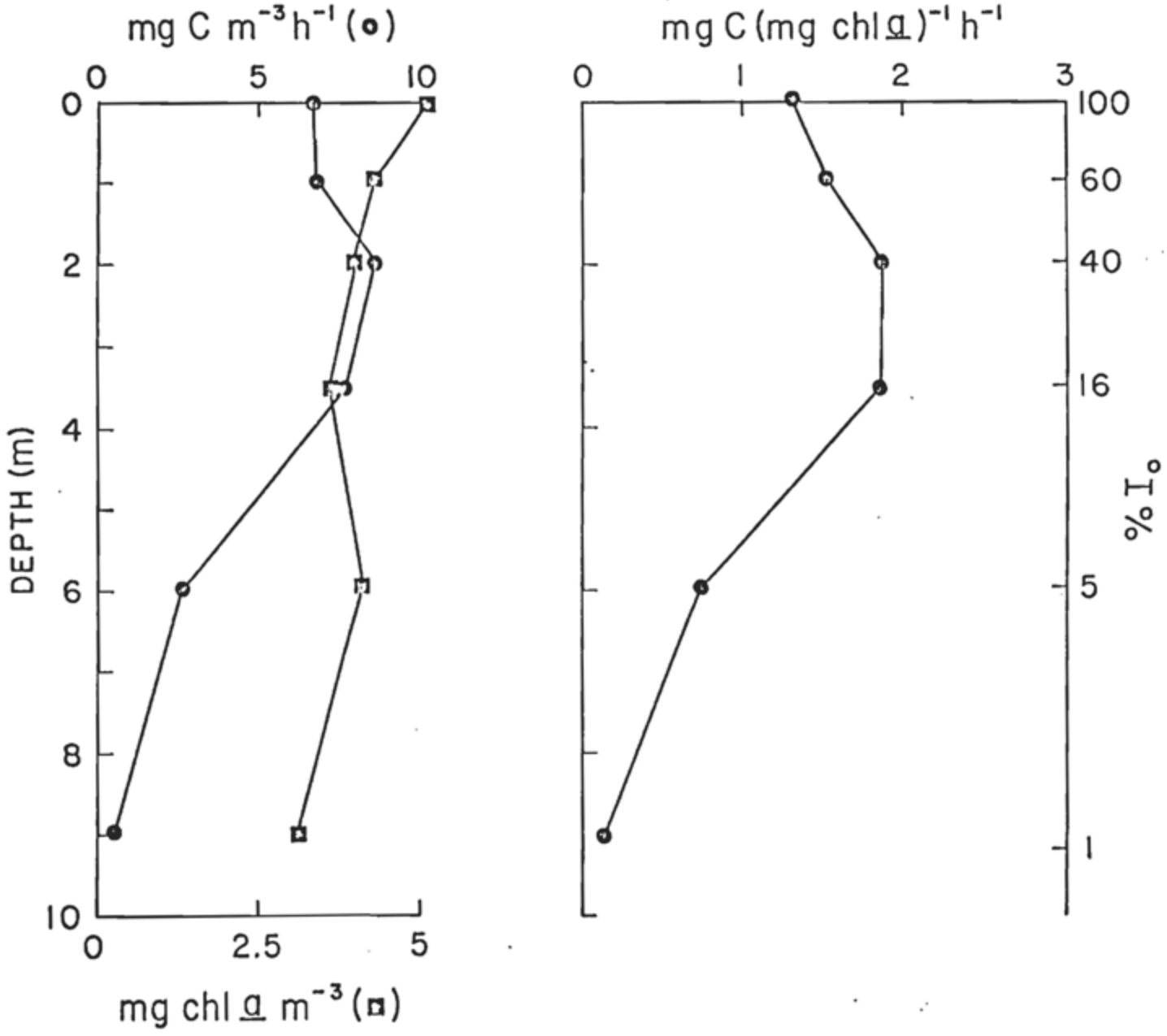

Figure VI-20. Depth distribution at station 6 of carbon assimilation (mgC mg^{-3} hr^{-1}), chlorophyll a concentration (mg chl a m^{-3}) and assimilation index [mgC (mg chl a)$^{-1}$ hr^{-1}] for the December baseline cruise.

that Pleurobrachia was the dominant ctenophore genus and Cyanea was the dominant scyphozoan genus. The preserved samples were subsampled for the nongelatinous zooplankton and species were enumerated for relative abundance offshore and inshore (Table VI-3).

While significant differences in the relative abundance of all species present were discovered among stations, in October, two species of copepods, Acartia tonsa and Paracalanus crassirostris, contributed greater than 90% of the total abundance of zooplankton at each station. In terms of biomass of small zooplankton, A. tonsa was the most important because of the larger size of individuals and their relative abundance.

During the December cruise, zooplankton abundances were low. The zooplankton samples were collected using vertically towed, metered 60 cm ring nets with 202 mm mesh nitex^{R}. Samples were immediately preserved in 10% formalin in seawater. Several of the whole samples were subsampled with a plankton splitter to minimize interference from the abundant ctenophores in the collections. Gelatinous animals did not preserve well and thus could not be enumerated. All recognizable zooplankton were identified and counted, their abundance is given in Table VI-4. The relatively low abundances cannot be attributed to clogging of the nets, and are typical of the winter zooplankton abundance minimum.

Table VI-3. Relative abundance of non-gelatinous zooplankton.

Zooplankton species	Station* 1	3	8	12
Acartia tonsa	318	383	221	233
Paracalanus crassirostris	103	61	131	50
Pseudodiaptomus coronatus	11	1	0	0
Centropages typicus	0	0	1	4
Centropages hamatus	1	4	0	0
Labidocera aestiva	1	1	2	2
Paracalanus parvus	1	0	4	0
Temora longicornis	0	0	0	2
Oithona similis	3	0	1	0
Farranula sp.	0	0	0	1
Microstella norvegica	1	0	0	0
Hyperiid amphipods	0	0	0	1
Decapod larvae	0	1	0	0
Cladocera (*Bosmina*)	0	0	3	17
Chaetognatha	0			
Total enumerated	439	451	363	311

*There are statistically significant differences among the stations in terms of the relative abundances of species listed, as revealed by RxC test of independence, using the G statistic (Sokal and Rohlf, 1969). $G = 192.95$, d.f. = 42 significant at $P < .500$) Critical value of $\chi^2_{42,0.005} = 69.336$

Table VI-4. Zooplankton abundance (animals m^{-3}) for the December 1978 cruise, excluding ctenophores.

Taxon		Sta. 1	Sta. 3	Sta. 9	Sta. 20	Mean +s. Dev
Copepoda:	Acartia clausii	11.7	313.6	24.6	65.2	103.77 ± 141.73
	Centropages hamatus	0.4	10.2	1.2	1.6	3.35 ± 4.59
	C. typicus	0.6	-	-	-	0.15 ± 0.30
	Paracalanus crassirostris	-	-	0.2	1.8	0.50 ± 0.87
	Oithona similis	-	2.1	-	1.4	0.87 ± 1.05
	Microsetella norvegica	-	-	0.3	-	0.07 ± 0.15
Gammarid amphipods:		0.2	-	0.2	0.2	0.15 ± 0.10
Meroplanktonic larvae:						
	Echinopulteus larvae	0.2	41.0	0.3	3.6	11.27 ± 19.88
	Polychaete larvae	0.2	-	0.3	1.0	0.37 ± 0.43
	TOTAL	13.2	375.1	27.1	74.8	122.55 ± 170.42

C. Benthic Community

1. Methodology

a. Sampling. Benthos sampling for baseline data in the vicinity of the project site was carried out over a grid of grab stations along four transects normal to the Fire Island shoreline. During the October cruise, 14 grab stations were sampled, of which four were unsatisfactory. In December, 12 grab stations were sampled with replicates of up to five samples taken at individual stations on each cruise. Station depths ranged from 17 m to 22 m over a sea bed of medium to coarse hard quartz sand, occasionally overlain by a thin surficial layer of mud. The positions of the benthos stations are shown in Figure VI-1.

The initial stations in October were sampled using a $0.04m^2$ Shipek sediment grab, model 8601. Although the sampler weighed 130 lbs., it often failed to properly penetrate the hard sand bottom and take an adequate sample. Subsequently, a heavy 0.1 m^2 Smith-McIntyre spring-loaded grab was employed for the sediment and benthic surveys because of its superior sampling capabilities on the hard sand bottom characteristic of the project site. The larger sediment samples taken with the Smith-McIntyre grab also provide more benthic organisms per sample.

b. Sample treatment. Each grab sample was washed successively through two sieve screens, with 2 mm and 1 mm mesh openings. A washing technique, using a copious water flow and rapid rotary agitation of the sieves, allowed

shorter sample processing times on deck, reduced sieve blockages, and minimized the physical damage to fragile benthic organisms. All organisms collected on the sieves were gently washed into storage jars which contained a few mls of Rose Bengal stain and some crystals of menthol at a temperature of 0° to 2°C. This process stained pink only the live animals, facilitating subsequent sorting, and narcotized them prior to preservation. On return to the laboratory the same day, samples were fixed with formalin buffered with sodium bicarbonate. The samples were subsequently transferred to 70% alcohol for permanent preservation. These procedures considerably increased efficiency by reducing sample handling and sorting times, both at sea and in the laboratory, while preserving the organisms in good condition.

2. Results

a. Fauna. Dominant organisms observed in the grab samples were the bivalves Tellina agilis and Astarte castanea, amphipods, Paraphoxus spinosus, Pseudunciola obliquua, including the haustorids Protohaustorius deichmannea, Prothaustorius wigleyi; sand dollars Echinarachnius parma; starfish, Asterias forbesi; and a diverse assemblage of some 30 species of polychaetes commonly including Nephthys picta, N. bucera, Lumbrineris fragilis, and occasional large colonies of Ampharete grubei. The results of the sorting and counts for the benthos stations are summarized generally in Tables VI-5

Table VI-5. Benthic species abundance by Phyla.

October Cruise

Station	5	6	9	10	11	12	13	14	15	16
Phyla										
Achelminthes	12	18		3	3	9		1	3	3
Annelida	18	12	33		13	19	12	17	4	12
Arthropoda	5	8			3			1		5
Mollusca			4	2	12	7	5	8		17
Bryozoa		3		1						
Echinodermata				2	2	16	6	1		2
Sipunculoida	1			1	2					
Total	36	41	37	9	35	51	23	28	7	39

December Cruise

Station	1	2	3	4	5	6A	7	8	9A	10A	11	12A
Phyla												
Achelminthes	4	8	20		2		4	2	12	6		2
Annelida	8	15	14	98	25	11	16	38	20	86	463	35
Arthropoda	25	55	16	32	1	4	44	1	3	25	28	6
Mollusca	45	74	21	27	30	20	18	58	59	45	24	63
Bryozoa		2								1		
Echinodermata	1	4		3		1	6			2	3	6
Sipunculoida			1	1	4		4	6		1		
Total	83	158	72	161	62	36	92	105	94	165	518	112

and VI-6 which list the numbers of infaunal benthic species by systematic groups and their wet total biomass for each station in October and December. Sand dollars, E. parma, were large and irregularly distributed in samples and were not included in these estimates. More detailed analyses of the benthos samples are given for each station in Tables VI-7 and VI-8 which list the numbers for different species for each cruise. A complete systematic listing of all species found is given in Table VI-9. Despite good technique, many animals were damaged during sieving, especially polycheate worms, and complete identification to species was not possible. This is reflected in the listing of genera or higher groups.

b. Biomass distribution. The measure used to estimate biomass (total wet weight of preserved species) was only semi-quantitative and variability was found between replicates from the same station, as expected. Benthic biomass appeared to be non-randomly distributed in the project area with the highest values for infaunal biomass (i.e. without sand dollars) found near the center of the station grid, in the vicinity of the Fire Island artificial reef (Figure VI-21).

c. Size of dominant macrobenthos. The growth and size distribution of animals may often provide a valuable index to use in making environmental comparisons and assessments. The size of some of the more common members of the benthic community was therefore routinely measured during the sorting of samples. The size distributions for three macrobenthic species, - the bivalves, Astarte castanea and Tellina agilis, and the sand dollar Echinarachnius parma, are shown as percent

Table VI-6a. Benthic Biomass by Phyla (wet weight, gm), October.

	Station Number									
	5	6A	6B	6C	6D	6E	9	10A	10B	10C
Achelminthes	0.0097	-	-	0.0032	0.0038	0.0017	0.001	0.0162	0.0012	0.047
Annelida	0.3613	0.6013	0.5949	0.7513	0.7701	0.4168	0.6002	0.2851	0.2545	0.2749
Arthropoda	-	0.0035	0.0053	0.0124	0.0124	0.0706	-	0.0046	-	0.0010
Mollusca	0.1980	8.5233	-	0.1997	0.0946	0.2076	0.0727	0.0450	0.8029	16.5051
Bryozoa	-	0.0003	0.2193	0.0003	-	-	-	0.0013	-	-
Echinodermata	-	-	0.1973	-	-	-	-	0.1892	7.7634	0.0588
Sipunculoida	0.0139	-	-	-	-	-	-	0.0011	-	0.0077
Total Biomass	0.5829	9.1284	1.0168	0.9669	0.8809	0.6967	0.6739	0.5425	8.8220	16.8945

	Station Number									
	11A	11B	11C	11D	11E	12	13	14	15	16
Achelminthes	-	0.0004	0.0095	0.0110	0.0140	0.0058	0.0015	0.0794	0.0001	0.0033
Annelida	0.5819	0.0362	0.1638	0.2352	0.5883	0.2501	0.1535	0.0362	0.1616	0.1163
Arthropoda	0.0199	0.0223	0.0224	0.0052	0.0906	-	-	0.0681	-	0.0538
Mollusca	0.1069	17.6642	0.0160	0.1358	0.0268	0.1627	0.7065	-	-	0.8967
Bryozoa	-	-	-	-	-	-	-	3.7051	-	-
Echinodermata	0.7802	-	-	-	-	1.9596	-	-	-	0.1051
Sipunculoida	0.0281	0.0003	-	-	-	-	-	-	-	-
Total Biomass	1.5170	17.7234	0.2117	0.3872	0.7197	2.3782	0.8615	3.8888	0.1615	1.1752

Table VI-6b. Benthic Biomass by Phyla (wet weight, gm), December.

	Station Number										
	1	2	3	4	5	6A	6B	6C	7	8	9A
Cnidaria	-	-	-	-	-	0.15	-	-	-	-	-
Achelminthes	0.0683	0.0046	0.0053	0.0054	0.0002	-	-	-	0.0008	-	0.0059
Annelida	0.2841	1.0421	0.2699	0.2750	0.3172	-	2.0716	4.7382	0.3815	0.4708	0.9784
Arthropoda	0.0639	0.1349	0.0330	0.2062	-	-	0.0358	0.2560	0.0070	0.0084	0.0129
Mollusca	0.2454	0.5288	1.4503	0.2336	0.0986	7.6271	0.4350	-	0.2320	0.2880	0.4903
Bryozoa	-	-	-	-	-	-	-	-	-	-	-
Echinodermata	4.000	17.1874	-	7.0460	-	-	0.0075	-	12.3972	-	-
Sipunculoida	-	-	0.0070	-	0.0573	-	-	-	0.0064	0.0906	-
Total Biomass	4.6621	18.8978	1.7655	7.7662	0.4733	7.7771	2.5499	4.9942	13.0249	0.8578	1.4875

	Station Number										
	9B	9C	9D	9E	10	11A	12A	12B	12C	12D	12E
Cnidaria	-	-	-	-	-	-	-	-	-	-	-
Achelminthes	-	-	-	-	0.0017	-	0.0007	-	0.0016	-	-
Annelida	0.3754	0.4038	0.1565	0.5138	0.8925	2.1400	0.6250	0.1205	0.0696	0.0130	0.1043
Arthropoda	0.0384	0.0164	-	-	0.1385	0.1707	0.0126	0.1055	0.0505	0.0359	0.4345
Mollusca	1.0153	0.3084	0.2300	0.1879	0.3189	9.5526	0.2301	0.1842	0.6179	0.0668	0.1444
Bryozoa	-	-	-	-	0.0013	-	-	-	-	-	-
Echinodermata	-	-	-	-	5.0281	0.2147	0.3795	0.2236	0.5019	-	0.0473
Sipnuculoida	0.3111	-	-	-	0.0028	-	0.0062	0.0969	0.1230	-	0.0023
Total Biomass	1.7402	0.7286	0.3865	0.7017	6.3838	12.078	1.2541	0.7307	1.3645	0.1157	0.07328

Table VI-7. Benthos Species Abundance, October.

Stations	5	6	9	10	11	12	13	14	15	16
Species										
Nematod spp.	12	18		3	3	9		1	3	3
Oligochaete A	5		9			1	2			
Oligochaete B		1								
Ampharete grubei	2	4	1			1	1			
Driloneris sp.	2					1				
Chaetopterid A		1						1		1
Cirratulus grandis	1									
Cirratulus cirratulus			1							
Cirratulus sp. A						3	5			
Glycera americana			1		3					1
Glycera capitata							4			
Goniada maculata		2	2							
Lumbrineris brevipes		1			1					
Lumbrineris tenuis								1		
Clymenella zonalis		1								
Nepthys bucera			1		3	2		2	2	1
Nepthys incisa	1		1							
Ammotrypane aulogaster			1							
Orbinia ornata	7		1		4	7		8	2	8
Scoloplos sp.		1								
Orbinid sp.			15					1		1
Harmothoe extenuata						1				
Chiriodotea coeca		1				1		2		
Neomysis americana								2		
Unciola irrorata					2	2				

Table VI-7. Benthos Species Abundance, October Continued.

Stations	5	6	9	10	11	12	13	14	15	16
Parahaustorius deichmannae								1		2
Protohaustorius wigleyi					2					3
Tanaidacea	5				1					
Nassarius trivittatus				1			1			1
Tellina agilis		8	4	1	6	4	4	8		16
Astarte castanea					6	3				
Bugula sp.		3		1						
Echinarachnius parma				2	2	16	6	1		2
Sipunculoid A	1			1	2					
TOTAL INDIVIDUALS	36	41	37	9	35	51	23	28	7	39

Table VI-8. Benthos Species Abundance, December.

Stations	1	2	3	4	5	6	7	8	9	10	11	12
Species												
Nematod spp.	4	8	20		2		4	2	12	6		2
Ampharete grubei	3	6	4	80	7		1	1	1	58	451	12
Driloneris longa				1	1							
Driloneris sp.						2						
Chaetopterid A									1			
Cirratulus grandis					2							
Cirratulus cirratulus										3		
Cirratulus sp			1	7	4	3					2	
Glycera americana			1									
Glycera capitata					1					1		
Glycera dibranchiata								5		1		
Glycera sp.	1									3	4	
Goniada maculata	2		1							1		7
Lumbrineris acuta								2	1			3
Lumbrineris fragilis		1	3			3	1	7		3	4	
Lumbrineris tenuis			1									
Nepthys bucera			2					6		11		10
Nepthys incisa				4			7	5	6	1		3
Nepthys spp.	2	1				1	2					
Orbinia ornata		2		3	1		2					
Orbinid sp.				1	1		2	2	9	1	1	
Harmothoe sp.			1									
Scalibregma inflatum		1					1					
Sigalion arenicola		4				2					1	
Spiophanes bombyx				1	2			2	2			
Spionid A				1	6			8				
Spionid B										2		

Table VI-8. Benthos Species Abundance, December Continued.

Stations / Species	1	2	3	4	5	6	7	8	9	10	11	12
Phyllodicid							1					
Chiridotea coeca		1				1	1			1	27	1
Cerastoderma pinnulatum										1		
Pseudunciola obliquua	20	49	5	15			13			12		5
Unciola irrorata						1				3		
Acanthohaustorius sp.							8					
Protohaustorius wigleyi			3	17			21		1		1	
Anoyx liljeborgi										4		
Photis macrocoxa						1						
Paraphoxus spinosus		4	5							4		
Trichophoxus epistomus						1		1				
Tanaidacea	5	1	3						2			
Pagurus sp.					1							1
Bivalve A	7	7	5	11	15	1	10	9	12	4		9
Cerastoderma pinnulatum		2				2						
Ensis directus	1			1				2				8
Tellina agilis	36	56	14	15	15	17	8	47	47	28	24	44
Astarte castanea	1	9	2							13		1
Bugula sp.		2								1		
Asterias forbesi						1					1	
Echinarachnius parma	1	4		3			6			2	2	6
Sipunculid A			1	1	4		4	6		1		
TOTAL INDIVUDALS	83	158	72	161	62	36	92	105	94	165	518	108

Table VI-9. Systematic list of species collected.

Cnidaria (Coelenterata)

Hydrozoa

Hydrozoa sp.

Anthozoa

Metridium senile (sea anemone)

Achelminthes

Nematoda (Round Worms)

unidentified spp.

Annelida

Oligochaeta

Oligochaete A

Oligochaete spp.

Polychaeta

Ampharetidae:

Ampharete grubi (tent.)

Arabellidae:

Drilonereis longa

Drilonereis sp.

Chaetopteridae:

Chaetopterid A

Cirratulidae:

Cirratulus grandis

Cirratulus cirratulus

Cirratulid

Tharyx sp.

Table VI-9 Continued

Glyceridae:

Glycera americana

Glycera capitata

Glycera dibranchiata

Glycera spp.

Goniada brunnea or *maculata*

Lumbriconerida:

Lumbrineris brevipes

Lumbrineris fragilis

Lumbrineris tenuis

Maldanidae:

Clymenella zonalis

Nepthyidae:

Nepthys bucera

Nepthys incisa

Nepthys spp.

Opheliidae:

Ammotrypane aulogaster

Orbiniidae:

Orbinia ornata

Orbiniid sp.

Scoloplos sp.

Phyllodocidae:

Phyllodocid A

Polynoidae:

Harmothoe extenuata

Harmothoe sp.

Table VI-9 Continued

Scalibregmidae:

Scalibregma inflatum

Sigalionidae:

Sigalion arenicola

Sigalionid sp.

Spionidae:

Spiophanes bombyx

Spionid A

Spionid B

Arthropoda - Crustacea

Isopoda

Chiridotea tuftsi

Chiridotea coeca

Mysidacea (Shrimp)

Neomysis americana

Cumacea

Oxyurostylis smithi

Amphipoda (Beach fleas, Scuds)

Aoridae:

Unciola irrorata

Pseudunciola obliquua

Lysianassidae:

Anoyx liljeborgi

Haustoriidae:

Parahaustorius deichmannae

Parahaustorius longimerus

Table VI-9 Continued

Protohaustorius wigley

Pseudohaustorius spp.

Acanthohaustorius spp.

Photis macrocoxa

Phoxcephalidae:

Paraphoxus spinosus

Trichophoxus epistomus

Decapoda

Caridae:

Cragon septemspinosis

Anomura:

Pagurus sp. (Hermit crab)

Brachuyra: (Crabs)

Brachyura spp.

Mollusca

Gastropoda (Snails)

Prosobranchia:

Lunatia heros

Nassarius trivittatus

Bivalvia (Clams)

Protobranchia:

Lamellibranchia:

Astarte castanea

Ensis directus

Tellina agilis

Table VI-9 Continued

Bryozoa

Bicellariidae:

Bugula sp.

Membraniporidae:

Membraniporida spp.

Echinodermata

Asteroida (Sea Stars)

Asterias forbesi

Echinoida: (Sand dollars)

Echinarachnius parma

Sipunculoida

Sipunculid A

Sipunculid B

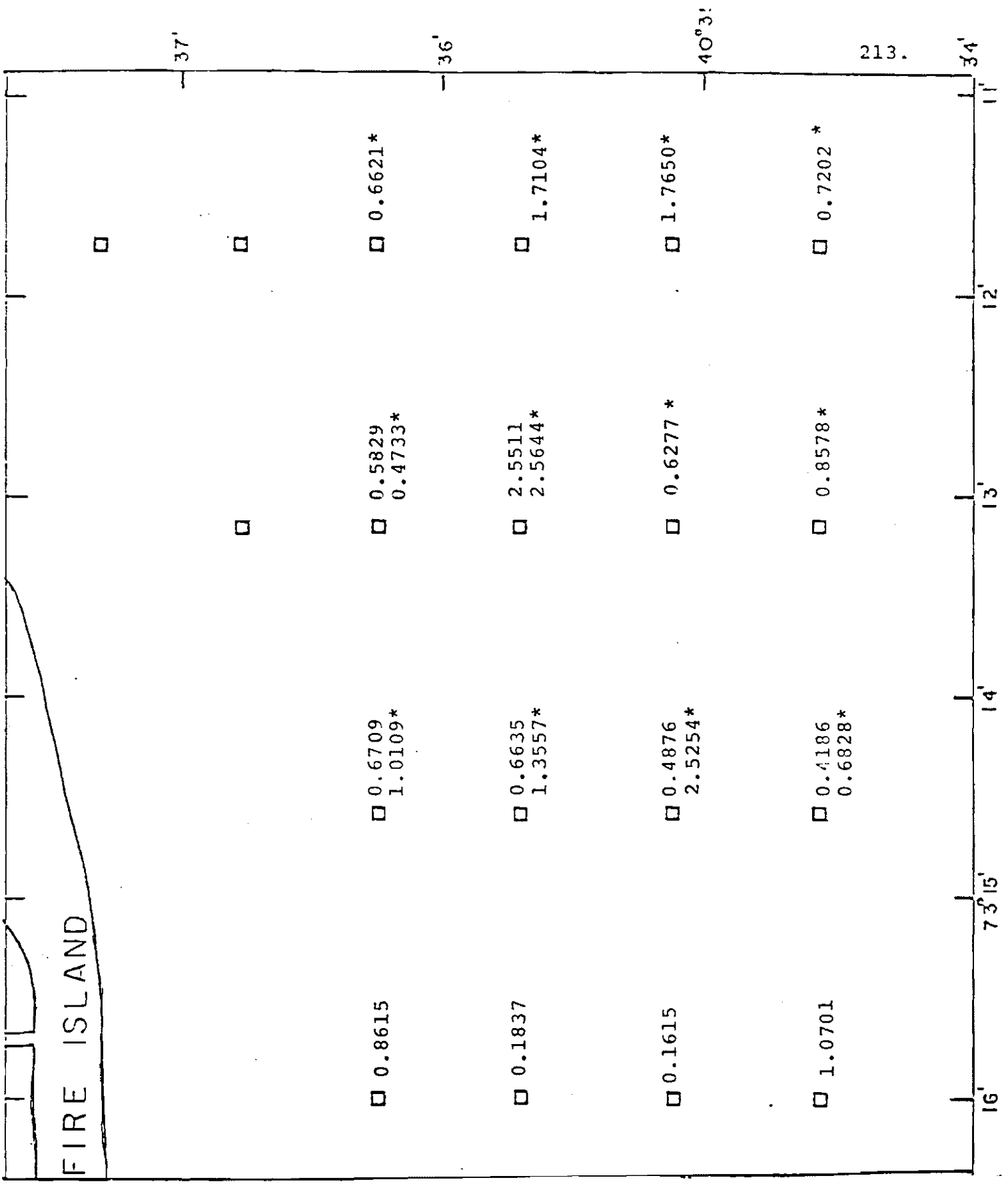

Figure VI-21. Distribution of infaunal benthic biomass (wet weight, gm) without surface sand dollars, E. parma, October and December.

* = December cruise.

size frequency for the October cruise in Figures VI-22, 23, and 24. For each organims, two or more size-classes appear to be present. These results were supported by the measurements made of the same animals in the samples taken during the December cruise.

D. Bulk Sediment Properties

1. Methodology

a. Sampling. Smith-McIntyre bottom grab samples were taken on 19 stations shown in Figure VI-1. A Smith-McIntyre grab sampler intercepts a sediment surface area of about 0.1 m^2 to an approximate depth of 10 cm of sediment.

b. Sediment texture. Analysis of grain-size distribution was performed by dry sieving according to standard methods described by Folk (1968). The limits and names of size grades used in this study are sand, for particle diameters between 2 and 0.063 mm and for material finer than 0.063 mm, the term mud is used. At stations 6, 10, and 11, replicate grabs were collected to determine the sampling variability (Table VI-10). Considering that sand is the dominant sediment component at the study site, the sampling variability is relatively small. In terms of gravel and mud fractions, however, the variability is large, approaching 100%.

c. Total carbon and nitrogen. Total carbon and nitrogen were determined on dried sediment samples using a CHN analyzer. Sampling and sample variability for carbon and nitrogen are given in Table VI-11.

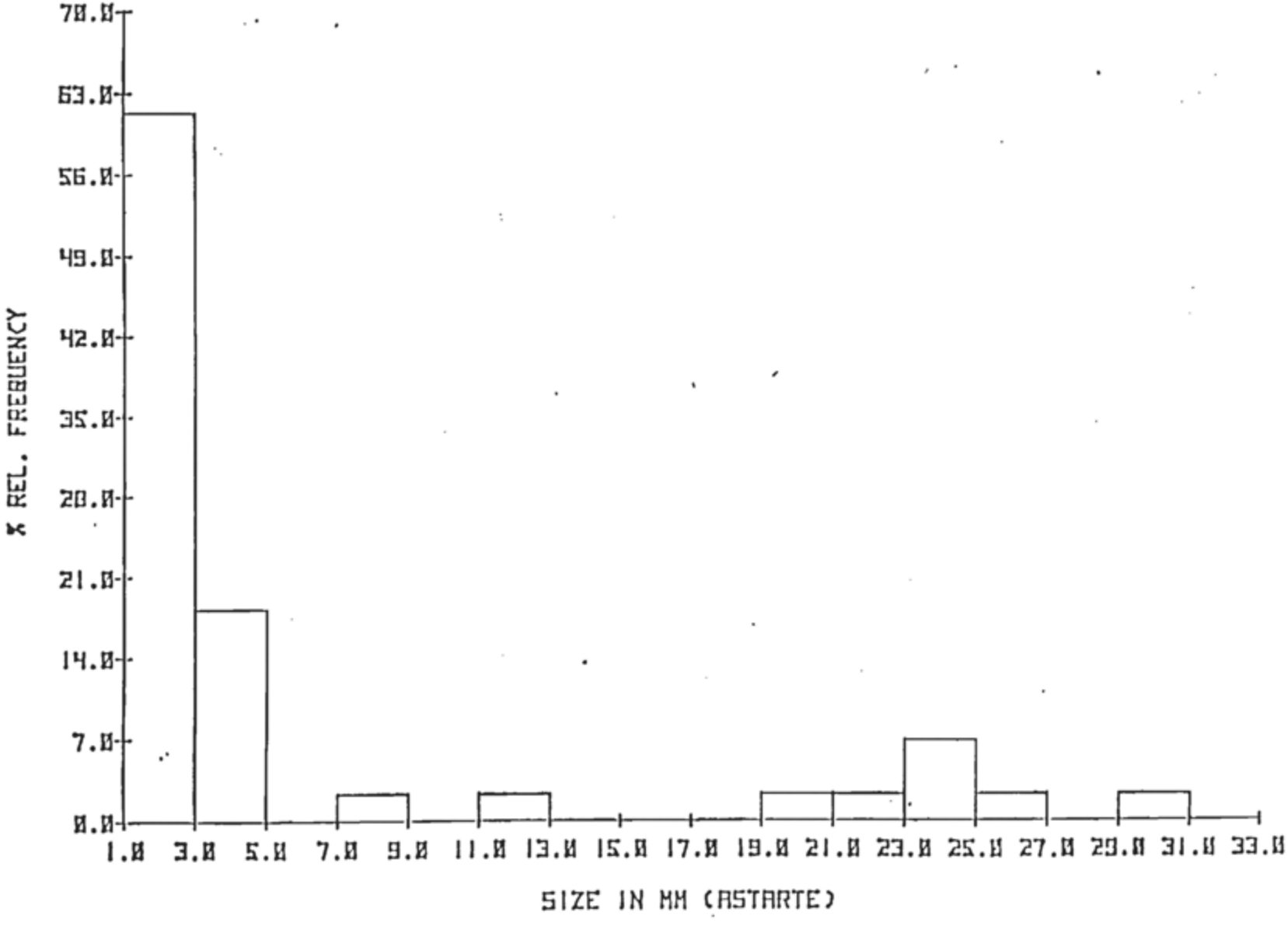

Figure VI-22. Shell lengths of Astarte castanea, percent frequency.

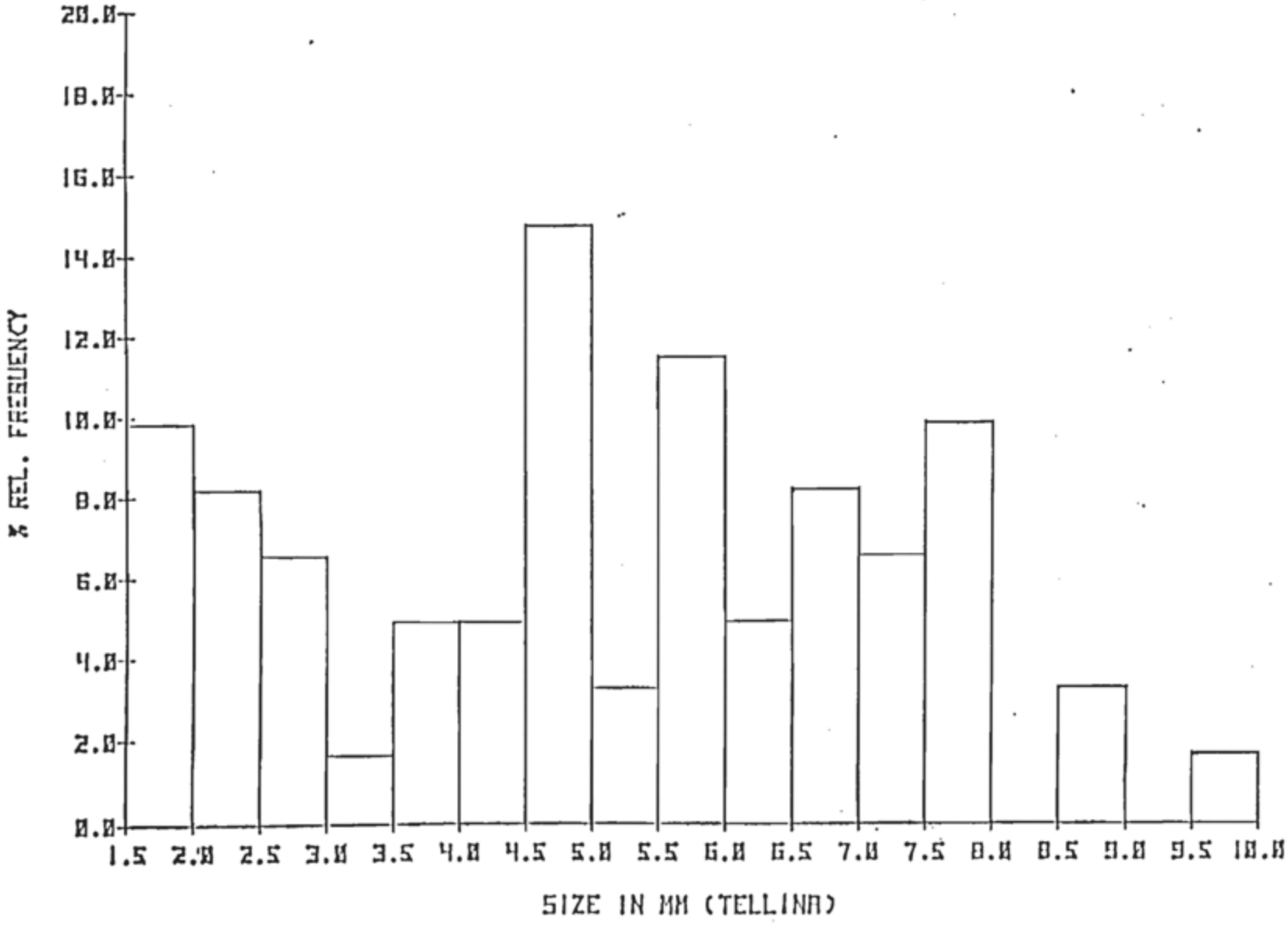

Figure VI-23. Shell lengths of Tellina agilis, percent frequency.

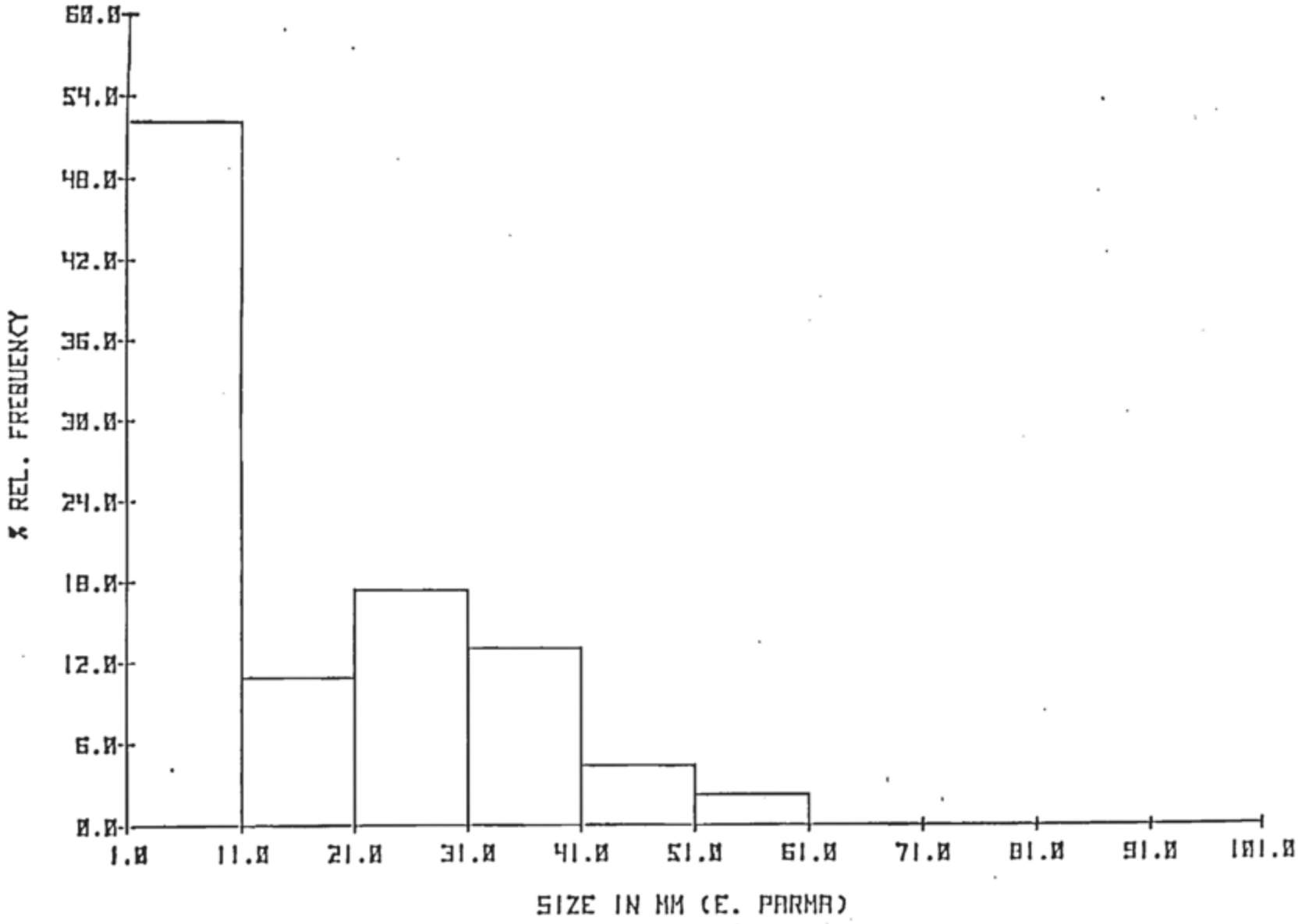

Figure VI-24. Diameter of sand-dollars, E. parma, percent frequency.

Table VI-10. Sediment textural data showing sampling variability at stations 6, 10 and 11 at the project site.

Station No.	No of Replicates	*	Weight Percent			
			Water Content	Gravel	Sand	Mud
6	4[x]	$\bar{x}$	18.5	2.79	96.5	0.66
		s	0.8	2.83	2.9	0.45
10	3[x]	$\bar{x}$	20.6	0.13	99.4	0.47
		s	0.8	0.03	0.3	0.22
11	5[x]	$\bar{x}$	18.0	0.29	99.6	0.11
		s	0.6	0.18	0.2	0.03

* $\bar{x}$ = mean value
s = standard deviation

x number of grab samples collected at each station

Table VI-11. Carbon and nitrogen content of sediment grabs collected at the project site.

Station No.	Weight Percent Carbon	Nitrogen
1	0.09	0.03
2	0.05	0.01
3	0.04	0.004
4	0.06	0.02
5	0.14	0.02
6*	0.29±.33	0.04±.04
7	0.05	0.05
8	0.07	0.02
9	0.08	0.01
10*	0.01±.10	0.01±.004
11*	0.04±.02	0.06±0.05
12	0.04	0.01
13	0.13	0.01
14	0.05	0.01
15	0.05	0.01
16	0.05	0.01
17**	0.05±.001	0.01±.001
18	0.09	0.02
19	0.08	0.02

* 4 grab samples were collected at station #6
3 grab samples were collected at station #10
5 grab samples were collected at station #11

** 1 grab sample was collected at station #17 analyzed 5x

d. Percent water. The mass percent water of sediment was determined gravimetrically by drying at 70°C until the weight was constant. The effect of sampling variability on water content at stations 6, 10, and 11 is given in Table VI-10.

e. Sediment trace element analysis. A sample of 2.5 g of oven-dried, finely-ground bulk sediment was weighed in an acid-cleaned 4 oz polyethylene bottle. The sample was digested in 10 ml of concentrated nitric acid on a sand bath at 80°C for 2 hr. The warm sample was filtered using Millipore filtration apparatus and the sediment residue was washed three times with 10 ml aliquots of distilled water. The filtrate and wash solution were collected in a 50 ml volumetric flask and the total volume was brought to 50 ml with distilled water. The resulting solution was analyzed for Cr, Zn, Pb, Cu, Fe, Mn, and Ni by flame atomic absorption spectrophotometry. Metal concentration data for replicate grabs collected at stations 6, 10, and 11 are given in Table VI-12. Also included is the metal data showing sample variability for sediment grab collected at station 5.

f. Pore water sampling. An in situ pore water sampler has been developed and will be tested in the field at the project site. A front view of the sampler is shown in Figure VI-25. This device allows in situ sampling of pore water contained in surrounding host sediment at discrete intervals along the length of the sampler. The sample

Table VI-12. Metal concentration data showing sampling and sample variability in sediment grabs collected at the project site.

tion ber	No of Replicates	*	Fe(%)	Mn(ppm)	Zn(ppm)	Cu(ppm)	Cr(ppm)	Ni(ppm)	Pb(ppm)
	3[a]	$\bar{x}$	0.47	133	15.88	1.89	6.09	1.60	8.84
		s	0.01	18	0.93	0.03	0.70	0.12	0.63
		CV	1.8	13.5%	6.2%	1.8%	11.5%	7.6%	7.1%
	4[b]	$\bar{x}$	0.19	48	7.33	1.55	2.62	0.99	4.27
		s	0.05	15	2.40	0.57	0.79	0.39	1.43
		CV	27.0	31.0%	32.8%	3.6%	30.5%	33.9%	33.5%
	3[c]	$\bar{x}$	0.28	84	9.25	1.23	3.79	0.95	5.92
		s	0.04	34	3.04	0.11	1.16	0.35	1.48
		CV	13.9	40.8%	32.9%	8.9%	30.3%	36.9%	25.1%
	5[d]	$\bar{x}$	0.12	24	3.6	0.68	1.44	0.34	2.12
		s	0.01	4	0.3	0.04	0.14	0.03	0.31
		CV	8.8	14.7%	9.2%	6.1%	9.9%	8.8%	15.5%

* $\bar{x}$ = mean value
s = standard deviation
CV = coefficient of variation

a Three sub-samples of a sediment grab collected at station 5
b Four grab samples collected station 6
c Three grab samples collected at station 10
d Five grab samples collected at station 11

Figure VI-25. In situ pore water sampler.

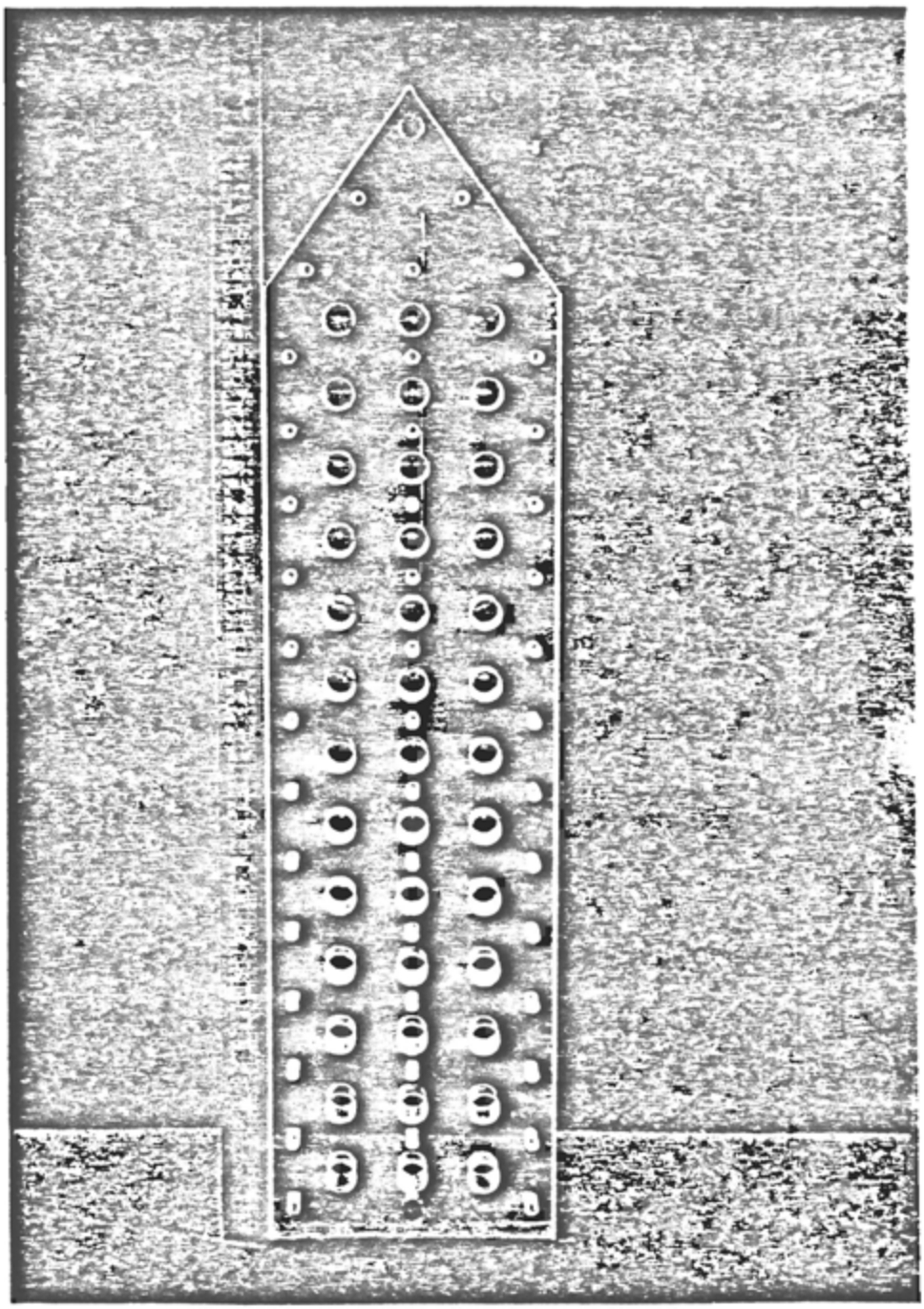

compartments are closely spaced at a constant interval of 2 cm. Three compartments at each depth allow replicate sampling of pore water at that particular depth.

2. Results and Discussion

Surficial dark gray mud was visibly present in a number of samples suggesting minimal washout of sediment during the sampling operation. Substantial amounts of surficial sediment were sub-sampled from each grab sample for the analyses of bulk sediment properties. Residual sediment was used for benthic infauna studies. A total number of 28 grab samples were collected; at least three replicates were sampled at stations 6, 10, and 11.

The sediments at the study site consist of generally medium to coarse light brown quartz sand. At several stations, this material is overlain by a surficial 1 cm thick layer of dark gray mud. In some samples, appreciable amounts of gravel containing rounded pebbles were observed. Grain size analysis shows that the sediment in the area is basically sand, with the sand content approaching 100% at some stations (Table VI-13). Microscopic examination of the sand fraction reveals that quartz is the dominant mineral. The quartz grains are often stained with a reddish-brown iron-oxide coating. X-ray diffraction analysis of the mud-fraction (2-63 μM) reveals the presence of quartz, feldspars, and goethite. It seems that the ironoxide coating observed on quartz grains is goethite.

Table VI-13. Textural data for sediment grabs collected at the project site.

:ation No.	Weight Percent			
	Water	Gravel	Sand	Mud
1	18.1	0.4	99.2	0.3
2	17.8	0.7	99.1	0.2
3	17.2	1.9	98.0	0.1
4	21.9	0.1	99.7	0.2
5	20.3	0.1	96.7	3.2
6 *	18.5	2.8	96.5	0.7
7	21.2	0.1	99.7	0.2
8	19.2	0.1	99.7	0.2
9	18.5	0.2	99.4	0.4
10 *	20.6	0.1	99.4	0.5
11 *	18.0	0.3	99.6	0.1
12	17.5	0.3	99.6	0.1
13	17.5	0.8	98.2	1.0
14	19.9	0.1	99.8	0.1
15	21.0	0.2	99.1	0.7
16	18.7	0.0	99.9	0.1
17	20.2	0.2	98.7	1.1
18	19.2	0.4	99.1	0.5
19	20.8	0.1	97.4	2.5

*4 grab samples were collected at station #6
3 grab samples were collected at station #10
5 grab samples were collected at station #11

The water content of sediment samples varies from 17.2 to 21.9% by weight, (Table VI-13). The observed values of water content are characteristic of surficial sandy sediment; small differences in water content of sediment from one station to another reflect lack of variation in sediment texture.

Flame atomic absorption analysis of the sediment acid-leachable component for trace metals is given in Table VI-14. The results show that the metals concentrations do not vary greatly from one station to another. This may be due to the lack of variation in sediment texture. Station No. 5, however, exhibits elevated concentrations for all metals as compared with other stations. The observed concentrations are typical of relatively uncontaminated coarse-grained coastal sediments.

The total carbon and nitrogen content of sediment samples is given in Table VI-11. Total carbon values range from 0.01% at station 10 to 0.29% at station 6. Interestingly enough, station 6 is located at the old reef site. Elevated metal concentrations have also been observed in this general area. The nitrogenous part of the organic matter also shows enrichment in this area as compared with other stations.

E. Sub-bottom Seismic Survey

In October, a seismic reflection survey was made to examine the details of the sub-surface structures at the reef site. An EG & G Uniboom Model 230-1 unit pulse seismic energy source was used and 15 n miles of seismic profile were made (Figure VI-26).

Table VI-14. Metal concentration data for sediment grabs collected at the project site.

ation No.	Acid-Leachable Metal Concentrations						
	Fe (%)	Mn(ppm)	Zn(ppm)	Cu(ppm)	Cr(ppm)	Ni(ppm)	Pb(ppm)
1	0.24	60	6.1	1.08	2.85	0.78	3.94
2	0.15	36	3.6	0.64	1.63	0.38	2.08
3	0.18	40	3.6	0.79	1.93	0.37	2.26
4	0.25	95	8.2	1.06	3.64	1.07	5.76
5x	0.47	133	15.8	1.89	6.09	1.60	8.84
6Y	0.19	48	7.3	1.55	2.62	0.99	4.27
7	0.39	210	10.8	1.19	5.63	1.11	6.82
8	0.11	22	3.8	0.87	1.62	0.53	2.45
9	0.18	30	5.9	0.95	2.54	0.48	3.53
0z	0.28	84	9.3	1.23	3.79	0.95	5.92
1	0.12	24	3.6	0.68	1.44	0.34	2.12
2	0.11	20	4.1	0.75	1.76	0.48	2.22
3	0.16	45	6.9	1.45	2.69	0.86	3.59
4	0.20	80	8.9	5.53	2.56	0.55	4.07
5	0.34	103	12.3	1.32	4.49	1.29	6.57
6	0.19	85	6.3	0.87	2.70	0.59	3.93
7	0.22	71	6.2	0.84	2.42	0.55	3.39
8	0.17	49	5.6	1.07	2.02	0.68	2.74
9	0.34	102	11.1	1.36	4.19	1.14	6.64

mean value of 3 sub-samples of a grab collected at station 5
mean value of 4 grab collected at station 6
mean value of 5 grabs collected at station 10

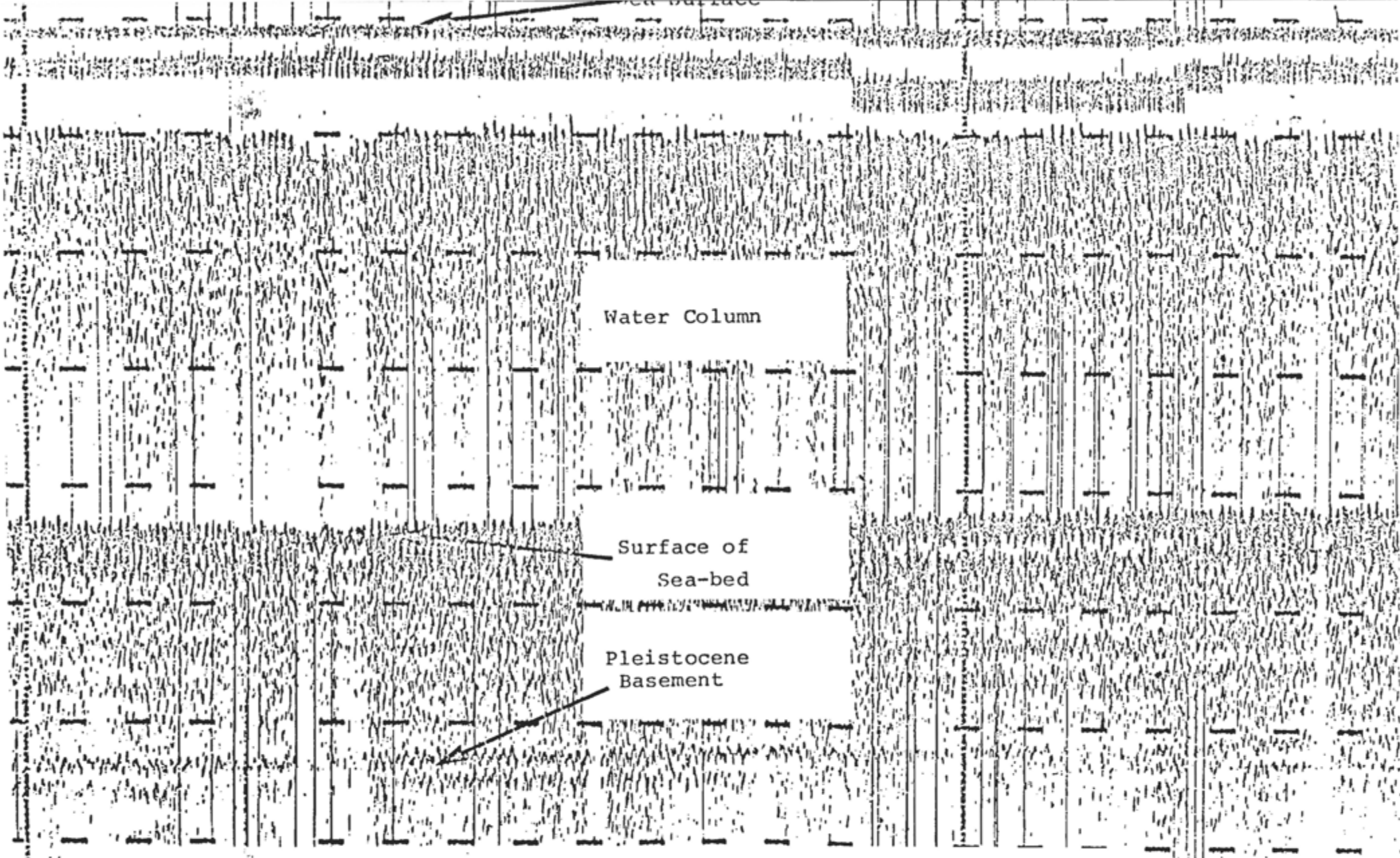

Figure VI-26. Seismic profile at the project site.

The bottom bathymetry at the project site is shown in Figure VI-27. With the equipment used in the survey, penetration was limited to the top 25-30 m of the sediment cover corresponding to depths about 50 m below sea level. This range was sufficient to detect an undulating reflector at a depth of 30-35 m which is identified as the Pleistocene Cretaceous Contact. Deeper stratigraphy, including the bedrock surface, could not be detected. Recent sediments overlying the Pleistocene material could not be distinguished. At the reef site, the cover of Pleistocene and Recent sands is 10-15 m thick (Figure VI-28). The sediments below this reflector are contorted; above the reflector the sediments are flat-lying and apparently homogenous. There is no indication of Recent estuarine muds buried at the reef site.

The regional geology off the south shore of Fire Island has been discussed by Williams (1976) based on a survey consisting of 960 miles of seismic reflection profiles and 152 vibratory cores and included the reef site; the post-glacial, sedimentary history of this is discussed by Sanders and Kumar (1975).

At Fire Island, the crystaline bedrock lies at a depth of about 610 m. The bedrock is overlain by strata of late Cretaceous and early Tertiary coastal plain sediments. The surface of the coastal plain sediments lies about 30 m below sea level at Fire Island. Pleistocene sediments overlie the coastal plain strata (Jensen and Soren, 1974).

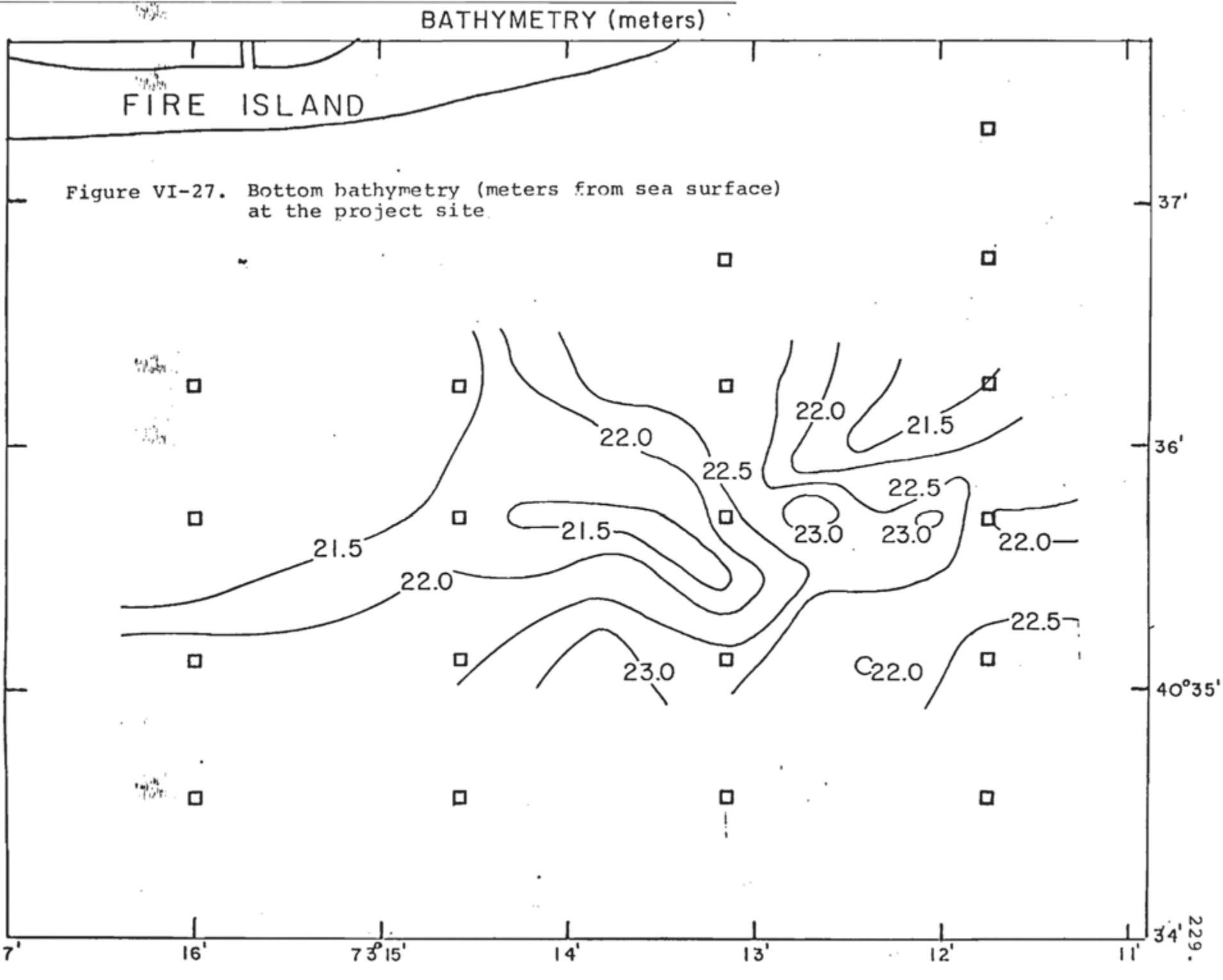

Figure VI-27. Bottom bathymetry (meters from sea surface) at the project site

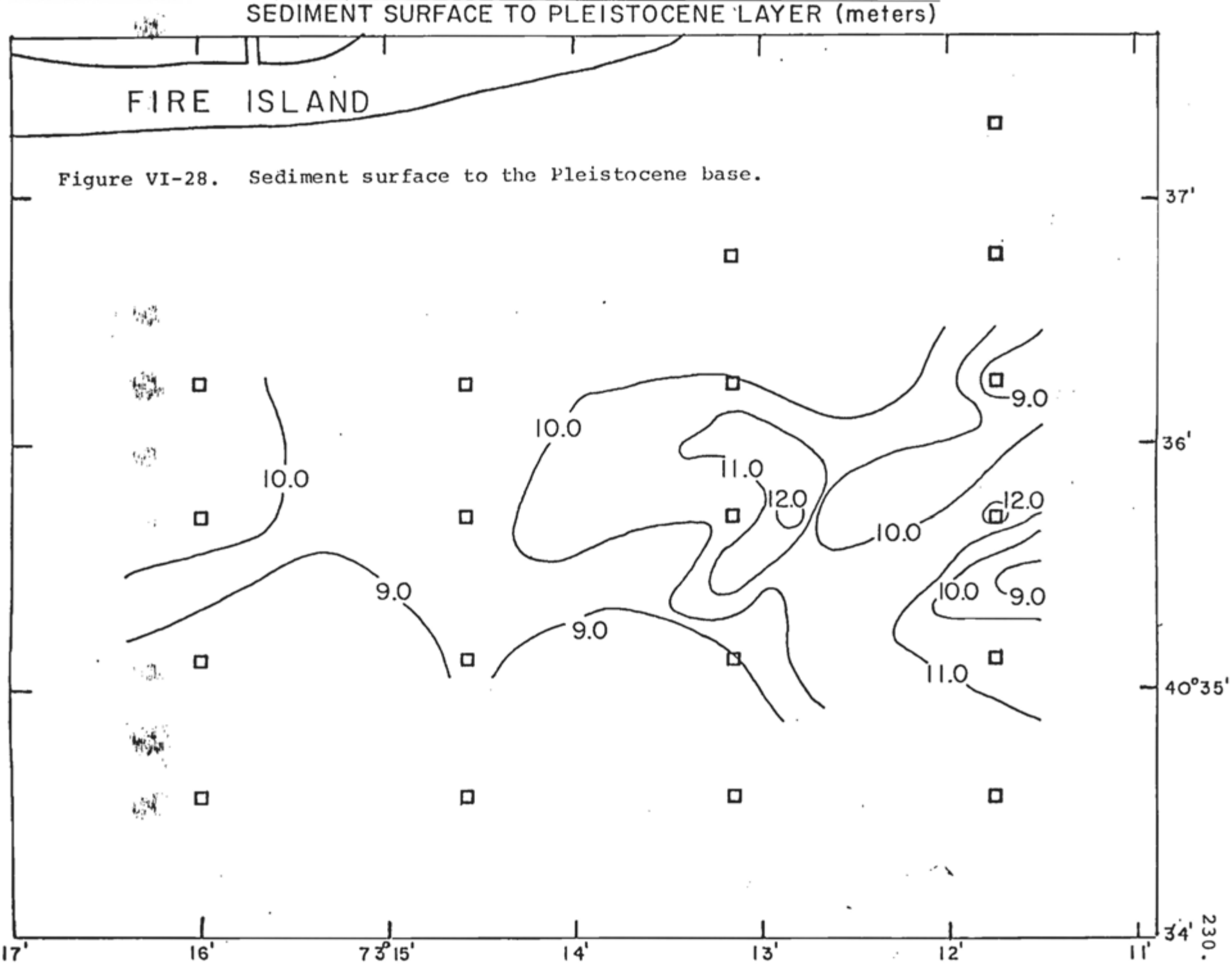

Figure VI-28. Sediment surface to the Pleistocene base.

In the study area, the Gardeners Clay (a lower unit of the Pleistocene group and a good acoustic reflector) lies at a depth of about 25 to 30 m. Above the Pleistocene sands is a thin cover of flatlying recent sediments (Williams, 1976).

F. Analyses for Trace Metals in Biota

During the baseline benthos community surveys, a number of the macrobenthic organisms taken in the Smith-McIntyre grab samples were collected for subsequent microchemical analysis. During the SCUBA surveys at the disposal project test site, and at the Fire Island Reef, other samples of epibenthos were collected by the divers for trace metal analysis. The organisms selected were placed in acid-washed plastic bags, sealed, and on return to the laboratory they were stored and frozen until analysis.

A procedure suitable for the preparation and digestion of the organisms has been developed by modification of the method of Boyden (1977). The frozen samples were returned to room temperature and, when necessary, the tissues carefully dissected from shells (avoiding metal instruments). The tissues were washed briefly with distilled water, surface-dried on clean filter papers and weighed, then oven dried at 85-95°C for 48 hr and reweighed. Digestion of the dried tissue was made with Ultrex concentrated nitric acid (5 to 25 ml) and, after preliminary cold digestion, the flasks were placed upon a hot plate at 100 - 200°C. During the entire procedure hollow glass drop-shaped bubbles were placed in the flask mouths allowing reflux of the acid to take place. Upon production of a clear liquor,

the glass bubbles were removed and the nitric acid driven off. When cool, the remaining salts were dissolved in a small volume (usually 10-25 ml) of 1 N-HCl. The solution was analyzed with an atomic absorption spectrophotometer for determination of individual elemental concentrations, as described in Chapter II, "Composition Mineralogy and Chemical Behavior of Stabilized FGD Sludge and Fly Ash". Using this technique for the digestion of organisms, analyses for the contents of heavy metals have begun on benthic animals collected during baseline surveys at the Atlantic project site.

VII. FIRE ISLAND ARTIFICIAL REEF

In 1962, the New York State Department of Environmental Conservation (NYSDEC) began the construction of an artificial fishing reef or fish haven, (the Fire Island Reef) close to the site proposed for the C-WARP project. This artificial reef includes large quantities (more than 20,000m^3) of natural rock, concrete, and building rubble together with some 10 sunken barges and more than 500 bales of automobile tires embedded in concrete. The reef lies about 4 km south of Fire Island, 8 km southeast of Fire Island Inlet, at a 20 to 21 m depth covering an area of about 1.6 km by 0.2 km.

A. Fauna

The Fire Island artificial reef has been heavily colonized by a diverse community of benthic organisms as well as inhabited by large populations of fish and will serve several useful purposes in the coal waste project. Surveys of the communities growing upon the rock and concrete in the Fire Island artificial reef will provide data for comparisons of the progress of colonization and the processes of biological succession on the coal waste blocks. These results will also allow assessment of sampling problems and sample variability which may be anticipated for the fauna growing on the coal waste blocks.

Preliminary underwater surveys to characterize the Fire Island reef were begun on the first cruises in October and November (Table I-1). Small stones and rocks, many of which could readily be identified as fragments of building bricks, clinker, shards of glass and concrete, were found on the sandy bottom in the vicinity of the reef. The larger fragments

and stones frequently had sessile benthic animals growing upon them, including: mussels, Mytilus edulis, and Modiolus sp.; bryozoans (species of Bugula were especially common); and hydroids and sponges (Figure VII-1). Starfish, Asterias forbesi, and sand dollars, Echinarachnius parma, occurred commonly on the sea bed at the reef site.

Measurements of the fauna growing on small rocks retrieved from the reef site revealed a diverse community. Barnacles, Balanus balanoides, occurred in densities of up to 200 or 300 per 100 cm^2 covering 40 to 60% of some of the surfaces. Ectoproct bryozoans, such as Bugula sp., were also dominant covering 15 to 30% of some rocks, as were sponges resembling Halichondria sp. Associated with such dominant epibenthic colonizers were numerous nematode worms, amphipods, isopods, caprellid shrimps, crabs, and many species of polychaete bristle worms.

The large rocks and other structures forming the artificial reef were heavily overgrown by epifauna. Feathery tuft-like growths of ectoproct bryozoans and hydroids abounded. Between them, small colonies of cup-corals, Astrangia danae, and aggregations of barnacles, B. balanoides, were very common. Other surfaces were crowded with colonies of sea anemones, apparently Metridium senile. The reef site appeared to be densely populated by fishes. In particular, bergals, Tautogolabrus adspersus, were ubiquitous. Other species seen at the

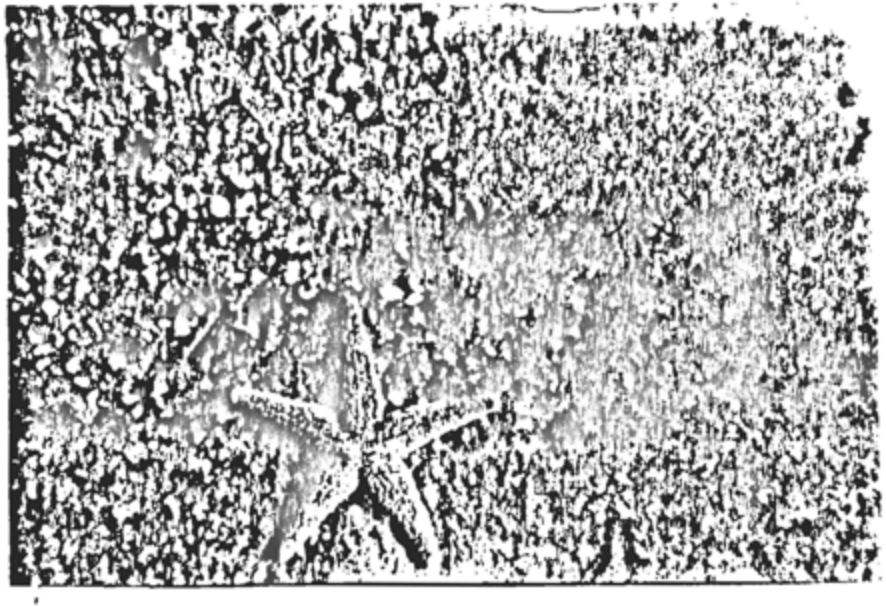

Coarse and fine sediments with star fish.

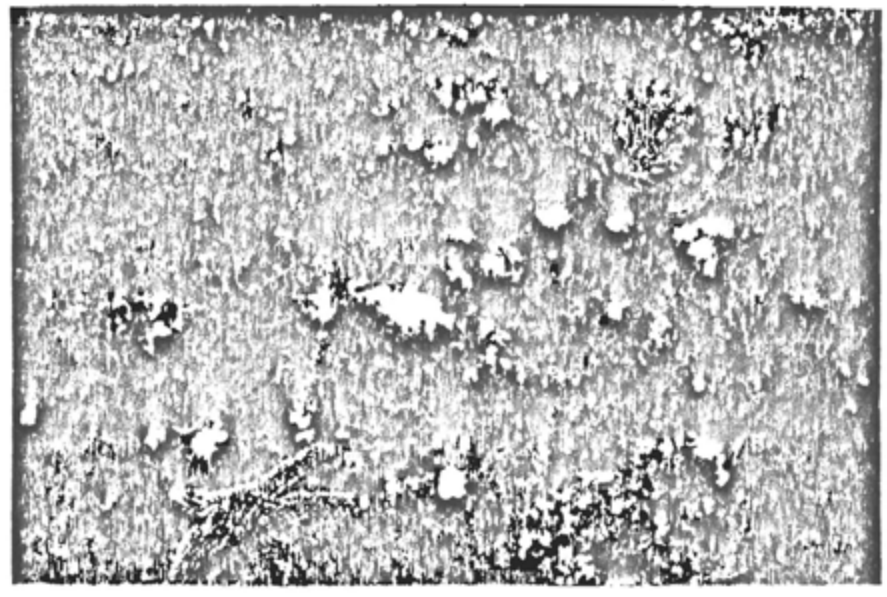

Epifauna growing on rocks and stones on the sea-bed-

Figure VII-1. Sea-bed at the reef site.

reef were blackfish, Tautoga onitis, black sea bass, Centropristis striata, scup, Stenotomus chrysops, and sea robin, Prionotus sp. Ocean pout, Macrozoarces americanus, red hake, Urophycis chuss, sea raven, Hemitripterus americanus, and winter flounder, Pseudopleuronectes americanus are common seasonal inhabitants at the reef. The more common large invertebrates included the rock crab, Cancer irroratus, Jonah crab, C. borealis, lobster, Homarus americanus, spider crab, Libinia dubia, and winter shrimp, Dichelopandalus leptocerus.

Some of the faunal communities presently inhabiting the artificial reef are illustrated in Figures VII-2, a-h.

From the figures, it is apprarent that the reef fauna is well-developed and of high biomass.

Smith-McIntyre grab samples for benthos were taken at the Fire Island Reef. The benthic samples had significantly higher biomass than was found for the project area as a whole. Animals found in the Fire Island Reef samples generally occurred elsewhere over the area of the baseline oceanographic surveys but some species appeared more numerously represented, as the dense aggregations of the sedentary polychaete, Ampherete grubei. The polycheate worm, Scalibregma inflatum, was common at the reef but not found elsewhere. Also found in smaller numbers were the amphipod, Photis macrocoxa, and worm Glycera americana. The branched bryozoan, Bugula sp., was abundant and, although it occurred in a few other grab samples, it

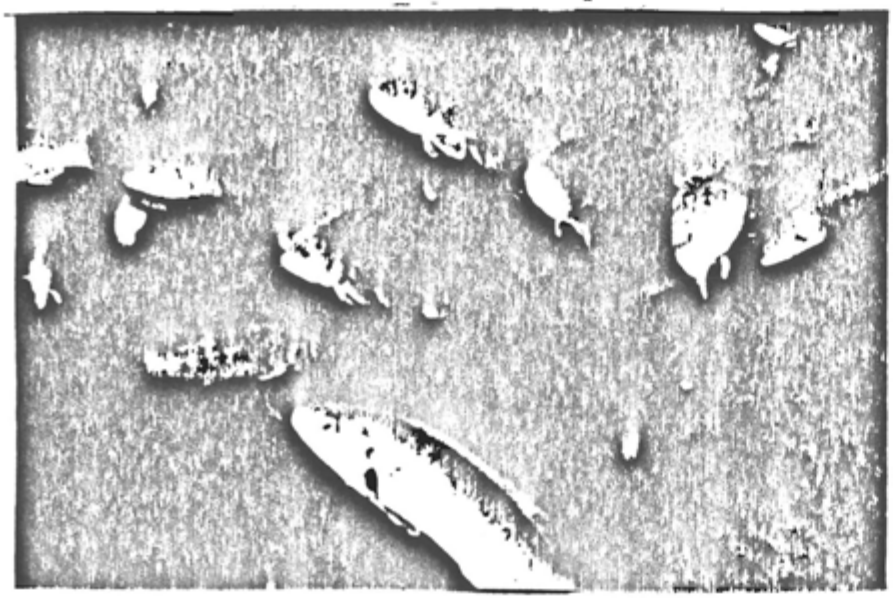

a) Fish on the reef

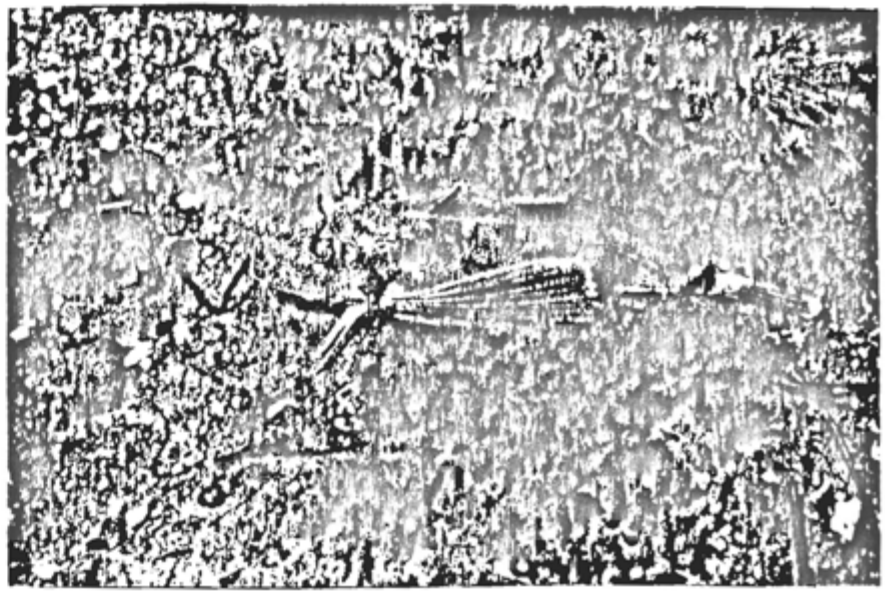

b) Sea robin

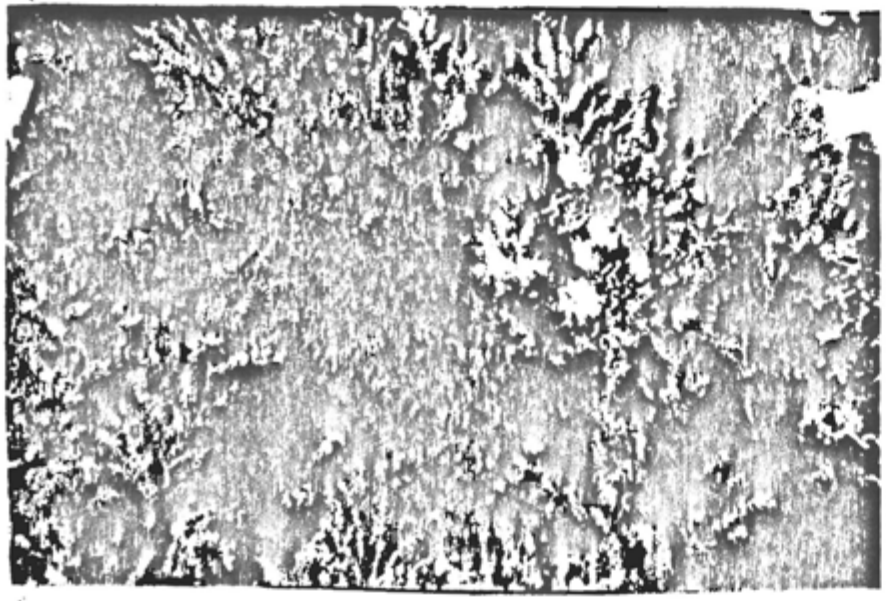

c) Bushy bryozoans, hydroids, corals

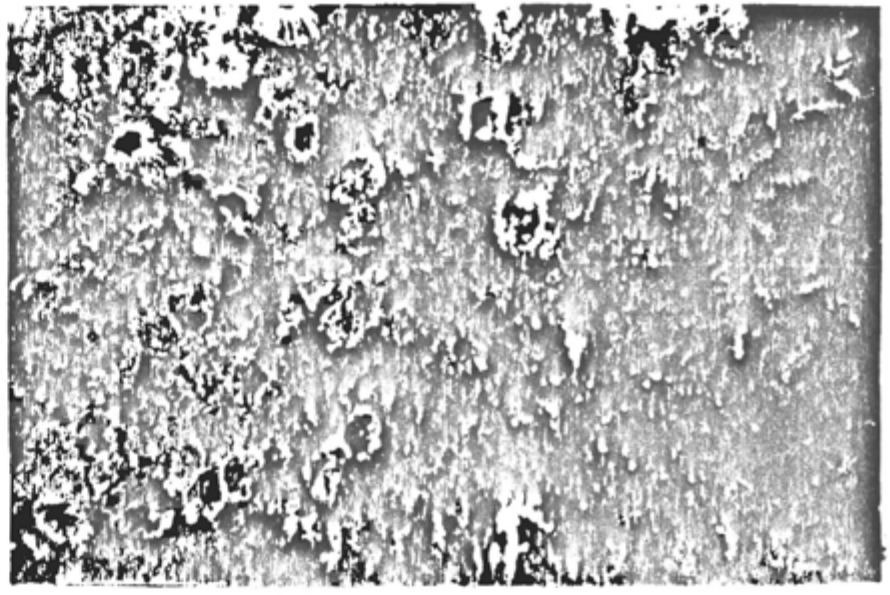

d) Barnacles and bryozoans

Figure VII-2. Fauna at the Fire Island Reef site.

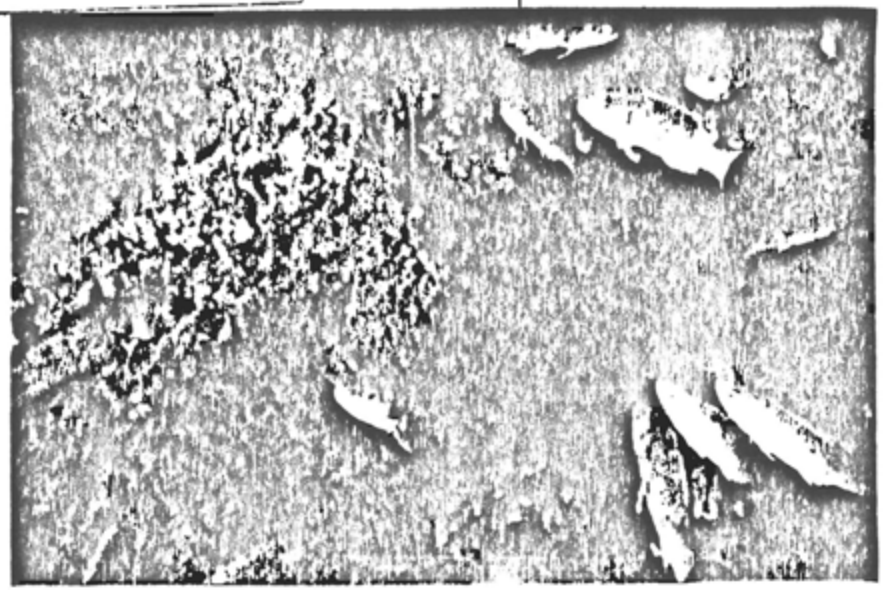

e) Bergals on the reef

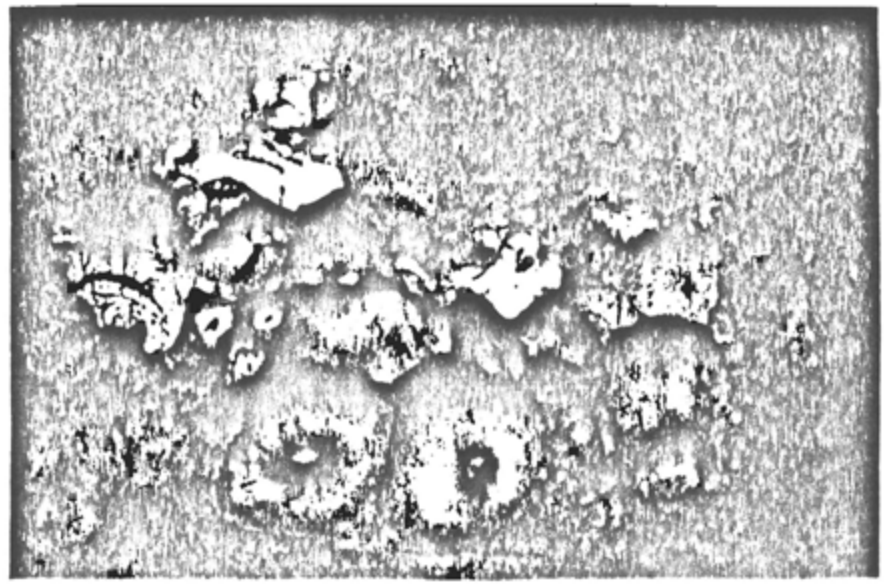

f) Sea-anemone colony

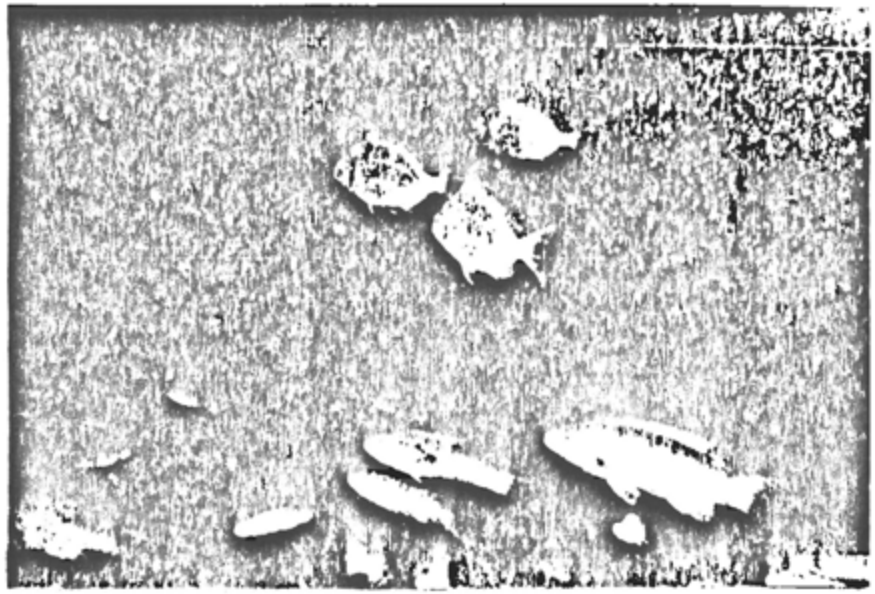

g) Porgies and bergals

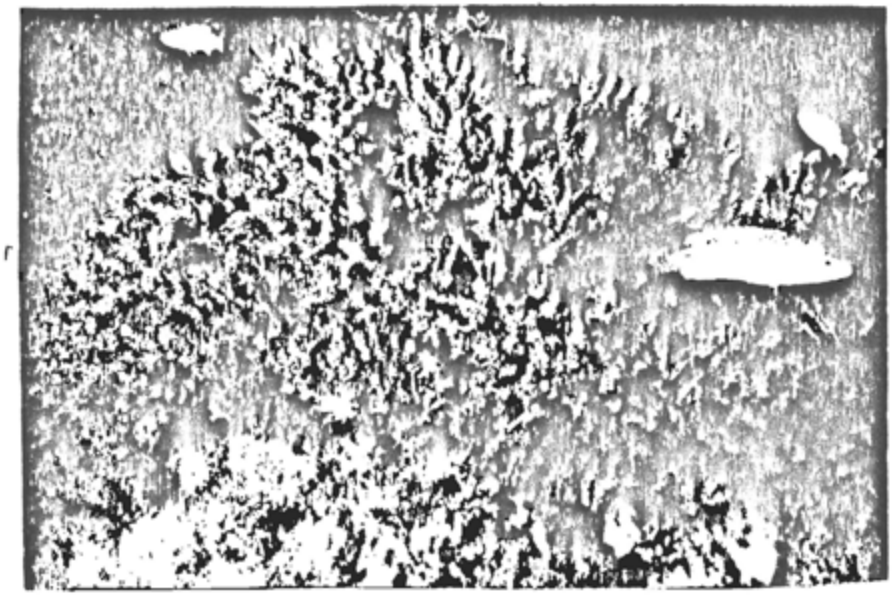

h) Bryozoans and corals

Figure VII-2 (continued)

appeared that such occurrences were of incidental fragments detached from the reef substrates and carried by water currents.

The Fire Island Reef appeared to sustain a very productive biological community, as well as supporting fish populations of a size to consistently attract sport fishermen. The reef is more productive than the surrounding sea-bed, and the benthic infauna associated with the reef appears to be of significantly greater biomass than the benthic fauna over the rest of the project area. It is anticipated that the large stabilized coal waste blocks placed at the project demonstration disposal site will provide surfaces for new biological settlement and overgrowth, will develop equally rich and productive reef communities, and will support populations of commercially desirable food fishes.

B. Sonar Surveys

Sonar has long been used to detect fish, usually in groups or schools in midwater or at the seabed. With refinements, sonar can be used to distinguish and count echoes from single fish. A horizontal scanning sonar has been added to the R/V ONRUST for the underwater sensing capability. After the large block (1 yd^3) reef has been established, the scanning sonar will be used to make repeated surveys from fixed positions. The positioning-posts, which can be detected with this sonar, will be driven into the seabed by SCUBA divers for such purposes.

It is anticipated that repeated surveys made from closely fixed positions around the reef will permit estimates of increases in fish populations with time. To this end, a series of tests have been run in the open seas using the scanning sonar equipment to sense a number of small buoys sunk on lines form the seabed. It has proved possible to detect single buoys, but weather conditions in mid-winter have significantly slowed the development of these techniques. With relatively slow scanning response at long ranges and winter swells running high the position of the ship had usually shifted by the time that echoes from targets returned, making CRT presentation of echoes difficult to interpret. Modification of the recording method to allow display of the echoes on a strip-chart is planned, and should significantly reduce noise interference with trace interpretation. The onset of better weather conditions will allow more effective use of the scanning sonar for fish surveys.

VIII. Block Fabrication Experimental Program

A. Phase I

Phase I was the first in a series of funded programs leading up to the production of cubic yard blocks for reef construction. Based on the results of the initial studies, two design mixes had been selected for eventual implementation in the cubic yard block production phase. These mixes were 1:1 (dry weight basis = dwb) fly ash:filtercake and 3:1 (dwb) fly ash:filtercake.

The Phase I program was developed with the purpose of examining in depth the physical and environmental properties of these mixes to assure their success in the cubic yard block phase. Additional emphasis was placed on evaluating the impact of variations of lime quality on these mix properties.

To meet these objectives, the work plan described below was formulated using Elrama filtercake, fly ash and quicklime as utility raw materials. These materials were selected on the basis of superior results obtained with Elrama materials in the initial Conscience Bay studies. However, subsequent information quantifying the fly ash content of the Elrama filtercake strongly influenced a change, in the later portion of Phase I, to Conesville fly ash and filtercake which was deemed more representative of current and future utility coal burning wastes. In addition, results of SUNY's environmental tests led to use of hydrated lime instead of quicklime.

To meet the objectives stated above, the following work program was developed:

Program Element	Description	Work Objective
Phase I-A	Lime Additive Evaluation	Select optimal lime additive type and quantity yielding required physical properties in design mixes
Phase I-B	Block and Proctor Production	Provide SUNY with stabilized design mixes for detailed environmental evaluations
Phase I-C	Fabrication, Design of 1 cu yd blocks	Construct and test 1 cu yd blocks for strength characteristics

The initial intent of the program was that these program elements proceed in sequence with Phase I-B following completion of I-A. However, feedback obtained from SUNY's block testing work necessitated changes in philosophy regarding lime additive with the result that the two program elements were completed more in parallel than sequentially.

1. Phase I-A, Lime Additive Evaluation

Preparation and evaluation of mixes prepared during initial studies had not fully characterized the impact of lime quality variability on stabilized mix properties. Since the design mixes in Phase I would ultimately be produced at an operating IUCS plant, the effect of typical plant lime variability on stabilized design mix properties (notably compressive strength) had to be quantified to obtain data on the range to be expected and to insure that all blocks would be acceptable regardless of lime quality. Two manufacturers supply

quicklime at the Elrama facility. Thus, at any given time the plant could be utilizing quicklime from Source #1 (manufacturer's name deleted), Source #2, or a mixture of both. To establish the range, mixes were prepared from each lime to observe what, if any, strength differences would occur.

Results shown in Table VIII-1 indicate lime Source #1 to be superior to Source #2, using lime at -30 mesh size. The difference in Mixes #1 & 2 are significant but still above the 300 psi criteria as are Mixes #3 & #4. Based on this data, the source of lime did not appear to be a point of concern. However, the reproducibility of the results, i.e., achievement of over 300 psi, needed to be verified.

Additional mixes using 4% and 6% Elrama quicklime additive were prepared as indicated in Tables VIII-2 and VIII-3. Strengths for 7 days at 38°C (7d38°) cures were markedly reduced in Mixes #1 - 3, compared to results in Table VIII-1. However, 28d23° cures yielded satisfactory strengths for 4% quicklime and excellent strengths for 6% quicklime additive. Tensile strengths were also significantly improved using 6% quicklime. Based on these results it was decided to use 6% quicklime in future mixes to provide an extra safety factory.

Two additional mixes, #5 & #6, were prepared which accounted for the fly ash content of the Elrama filtercake which was 65% (dwb) in this case. Strength was significantly lower in these mixes.

The 6% quicklime figure was applied to cubic foot block production of the Elrama mixes, using a somewhat coarser

Table VIII-1. Lime source evaluation for Elrama test mixes.

Mix	Mix Design (dwb)*	Wet Weight Lb/Ft^3	Dry Weight Lb/Ft^3	%Solids	Lime Source	%Lime	Comp.Strengt 7d38°
1	1:1	98.5	74.7	75.8	#1	4%	599
2	1:1	98.1	74.4	75.8	#2	4%	448
3	3:1	94.8	72.2	76.1	#1	4%	374
4	3:1	94.7	72.0	76.1	#2	4%	385

* Fly ash:filtercake ratio (dwb).

Table VIII-2. Compressive strength vs quicklime content for Elrama mixes.

Mix	Mix Design (dwb)*	%Solids	% Lime Additive	Compressive strength (PSI) 1d23°	3d23°	7d23°	28d23°	7d38°
1	1:1 (4.7:1)	72	4%	**	**	13	332	150
2	1:1 (4.7:1)	77	6%	12	13	26	719	125
3	3:1(10.4:1)	73	4%	11	19	64	427	215
4	3:1(10.4:1)	79	6%	16	-	51	905	534
5	0.38:1(3:1)	72	4%	**	**	13	182	74
6	0.0:1(1.9:1)	57	4%	**	**	4	124	13

* Fly ash:filtercake, (dwb) given, total fly ash content, actual scrubber sludge (dwb) listed in parentheses.

** Too soft to test.

Table VIII-3. Tensile strength vs quicklime content for Elrama mixes.

Mix	Mix Design (dwb)*	%Solids	% Lime Additive	Tensile Strength PSI 1d23°	3d23°	7d23°	28d23°	7d38°
1	1:1 (4.7:1)	72	4	**	**	9	136	36
2	1:1 (4.7:1)	77	6	5	7	44	348	158
3	3:1(10.4:1)	73	4	1	2	56	146	77
4	3:1(10.4:1)	79	6	8	-	125	375	215

* Fly ash (dwb):filtercake given, total fly ash content, (dwb) listed in parentheses: actual scrubber sludge.

** Too soft to test

quicklime (-10 mesh) than added to the proctors (-30 mesh) tested in Tables VIII-2 and VIII-3. Upon testing and inspection by SUNY personnel, the cured blocks were found to be subject to cracks and stresses, especially in the vicinity of coarser quicklime particles. In addition, the coarse (relative to hydrated lime) quicklime was not readily dispersed throughout the blocks, leaving nodules of fly ash and scrubber sludge unstabilized due to lack of lime contact for reaction. These nodules did not contribute to structural strength and were readily eroded by seawater.

Inasmuch as the quicklime used in block production was as coarse as typical plant lime, there was concern that plant lime would not produce acceptable blocks in full scale production. Thus, it was decided to switch to high calcium hydrated lime, a much finer, more easily dispersed lime of more uniform, predictable quality. This lime was used in subsequent block formulations at a 4% additive rate as detailed in the following section of block production.

2. Phase I-B, Block and Proctor Production

To enable SUNY to properly characterize the physical and environmental properties of the design mixes, proctor cylinders and cubic foot blocks were manufactured and cured at IUCS Pilot Plant and Tec Center. Leachate analyses, the structural integrity of blocks under many feet of seawater, and the effect of blocks on aquatic life were among the factors SUNY

wished to examine. These tests would confirm the environmental acceptability of the design mixes indicated during the initial studies and provide pilot scale data on the cubic yard blocks to follow.

The initial set of Phase I-B blocks was produced in September and October of 1978, using the Elrama design mixes. Reports from SUNY indicated that the 9/78 batch (E1) of blocks were of inferior quality, exhibiting poor compressive strength. (E1 is SUNY's notation for first batch of Elrama blocks received.) As Table VIII-4 indicates, the batch of blocks was formulated with coarse, uncrushed Elrama plant lime and cured under a loosely secured tarp. Accordingly, the subsequent E2 (10/78) batch was manufactured with crushed Elrama plant lime to what was considered more typical of the particle size observed in plant quality control analyses. Blocks were then cured under several more securely fastened tarps. Water was sprinkled at regular intervals to prevent block dehydration. Overall block quality was much improved. Proctor cylinders were made from the same Poz-O-Tec batches used in block manufacture, cured 7d38°, and tested for compressive strength, as shown in Table VIII-5. Strength was satisfactory, in excess of the 300 psi criteria for both mixes. However, it should be noted that the strength values of cylinders cured 7d38° are just approximations of 28d23° strength which is considered more representative of field conditions.

Table VIII-4. Phase 1B, block and proctor production.

Background data	1:1, fly ash:filtercake						3:1, fly ash:filtercake					
Date Made	9/1/78	10/78	12/78	1/79	12/78	1/79	9/78	10/78	1/79	1/79	12/78	1/79
SUNY Code	E1C1	E2C1	E3F1	E4F1	C3F1	C4F1	E1C3	E2C3	E4F3	E4F3	C3F3	C4F3
Mix Form												
Block	x	x	x	x	x		x	x	x	x	x	
Proctor						x						x
Raw Materials												
Elrama filtercake	x	x	x	x			x	x	x	x		
Elrama fly ash	x			x			x			x		
Phillips fly ash		x	x		x			x	x		x	
Conesville filtercake					x	x					x	x
Conesville fly ash						x						x
Elrama quicklime												
Crushed		x						x				
Uncrushed	x						x					
Hical hydrated lime			x	x	x	x			x	x	x	x
Lime additive, %	6%	6%	4%	4%	4%	4%	6%	6%	4%	4%	4%	4%
Curing conditions												
Mass Covering												
Loose	x						x					
Tight		x						x				
Individual wrap			x	x	x			x	x	x		
Curing chamber			x	x	x							x
Quantity made	10	23	5	16	3	12	10	23	5	2	4	12
True mix design fly ash:sludge (dwb)	4.7:1	3:1*	3:1*	2.7:1	1:1	1:1	10.4:1	7:1*	7:1*	6.4:1	3:1	3:1

* Estimate based on typical analysis.

ble VIII-5. Block and proctor quality control data.

arameter	Mix Design (dwb) 1:1 Fly ash:filtercake			3:1 Fly ash:filtercake		
ix Form						
Block	x	x		x	x	
Proctor			x			x
roduction Data						
SUNY Code	E2C1	E4F1	C4F1	E2C3	E3F3	C4F3
Date Made	10/78	1/79	1/79	10/78	12/78	1/79
Fly Ash	Phillips	Elrama	Conesville	Phillips	Phillips	Conesville
Filtercake	Elrama	Elrama	Conesville	Elrama	Elrama	Conesville
Lime Type	QL*	HCHL*	HCHL	QL	HCHL	HCHL
Lime Additive %	6%	4%	4%	6%	4%	4%
ompressive trength	(7d38°)	(28d23°)	(28d23°)	(7d38°)	(7d38°)	(28d23°)
Maximum	532	1040	-	492	-	-
Minimum	305	240	-	355	-	-
Mean	398	531	130	424	209	373

L = Quicklime, HCHL = High Calcium Hydrated Lime.

One other fact distinguished the E2 batch from the E1 batch and that was the type of fly ash used in the formulations. The first batch was manufactured with Elrama fly ash while the E2 batch of blocks was prepared with Phillips fly ash. However, as the analyses in Table VIII-6 indicate, the two are very similar in terms of historical data. Additionally, SUNY's analyses (see Table II-9, Chapter II) of fly ash shows that the trace element concentrations of the Elrama and Phillips fly ashes to be very similar. Furthermore, a comparison of the Elrama ash used in the E1 blocks and the Phillips ash used in the E2 blocks show them to be virtually identical in silica content and pozzolanic reactivity and very close in particle size distribution. This is not totally surprising since both Phillips and Elrama ashes come from the same coal which is combusted in plants (both owned by Duquesne Light) of similar type and age.

The detailed ash comparison turned out to be less of an issue since materials were soon changed from Elrama and Phillips to Conesville. The sudden change was precipitated by the recognition of the magnitude of the fly ash content in the Elrama filtercake. Filtercake may be defined as the dewatered sludge resulting from the scrubbing of flue gases with a lime solution. In newer power plants, virtually all the fly ash is removed from the flue gas prior to the scrubbing process. Hence, the scrubber sludge and its dewatered form, filtercake, consist primarily of the reaction products of the

Table VIII-6. Fly ash analyses (%).

	Historical Averages			Analyses Performed 10/78	
Paramater	Elrama	Phillips	Conesville	Elrama	Phillips
LOI	8.2	5.3	1.09	-	-
SiO	44.6	50.3	41.7	46.9	46.5
Fe_2O_3	17.6	(36.9)	27.5	-	-
Al_2O_3	23.5		21.6	-	-
CaO	1.15	2.98	3.01	-	-
MgO	0.87	1.80	2.03	-	-
SO_3	0.20	0.80	-	-	-
SO_4	-	-	0.97	-	-
Carbon	-	-	0.96		-
Specific Gravity	2.24	2.30	2.73	-	-
Sieve Analysis					
% Passing 100	-	95.2	97.8	97.7	94.8
%Passing 200	-	86.3	92.8	88.4	83.4
%Passing 325	-	72.8	81.9	80.2	73.9
Pozzolanic Reactivity	-	-	-	736	725

flue gas-lime solution reaction. These reaction products are $CaSO_3 \cdot 1/2H_2O$, $CaSO_4 \cdot 2H_2O$, and occasional minor amounts of $CaCO_3$. At Elrama, all the fly ash is not removed from the flue gas prior to the scrubbing process. As a result, the scrubber sludge and its dewatered form, filtercake, contain not only the reaction products mentioned previously, but the fly ash that was still present in the flue gas.

The mix designs selected by SUNY were expressed as the ratio (dwb) of the weight of fly ash to filtercake. Thus, a 1:1 ratio was interpreted as the ratio of fly ash to reaction products since filtercake was assumed to be predominantly reaction products. However, as the analyses in Table VIII-7 indicate, the Elrama filtercake contains an average of 40% fly ash with a maximum of 65% observed in the filtercake used in the El block formulations. Thus a 1:1 ratio of fly ash to filtercake turns out to be not 1:1 but a 1.65:0.35 or 4.7:1 ratio for the case of 65% fly ash.

The mix designs in the column headings, Table VIII-4 and VIII-5, designated as "fly ash:filtercake" are technically correct but do not reflect the ratio of fly ash to reaction products which is given at the bottom of Table VIII-4 as "true mix design". For convenience sake, the "true mix design" which is the ratio of fly ash to reaction products will henceforth be referred to as the fly ash:sludge ratio. The mix designs not distinguishing the fly

Table VIII-7. Filtercake analyses (%).

Parameter	Elrama (1978)	Conesville	Elrama (Pre-1978)
LOI	-	9.84	-
$CaCO_3$	-	13.07	Avg. 5%
$CaSO_3 \cdot \frac{1}{2}H_2O$	33.0	68.10	Avg. 5%
$CaSO_4 \cdot 2H_2O$	11.0	5.36	Avg. 50%
$Ca(OH)_2$	-	0.50	-
Specific gravity	-	2.35	-
% Passing 325 Sieve	-	97.5%	-
% Fly ash (DWB)	Avg. 40% Range 22- 65%	Minimal	Avg. 35%

ash content of the sludge will be referred to as the fly ash:filtercake ratio.

Once the discrepancy between the fly ash to filtercake ratio and fly ash to sludge ratio was known, it was necessary to find a utility where fly ash to sludge ratios of 1:1 and 3:1 could be achieved. That facility was Conesville where the (predominantly $CaSO_3 \cdot 1/2H_2O$) filtercake contains little, if any, fly ash and as a consequence the fly ash:filtercake ratio and the fly ash:sludge ratio were virtually identical.

At this time, a change in the type of lime was also being strongly considered. The variability of the quicklime in terms of its particle size and ease of dispersion was a source of concern. Accordingly, experiments were proposed using blocks formulated with high calcium hydrated lime, a finer, more easily dispersed lime.

The blocks and Proctors manufactured 12/78 (E3, C3) and 1/79 (E4,C4) reflect the concerns over the source of utility, materials, and the type of lime. The 1:1 (fly ash:filtercake) Elrama mixes were prepared with the hydrated lime to allow comparison to previous blocks made with quicklime. Quality control data in Table VIII-5 for proctors cured 28d23° suggest equal or better strength for a 4% hydrated lime additive. Additional blocks and proctors were prepared with Conesville filtercake at 1:1 and 3:1 fly ash to sludge

ratios. All blocks in the E3, C3 (12/78) and E4, C4 (1/79) series were individually wrapped for optimum curing.

Thus, Phase I-B ended with the selection of Conesville materials as the choice for the design mixes of the cubic yard blocks. Quicklime had been replaced by the finer, more easily dispersed hydrated lime and the need for securely wrapped blocks for curing had been reaffirmed.

3. Phase I-C, Design and Fabrication of 1 yd^3 Blocks

Phase I-C was developed with the objective of determining the feasibility and detailed fabrication methods of manufacturing one cubic yard blocks from the design mixes evaluated in Phase I-A & B. The prime criteria of Phase I-C was to accomplish the size increase from one cubic foot to one cubic yard while maintaining the structural and environmental properties necessary for the handling, shipping, and ocean placement of the large blocks. Information derived from Phase I-C would allow previous time and cost estimates for Phase II, full scale cubic yard block production, to be modified as necessary to final form.

A simplified version of Phase I-C was initiated in October 1978 at Elrama to provide the project team with preliminary estimates of cubic yard block feasibility and logistics, with the understanding that a more in-depth study would follow at a more propitious time. The change to Conesville materials described in Phase I-B necessitated a shift from Elrama to Conesville as the site for big block production tentatively scheduled to commence in March 1979.

The work program outlined below represents the initial concepts of Phase I-C. The program pursues the tasks outlined below. The Elrama program was intended only as a preliminary study designed to supply initial data on cubic yard block formulation, data which could be used to supplement the Conesville program which would meet the objectives of the initial concepts of Phase I-C.

Phase I-C Work Program Concepts

Program Element	Areas of Interest	Comments
Plant Quality Control	Mix Variability	Mix analyses for lime and fly ash variation
	Mix Stockpile	Evaluate efficiency of mix stockpile
Block Forming Methods	Compaction Methods	Hand tamping vs. vibratory, mechanical compaction
	Mold Release Agents	Efficacy of release agents
	Block Reinforcement	Need for it based on tensile strength
Block Testing	Stripping of Molds	Minimum cure time til stripping
	Block Handling	Forklift, crane, internal supports, cure time required to move blocks, strength testing

a. Elrama Program. This program explored two of the elements listed in the previous section, block forming methods and block testing. The initial work focused on tensile strength testing of the design mixes to assess the need for

block reinforcement, one of the areas of interest under block forming methods.

Tensile strength tests were performed on the two Elrama design mixes at two lime additive levels. Results shown in Table VIII-8 indicate distinctly superior strength at the 6% additive level. In addition, significant tensile strength developed after seven days curing at 23°C with high strength achieved at 28 days curing. On the basis of these results, little need was seen for block reinforcement.

The field experiment commenced at Elrama the week of 10/17/78. Primary objectives of the program were to obtain familiarity with the block molds and compaction equipment, test mold release agents, and evaluate block handling properties. Testing was to be performed on mixes approximating the Elrama design mix ratios of 1:1 and 3:1 fly ash: filtercake, (dwb).

A total of five cubic yard blocks were formed in the program, as indicated in Table VIII-9 (see Figures VIII-1-4). Logistics at the plant limited mix flexibility that week with the result that 0.73:1 and 2:1 mixes, not 1:1 and 3:1 mixes, were prepared. In actuality, these were not far off the mark. A 3:1 mix using filtercake at 47.5% solids and lime at 4.8% would be on the order of 79% solids. However, cubic foot block production had shown this to be too dry with water addition required to reach 73% solids, more preferable for optimum compaction. Thus, while the mix design at 2:1

Table VIII-8. Tensile strength properties.

Mix	Fly Ash: Sludge	Fly Ash: Filtercake	% Solids	% Lime** Additive	1d23°	3d23°	7d23°	28d23°	7d23°
1	4.7:1	1:1	72	4	*	*	9	136	36
2	4.7:1	1:1	77	6	5	7	44	348	158
3	10.4:1	3:1	73	4	1	2	56	146	77
4	10.4:1	3:1	79	6	8	-	125	375	215

* Too soft to test

** Quicklime Sieved to -30 mesh

Table VIII-9. Phase 11-A Block Formulation.

Block	% Solids	% Lime	Filtercake % Solids	Mix Design (dwb) Fly ash: Filtercake	Compaction Method
1	74%	4.8%	47.5%	2:1	Pneumatic compact
2	74%	4.8%	47.5%	2:1	Hand tamped
3	64%	>3%*	49%	.73:1	Hand tamped
4	64%	>3%*	49%	.73:1	Hand tamped
5	56%	>3%*	49%	.73:1	no compaction

* Estimate

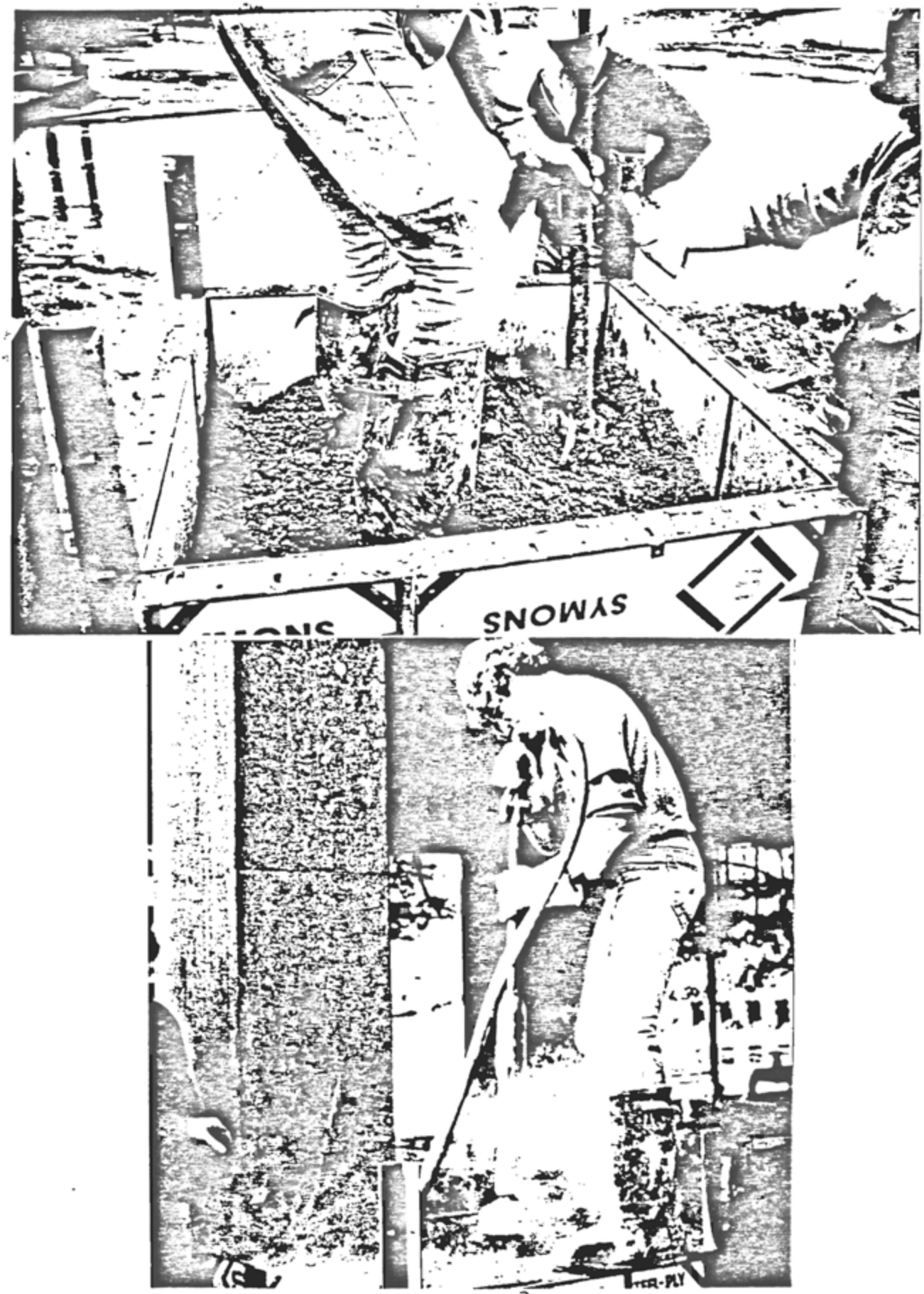

Figure VIII-1. Compacting a 1 yd^3 block.

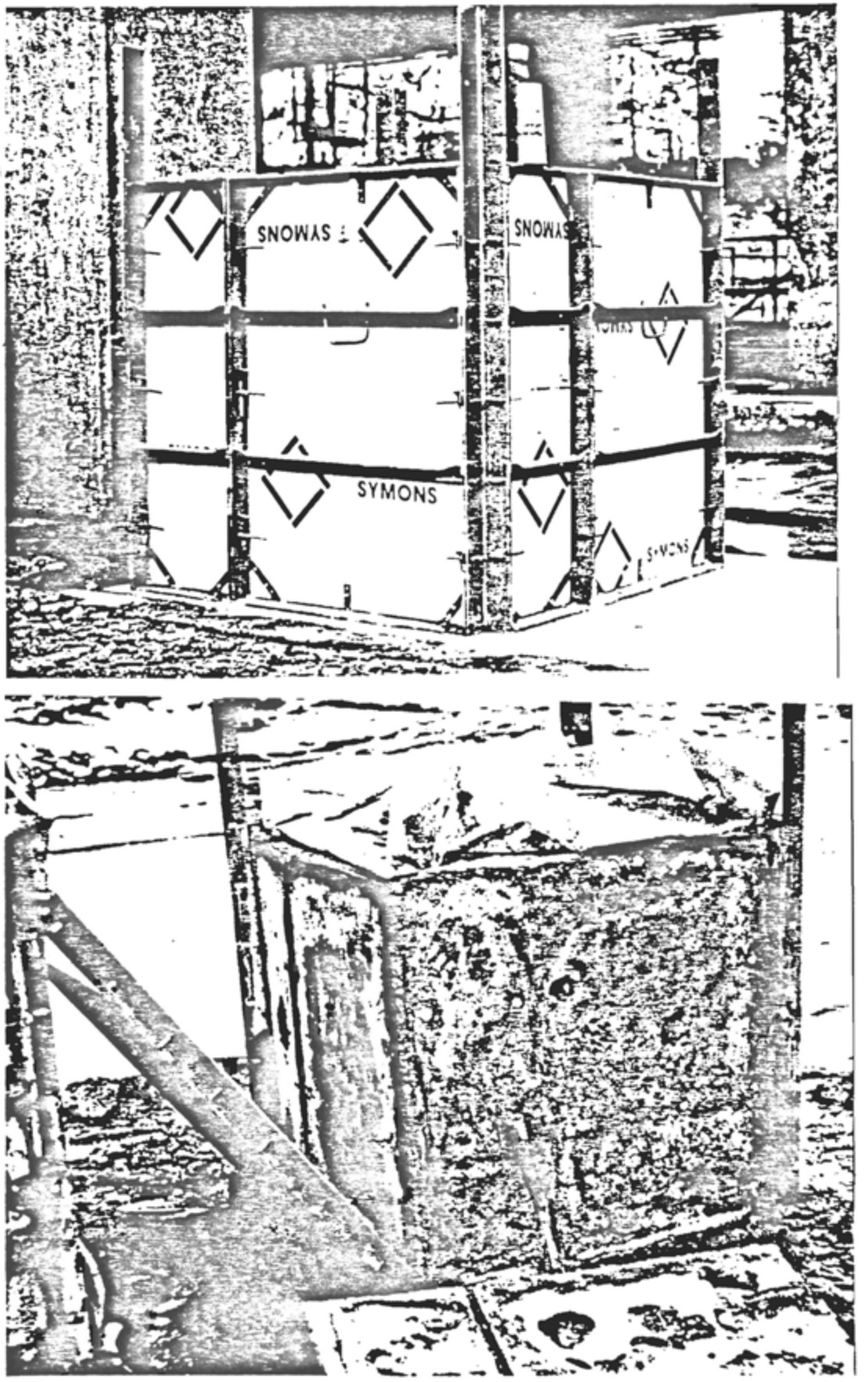

Figure VIII-2. Removal of mold.

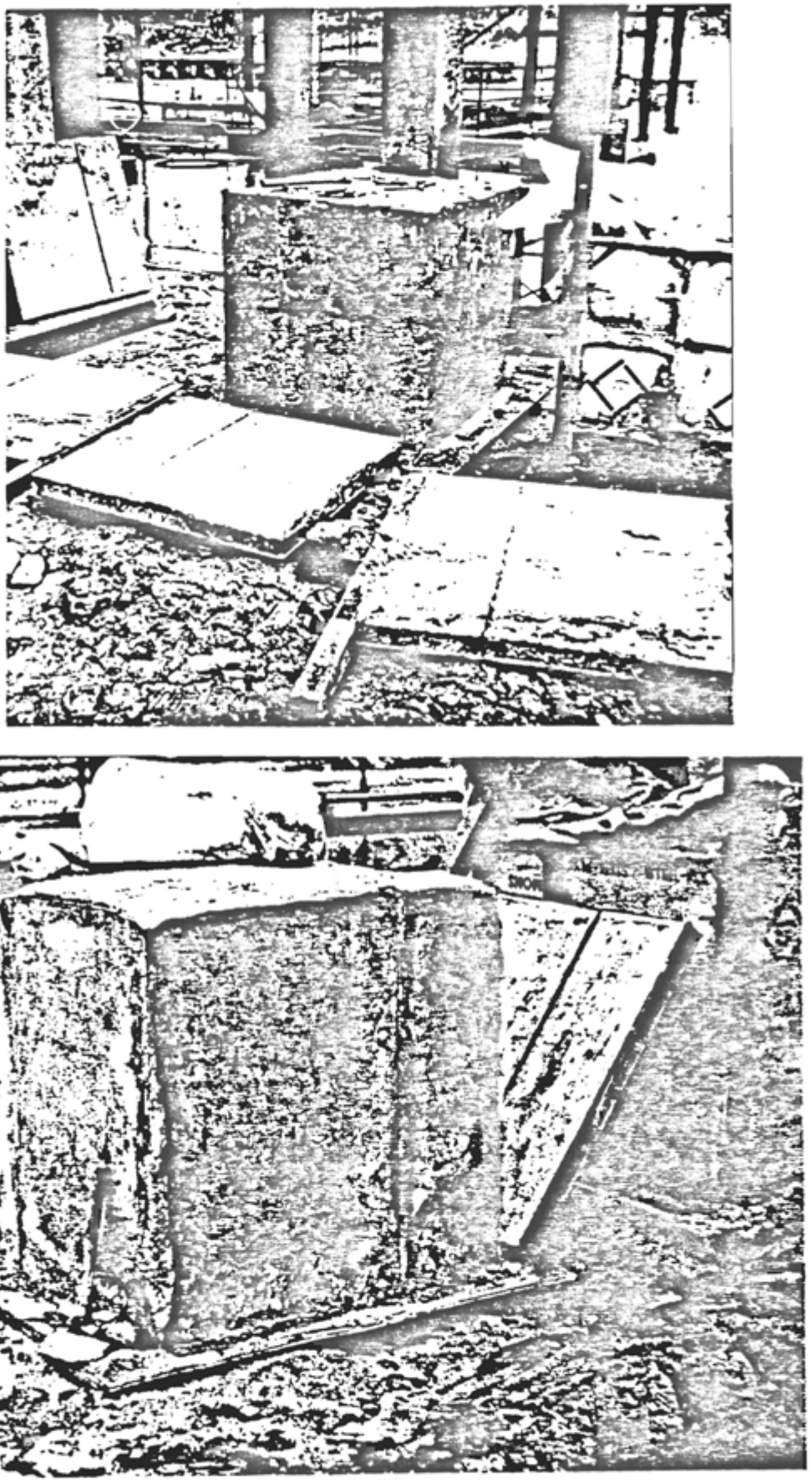

Figure VIII-3. Cubic yard blocks of stabilized scrubber sludge and fly ash.

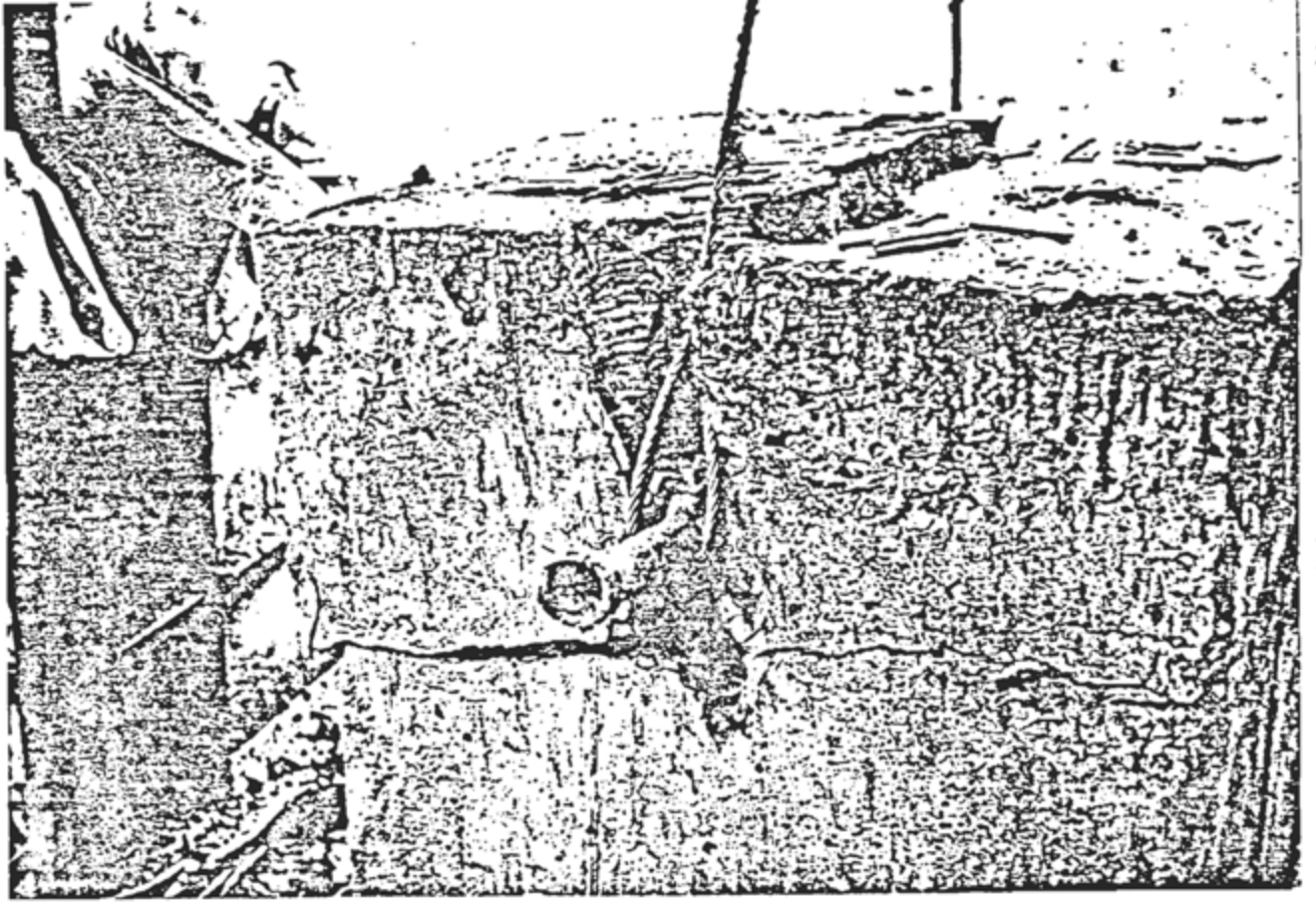

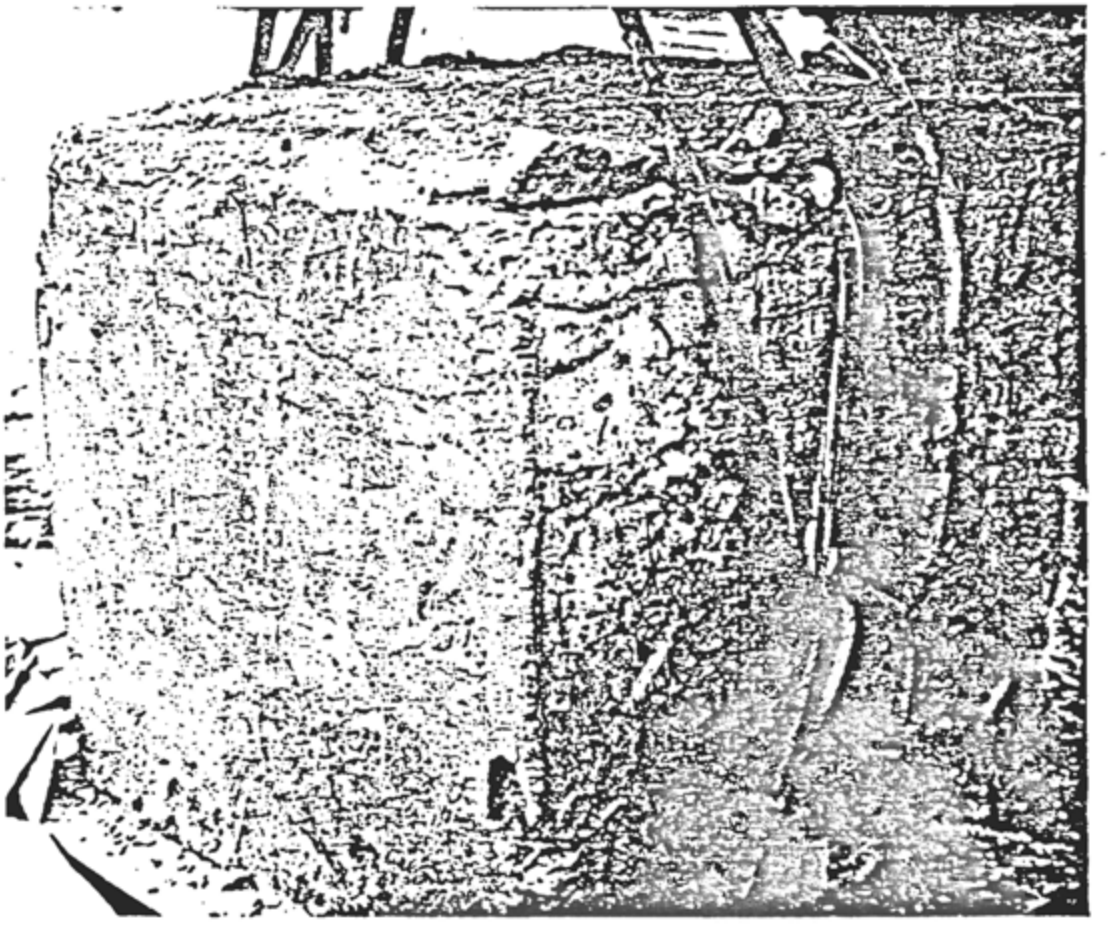

Figure VIII-4. Handling tests.

was somewhat off the mark, materials consistency was near the predetermined optimum allowing for a better evaluation of block forming, compaction and stripping methods.

The 0.73:1 mix at 64% solids, was wetter than cubic foot block 1:1 mixes prepared in Phase 1-A & B at 70% to 75% solids. The higher solids content in Phase I-A and B blocks is attributable to the gradual drying of stored filtercake and the increased fly ash content of a 1:1 mix as opposed to a 0.73:1 fly ash:filtercake (dwb) mix. However, rather than producing a 0.73:1 block at 70-75% solids, essentially the same consistency of the 3:1 blocks, the mix was evaluated at its produced solids content of 64%. It was felt that test data was needed on a wet plastic mix to provide background information in the event that a "worst case"scenario of unavoidably wet mixes occurred at some later date.

Going one step further, a mix of pourable consistency was prepared by adding water to the 0.73:1 mix in a small cement mixer and blending until uniform. This approach was investigated to evaluate the possibility of adding water to design mixes and pouring them into molds, saving the compaction step.

The block molds were found to be easily set up and stripped from the blocks. Each four-sided mold required about 15 minutes to assemble and place on a plywood base

set on a pallet. Stripping the mold from the block could be accomplished in five minutes. Molds stripped rather cleanly with those sprayed with Symons Magic Kote exhibiting a somewhat cleaner surface than unsprayed molds and much cleaner surface than molds smeared with grease. The Symons agent was easily applied to all surfaces with a spray can in less than a minute. Cleaning of stripped molds sprayed with Magic Kote could be accomplished in 15 minutes.

Two methods of block compaction were evaluated, hand tamping and pneumatic compactor. The pneumatic compactor was a jackhammer type device powered by air pressure with a 6-inch disc at the bottom. The pneumatic compactor was tested on Block #1 on Poz-O-Tec of different depths. It was found to scatter the material, prolonging the compaction process. In addition, it was heavy and awkward to maneuver. If the compaction disc were larger and flatter, the compaction stroke shorter, and the compactor lighter, it would be more flexible. As it was, it was found unsuitable for further use.

The hand tamper was simply a long wooden broom handle attached to a 7-1/2 in square steel plate. It was easier to maneuver, did not scatter the mix material, and compacted it to a somewhat greater density than the pneumatic compactor. Use of the hand tamper on Blocks #3 and #4 altered the initially firm Poz-O-Tec mix material

to a somewhat plastic consistency that quaked like firm Jello. This was not surprising since Poz-O-Tec in the 60-70% range is thixotropic in that repeated compaction or working of the material will reduce it from an initially firm, solid texture to a plastic, putty-like form. As a result, the thixotropic nature prolonged the compaction process by requiring additional compaction to achieve this consistency change and additional effort to free the tamper from the increasingly sticky surface.

Blocks #1 and #2 formulated from non-thixotropic material were judged firm enough to allow molds to be stripped the same day they were made. Once stripped they showed no signs of slumping or deformation. Edge and surface quality was good to excellent, with no air pockets or layer effects observed. Blocks #3 and #4 remained in the molds for 4 and 14 weeks respectively prior to stripping. Block #3 had firmed up somewhat during the 4-week period. Mold stripping was clean and block edge and surface quality good to excellent. Similar results were obtained for Block #4. Block #5 was too fluid to consider immediate stripping and still soft at 4 weeks. After 14 weeks it was frozen solid (January 23) so no long-term evaluation was possible.

Once blocks were stripped from their molds they were subjected to two handling tests. Each block had been formed with a 2" diameter plastic pipe through the center and two steel channels on the bottom, each approximately 5 in. wide

by 2 in. high and 36 in. long. The two handling tests involved lifting the blocks by straps slung through the grooves in the steel channel under the blocks, or lifting by attaching chains to each end of a steel rod slipped through the plastic pipe. The latter test was performed on Blocks #1 and #3, both of which cracked and broke under the strain. Lifting via straps slung through the channel was performed on Block #2 and 4 weeks of outdoor curing and proved successful.

Block curing was not optimal, inasmuch as they were left covered outdoors during October and November with daytime temperatures generally between 10-16°C and nightly lows around 0-4°C. Cubic foot blocks and proctors generally receive 23°C curing since temperatures under 16°C inhibit strength development and under 7°C often halt it entirely. As a consequence, the blocks exhibited little, if any, strength development, pointing out the need for controlled curing, i.e., warehouse, during the Phase II program.

In conclusion, the work completed in the Elrama program was a useful exercise. The molds and release agent had been found to be easy to use and apply. Mixes of nonthixotropic consistency were more easily compacted than those of a thixotropic nature. Mix compaction was more effective via hand tamper than pneumatic compactor, although alternate models might be equally satisfactory. Lifting of uncured blocks can be accomplished if sufficient block support is

by 2 in. high and 36 in. long. The two handling tests involved lifting the blocks by straps slung through the grooves in the steel channel under the blocks, or lifting by attaching chains to each end of a steel rod slipped through the plastic pipe. The latter test was performed on Blocks #1 and #3, both of which cracked and broke under the strain. Lifting via straps slung through the channel was performed on Block #2 and 4 weeks of outdoor curing and proved successful.

Block curing was not optimal, inasmuch as they were left covered outdoors during October and November with daytime temperatures generally between 10-16°C and nightly lows around 0-4°C. Cubic foot blocks and proctors generally receive 23°C curing since temperatures under 16°C inhibit strength development and under 7°C often halt it entirely. As a consequence, the blocks exhibited little, if any, strength development, pointing out the need for controlled curing, i.e., warehouse, during the Phase II program.

In conclusion, the work completed in the Elrama program was a useful exercise. The molds and release agent had been found to be easy to use and apply. Mixes of nonthixotropic consistency were more easily compacted than those of a thixotropic nature. Mix compaction was more effective via hand tamper than pneumatic compactor, although alternate models might be equally satisfactory. Lifting of uncured blocks can be accomplished if sufficient block support is

provided. Finally, curing had been confirmed to be temperature sensitive, necessitating controlled curing conditions, i.e., warehouse for Phase II.

b. Conesville Program. The information provided by the Elrama program was applied to the work program concepts initially developed for Phase I-C to formulate this program. The program outlined below is tentatively scheduled to commence in March 1979.

Conesville Plant Program

Quality Control	Establish design process equipment settings for each mix by testing Poz-O-Tec mixes for lime and fly ash content. Establish variability of leach design mix at equipment settings.
Mix Production	Determine stockpiling time required to allow Poz-O-Tec mix material to reach proper consistency.

Block Formulation

Block Compaction	Evaluate efficacy of hand tamping, automatic tamping and vibrating plant compaction versus lift depth in block to produce method yielding maximum practical block density.
Block Quality Control	Prepare three separate sets of proctor cylinders from each batch of Pcz-O-Tec used to form cubic yard blocks. Prepare cylinders at block density testing material for lime and fly ash content. Cure proctors at internal block temperature.

Block Testing

Temperature Monitoring	Measure block internal temperature during curing.

Block Testing - Continued

Block Stripping	Establish minimum cure time required prior to stripping molds from blocks.
Physical Testing	Establish minimum curing time needed for blocks to develop sufficient strength to permit forklifting handling, trucking and other physical stresses. Test blocks and block quality control weekly for compressive strength.

The Conesville program will take six to seven weeks. The onsite plant program will take one to two weeks. Block formulation will end by the third week with block testing complete by the end of the 7th week.

The program is reasonably self-explanatory, though some amplification will serve to clarify a few points. The reproducibility of the Poz-O-Tec produced at a given equipment setting will bracket the range of mixes anticipated in Phase II, i.e., 1:1 could range from 0.8:1 to 1.2:1. The term "lift depth" mentioned in block formulation refers to the thickness of the layers of material successively placed and compacted inside the block mold.

Internal block temperature measurements were specified to determine whether the heat of the pozzolanic reaction will be significantly higher than the air temperature for curing (23°C) allowing for accelerated strength development at the higher temperature. Proctor cylinders cured at the internal block temperature, and tested for compressive strength, will then accurately reflect actual block strength.

The physical testing aspect of the program will accurately define the day-to-day logistics of block storage, handling and transport processes in Phase II by determining the strength (and hence the curing time) required to permit these processes.

B. Phase II

1. Introduction

IU Conversion Systems, Inc. will manufacture, transport and dump by ocean barge approximately 350 blocks consisting of approximately a 3:1 ratio of fly ash mixed with sludge and 350 blocks consisting of approximately a 1:1 ratio of fly ash mixed with sludge. The fly ash to sludge ratio is intended to simulate the waste products generated by the proposed Arthur Kill Electric Generating Station to be erected in Staten Island, New York. The designated manufacturing facility selected is the Columbus and Southern Ohio Electric Power Plant located in Conesville, Ohio. The blocks manufactured will be one cubic yeard in size and weigh approximately 2,700 pounds. Manufacture of the blocks will be in an enclosed, covered, heated if required, and protected area located outside the power plant in order to preserve the normal operation of the utility.

2. Manufacturing Procedures

The two formulations of blocks require different methods of manufacture, thereby necessitating the use of different equipment, procedures, quality control and resources. Manufacture of the 3:1 blocks will consist of erection of the molds on specially designed pallets in which the material will be placed and compacted in lifts ranging from 6 to 12 inches. Each lift will be independently compacted and samples taken for analysis. Due to the impact induced by

the compaction equipment, it becomes imperative that special extra rigid pallets be provided in order to minimize deflection during the compaction period and also serve as a rigid support during transporting. Each of the 3:1 consistency blocks will be marked on four faces with one circular indentation of size and depth to be determined at a later date. All blocks will be supplied with chamfered corners of approximately 1 in x 1 in. The 1:1 consistency blocks will not be marked. After compaction of the 3:1 blocks, the molds will be removed and the blocks moved to a designated curing area where they will remain until the curing cycle is complete. The molds will be reassembled and utilized in the manufacture of the 1:1 block formulations. This method of utilizing the molds is advantageous since the 3:1 blocks can have the molds removed in a short period of time after manufacture; however, the 1:1 block formulations require the molds to remain in place during the curing cycle. Each of the above processes will be accomplished utilizing a biodegradable form release agent which has proved acceptable during our previously conducted block manufacturing activities. Each of the block formulations would be constructed without the use of any foreign material in the blocks.

3. Testing Procedure

The testing procedure will consist of proctors provided from each block (as many as is deemed necessary) in order to

to adequately regulate the curing process. The individual samples will undergo analysis in order to determine the actual consistency of each block. It is intended to provide a full scale compressive test on one block of each of the two formulations in order to ascertain and verify the compressive strength. IUCS is in the process of constructing a curing chamber for these proctors which is supplied with an adjustable heat source in order to regulate the heat intensity and thereby regulate the curing cycle.

4. Quality Control

IU Conversion Systems realizes that this operation warrants the use of a quality control procedure; therefore, the operating plant will be adjusted to insure that the block formulations are within the range of practicality. This operation will be supervised by highly qualified technical personnel as provided by IUCS. Since all mechanical equipment contains a degree of error, this will be corrected for the collection of a large quantity of material in order to minimize the error. In addition, it is apparent that hydrated lime will provide better distribution throughout the block formulation. Therefore, IUCS will adapt the plant silo and associated feed equipment from its normal use of pebble lime to deliver hydrated lime at a predetermined rate. This modification of equipment and the additional cost associated with purchasing and delivery of hydrated lime will be borne by IU Conversion Systems.

5. Transporting

The blocks once cured and approved satisfactory for transporting from the Conesville area to Fire Island will be loaded on either of two transportation methods (tractor trailer or railcar) whichever proves more feasible for rapid delivery and the least amount of handling. IUCS has obtained a loading/unloading site available in Bayonne New Jersey suitable for either of the two transporting methods and has made tentative arrangements for the barge to be positioned in order to facilitate loading and correct placement of the blocks.

6. Loading/Unloading

Due to the nature of the blocks, it is IUCS' option that the blocks can be loaded and unloaded with the use of a mechanical device that would lift three blocks simultaneously. The device is similar to a set of ice tongs except that instead of points, the device would depend on friction to lift the blocks. To this end, IUCS has proceeded to test the one cubic foot blocks in order to establish the nominal static friction factor induced by this material composition. The lifting device would be of special design and would therefore be designed, fabricated and supplied by IUCS.

7. Ocean Dumping

Placement of the blocks on the bottom of a bottom dumping barge is a critical factor since it necessitates that when dumping occurs, the blocks do not become jammed or wedged

in the doors. To this end, a feasibility study was conducted with the bottom dump barge supplier in order to establish the correct placement of the blocks. It is the intent to load the barge, one end being the 1:1 blocks and the other being the 3:1 blocks, in the Bayonne, New Jersey area and then tow the barge to the Fire Island designated dump site, where the blocks would be released.

IX. COST ESTIMATES FOR COAL WASTE DISPOSAL

The economic assessment proposes to address:

a) definition of the system of waste disposal, and estimation of the quantities of wastes to be handled,

b) review of published disposal cost estimates, update them and summarize our estimates, and

c) identification of some problems which may affect cost estimates related to the disposal process for coal waste blocks.

A. Rate of Waste Production

The assessment takes a strictly post-scrubber view of disposal, shown in Figure IX-1 (from the Power Authority of the State of New York). Quantities of scrubber sludge and ash are assumed to be available. The alternatives involve techniques for stabilization of sludge and/or block construction and subsequent transportation and disposal costs. The quantities of coal waste produced by coal burning power plants are large. As a waste computation basis, shown in Table IX-1, we postulate a 500 MW power plant on the Hudson River Estuary with typical 65% load factor. The coal is 3% sulfur and 15% ash content. Typical control measures for a modern power plant are assumed - 90% SO_2 removal in the scrubber and above 99% particulate removal in the precipitator. The resulting waste production (sludge plus fly ash) is 1650 tons daily.

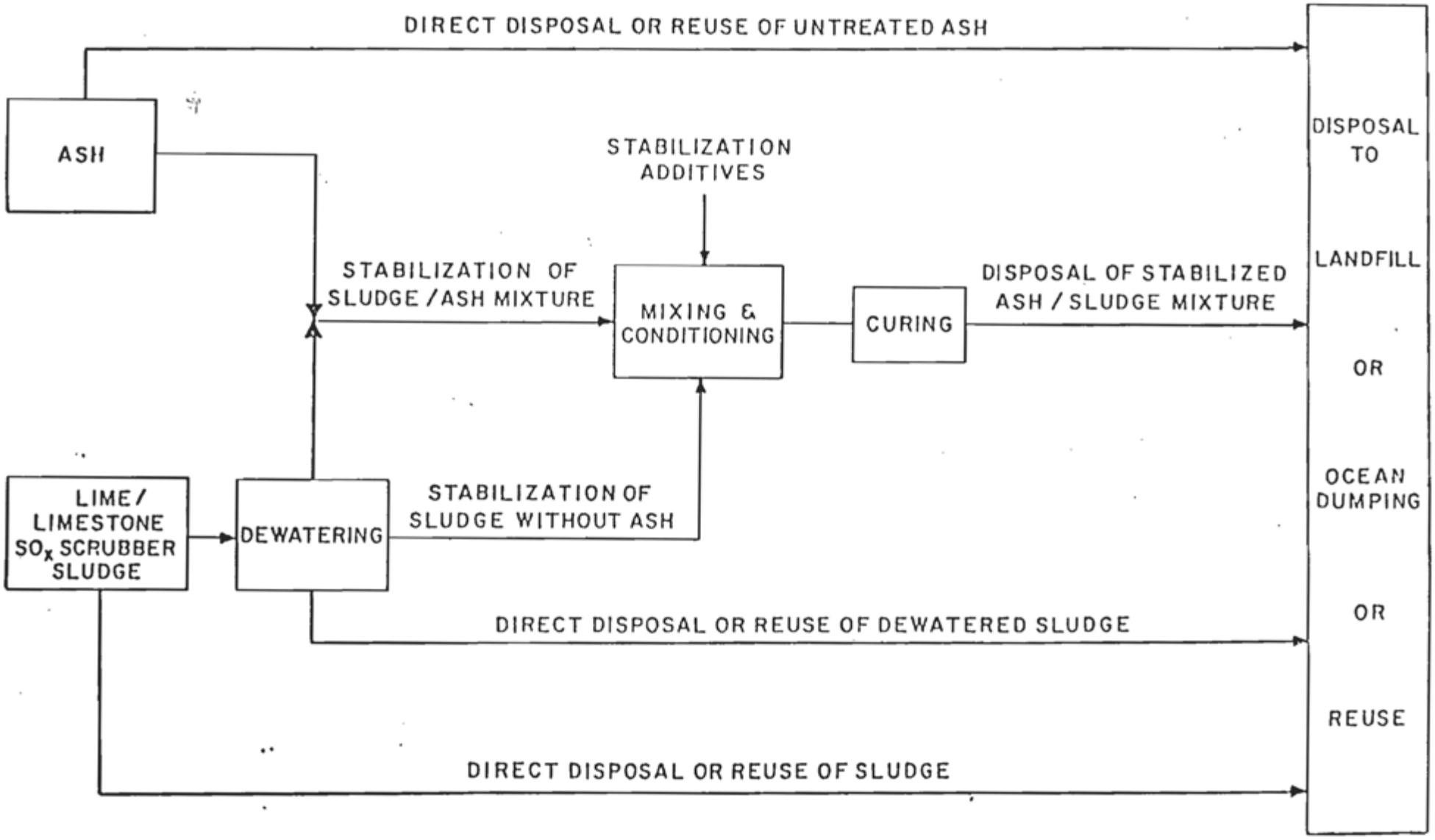

Figure XI-I. Alternative Ash and Sludge Handling Systems (from PASNY, 1975).

Table IX-1. Waste Production Estimate.

Plant:	50 MW, 65% load factor
Coal:	0.76 lbs coal/kWh (12500 Btu/lb coal and 9500 Btu/kWh heat rate)
	3% sulfur, 15% ash
Control:	90% SO_2 removal (scrubber)
	99+% particulate removal (precipitator)
Sludge production:	sulfur 137×10^3 tons annual
	ash 162×10^3 tons annual
	total (dry) 300×10^3 tons annual
	at 50% solids:
	Total (wet) 600×10^3 tons annual
	1650 tons daily

Computation Basis

Plant

$$500 \text{ MW } (8{,}760 \text{ hrs})(0.65) = 2.85 \times 10^9 \text{ kWh}$$

Coal

$$2.85 \times 10^9 \text{ kWh} \times (0.76 \text{ lbs/kWh}) = 2.17 \times 10^9 \text{ lbs/yr}$$

$$= 1.08 \times 10^6 \text{ ton/yr}$$

Sulfur

$$S(1 \text{ mole}) + SO_2(2 \text{ moles}) \rightarrow CaSO_4 \quad 4.25 \text{ moles}$$

(+10% reacted CaC_3) +0.42

3% 3%(90%)(4.7) = 0.127

$1.08 \times 10^6 \times 0.127 = 137 \times 10^3$ ton/yr

= 375 ton/day

Ash

15%(00+%) $= 163 \times 10^3$ ton/yr

= 440 ton/day

TOTAL (Sulfur plus ash)

dry = 815 ton/day

(50% solids) wet =1,630 ton/day

Disposal of quantities of this magnitude would require either several large barges, a number of rail cars, some type of conveyor system, or fleets of trucks. The only practical methods which achieve economical costs, and will be reviewed here, are barge disposal either of a stabilized sludge directly to a land fill or of stabilized sludge and/or block disposal at ocean sites.

B. Economic Estimates and Review

In Table IX-2 is a review of existing cost estimates for stabilization and barge transportation for both landfill and ocean disposal. The uniform cost basis which we establish will be cost per ton at 50% solids by weight. There is little apparent difference between the weight of stabilized slurry and that of block, since it appears that the curing of stabilized waste into the blocks does not occur by evaporation of water but rather by its "locking" into interstitial locations. Where costs were given in prior studies (Table IX-3) as "dry", these were generally estimated on the basis of a "wet" (50% solid) slurry. Consequently the dry costs were divided by two to estimate the cost per ton at a 50% solid mixture for Table IX-2. In addition, all costs from prior studies (Table IX-3) were adjusted to 1979 dollars by assuming a 10% annual inflation rate. The basis for the most recent cost estimate for barge transportation is that of Carroll and Dicker,

Table IX-2. Cost review (1979 dollars)*

	Stabilization (including handling)	Transportation (Barge-100n.m.)	Total
Landfill			
Workman and Rothfuss (1978)	$1.55/ton	-	-
Jones, Rosoff, and Rossi (1976)	-	-	$5.10-8.00/to
Goodwin and Gleason (1978)	$1.70/ton	-	-
EPA (1977)	-	-	$7.00/ton
Lunt et al. (1977)	-	$4.80/ton	-
Lilley (1976)	$2.80-5.60/ton	$2.80/ton	$5.60-8.40/to
Duvel et al.	$2.70/ton	-	$6.80/ton
Ocean application			
Lunt et al. (1977)	-	$2.70/ton	-
Lilley (1976)	$2.80-5.60/ton	$2.80/ton	$5.60-8.40/to
Carroll and Dicker (1979)	-	$4.00/ton	-

* Based on 10% annual rise in costs. Cost per dry ton equals twice cost per wet (50% solids) ton.

Table IX-3. Cost data (see Table IX-4 for sources).

	Stabilization (including handling)	Transportation	Total
Landfill			
Workman and Rothfuss (1978)	$3/ton dry	-	-
Jones, Rossoff, and Rossi (1976)	-	-	$7.30-11.40/ ton dry
Goodwin and Gleason (1978)	$3.08/ton	-	-
EPA (1977)	-	-	$5.82/ton
Lunt et al. (1977)	-	$6.50-8.00/ ton dry	
Lilley (1976) (1975)	$1-2/ton	$1-2/ton	$2-4/ton
Duvel et al. (1978)	$2.50/ton	-	$12.40/ton dr
Ocean dumping			
Lunt et al. (1977)	-	$4-5/ton dry (25 n.m.)	-
Lilley (1976) (1975)	$2-4/ton	$1-2/ton	$3-6/ton
Carroll and Dicker (1979)	-	$4/ton (100 n.m.)	-

Table IX-4. Reference sources for Table IX-3.

K. H. Workman and E. H. Rothfuss, Jr. "FGD Waste Disposal Effective Despite Surprises", Power Engineering (Nov. '78).

J. W. Jones, J. Rossoff, and R. C. Rossi, "Flue Gas Cleaning Waste Characterization and Disposal Evaluation", Fourth Annual International Ash Utilization Symposium (St. Louis, Mar. '76).

R. W. Goodwin and R. J. Gleason, "Options for Treating and Disposing of Scrubber Sludge" American Powers Conference (Chicago, Apr. '78).

Anon 1977 "Coal Cleaning with Scrubbing for Sulfur Control: An Engineering/Economic Summary" U. S. EPA Office of Energy, Minerals, and Industry (Aug. '77).

R. R. Lunt, et al., "An Evaluation of the Disposal of Flue Gas Desulfurization Wastes in Mines and the Ocean", Technical Report to EPA (EPA-600/7-77-051), A. D. Little (Cambridge, May '77).

W. A. Duvel, et al., "State-of-the-Art of FGD Sludge Fixation", Technical Report to Electric Power Research Institute (FP-671/project 786-1), Michael Baker Consulting Engineers (Beaver, Pa., Jan. '78).

W. D. Lilley, "Economic Feasibility Study of Disposal Alternatives for SO_2 Sludge", Office of Environmental Planning, New York State Public Service Commission (Aug. '76).

Anon 1976 "Alternatives for New York-New Jersey Metropolitan Area Sewage Sludge Disposal Management Program", Technical Report to Interstate Sanitation Commission (June '76).

which reflects present tug and barge costs shown in Table IX-5.

Stabilization costs are presently in the range $2-4 per ton. Transportation costs for landfill disposal are in the range $3-5 per ton. Ocean disposal transportation costs to 100 nautical miles are estimated in prior studies at $3-4 per ton, while our inquiry with Moran Towing, a large barging firm operating out of New York City, provide a current estimated cost of $4 per ton. The consistency of stabilization costs and transportation costs estimated by different methods in these different studies (for example, sometimes from electric utility information and in other cases by construction of hypothetical disposal systems and estimating the capital, operating, and maintence costs for these) gives some assurance that these cost estimates are relatively accurate and would apply in practice. Also, it is significant that the range of estimates is quite narrow, even comparing costs estimated by entirely different methods, so that again, there is some assurance of the relative accuracy of the estimated costs.

C. Cost Associated Considerations

There are several problem areas associated with the coal waste disposal which are significant in terms of their implications for the physical design of a disposal system and/or their implications in terms of cost. These

Table IX-5. Transport cost estimate (Carroll and Dicker, 1979)

Tug and Barge costs (Moran Towing and Transfer, N.Y.C.).

tug (incl. crew)	$ 4,000/day
barge (1500 yd^3) - 2	6,000/day
	$10,000/day

Disposal distance

7 knots x 24 hrs/day = 168 n.m./round-trip daily

Cost per trip (100 n.m. off shore)

$\$10{,}000/day \frac{200}{168} = \$1{,}200/trip$

Block density (based on MSRC data)

1.4 gm/cm^3 (0.98 $tons/yd^3$)

Cost per ton* (100n.m. offshore site)

$$\$12{,}000/trip \times \frac{1\ trip}{3{,}000\ yd^3} \frac{1\ yd^3}{0.98\ ton} = \$4/ton$$

---

* Barge capacity assumed selected to meet power plant waste quantity. If single barge towing, cost becomes $7,000/1,500 ton = $4.65/ton.

represent not insurmountable problems but indicate a) the need for some refinement in detailed engineering design of the disposal system and b) the potential for some minor changes in cost estimates depending upon details of the disposal process. However, the disposal system design must await more detailed findings on the size, strength, and response to handling and ocean dumping of the stabilized waste blocks.

1. Handling/Transfer

The blocks under current consideration are about one yard cubes and would weigh about 1 ton each. Our discussions with barge companies indicate difficulty in handling with crane or lift. If the block size were, for example, one foot cubes, these could be easily dumped on conveyor belts for barge loading. At this time it is not clear what would be the most appropriate size for the blocks, we merely suggest that some detailed thought needs to be given to the physical process of barge loading. While this is not a large element in the overall cost of the disposal system, it does offer some opportunity for slight adjustments in the cost with proper design of block handling.

Block and/or stabilized sludge barge loading operations represent no more than 10-15% of transportation cost. Sludge produced at 1650 tons daily, loaded at

4000 gpm would require about one hour for loading. Block loading time would likely be somewhat longer. Using the daily tug-and-barge rental in Table IX-5, the loading delay is estimated to cost about $.50 per ton. For landfill operations, the sludge must be both loaded on barges and later unloaded again and the total charge is about $1.00 per ton. In the studies reviewed in Table IX-2, we note stabilization (including handling) which appears to include these transfer operations.

2. Storage Space

The estimated curing time for the stabilized blocks is approximately three weeks. Consequently, some substantial storage area will be required. We assume the 1 yd^3 blocks cannot initially be stacked since they have little strength during the early stages of maturing. In a single layer, the curing blocks will cover up to approximately 8 acres. Of course, this area might be reduced substantially by stacking after the initial curing period but at present there is too little data on large block strength to assess this possibility in detail. The land requirement is not large; it is likely to present minor difficulty with respect to the mechanical movements associated with the pouring of blocks and transfer of blocks from the storage area to barge. In addition, a storage yard of this size is likely to add relatively little to the total cost of disposal of stabilized blocks.

3. Modes of Transportation

Because stabilization costs appear to not vary markedly with the type of stabilization ($2-$4/ton), the cost of the mode of transportation associated with each of the various types takes on added weight. The Arthur Kill study of coal waste disposal (ash and sludge) to quarries about 100 miles up the Hudson River indicates that the preferred transportation mode is barging. Although that study did not particularly address economic comparisons, it pointed out that because of the enormous quantities of waste to be expected from the plant an extensive fleet of trucks would be necessary to transport the material to the quarry. The costs of trucking are strongly site and job specific but are much more expensive than barges. Also, trucking uses much more energy than other transportation alternatives. Trucking has undesireable environmental impacts, discussed in subsection 4, below. On the other hand, rail transportation, which would be feasible, has other costly shortcomings. These include acquisition of rights-of-way, road-bed construction and laying down track, substantial loading areas, and other aspects of a volume-intensive transport system, all of which would have to be amortized over a relatively short time period - until the quarry is filled. Finally, the cost per ton-mile moved by truck and/or rail are more than double the costs of barge transport (Interstate Commerce Commission, 1976).

It appears from the considerations above that whether the coal waste is in the form of ash and sludge, or in blocks, the flexibility and capacity of barging would make it the preferred choice. The transportation cost would be about the same, therefore, for either form of waste hauled the same distance.

Loading and unloading costs would be different and would depend primarily upon the disposal type and location. With the proposed Arthur Kill plant, for example, where the quarry is relatively close to the barge docks, a conveyor system could efficiently transfer ash/sludge from the barges to the quarry where bulldozers would then spread the deposited material. But where the barge discharge facility is at some miles from the landfill conveyors may be too expensive, and trucking may be required for transport to the landfill, substantially increasing transportation costs. However, although it may appear that when the disposal site is close to the barge dock, the disposal of coal waste is more economical, ultimately the capacity of the quarry capacity will be exhausted (for the Arthur Kill plant this is projected as 16 years) so that additional sites will have to be developed. The likelihood is that future sites would require truck transportation from the barge to the disposal site. In such instances, the cost advantage of ash/sludge waste disposal shrinks appreciably.

The type of disposal site, is, evidentally, of prime

economic importance. A quarry disposal requires an initial cost, site preparation, perhaps a lining to inhibit leachate seepage, and ultimately, additional site work to shape the ground. And, of course, sooner or later its useable volume is depleted. Ocean dumping, on the other hand, requires none of the above: there is no cost of land and, it would take 10,000 years for the quantity of waste from the 500 MW plant to fill a volume 10 miles by 10 miles by sixty feet deep. However, in order to be environmentally acceptable the waste must be of a non-polluting form. In view of the foregoing data, the conversion of the waste to a stable block is promising.

4. Environmental and Social Costs

As noted above, the amounts of material to be disposed are large. In the above example, we cite some 1650 tons daily of material from a single power plant. As a result, even substantial landfills are likely to have limited life. For example, the Arthur Kill Quarry Disposal is estimated to have only a sixteen year life. As urban areas expand and coal-burning continues to increase, landfill areas become increasingly remote, as is already the case in the Metropolitan area. Substantial lead time is required for site selection and preparation. Consequently, landfill disposal must be viewed as, at best, a short-term measure while a search continues for a more permanent method of handling waste. By comparison,

ocean disposal offers a clear advantage of long-term accessability to a dumping area.

Initial purchase, land taxes, and site preparation should add no more than about $.30/ton to landfill disposal costs. However, eventual land rehabilitation and correction of such problems as entry of leachates into ground water where they arise, could become expensive. Difficulties might also arise in ocean disposal and careful monitoring, coupled with developing research, will be required to better define and predict waste behavior after disposal.

The handling/transfer/disposal of coal wastes in or near areas of population presents inherent problems and a set of often unrecognized social costs. Loading/unloading areas always exhibit some leakage, accidents, and the like. Truck, rail, or barge transit expose inhabitants of areas near the rights-of-way to possible residuals. Because only a relatively small volume can be handled at a time by trucks, the resulting frequency of handling causes increased traffic congestion as well as roadway damage, air and noise pollution and is particularly detrimental if trucks must pass through a residential neighborhood. Direct social - economic costs are also incurred. For example, while truck movement is taxed along major highways, the heavy truck traffic required for coal waste imposes serve wear upon local arterials. The maintenance cost is borne by the local community

rather than the coal waste disposal system.

The myriad of such environmental and social costs will be difficult to assess with any precision. However, because of its inherent movement of waste away from populated areas and research which, thus far, indicates environmental acceptability of stabilized coal wastes in the sea, ocean disposal seems to offer advantages in reduced environmental-social cost.

5. Artificial Fishing Reefs

The artificial reef is a means for increasing local biological productivity and aggregating fish for fishing. Suitably placed in selected areas, they may enhance fisheries on grounds close to access points, or, in areas of smooth seabed, they may improve the quality of fishing by providing a different environment for habitation by a diversity of "rough bottom" fish. There is, therefore, great appeal to using stabilized scrubber sludge and fly ash wastes for artificial reef construction, especially when compared with the simple ocean dumping of the unstabilized wastes -- the effects of which are entirely deleterious (Lunt et al., 1977). There seem to be few aspects of artificial reefs that differ fundamentally from natural reefs in the sea except in the characteristics of the materials used for their construction (The Conservation Foundation, 1974).

Artificial reefs can significantly increase fishing productivity. Although few estimates of their productivity

are available, long-term studies in South Carolina have estimated the value to the sport fishery of such reefs in excess of three million dollars per annum. With economic magnification effects, the income from the reefs were valued at more than ten million dollars.

The waters of New York Bight are subject to heavy sport fishing, mainly for pelagic species because the Bight floor is a relatively featureless, sandy plain with small populations of bottom species (less than 3% of the extensive sand covered continental shelf consists of hard bottom). Habitat improvement to create reefs would attract and hold bottom species of fish and enhance opportunities for sport fishermen. The Bight is an ideal region for such artificial reef building. In New York alone, there is an estimated total of 1.8 million salt-water anglers (Jensen, 1975),--a large constituency.

Undoubtedly, the environmental and recreational benefits from reef-building must be important considerations in ocean disposal of coal waste blocks, but adequate data is not currently available to factor such considerations into this cost assessment.

6. Assumptions for IU Conversion Systems Facility

The overall cost of stabilized coal waste disposal may be minimized if certain planning decisions are taken. The conversion-stabilization facility should be at the

power plant site, adjacent to the plant. Its receiving points for ash and sludge should be at the power plant's points of discharge, in order to reduce the amount of handling or storage required. Equally, block fabrication, maturation,and storage should be adjacent to the conversion facility. Because the blocks will ultimately be water borne and dropped into the ocean, the plant site should be close to the water's edge, preferably on a river, estuary,or bay so that barge docks are integral with the facility. This is in order to avoid a transfer step. Ideally the forms or molds for the block would be on each barge so that the solidfying process could take place during the voyage to the dumping site. This would imply a rapid block curing process. However, at present, the curing time is a few weeks, whereas the round barge trip is only about one or two days. An alternative scheme which avoids the handling of individual blocks, may be to form the blocks on pallets located on dockside storage for subsequent barge loading with minimal handling.

X. REFERENCES

American Public Health Association (1975) Standard methods for the examination of water and wastewater. American Public Health Association, Washington.

Berner, R. A. (1971) Principles of chemical sedimentology. McGraw-Hill, New York.

Boyden, C. R. (1977) Effect of size upon metal content of shellfish. Journal Marine Biological Association, U.K., 57, 675-714.

Carrol, O. and D. Dicker (1979) Chapter IX this report.

Carpenter, J. W. (1965) The Chesapeake Bay Institute technique for the Winkler dissolved oxygen method. Liminology and Oceanography, 10, 141-143.

Curl, H. and L. F. Small (1965) Variations in photosynthetic assimilation ratios in natural marine phytoplankton communities. Limnology and Oceanography, 10, supplement, R67-R73.

Dayal, R., S. Oakley, and I. W. Duedall (1978) Sediment geochemical studies at the 2800 m Atlantic nuclear waste disposal site. Report to the Office of Radiation Division, U.S. Environmental Protection Agency, Washington.

Dikeou, J. T. (undated) Fly ash increases resistance of concrete to sulfate attack. Research report No. 23, Water Resources Technical Publication, Bureau of Reclamation, Washington.

Duvel, W. A., W. R. Gallagher, R. G. Knight, C. R. Kolarz and R. J. McLaren (1978) State-of-the-art of FGD sludge fixation. EPRI report No. FP-671, Electric Power Research Institute, Palo Alto.

Environmental Protection Agency (1977) Coal cleaning with scrubbing for sulfur control: An engineering economic summary. U.S. Environmental Protection Agency Office of Energy, Minerals, and Industry, Washington.

Environmental Protection Agency (1978) Bioassay procedures for the ocean disposal permit program. EPA report No. 600/9-78-010. Office of Research and Development, U.S. Environmental Protection Agency, Gulf Breeze, Fl.

Folk, R. L. (1968) Petrology of Sedimentary Rocks. Hemphill's, Austin.

Garrels, R. M. and C. H. Christ (1965) Solutions, minerals, and equilibria. Harper and Row, New York

Goodwin, R. W. and R. J. Gleason (1978) Operations for treating and disposing of scrubber sludge. Paper presented at the 40th Annual meeting of the American Power Conference, April 24-26, 1978, Chicago.

Hardy, C. D. (1973) In Final report of the oceanographic and biological study for the Southwest Sewer District No. 3 Suffolk County, New York. Report prepared for the Bowe Walsh Associates. Marine Sciences Research Center, State University of New York, Stony Brook.

Herlihy, J. (1977) Flue gas desulfurization in power plants. Status report (April, 1977). Division of Stationary Source Enforcement, Office of Enforcement, U.S. Environmental Protection Agency, Washington.

Hulse, G. (1975) The Plunket, a shipboard water quality monitoring system. Technical report 22. Marine Sciences Research Center, State University of New York, Stony Brook.

Interstate Sanitation Commission (1976) Alternatives for New York-New Jersey metropolitan area sewage sludge disposal management program. Interstate Sanitation Commission, 10 Columbus Circle, New York.

Jensen, A. C. (1975) Artifical fishing reefs. MESA New York Bight Atlas Monograph 18. New York Sea Grant Institute, Albany.

Jensen, H. and J. Soren (1974) Hydrogeology of Suffolk County, Long Island, New York. U.S. Geological Survey Atlas HA-501.

Jones, J. W., J. Rossoff, and R. C. Rossi (1976) Flue gas cleaning waste characterization and disposal evaluation. Paper presented at Fourth Annual International Ash Utilization Symposium (St. Louis, March 1976)..

Klein-MacPhee, G. K. (1978) Synopsis of biological data for the winter flounder, Pseudopleuronectes americanus (Walbaum). NOAA technical report NMFS circular 414, U.S. Department of Commerce, Washington.

Lilley, W. D. (1976) Economic feasibility study of disposal alternatives for SO_2 sludge. Office of Environmental Planning, New York State Public Service Commission (August, 1976).